WT-1464

AEC Category: HEALTH AND SAFETY
Military Categories: 5-26 and 5-28

OPERATION PLUMBBOB

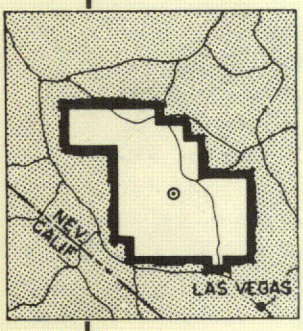

NEVADA TEST SITE
MAY-OCTOBER 1957

Project 32.3

EVALUATION OF COUNTERMEASURE SYSTEM COMPONENTS AND OPERATIONAL PROCEDURES

Issuance Date: September 15, 1959

CIVIL EFFECTS TEST GROUP

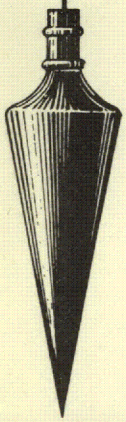

NOTICE

This report is published in the interest of providing information which may prove of value to the reader in his study of effects data derived principally from nuclear weapons tests.

This document is based on information available at the time of preparation which may have subsequently been expanded and re-evaluated. Also, in preparing this report for publication, some classified material may have been removed. Users are cautioned to avoid interpretations and conclusions based on unknown or incomplete data.

PRINTED IN USA
Price $3.00. Available from the Office of
Technical Services, Department of Commerce,
Washington 25, D. C.

AEC Technical Information Service Extension
Oak Ridge, Tennessee

Report to the Test Director

EVALUATION OF COUNTERMEASURE SYSTEM COMPONENTS AND OPERATIONAL PROCEDURES

By

W. E. Strope

Approved by: C. F. MILLER
Director
Program 32

Approved by: R. L. CORSBIE
Director
Civil Effects Test Group

U. S. Naval Radiological Defense Laboratory
San Francisco, California
August 14, 1958

ABSTRACT

The objective of Project 32.3 was to evaluate some operational characteristics of a radiological shelter and to determine values for some countermeasures-system parameters. The operation consisted of two phases, the first involving measurements made by project personnel in a manned station having the characteristics of a high-performance radiological shelter and the second involving monitoring and reclamation operations in an area near the shelter beginning about 1 hr after burst.

Measurements were made inside the shelter beginning at shot time to (1) test a simple shelter monitoring system, (2) test a proposed ventilation intake configuration intended to eliminate a requirement for filtration of the shelter air supply, (3) determine the effective gamma-radiation shielding afforded by an operational shelter, including two different exhaust ventilation configurations and a simple entrance configuration, and (4) determine those radiation and fallout characteristics needed to evaluate the operational measurements. The second phase involved (1) the test of a key-point initial monitoring technique, (2) the test of two proposed techniques for determining reclamation effectiveness in advance of reclamation operations, (3) the test of the feasibility of achieving a residual number of 0.01 in a cleared area, and (4) the test of a barrier as an alternative to a buffer zone.

Data were obtained on two shots (Diablo and Shasta). The shelter, having a minimum earth-cover thickness of 3 ft, provided an average shielding reduction factor of about 10,000. All openings in the earth cover for ventilation and other purposes were satisfactory from a radiological point of view with the exception of the straight entrance way. The shelter monitoring system provided adequate information. The air-filter data showed no requirement for air filtration at air intake flow rates of 300 to 600 cfm with the intake configuration used. All objectives in the second phase were successfully met with one exception. It was not possible to obtain an adequate test of the feasibility of achieving a residual number of 0.01 in the staging area because of the poor condition of the test area.

ACKNOWLEDGMENTS

This project was approved only 16 days before the first readiness date. That the shelter and reclamation areas were constructed, instrumentation installed and calibrated, and dry-runs of the procedure accomplished in time to achieve a very successful participation on shot Diablo was due in large part to the willingness and capability of the participants brought together for the project. The participants were:

SHOT DIABLO:

P. E. Brown, Oak Ridge National Laboratory, Oak Ridge, Tenn.
G. H. Giboney, USAEC, Savannah River Operations
D. G. Harris, USAEC, Grand Junction, Colo.
J. E. Jamison, Mason and Hanger, Silas Mason Co., Inc., Burlington, Iowa
J. A. LaSpada, USNRDL
R. K. Laurino, USNRDL
Hong Lee, USNRDL
C. F. Miller, USNRDL
M. J. Nuckolls, USNRDL
H. Phillips, Mason and Hanger, Silas Mason Co., Inc., Burlington, Iowa
W. E. Strope, USNRDL
B. A. Sword, USNRDL
J. E. Thrall, USAEC, Idaho Falls Operations Office
W. F. Trolenberg, USAEC, NYOO, Schenectady, N. Y.
C. M. Unruh, General Electric Corp., Hanford Operations Office, Richland, Wash.
G. A. Work, USNRDL

SHOT SHASTA:

P. A. Covey, USNRDL
L. D. Johnson, USNRDL
C. F. Miller, USNRDL
M. J. Nuckolls, USNRDL
T. E. Sivley, USNRDL

Thanks for invaluable aid are also due R. L. Corsbie, W. W. Schroebel, and E. R. Saunders of the Civil Effects Test Group (CETG) and L. E. Egeberg, Project 32.4; J. E. Barnett, Program 35; and S. Sigoloff, Project 39.1.

Acknowledgment is given to P. Zigman, J. Mackin, P. Strom, D. Love, M. Honma, D. Sam, and other members of the Analytical and Standards Branch, USNRDL, who made all the laboratory analyses on the fallout samples.

The project officer desires to pay special tribute to Carl F. Miller, who took charge of the shot Shasta participation in the project officer's absence, was responsible for planning all supporting technical measurements, and is responsible for the data analysis in Sec. 3.3 and Appendix D of this report.

This study was funded by the Division of Biology and Medicine, U. S. Atomic Energy Commission.

CONTENTS

CONTENTS (Continued)

ILLUSTRATIONS

ILLUSTRATIONS (Continued)

CHAPTER 2 PROCEDURE

CHAPTER 3 RESULTS

ILLUSTRATIONS (Continued)

ILLUSTRATIONS (Continued)

TABLES

TABLES (Continued)

Chapter 1

INTRODUCTION

1.1 OBJECTIVE

The objective of Project 32.3 was to evaluate the performance of a number of important components of a radiological countermeasures system[1,2] in order to fix minimum performance requirements or to establish the feasibility of procedures proposed on theoretical grounds. One group of components is involved in the emergency phase of the system and is associated with a radiological shelter in a fallout area. This group of components was the subject of phase I of the project. A second group of components is concerned with the operational recovery phase of the system and involves operations in the fallout area outside the shelter. This group was the subject of phase II.

1.1.1 Phase I Objectives

All phase I objectives involved measurements made within, and from within, an occupied underground shelter located in the local fallout area but beyond the region of significant blast damage. These objectives were as follows:

(a) Operational Monitor System: To evaluate the operational suitability and accuracy of a simple low-cost device for determining from within the shelter the radiological situation outside the shelter.

(b) Ingress of Contaminated Air: To evaluate the ability of a simple low-cost configuration of the shelter ventilation system to satisfactorily prevent the entry of hazardous amounts of radiological fallout into the shelter and to determine whether or not filtration of the air supply would be a requirement of shelter design.

(c) Effects of Openings on Shielding: To evaluate the effective shielding provided by an underground shelter and to determine the effect of the shelter entrance and two different ventilation-opening configurations on the effective shielding.

(d) Supporting Technical Studies: To obtain information on radiological decay, energy spectra, and physicochemical characteristics of fallout necessary to interpret the results of the operational measurements.

1.1.2 Phase II Objectives

Phase II objectives involved measurements outside the shelter following phase I. Most objectives are concerned with the establishment of a suitable staging area for operational recovery. These were as follows:

(a) Initial Monitoring from Shelter: To evaluate a standard procedure for determining essential radiological information in a minimum amount of time and with a minimum exposure of personnel.

(b) Staging-area Reclamation: To establish the feasibility of achieving a residual number of 0.01* in the preparation of a cleared staging area and to determine the operational residual numbers associated with this effort.

(c) Reclamation Test Methods: To obtain an initial feasibility judgment on two techniques, proposed on theoretical grounds, for determining the effectiveness of a reclamation method on a small representative area before committing personnel to a large-scale operation.

(d) Alternative Buffer-zone Techniques: To determine the relative effectiveness, as a function of effort expended, of a barrier technique vs. a buffer-zone method.

1.2 BACKGROUND

The radiological-defense system[3–5] consists of three time phases of action following a contaminating nuclear event: (1) emergency phase, (2) operational recovery phase, and (3) final

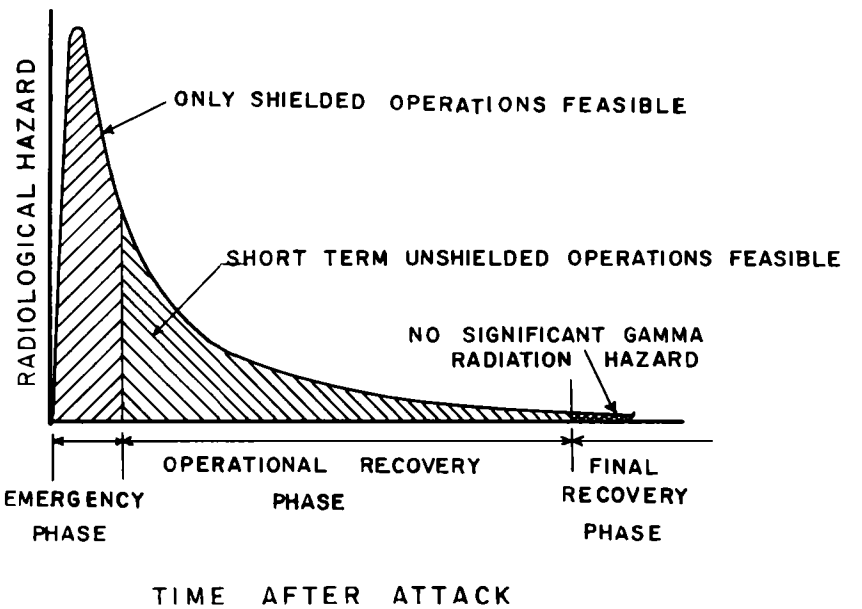

Fig. 1.1 — Phases of radiological defense.

recovery phase.[1] The technical basis for this phasing lies principally in the manner in which the gamma-radiation hazard decreases with increasing time after burst. In general, the gamma radiation decays very rapidly at early times and more and more slowly at later times after burst. Operations, consequently, must be geared to this decay rate. In the central regions of a fallout area, there exists a time period immediately following the arrival of fallout in which the gamma-radiation hazard may be so high that no unshielded operations are feasible without casualties (or without exceeding the allowable personnel exposure). This time period constitutes the emergency phase, as shown in Fig. 1.1. All operations during this phase must take place in shelters that provide adequate shielding against the gamma radiation. The fundamental objective during this phase is the survival of personnel. Therefore, adequate personnel shelters are the minimum requirement for defense during this phase.

At some time after fallout has ceased, the gamma-radiation hazard will have decreased to the point where short-term unshielded operations are feasible, although long-term or normal

*Residual number is a measure of radiological countermeasure effectiveness and is defined as the ratio of the measurement with the countermeasure to the corresponding measurement without the countermeasure.

functions are not. At this time the ability to perform short-term functions can be used to create the necessary conditions for the resumption of the longer term functions. The principal means available for this purpose is reclamation. This time period, which has as its objective the recovery and operation of the essential unprotected facilities, is the operational recovery phase.

At a much later time, about one to two years for most of the contaminated area, the gamma-radiation hazard will have decreased to a level where it is no longer significant. This may be conveniently taken as the level at which the present permissible exposure of 0.3 r/week would not be exceeded. The final recovery phase will begin at this time and will continue indefinitely. Nonessential areas bypassed during the operational recovery phase can then be reoccupied. External gamma radiation would no longer be a significant hazard, but the control of the internal alpha- and beta-radiation hazards could constitute a major public-health problem.

Participation was scheduled for Diablo and Shasta shots, with participation in Whitney and possibly other shots conditional on the success or failure of the earlier participations.

The shelter (a standard ammunition-storage magazine of the type previously tested to 25 psi) was located in the most probable fallout area at a distance where the predicted blast overpressure would not exceed 3 psi. Average gamma-radiation intensity anticipated at this range (assuming that the shelter was downwind) was about 100 mr/hr measured 1 hr after burst; maximum radiation intensity expected was about 1 r/hr measured at 1 hr. Since fallout arrival time would be a matter of minutes after burst, much higher transient intensities were anticipated. Nevertheless, the relatively low levels of fallout anticipated indicated that measurements within the shelter would be difficult and that phase II operations must be accomplished beginning about 1 hr after burst. These conditions influenced the choice of objectives and the experimental procedure.

REFERENCES

1. W. E. Strope, Radiological Defense Measures as a Countermeasure System, Report USNRDL-TR-74, Feb. 15, 1956.
2. Atomic Warfare Defense, NavDocks TP-PL-2, July 1, 1956.
3. Radiological Recovery of Fixed Military Installations, NavDocks TP-PL-13, June 1, 1957.
4. J. R. Earl et al., Operation Jangle Report, WT-400, 1952.
5. J. D. Sartor, H. B. Curtis, H. Lee, and W. L. Owen, Cost and Effectiveness of Decontamination Procedures for Land Targets, Report USNRDL-TR-196, Dec. 27, 1957.

Chapter 2

PROCEDURE

2.1 GENERAL PLAN

The operating area for the project is shown in Fig. 2.1. The general procedure was to man the shelter on D−1 night with designated personnel (about 15 people). At H−30 min mechanical ventilation was shut down, and blast closures were secured on all openings. Shelter status was reported to the Control Point (CP) at required intervals via phone (Appendix C). Telephone link was backed by emergency radio link. Immediately after the detonation, closures were removed, and ventilation was activated. Predicted fallout arrival time was 6 to 10 min after burst. The intensity was expected to peak about 20 min after burst, and fallout was expected to be complete approximately 30 min after burst. Phase I measurements were made during the first hour. Approximately 45 min to 1 hr after burst, the exact time depending on the radiological situation resulting at the shelter, the phase II initial monitoring routine was carried out. Information obtained was relayed to the shelter by voice radio. If none of the three prelocated areas had received a suitable level of fallout, no operations would be conducted on that shot.

Phase I operations were conducted inside the underground radiological shelter (Fig. 2.2). The shelter, a standard 25- by 48-ft Armco Multi-plate ammunition-storage magazine, was modified as shown in Fig. A.1. The new entrance unit, containing a Navy standard quick-acting watertight door and two hooded ventilation intakes, was reached by an open ramp and a covered passageway approximately 30 ft long (Fig. 2.3). The shelter was buried side-on to the shot area beneath 3 ft of earth cover, the entrance facing away from Ground Zero (GZ). The roof of the shelter housed two exhaust ventilators of differing configuration, two dosimeter tubes, a periscope housing, and an antenna lead tube. A small buried sample-collection room was located adjacent to the end of the shelter which was opposite the entrance. It was entered from the shelter through a crawl space. The shelter was ventilated by two M6 collective protectors, with a total capacity of 600 cfm. Design details of the shelter are given in Appendix A.

Phase II operations were conducted in an area measuring 500 ft on a side. Three such areas were predesignated and staked prior to shot time. These areas are shown in Fig. 2.1. The areas offered very difficult conditions for land reclamation, compared with areas reclaimed at Operation Jangle,[1] because of the rocky condition of the soil and the presence of gullies and washes. Because of this, extensive preparation of the areas was necessary to provide even minimum conditions for successful land reclamation by scraping. Large numbers of stones and boulders were removed from these areas. Even with these efforts, scraping was substituted for plowing as the only practicable buffer-zone method. Land-reclamation equipment and other vehicles were located about 3 miles southwest of the shot towers, and the jeeps were located to the rear of the shelter near the entrance. The jeeps were revetted and covered with tarpaulins during the fallout event.

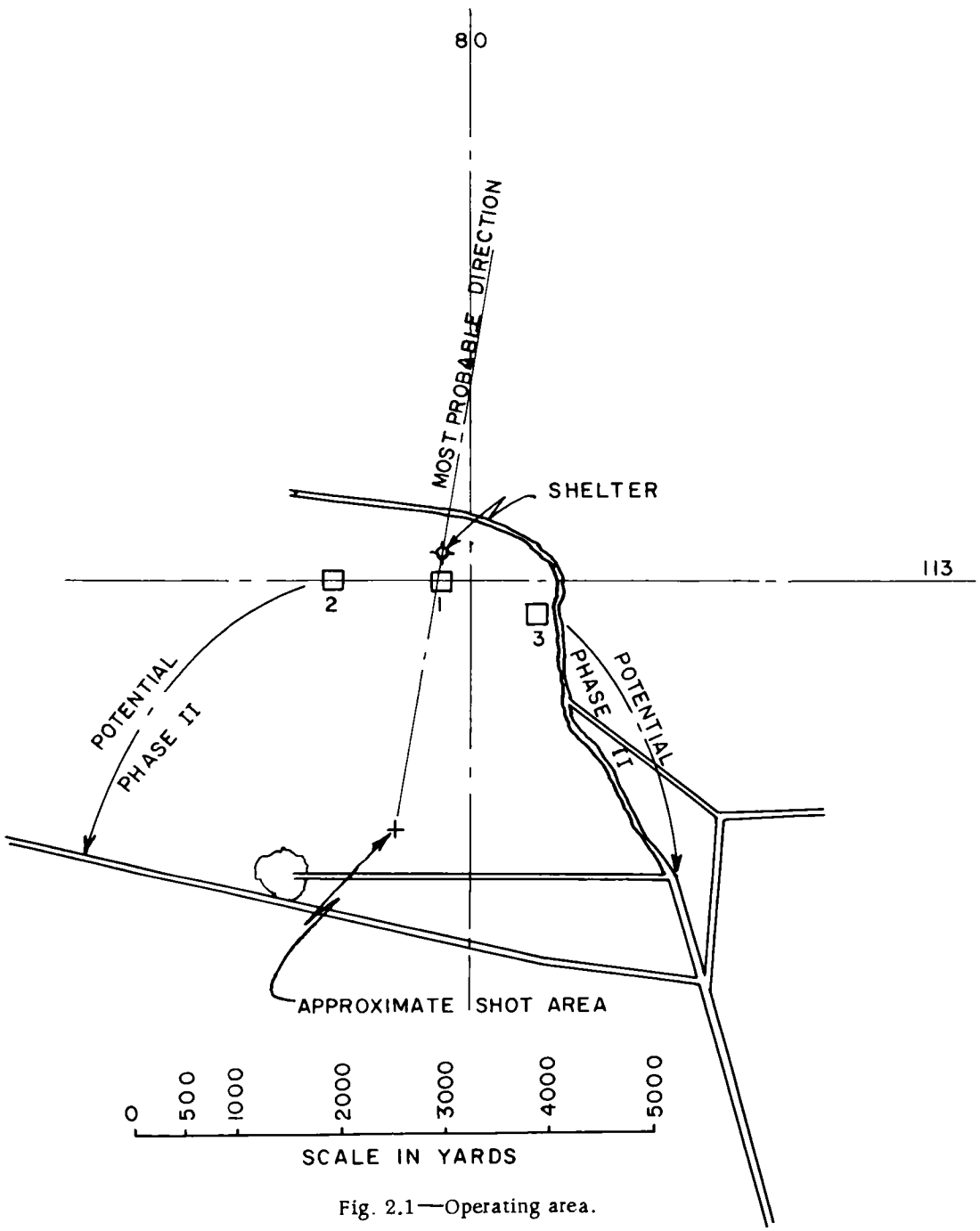

Fig. 2.1—Operating area.

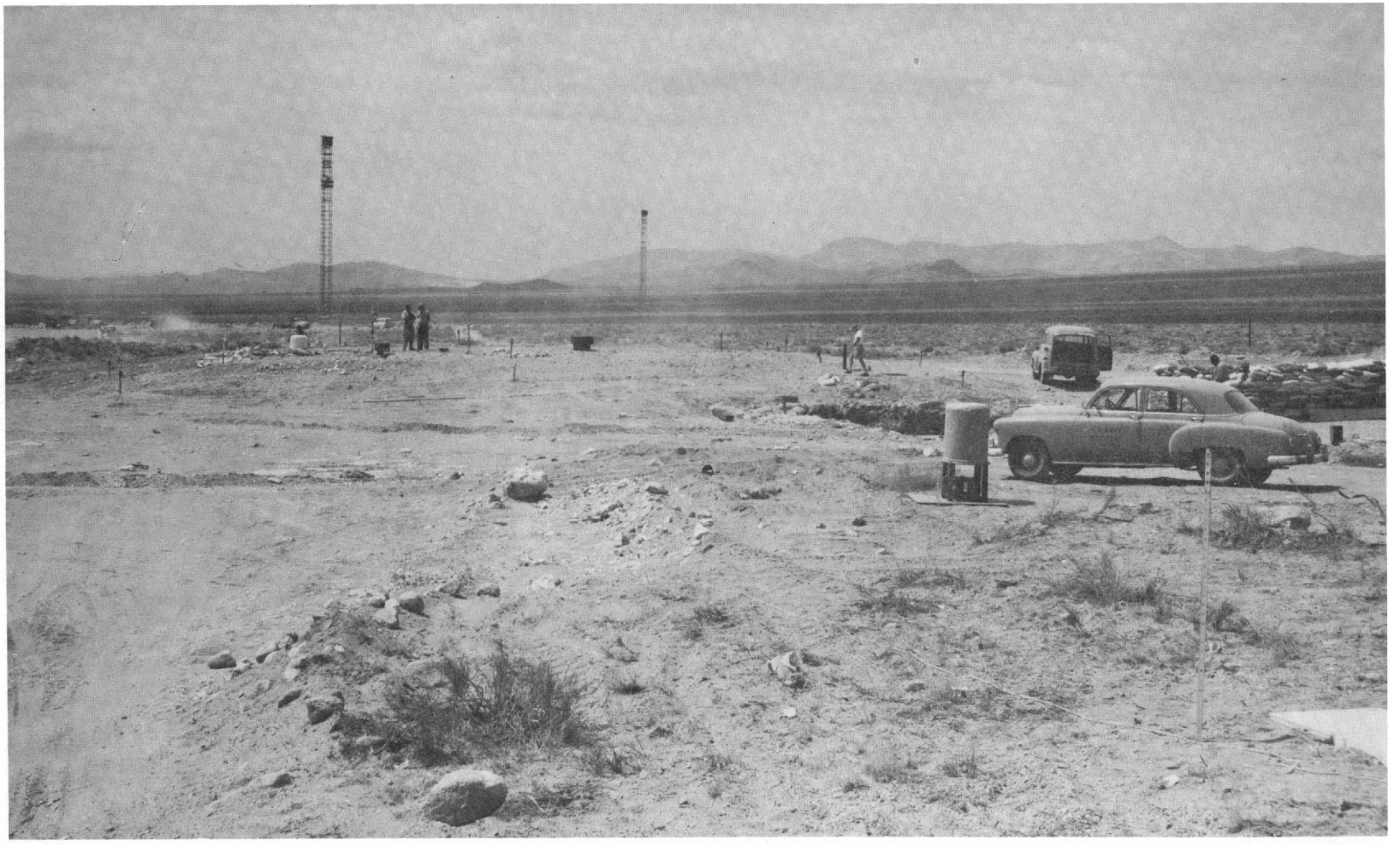

Fig. 2.2—View of shelter, looking toward shot area.

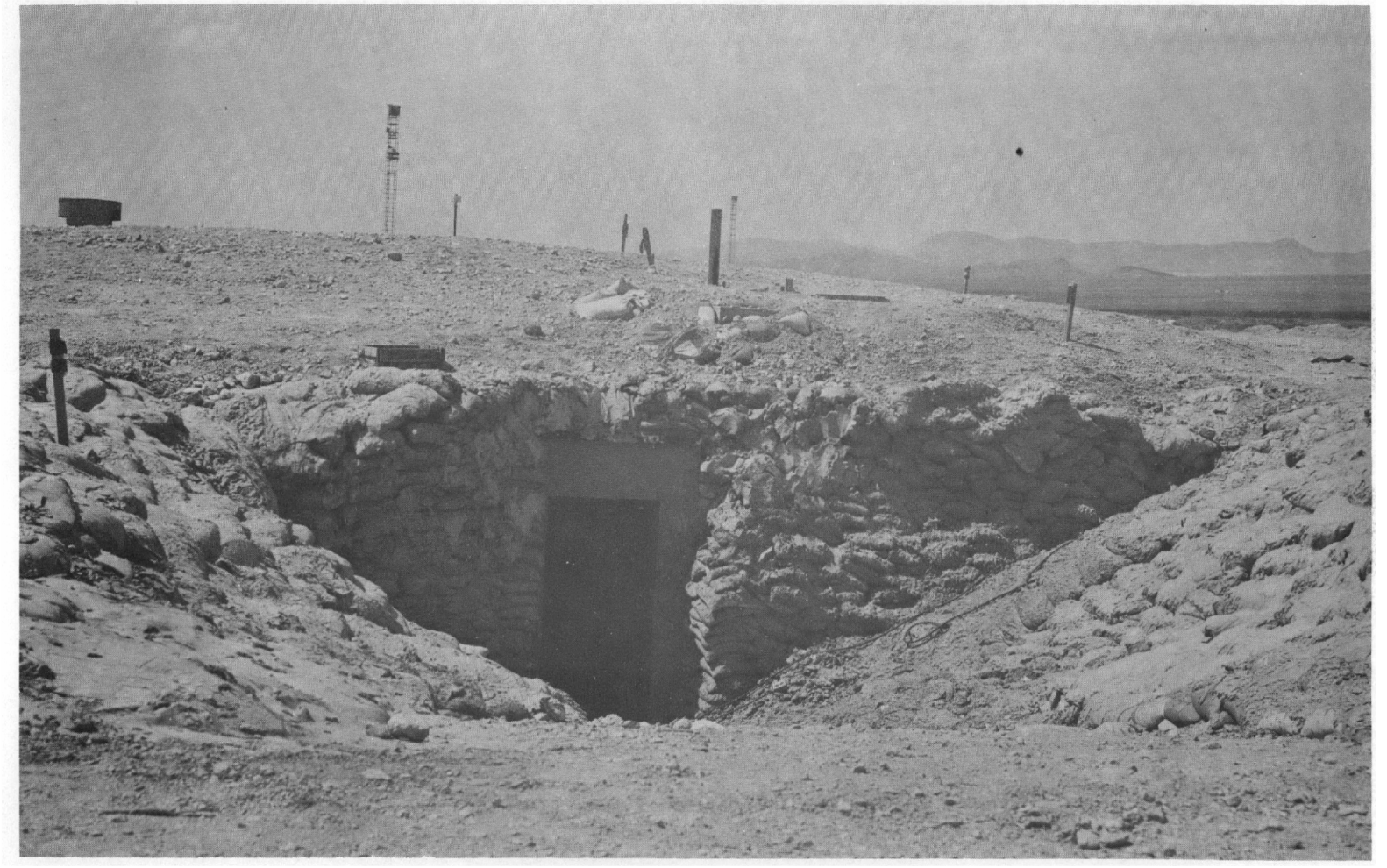

Fig. 2.3—Entrance ramp, showing tunnel opening.

2.2 OPERATIONAL MONITOR SYSTEM

Objective I(a) involved the evaluation of the low-cost monitoring device shown in Fig. 2.4. The system consists of a 1-in. steel pipe projecting above the shelter roof which is fitted with a wooden rod drilled at the upper end to receive a standard IM-9 self-reading dosimeter. The dosimeter is charged within the shelter, run up to the exposed position for a measured period of time, and withdrawn; the dose is then read. The gamma-radiation intensity is obtained by the following relation:

$$I = \frac{D \times 60}{t}$$

where I is the intensity in roentgens per hour, D is the dose in roentgens as read on the dosimeter, and t is the time of exposure in minutes.

The value of I thus calculated is associated with the time after burst corresponding to the mid-point of the exposure period. The experimental procedure involves a variable exposure period ranging between 1 and 6 min, depending on the dose recorded on the previous exposure, and a constant 1-min down time while the dosimeter is being read, the reading is being recorded, and the dosimeter is being recharged, if necessary.

Two such systems were fitted in the shelter for purposes of intercomparison, one at each end of the shelter. The forward dosimeter tube is shown in Fig. 2.5. The exposure schedules for the two systems were arranged to provide exposure by one system during the down time of the other system, thus providing better resolution of the arrival time and peaking time.

The following information was to be obtained from the system:

1. Time of arrival of fallout
2. Time and absolute value of peak intensity
3. Time of fallout cessation
4. A prediction of the standard intensity (roentgens per hour at 1 hr) based on readings taken at about fallout cessation (about 30 min after burst)

Items 1 and 2 were obtained directly from the intensity measurements; items 3 and 4 were obtained by correcting the intensity measurements to 1 hr by means of the decay curve shown in Fig. 2.6. Information obtained was evaluated following the event by comparison with data obtained under objective I(d) and data obtained by Project 32.4.

2.3 INGRESS OF AIRBORNE ACTIVITY

Objective I(b) was concerned with the evaluation of a simple ventilation intake configuration for the shelter which previous experiments had indicated should prevent significant amounts of fallout from entering the shelter (Fig. A.1). Air is drawn through the entrance tunnel, which acts as a plenum chamber. At the shelter two intakes, protected by mushroom heads that force a reversal of air direction, are located adjacent to the door. Air is taken into the shelter by two M6 collective protectors,[2] delivering a total volume of 600 cfm (Fig. 2.7). Air velocity across the face of the entrance tunnel is approximately 30 ft/min. The combination of low air velocity in the tunnel and mushroom vent caps on the air intakes was the configuration being tested.

The ingress of contaminated air through the configuration was determined from activity collected on the particulate filters in the collective protectors. These measurements were to be made at USNRDL after shot participation.

It was necessary to relate the activity concentration in the air moving through the system to the activity concentration in the air external to the shelter in order to further define the conditions of test so that the results could be evaluated for other contaminating events. For this purpose measurements were made both inside and outside the shelter to determine the activity concentration as a function of time and the average activity concentration during the fallout period.

Four aerosol sampling units and two collective protector units were used to obtain the data. Two aerosol sampling units (one automatic incremental sampler and one Porta-Vac

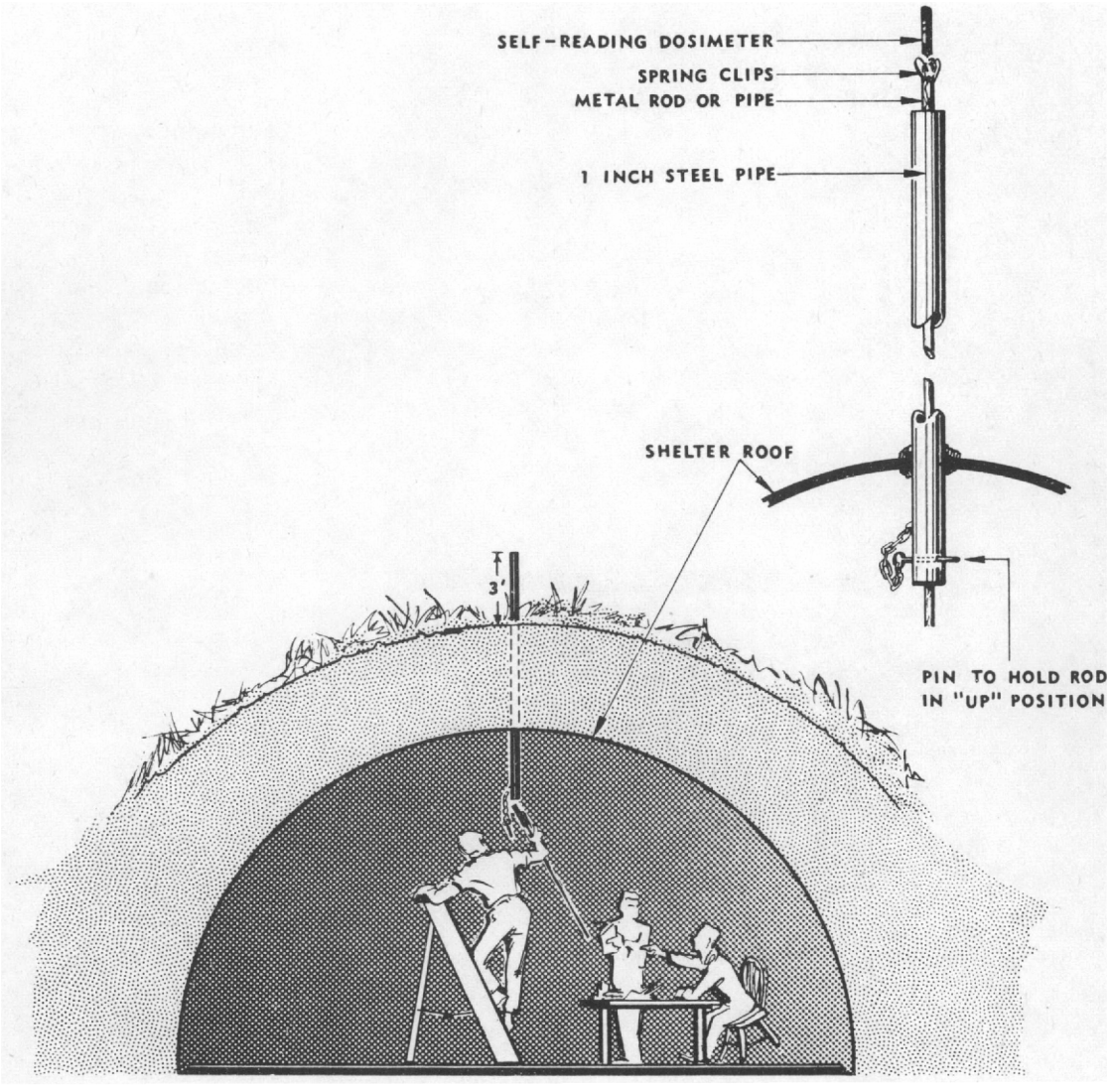

Fig. 2.4—Simple radiation-measuring device for use in shelter.

Fig. 2.5—Exterior view of forward dosimeter tube.

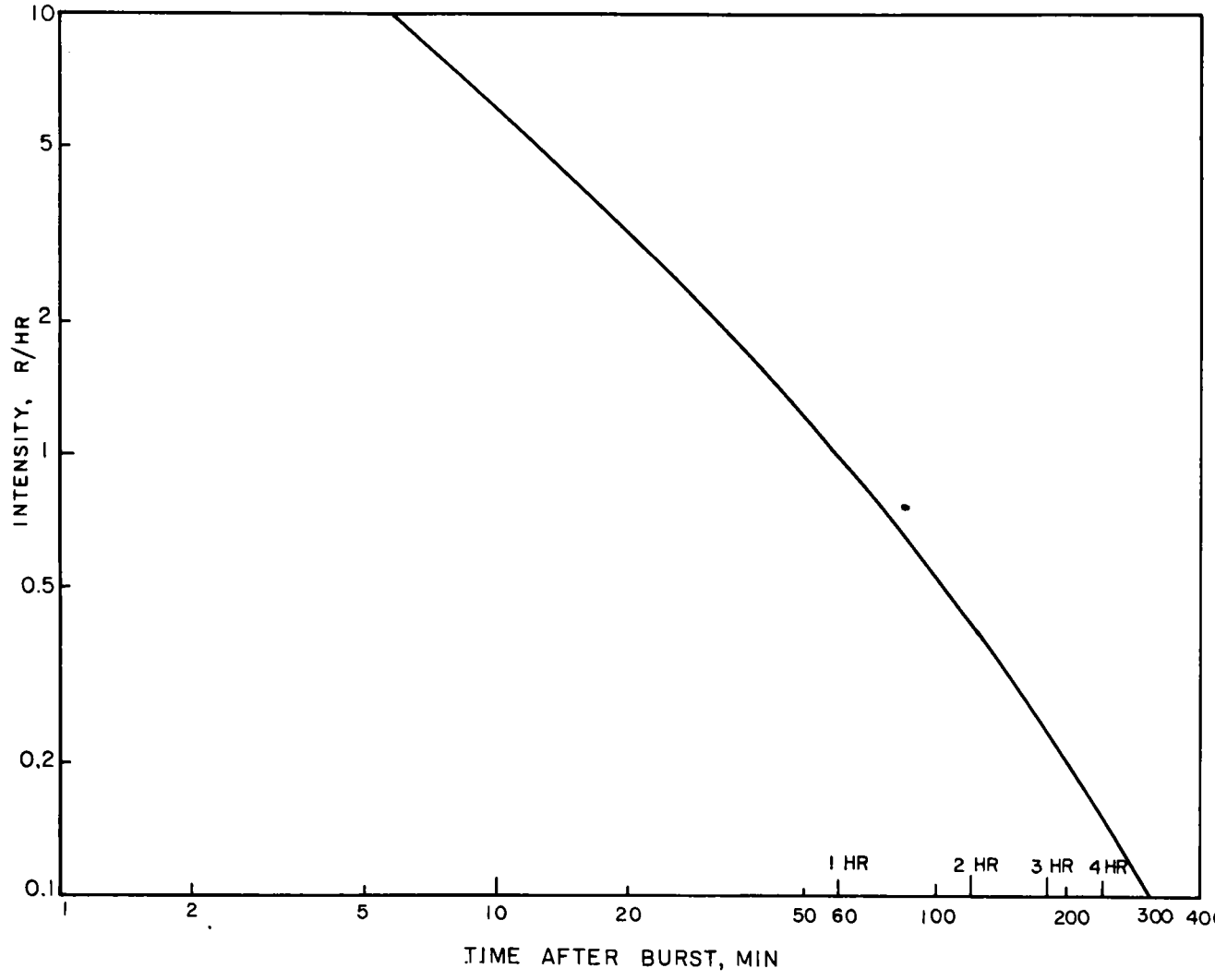

Fig. 2.6—Planning decay curve, normalized to unit standard intensity.

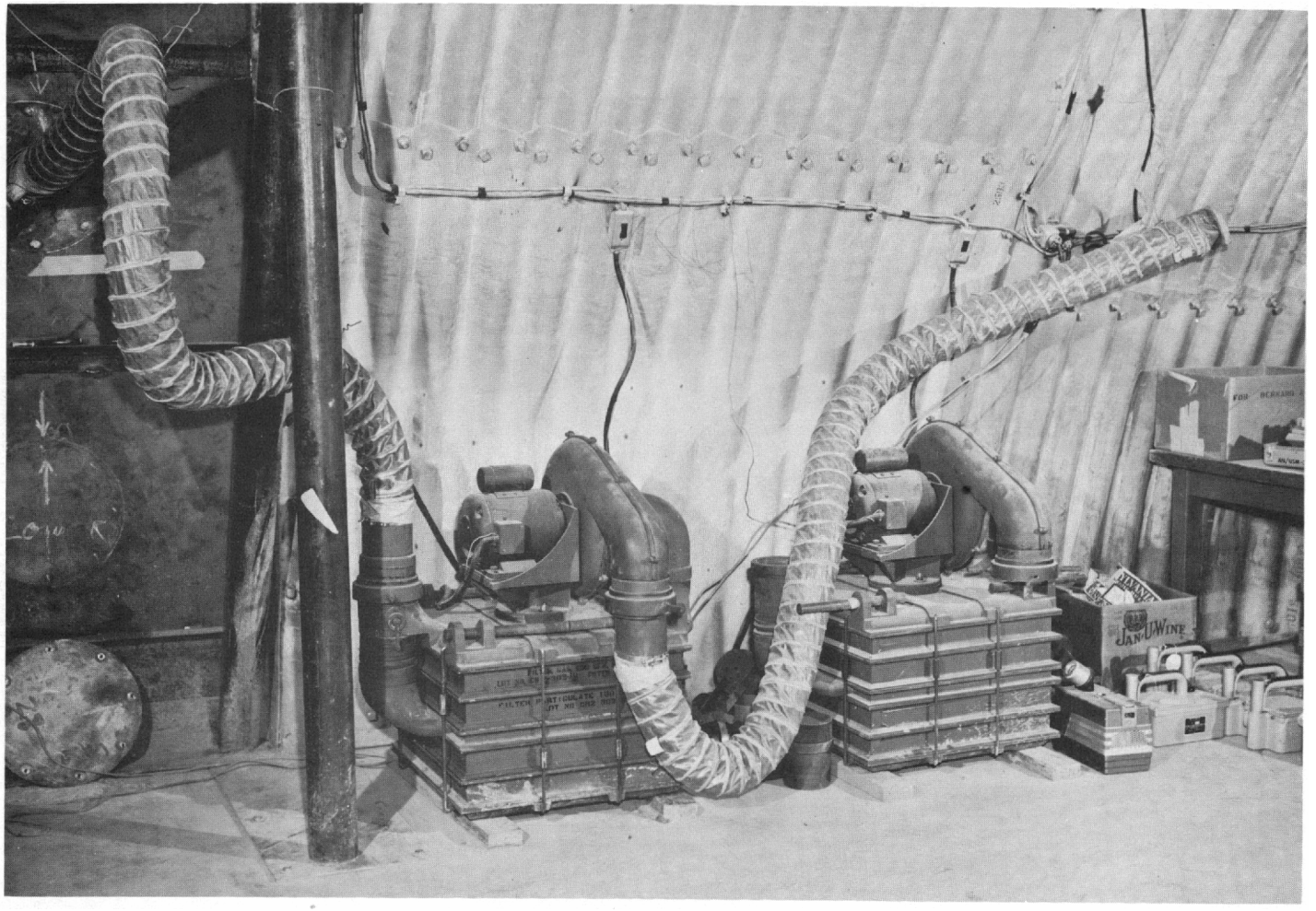

Fig. 2.7 — M6 collective protectors in shelter.

sampler) were placed outside the shelter entrance (Fig. 2.8) to measure activity concentration with time and total activity during the fallout period in the open atmosphere. Two sampling units (both Porto-Vac samplers) and the M6 units were located inside the shelter. One sampler was used to measure the activity concentration in the plenum chamber through an opening in the door, and the other unit was used to measure the activity concentration in the intake of the M6 unit (Fig. 2.9).

Aerosol sampling began when fallout reached the vicinity of the shelter indicated by the Project 32.4 gamma intensity-time recorder (GITR) located outside the shelter. At this time outside samplers were switched on. The two samplers inside the shelter were operated for sampling periods of 2-min duration with 1-min intervals between sampling periods. Filters from shelter samplers were replaced after each sampling period and were stored for counting after the end of the fallout event.

Aerosol sampling inside and outside the shelter was stopped shortly after the end of the fallout event. When the intensity outside the shelter permitted, personnel recovered the filters from the outside samplers for counting.

2.4 EFFECTS OF OPENINGS ON SHIELDING

Objective I(c) was concerned with evaluation of the effective shielding against fallout radiation provided by an underground shelter having approximately 3 ft of earth cover over the crown. It has been pointed out[3] that, although 3 ft of earth cover may be expected to provide a residual number between 0.001 and 0.0005, the effective shielding afforded by an operational shelter will be controlled by openings in the earth cover required for entrances, ventilation ducts, and other shelter appurtenances. In addition, a cylindrical shelter with a level fill will have an increasing thickness of earth cover for areas not on the center line.

The shielding effectiveness of the shelter in the vicinity of the air vents and entrance was determined by measurements of gamma intensity and gamma dose inside and outside the shelter and by measurements of the gamma-energy spectrum inside the shelter. On the exterior the needed data were obtained by (1) continuous measurement and recording of intensity and dose at fixed locations above and near the shelter, (2) a gamma survey on and around the shelter, and (3) measurements made by Project 32.4 on total and incremental fallout collectors around the shelter. Inside the shelter data were obtained by (1) measurement of gamma intensity and dose at a few fixed stations, (2) survey measurements at a large number of other stations distributed throughout the shelter, (3) a directional gamma-radiation survey along the center line of the shelter, and (4) measurements of gamma-energy spectra using a single-channel pulse-height analyzer.

2.4.1 Dose Measurements

Dose measurements outside the shelter were made with film-badge dosimeters. Film badges were secured near the top of the dosimeter tubes (about 2 ft 6 in. above the ground) and to the center ventilator (about 6 in. above the ground) (Figs. 2.5 and 2.10). These dosimeters were collected upon completion of phase I; they recorded the dose both from initial gamma radiation and from fallout up to the time of collection. About 2 min after burst, when the dose from initial gamma radiation had been received, another set of film badges was introduced into the above locations from inside the shelter. Several film badges were pushed up each dosimeter tube and dropped into a cup attached near the top of the tube (Fig. 2.5). Other film badges attached to metal rods were pushed up the center vent to an exposed location. These badges recorded only fallout dose and were collected at the same time as the original group. The difference between the doses recorded by the two sets of badges was attributed to initial gamma radiation.

A limited number of dose measurements were made inside the shelter. Because of the high degree of protection afforded by the shelter, film-badge dosimeters were too insensitive to be used. Near shelter openings, where the highest doses were expected, self-reading electroscope dosimeters (0 to 200 mr) were used. A line of dosimeters was strung vertically below the ventilation openings. Measurement heights on the vertical line were 3, 6, 9, and 12 ft above the shelter floor. Three dosimeters were located near the shelter door. All self-

Fig. 2.8—Exterior air samplers near shelter entrance.

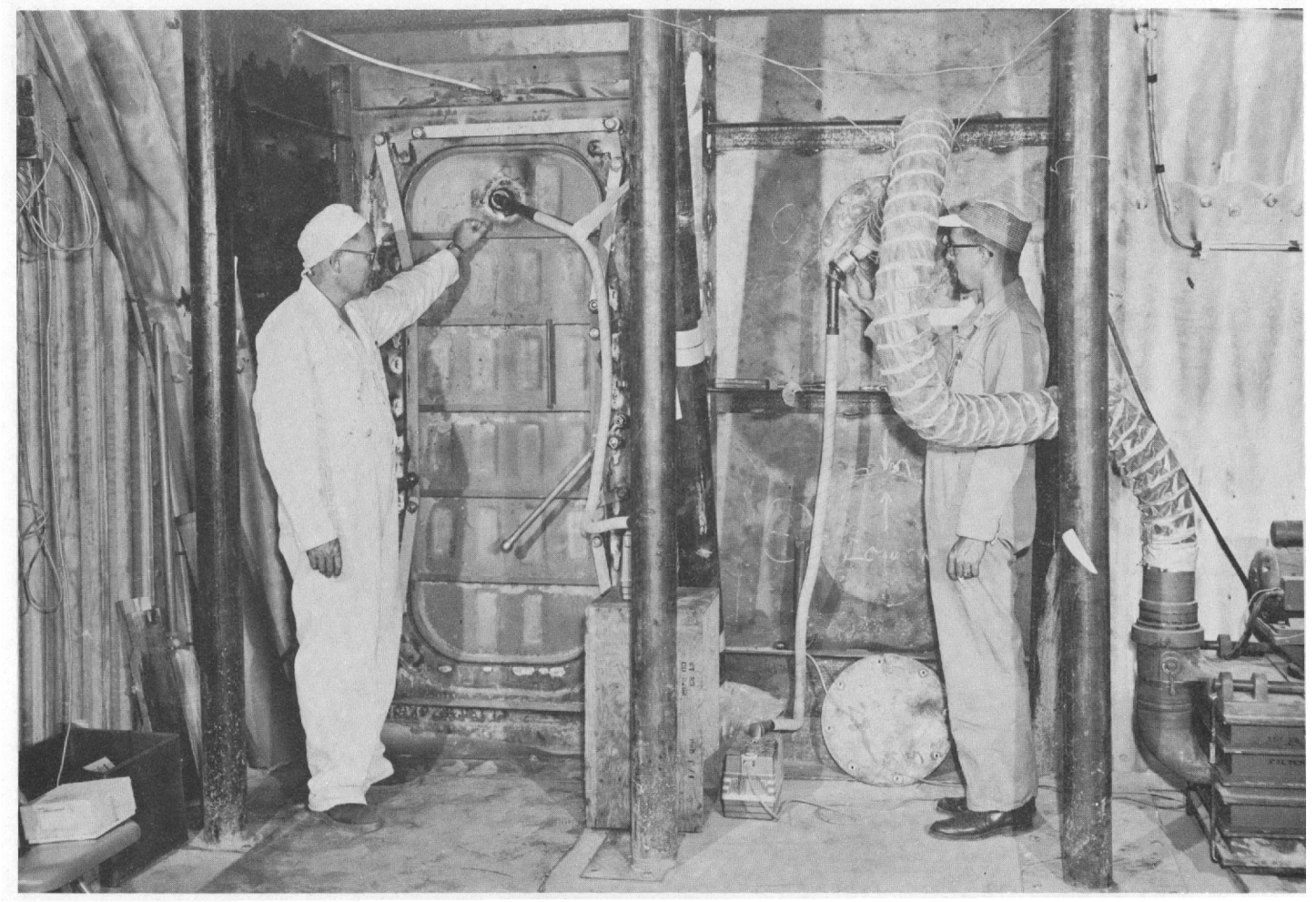

Fig. 2.9—Interior of air-sampling arrangement.

Fig. 2.10—View of center ventilator, showing location of film-badge dosimeters.

reading dosimeters were read about 2 min after burst to determine the dose from initial gamma radiation; final readings were made at the completion of phase I.

In addition to the above, a number of Victoreen background dosimeters (0 to 10 mr) were charged by a manometer charger-reader about 2 min after burst and were placed in the well-protected parts of the shelter to measure the anticipated low doses at these points (Fig. 2.11).

2.4.2 Intensity Measurements

Continuous measurement of intensity at a fixed location on top of the shelter (Fig. 2.12) was provided by a Project 32.4 GITR with the recording console inside the shelter. This instrument was switched on 2 hr before shot time and continued to record until the completion of phase II.

About 1 hr after burst, depending on the radiological situation, a gamma-intensity survey was made using the AN/PDR-27C and AN/PDR-39(T1B) survey meters at the points shown in Fig. 2.13. At the time these measurements were made the top of the center exhaust vent was decontaminated by broom, and sandbags were piled around the vent to reduce the contribution of the vent to the radiation field inside the shelter to a low level. A second survey was then performed within the shelter.

Intensity measurements inside the shelter were made using modified AN/PDR-27C instruments. Seven such instruments were connected by cables to one 12-channel Heiland recorder. These instruments were used to take detailed survey measurements at a large number of survey stations inside the shelter. The survey was initiated after fallout cessation (about 30 min after burst). Initially, monitors lined up at stations in row A (stations A1, A2, A3, etc., in Fig. 2.11). On signal, all monitors read the instrument at the 3-ft height above the floor and recorded the readings. At the same time the instruments were recorded for 10 sec on the Heiland recorder. Monitors then moved to row B, and the process was repeated. Measurements were also made at other heights of interest (6, 9, and 12 ft above the floor). A second survey was made after the center vent had been shielded.

In addition to the above, AN/PDR-27C instruments, modified to record individually on Brown recorders, were located as shown in Fig. 2.11; they recorded continuously.

2.4.3 Directional Measurements

The source of radiation inside the shelter was investigated with a directional gamma-intensity meter (see Appendix B). Measurements were initiated at fallout arrival time at locations along the center line of the shelter (row C). At each location the instrument was rotated in a plane including the nearest shelter opening (entrance or ventilators).

2.4.4 Energy-spectrum Measurements

A single-channel pulse-height analyzer (Appendix B) was located at position A6. This instrument was used intermittently to determine the gamma spectrum at this point within the shelter.

2.5 SUPPORTING TECHNICAL STUDIES

Objective I(d) included a series of precise measurements to define more completely the radiological situation at the shelter. The instrumented area on top of the shelter is shown in Fig. 2.12.

2.5.1 Interval-collector Data

Two interval collectors placed near the shelter were activated at about H+2 min. The collecting surface was a grease-covered plastic disk about 3 in. in diameter. Each disk was exposed for a period of 1 min, and the collectors were operated to collect fallout up to about H+1 hr. At about H+2 hr, Project 32.4 personnel recovered the samples and returned them to USNRDL for analysis. These analyses were used to determine the time of arrival of fallout at the shelter, the rate of arrival of fallout, the time of cessation of fallout, and, together with

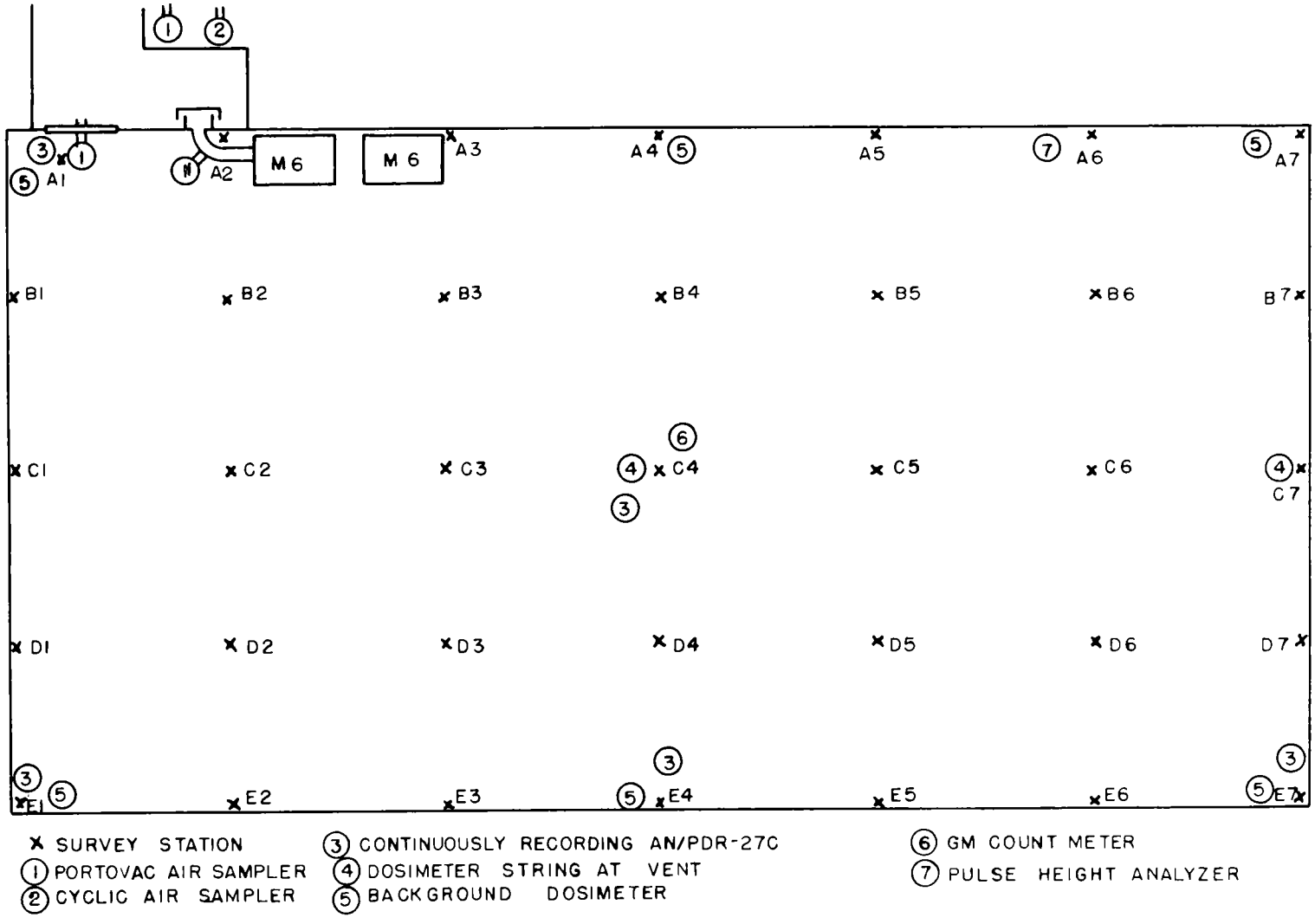

Fig. 2.11—Location of instruments and survey stations at the shelter.

Fig. 2.12—View of instrument location on top of shelter, showing (left to right) antenna, periscope housing, after dosimeter tube, rear exhaust vent, recording anemometer, GITR, sample elevator, and incremental collector.

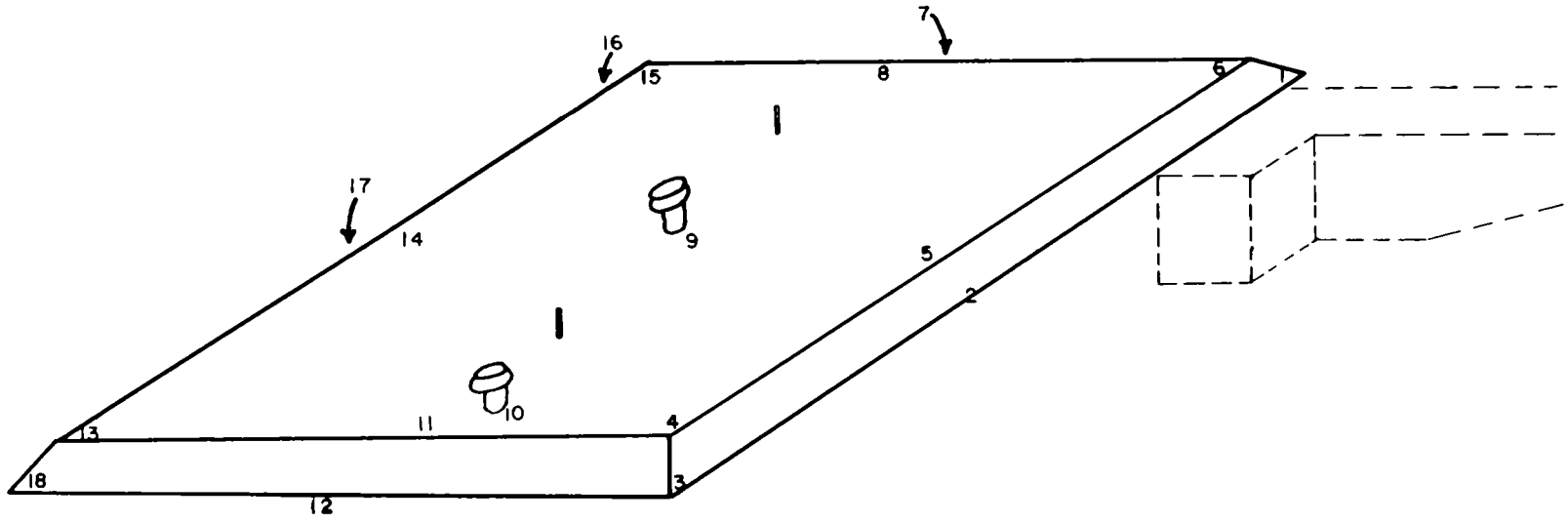

Fig. 2.13—Location of exterior survey stations.

the GITR records and decay measurements, the transit dose at the shelter. In addition, the samples were used to determine the range of fallout-particle sizes at the shelter.

2.5.2 Early-time Decay of Fallout Samples

Samples of fallout were collected by aluminum and plastic hexcell collectors and a hand-operated elevator located in the shelter sample room. An aluminum tray was exposed at H−30 min and retrieved at H+2 min as a collection of possible throw-out material. After recovery of the aluminum tray, a 6- × 6-in. hexcell collector was placed on the elevator and raised into collecting position. As soon as the GITR showed a rapid rise in the field intensity, the first hexcell was recovered and a second was exposed. The second hexcell collector was exposed until cessation of fallout (or until such time as the first sample had decayed to a low level).

Decay of the samples was measured in the USNRDL 4π ion chamber, an argon-gas ionization chamber operated at 600 psig with a previously determined photon-energy response.[4]

2.5.3 Early-time Photon Spectra of Fallout Samples

At H+5 min (shot Diablo) a helicopter left the CP area and picked up an open-close collector located 75 yards east of the shelter. The sample was returned to the Project 2.2 trailer located at Mercury. A counting sample was prepared, and the first spectrum was taken as soon as possible on the 100-channel analyzer. Spectra of the sample were taken at periodic intervals. Spectra of fallout samples were also obtained from the single-channel analyzer located in the shelter. These data, together with the decay data and instrument response, were to be used to determine an air-ionization (roentgens per hour) decay curve for the fallout.

2.5.4 Nature of the Fallout

The nature and amount of fallout at the shelter were determined from radiochemical and quantitative analyses made on the six open-close collector samples exposed above and about the shelter by Project 32.4. The collectors were actuated from within the shelter at H+2 min and closed at H+1 hr (or after cessation of fallout). They were recovered by Project 32.4 and returned to USNRDL by air for analysis. The samples were analyzed for gross gamma activity, gross mass of fallout, fission-product tracer nuclides, induced activities, iron, and soil minerals.

2.6 INITIAL MONITORING FROM SHELTER

The initial effort in phase II was monitoring of the three prelocated reclamation areas. A two-stage key-point monitoring procedure was followed. The first stage was to measure the radiation-field intensity at the center of the area with an AN/PDR-27C. This reading, made at 3 ft above the ground, was reported by radio to the shelter. The single center reading was the basis for selection of the area to be reclaimed. The second stage was to measure and report in a similar fashion the intensity at the four corners of each area. These measurements gave additional information, including the gradient over the area. Radiological information based on these key-point measurements was compared subsequently with the more detailed information obtained in the next step to determine the minimum information required for decisions at the beginning of the operational recovery phase.

2.7 STAGING-AREA RECLAMATION AND TEST METHODS

Objectives II(b) and (c) were accomplished simultaneously. After selection of a satisfactory area, personnel (three supervisors and five monitor-recorders) were dispatched to the area. When these personnel left the shelter, the reclamation-equipment operators (stationed at a more distant location) were alerted to move toward the area. Detailed monitoring was made of the area. Each of four monitors in turn started from the center in the direction of one of the four sides of the area. Readings were made at the center at 3-ft, 2-ft, and 1-ft heights (Fig. 2.14). Each monitor then paced toward his perimeter, taking the 3-ft, 2-ft, and

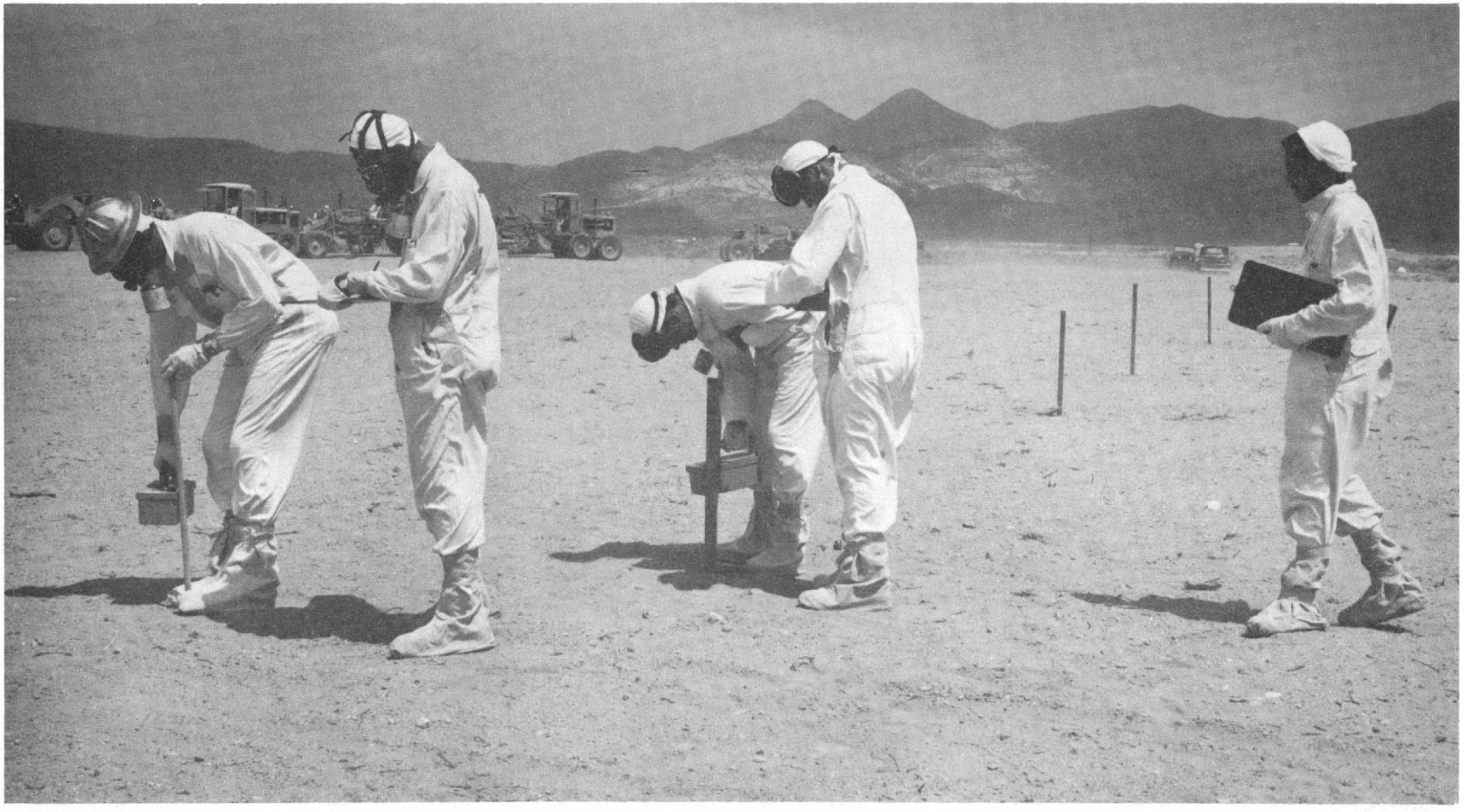

Fig. 2.14—Monitors taking measurements in reclamation area.

Fig. 2.15—Equipment used in land reclamation.

1-ft measurements at 2 paces and a single 3-ft measurement at 4, 5, 7, 10, 15, 20, 30, and 50 paces and at the 500-ft perimeter line. A fifth monitor took readings at two separate check points outside the area at 15-min intervals during the first hour and at 30-min intervals thereafter. All measurements were recorded along with the time of measurement.

As soon as the survey team had cleared the central area, an area 40 by 40 ft was cleared by motor-grader. Three motor-graders and a motorized scraper were maneuvered into position at the cross-wind side of the 500-ft perimeter line while the above monitoring was being done. They assumed a slant formation, with the scraper at the rear of the slant (Fig. 2.15). The motor-graders were set for a 2-in. cut at the 40-ft perimeter line, and the blades were set to move the windrow downwind toward the motorized scraper. The first grader cut and built the first windrow, the second grader picked up the first windrow and cut and formed a second windrow, the third grader cut and moved the windrow to the final position. The scraper was set for zero cut and picked up the windrow for disposal beyond the 500-ft perimeter. Two passes were needed to create a 40- by 40-ft cleared area since the width from the forward edge of the first grader to the rear edge of the third grader was 20 ft.

The 40- by 40-ft cleared area was then surveyed by conducting the previous survey to the edge of the cleared area.

Next, the cleared area was enlarged to 60 by 60 ft by making a 10-ft pass around the 40- by 40-ft area. Sides were done in order, north, south, west, and east. The windrow was left at the outer edge by the graders and picked up by the scraper. The 60- by 60-ft area was then surveyed as before.

Finally, the area was enlarged to 100 by 100 ft by making a 20-ft pass around the previously cleared area. Several trips of the scraper were required to remove the 100-ft windrows. The 100- by 100-ft area was then surveyed as before.

The area between the 100-ft perimeter and the 500-ft perimeter (a width of 200 ft) was then scraped, using three motor-graders, two scrapers, and a follow-up grader. A final survey was then made which was identical with the initial survey.

During the above operations all personnel carried film badges and pocket dosimeters so that operational-dose data could be obtained. The movement of all personnel was timed. If the residual number at the center of the cleared area was greater than 0.01, the area was scraped again and resurveyed. Clearing operations in the 100- by 100-ft area were continued until a residual number of 0.01 was achieved, or until it was obvious that further improvement was impossible.

2.8 ALTERNATIVE BUFFER-ZONE TECHNIQUE

Objective II(d), concerned with the test of an earth barrier as a substitute for a buffer zone, was conducted separately and at a different time from the operations described in Sec. 2.7. A 100- by 100-ft area was surveyed and then cleared by motor-grader and scraper. The area was then resurveyed. A 3-ft-high earth barrier was then constructed around the periphery of the scraped area by bulldozers. A final survey completed the operation.

REFERENCES

1. J. R. Earl et al., Operation Jangle Report, WT-400, 1952.
2. Department of Army Technical Bulletin 3-350-2.
3. A. B. Chilton and L. N. Saunders, Fallout Radiation Protection Afforded by Below-ground Structures, BuDocks Technical Digest No. 74.
4. C. F. Miller, Response Curves for USNRDL 4π Ion Chamber, Report USNRDL-TR-155, May 17, 1957.

Chapter 3

RESULTS

3.1 GENERAL

Participation occurred in three shots, Diablo, Kepler, and Shasta. Full participation was attempted on the first two shots; participation on Shasta was limited to the acquisition of additional supporting technical data.

3.1.1 Shot Diablo

Shot Diablo was fired on a 500-ft tower 5300 ft south of the shelter at 0430 PDT on July 15, 1957. The predicted wind structure was favorable for fallout at the shelter. Sixteen persons occupied the shelter at the time of burst. The event schedule followed is given in Appendix C. About 1 sec after the shot a light double-peaked ground shock wave was felt; at about 3½ sec the air blast wave arrived. Some dust was raised in the shelter, but no damage was evident. Later it was determined that the only blast damage consisted in the following: (1) the plywood wall between the entrance tunnel and the motor-generator room was blown in (Fig. 3.1); (2) the tarpaulins were stripped from the jeeps; and (3) the jeep revetment was partially demolished (Fig. 3.2).

The only damage that affected the experimental results was that to the wall since it caused the motor-generator to draw its cooling air from the entrance tunnel, greatly increasing the flow rate in the tunnel.

Fallout arrival occurred at about 6 min after burst. Intensity rapidly increased to a peak of 55 r/hr (GITR reading) at about 15 min. Intensity at 1 hr (GITR reading) was 14 r/hr. These intensities were considerably higher than anticipated, and they forced adjustments in the experimental schedule. Phase II was postponed until D+2 day. Exterior measurements on top of the shelter were made at about 5½ hr after shot time using AN/PDR-T1B radiacs. Shelter personnel left the area at about H+8 hr, two persons remaining to continue data collection.

3.1.2 Shot Kepler

Shot Kepler was fired on a 500-ft tower 4.75 miles south of the shelter at 0450 PDT on July 24, 1957. The wind structure at time of burst was favorable for fallout at the shelter. However, the yield of Kepler was less than anticipated; consequently fallout was negligible. No useful data were collected on this shot.

3.1.3 Shot Shasta

Shot Shasta was fired on a 500-ft tower 2 miles south of the shelter at 0500 on Aug. 18, 1957. The predicted wind structure was very favorable for fallout at the shelter. Five persons occupied the shelter at the time of burst. The event schedule followed is given in Appendix C. About 8 sec after the shot a very light double-peaked ground shock was felt; at

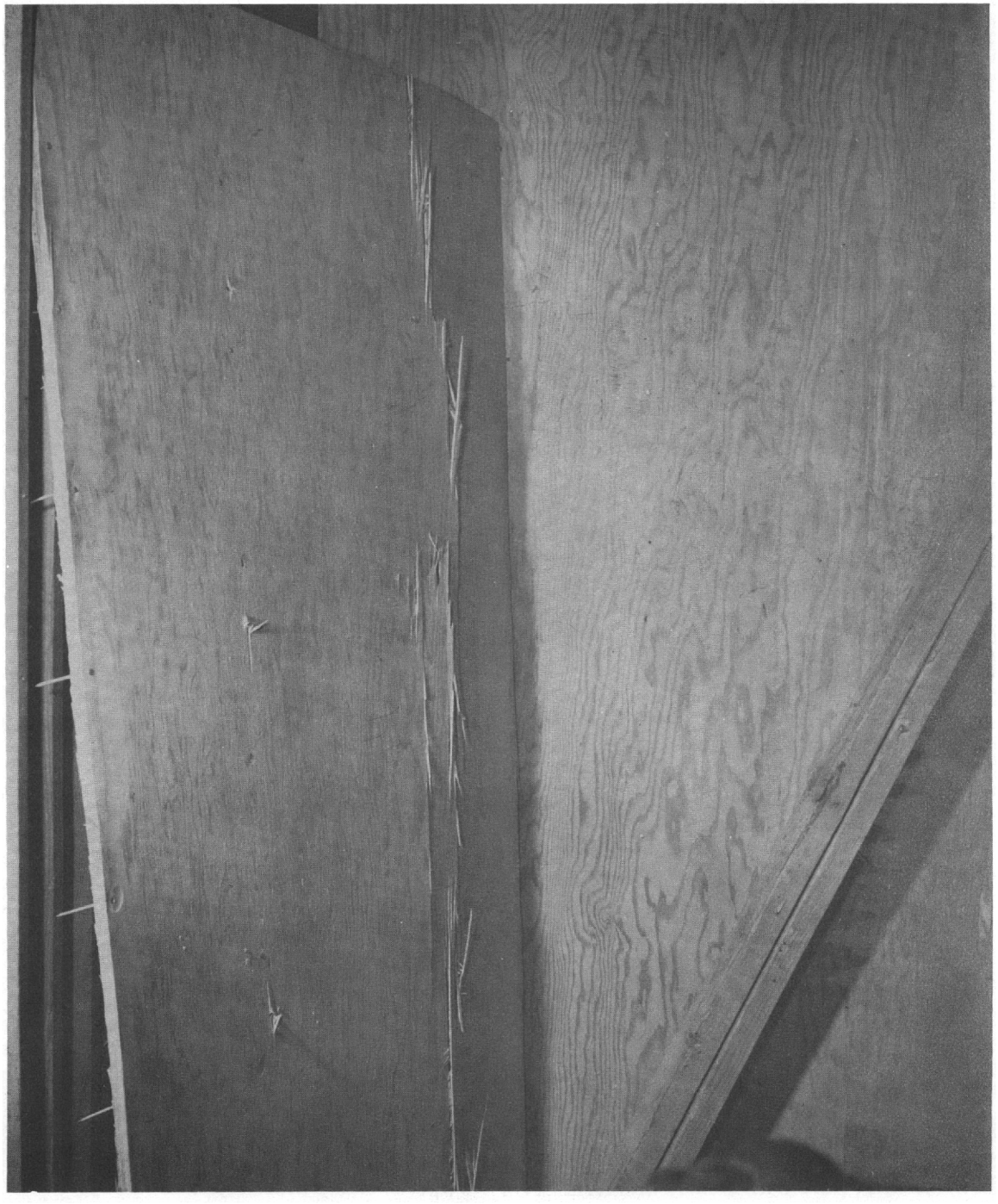

Fig. 3.1—Damage to wall between entrance tunnel and generator room after shot Diablo.

Fig. 3.2—Damage to jeep revetment and tarpaulins after shot Diablo.

about 10 sec the air blast wave arrived. The air blast wave was shorter than experienced on shot Diablo. No dust was raised in the shelter, and no damage was sustained by any of the outside equipment.

No initial radiation during the first minute after burst was detected on the portable radiacs; the Geiger-tube monitor under the center vent registered a pulse of radiation from 0.05 to 0.2 min with a peak at 0.12 min of 0.1 mr/hr. (Preshot background was 0.03 mr/hr.) Radiation from the rising cloud, as measured by this instrument, increased the radiation intensity under the center vent from about 0.07 mr/hr at 0.8 min to a peak of 1.1 mr/hr at 4 min. The intensity then decreased to 0.3 mr/hr at 9.7 min, after which time fallout started to arrive.

After fallout arrival the intensity outside rapidly increased to a peak of about 120 r/hr (GITR reading) at about 18 min. Intensity at 1 hr was 25 r/hr (GITR reading). These intensities were near those anticipated based on the data from shot Diablo and the predictions of fallout from the H−½ hr wind data. No reclamation experiments were planned for shot Shasta.

3.2 OPERATIONAL MONITOR SYSTEM

3.2.1 Shot Diablo

Data obtained on the two dosimeter tubes during the first hour after burst are shown in Tables 3.1 and 3.2. Standard intensities shown in the final column were obtained by correcting measured intensities to 1 hr by the decay curve in Fig. 2.6. These data are plotted in Fig. 3.3, along with the intensity-time record obtained by the GITR. Dosimeter-tube data are in good agreement with GITR data, except for the absolute measurements of intensity. It was determined that the threefold increase in the dosimeter-tube data was due to the collection of fallout in the cups attached to the top of the dosimeter tubes to receive film badges after the initial gamma radiation had been received. These cups were cleaned out when the exterior measurements were made, about 5 hr after burst. Data were again taken and were found to be in good agreement with the exterior measurements made with calibrated AN/PDR-39(T1B) radiacs. These results are shown in Table 3.3; the GITR reading was lower than the other measurements.

Data obtained from dosimeter tubes were evaluated in the shelter during the period of measurement just as they would be in an operational shelter. Conclusions drawn were (1) fallout arrived at about H+7 min, (2) peak intensity occurred at about H+15 min, (3) fallout cessation occurred at about H+30 min, and (4) the predicted standard intensity was about 55 to 80 r/hr.

3.2.2 Shot Shasta

The dosimeter tubes were not operated during fallout arrival owing to the lack of operators. Data taken at later times are given in Table 3.4; the GITR readings are included for comparison. The dosimeter-tube data are consistently higher than the GITR readings. The film-badge cups used on shot Diablo had been replaced with wire-screen cups; thus the difference was similar to the data obtained on shot Diablo after the dosimeter cups had been cleaned out.

3.3 INGRESS OF AIRBORNE ACTIVITY

3.3.1 Shot Diablo

Data pertaining to the intake ventilation configuration were obtained from the four air-sampling units and from the particulate filters of one M6 collective protector. The filter samples were counted either with a calibrated well-crystal (NaI) gamma counter or a calibrated end-window crystal (NaI) gamma counter. The count rates were all converted to number of fissions in the samples from ratios based on the radiochemical analysis of the Mo^{99} content of some of the samples and their count rates. The data for the cyclic air sampler are given in Table 3.5. The sample from the exterior Porta-Vac, which sampled continuously from

TABLE 3.1—FORWARD DOSIMETER-TUBE DATA, SHOT DIABLO

Time after burst, min			Exposure period, min	Dosimeter reading, r	Measured intensity, r/hr	Standard intensity, r/hr
Up	Down	Mean				
3	7	5	4	0.04	0.6	0.072
8	10	9	2	0.160+	4.8+	0.072+*
14	15	14.5	1	3.0	180	42.0
18	19	18.5	1	3.0	180	53.0
20	21	20.5	1	3.0	180	58.5
27	28	27.5	1	3.0	180	77.1
29	30	29.5	1	3.0	180	83.2
31	32	31.5	1	2.5	150	73.8
33	34	33.5	1	2.0	120	63.4
35	36	35.5	1	2.0	120	66.5
37	38	37.5	1	1.8	108	63.8
39	40	39.5	1	1.6	96	60.0
41	42	41.5	1	1.4	84	55.0
43	44	43.5	1	1.2	72	49.7
45	46	45.5	1	0.4	24	17.0 } (?)
47	50	48.5	3	4.4	88	68.5 }
51	54	52.5	3	2.4	48	41.0
55	58	56.5	3	2.2	44	41.0
59	62	60.5	3	2.4	48	48
63	65	64	2	1.2	36	39

*Off scale.

TABLE 3.2—AFTER DOSIMETER-TUBE DATA, SHOT DIABLO

Time after burst, min			Exposure period, min	Dosimeter reading, r	Measured intensity, r/hr	Standard intensity, r/hr at 1 hr
Up	Down	Mean				
6	9	7.5	3	0.20+	4+*	0.51+*
15	16	15.5	1	3.0	180	44.5
17	18	17.5	1	2.8	168	46.6
19	20	19.5	1	2.2	132	40.5
23	24	23.5	1	2.2	132	48.8
25	26	25.5	1	2.2	132	52.8
27	28	27.5	1	2.0	120	51.5
29	30	29.5	1	2.0	120	55.5
31	32	31.5	1	1.8	108	53.2
33	34	33.5	1	1.6	96	50.8
35	36	35.5	1	1.5	90	50
37	38	37.5	1	1.3	78	46
39	40	39.5	1	1.3	78	48.5
41	42	41.5	1	1.3	78	50.8
43	44	43.5	1	1.2	72	49.7
45	46	45.5	1	1.1	66	48.2
47	48	47.5	1	1.0	60	45.8
49	50	49.5	1	0.9	54	43.0
51	52	51.5	1	0.9	54	45.0
53	54	53.5	1	0.7	42	37.0
55	56	55.5	1	0.8	48	43.6
57	58	57.5	1	0.6	36	34
59	60	59.5	1	0.7	42	42
61	62	61.5	1	0.5	30	31
63	64	67.5	1	0.7	42	45

*Off scale.

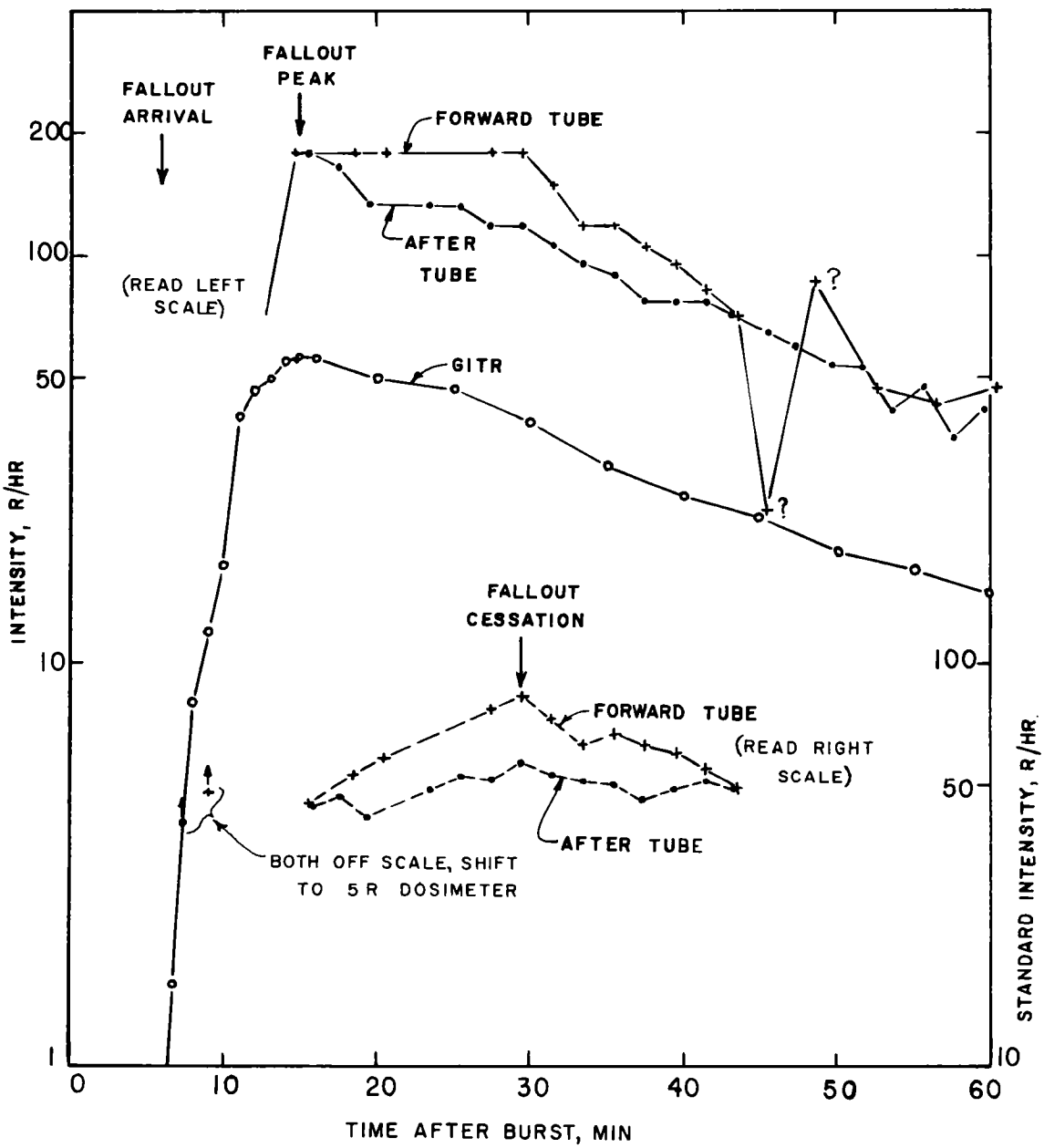

Fig. 3.3—Dosimeter-tube results, shot Diablo.

TABLE 3.3—COMPARISON OF INTENSITY READINGS 5 HR 30 MIN AFTER BURST, SHOT DIABLO

Instrument	Reading, r/hr
Foreward dosimeter tube	2.5
After dosimeter tube	2.1
AN/PDR-T1B at 3-ft height	2.2*
GITR	1.5

*See Table 3.23.

TABLE 3.4—AFTER DOSIMETER-TUBE DATA, SHOT SHASTA

Time after burst, hr	Exposure period, min	Dosimeter reading, r	Measured intensity, r/hr	GITR reading, r/hr
18.0	7	0.103	0.88	0.67
18.7	6	0.083	0.83	0.66
19.7	6	0.074	0.74	0.62
20.8	8	0.096	0.72	0.59
27.4	10	0.084	0.50	0.45
27.8	12	0.107	0.54	0.44

TABLE 3.5—CYCLIC AIR-SAMPLER DATA, SHOT DIABLO

Sample No.	Sampling period, min after burst	Activity, fissions $\times 10^{-10}$	Cumulative activity, fissions $\times 10^{-10}$
0*	0–9	0.0956	0.0956
1	9–11	0.366	0.461
2	11–13	2.338	2.799
3	13–15	1.583	4.382
4	15–17	0.994	5.376
5	17–19	0.822	6.198
6	19–21	0.946	7.144
7	21–23	0.860	8.004
8	23–25	0.269	8.273
9	25–27	0.152	8.425
10	27–29	0.0410	8.466
11	29–31	0.0151	8.481
12	31–33	0.0168	8.498
13	33–35	0.00993	8.507
14	35–37	0.00923	8.517
15	37–39	0.00535	8.522
16	39–41	0.00983	8.532
17	41–43	0.312	8.844
18	43–45	0.0152	8.859
19	45–47	0.00503	8.864

*Sample in position at time of blast; sampler not operating.

9 to 47 min, contained 9.57×10^{10} fissions. The data for the cyclic air sampler are plotted in Fig. 3.4. Interior air-sampler data are given in Table 3.6 and are plotted in Fig. 3.5. Over the sampling period, 9 to 47 min, the two outside samplers collected nearly the same total amount of activity. The cyclic sampler, being exposed upwards, apparently did not collect a single large particle since the large particles contained much more than 10^{10} fissions and the largest observed activity was only 2×10^{10} fissions. At early times the shelter-door sampler collected at a rate as much as five times that of the M6 intake sampler; at later times, however, it was collecting at about one-half the rate of the M6 intake sampler. Although the M6 sampler was, in part, sampling against the pull of the M6 protective collector (300 cfm vs. 9 cfm), the data suggest that the lower sampling rate of the M6 sampler at early times was due to some fractional size separations by the hood cap on the M6 intake.

A few of the filter samples were examined with a wide-field stereomicroscope (45×). The observations are given in Table 3.7. The observations show that a few particles as large as 500 μ in diameter reached the shelter door but that most were less than about 20 μ, with sizes up to 120 μ present in detectable concentration.

3.3.2 Shot Shasta

Data pertaining to the intake ventilation configuration were obtained in a manner similar to that used for shot Diablo, except that only one M6 protective collector unit was operated to give a plenum-chamber air velocity of 15 ft/min. The generator-room door and wall remained intact during the event.

The data for the cyclic air sampler are given in Table 3.8. The sample from the exterior Porta-Vac, which sampled continuously from 18 to 71 min, contained 1.71×10^{12} fissions. The cyclic air-sampler data are plotted in Fig. 3.6. The interior air-sampler data are given in Table 3.9 and are plotted in Fig. 3.7. Over the sampling period, 18 to 71 min, the outside Porta-Vac sampler collected almost twice as much activity as the cyclic sampler collected. For shot Diablo the cyclic sampler apparently collected no large fallout particles (black spheres). The shelter-door sampler generally collected at a rate 1.5 to 2.0 times that of the M6 intake sampler over most of the sampling period. The decrease in aerosol concentration outside the shelter at 68 to 70 min (Fig. 3.6) was only partially manifested by the interior sampler data in the samples taken from 68 to 71 min.

Results of a microscope examination of a few of the filters are summarized in Table 3.10. The observations show, in general, that few particles as large as 300 μ in diameter were collected but that most were less than 15 μ, with sizes up to 80 μ present in detectable quantities.

3.3.3 Reduction of Air-sampler Data

The air-sampler data were reduced in order to estimate the concentration of activity in the shelter during the fallout period if no filters had been used. The limitations on generalization and extrapolation of the data to other shot conditions are discussed in Sec. 4.2.

It will be assumed in reducing the data that the M6 collective protector filter was an absolute fallout filter; therefore all particles that were drawn through the ventilation opening were collected on the filter. For the M6 collective protector this is a valid assumption; in each shot the back-up charcoal filter readings were background; therefore the relative amount passing through must have been less than $1/1000$, and hence the total collected on the main filter was within 0.1 per cent of the total in the entering air.

The total collected on the M6 filter will be assumed to arrive at a rate proportional to that observed for the M6 intake sampler. The factor of proportionality would be the ratio of the total collected by each over the same sampling period. The M6 intake sampler was not operated to collect at consecutive time intervals as was the cyclic air sampler; therefore the rate curves given by Figs. 3.5 and 3.7 were integrated to obtain an estimate of the total activity that would have been collected up to a given time of continuous collection. The additional complications were that (1) the M6 collective protector was used as a source of ventilation air up to D+2 on shot Diablo and D+1 on shot Shasta before the filters were removed and (2) the interior air samples up to 71 min for shot Shasta did not cover the complete fallout period. The data for Diablo show rates of collection after fallout ceased (29 min)

(Text continues on page 53.)

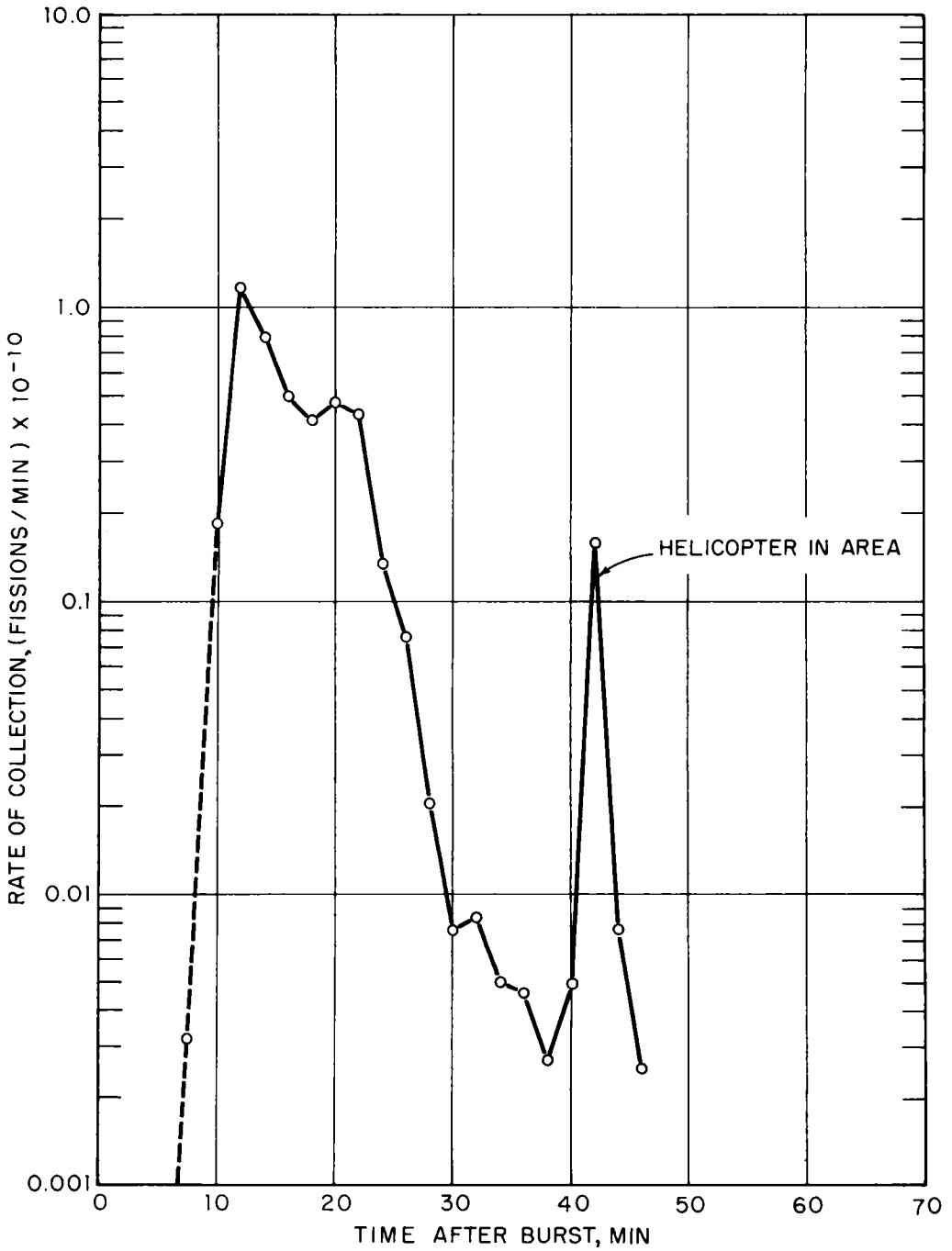

Fig. 3.4—Average (2-min) rate of collection by cyclic air sampler outside shelter, shot Diablo.

TABLE 3.6—INTERIOR AIR-SAMPLER DATA, SHOT DIABLO

Shelter-door sampler			M6 intake sampler		
Sample No.	Sampling period, min after burst	Activity, fissions $\times 10^{-10}$	Sample No.	Sampling period, min after burst	Activity, fissions $\times 10^{-10}$
1	7–9	0.104	1	7–9	0.0256
2	10–12	2.79	2	10–12	0.549
3	13–15	3.94	3	13–15	1.09
4	16–18	2.18	4	16–18	0.581
5	19–21	2.19	5	19–21	0.481
6	22–24	1.87	6	22–24	0.373
7	25–27	0.310	7	25–27	0.107
8	28–30	0.000542	8	28–30	0.0563
9	31–33	0.00976	9	31–33	0.158
10	34–36	0.00894	10	34–36	0.0162
11	37–39	0.00778	11	37–39	0.0244
12	40–42	0.00850	12	40–42	0.0133
13	43–45	0.254	13	43–45	0.102
14	46–48	0.00708	14	46–48	0.0189
15	49–51	0.0137	15	49–51	0.0140
16	52–54	0.00739	16	52–54	0.0121
17	55–57	0.00634	17	55–57	0.00849
18	58–60	0.00588	18	58–60	0.00512
19	61–63	0.00315	19	61–63	0.00705
20	64–66	0.00393	20	64–66	0.00789
21	67–72	0.00708	21	67–72	0.0127
22*			22	73–78	0.0116
23	79–94	0.00772	23	79–109	0.0474
24	95–105	0.118	24	~240–~260	0.0534

*Missing.

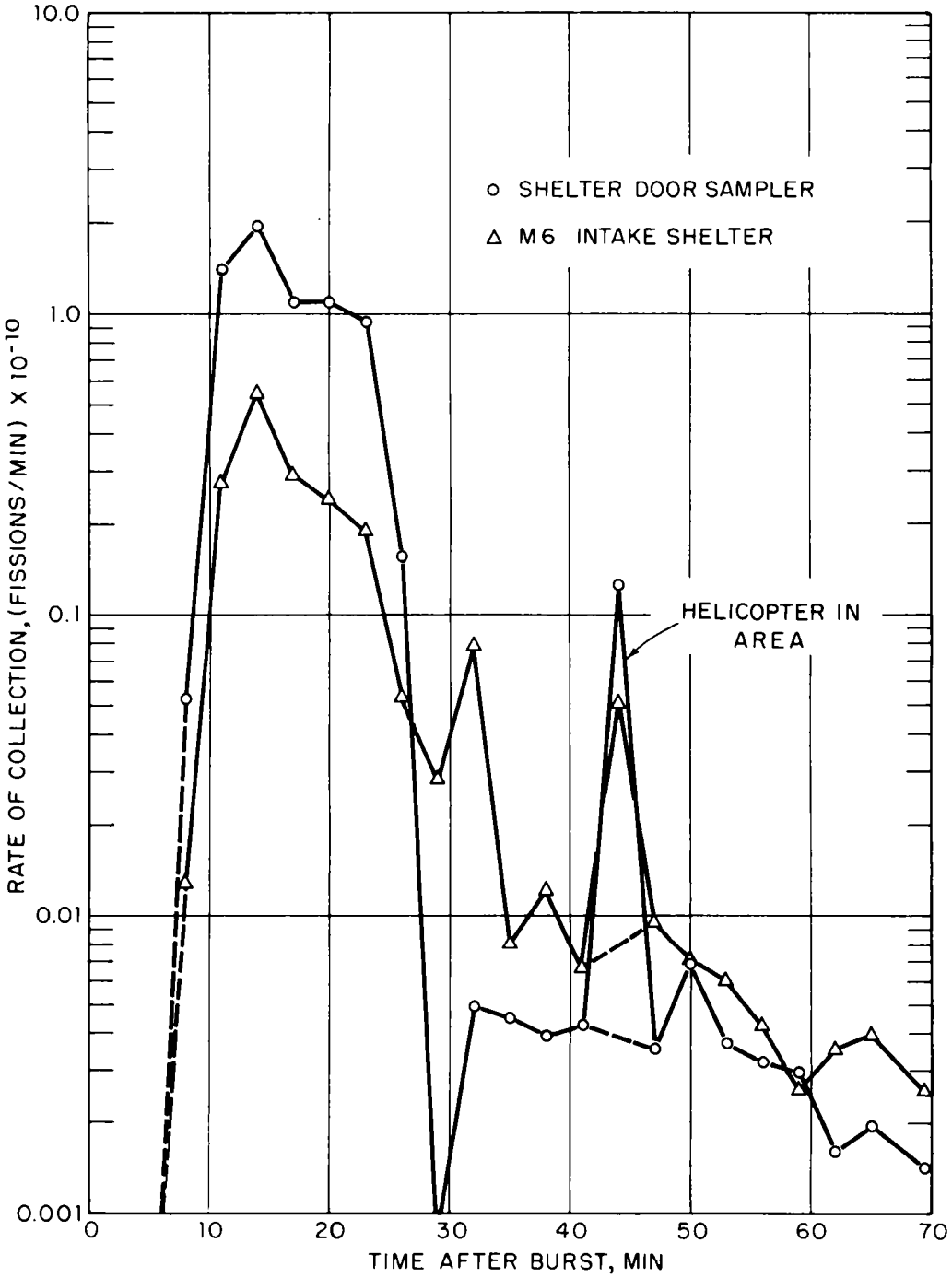

Fig. 3.5—Average (2-min) rate of collection by interior Porta-Vac samplers, shot Diablo.

TABLE 3.7 — MICROSCOPE EXAMINATION OF FILTER SAMPLES FROM SHELTER-DOOR SAMPLER, SHOT DIABLO

Sample No.	Observations
4	A few surface grains and black filaments up to 500 μ. A fairly dense concentration of black irregular particles 10 to 20 μ in size and spheres from 10 to 120 μ in size. Also yellow irregular particles up to 120 μ. Approximate number of spheres per field of view:
	Diameter, μ — Concentration, No./field: 10 — 1; 15 — 1; 20 — 2; 30 — 4; 40 — 1; 50 — 1; 60 — 1; 85 — 1; 100 — 1; 120 — 1
5	Similar to No. 4. General dispersion of material less than 15 μ. Yellow filaments and irregular particles up to about 120 μ.
6	Similar to No. 4. Slightly lower concentration of fines and fewer larger spheres. Number of spheres per field of view:
	Diameter, μ — Concentration, No./field: 10 — 1; 18 — 1; 20 — 2; 30 — 2; 40 — 2; 50 — 1
20	Imbedded yellow and black irregular particles of about 10 μ in size. Many yellow irregular particles up to 70 μ and a few up to 150 μ and occasionally up to 500 μ. No spheres present.

TABLE 3.8 — CYCLIC AIR-SAMPLER DATA, SHOT SHASTA

Sample No.	Sampling period, min after burst	Activity, fissions × 10^{-10}	Cumulative activity, fissions × 10^{-10}
0*	0–18	0.0876	0.0876
1	18–20	5.02	5.11
2	20–22	3.27	8.38
3	22–24	3.22	11.60
4	24–26	3.26	14.86
5	26–28	4.06	18.92
6	28–30	3.91	22.83
7	30–32	3.95	26.78
8	32–34	4.52	31.30
9	34–36	3.72	35.02
10	36–38	5.07	40.09
11	38–40	6.60	46.69
12	40–42	5.72	52.41
13	42–44	4.65	57.06
14	44–46	4.60	61.66
15	46–48	5.13	66.79
16	48–50	4.82	71.61
17	50–52	4.07	75.68
18	52–54	3.39	79.07
19	54–56	2.78	81.85
20	56–58	2.88	84.73
21	58–60	2.16	86.89
22	60–62	1.64	88.53
23	62–64	2.05	90.58
24	64–66	1.64	92.22
25	66–68	1.53	93.75
26	68–70	0.0848	93.84
27	70–71	0.0418	93.88

*Exposed from zero time.

TABLE 3.9 — INTERIOR AIR-SAMPLER DATA, SHOT SHASTA

Shelter-door sampler			M6 intake sampler		
Sample No.	Sampling period, min after burst	Activity, fissions × 10^{-10}	Sample No.	Sampling period, min after burst	Activity, fissions × 10^{-10}
1	11.8–13.8	0.000303	1	11.8 –13.8	0.0304
2	14.5–17.5	0.00352	2	14.5 –17.5	0.000787
3	18.5–21.5	7.02	3	18.5– 21.5	3.68
4	22.7–25.7	3.43	4	22.7 –25.7	0.952
5	26.5–29.5	7.87	5	26.5 –29.5	4.39
6	30.5–33.5	6.91	6	30.5 –33.5	3.67
7	34.5–37.5	9.05	7	34.5 –37.5	5.73
8	38.5–41.5	12.1	8	38.5 –41.5	7.53
9	42.5–45.5	11.1	9	42.5 –45.5	6.80
10	46.5–49.5	13.4	10	46.5 –49.5	8.09
11	51.5–54.5	8.32	11	51.5– 54.5	5.23
12	55.5–58.5	4.94	12	55.5 –58.5	3.37
13	59.5–62.5	4.21	13	59.5 –62.5	2.80
14	63.5–66.5	3.65	14	63.5 –66.5	2.45
15	68.0–71.0	2.16	15	68.0 –71.0	1.89

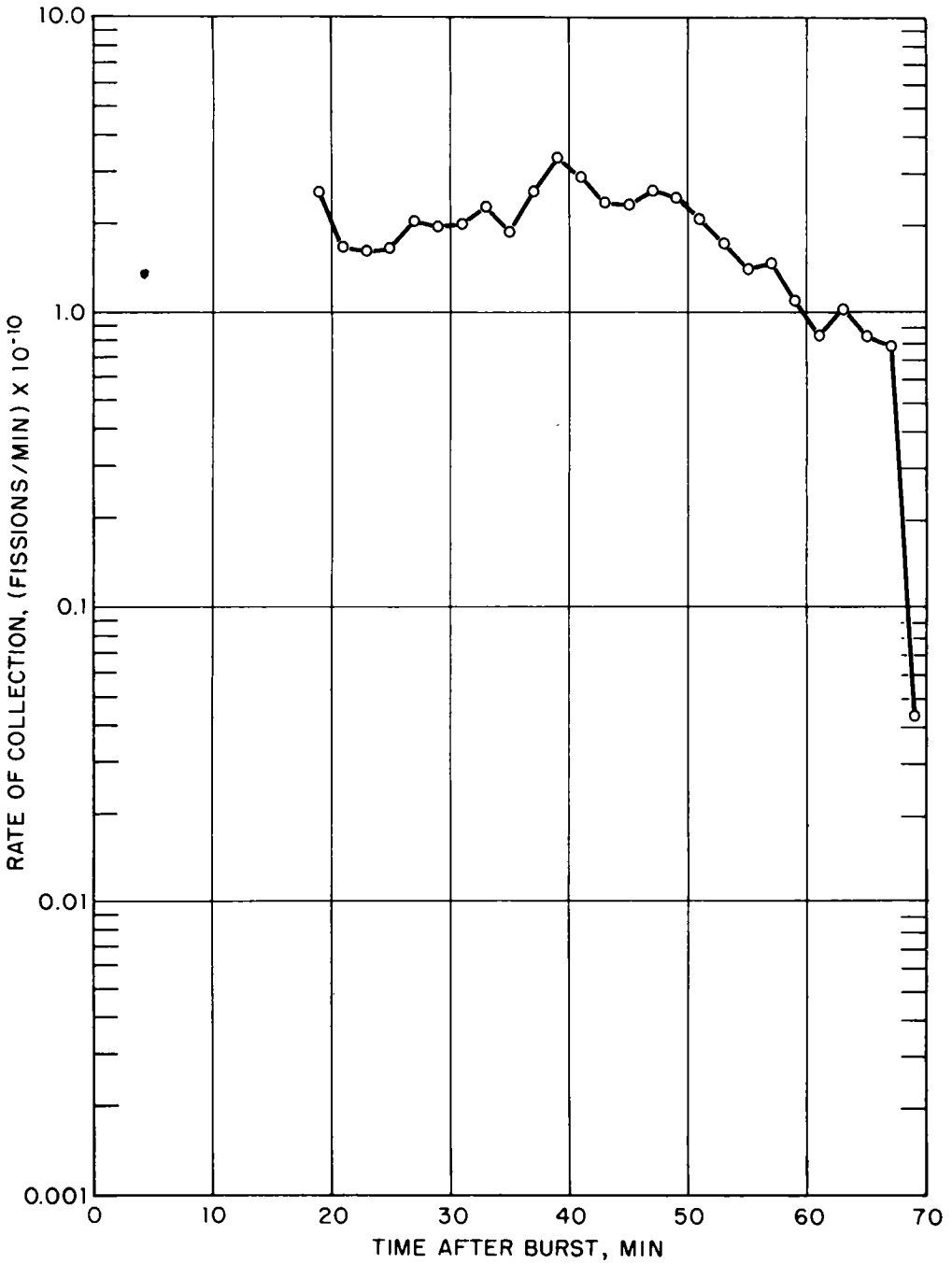

Fig. 3.6—Average (2-min) rate of collection by cyclic air sampler outside shelter, shot Shasta.

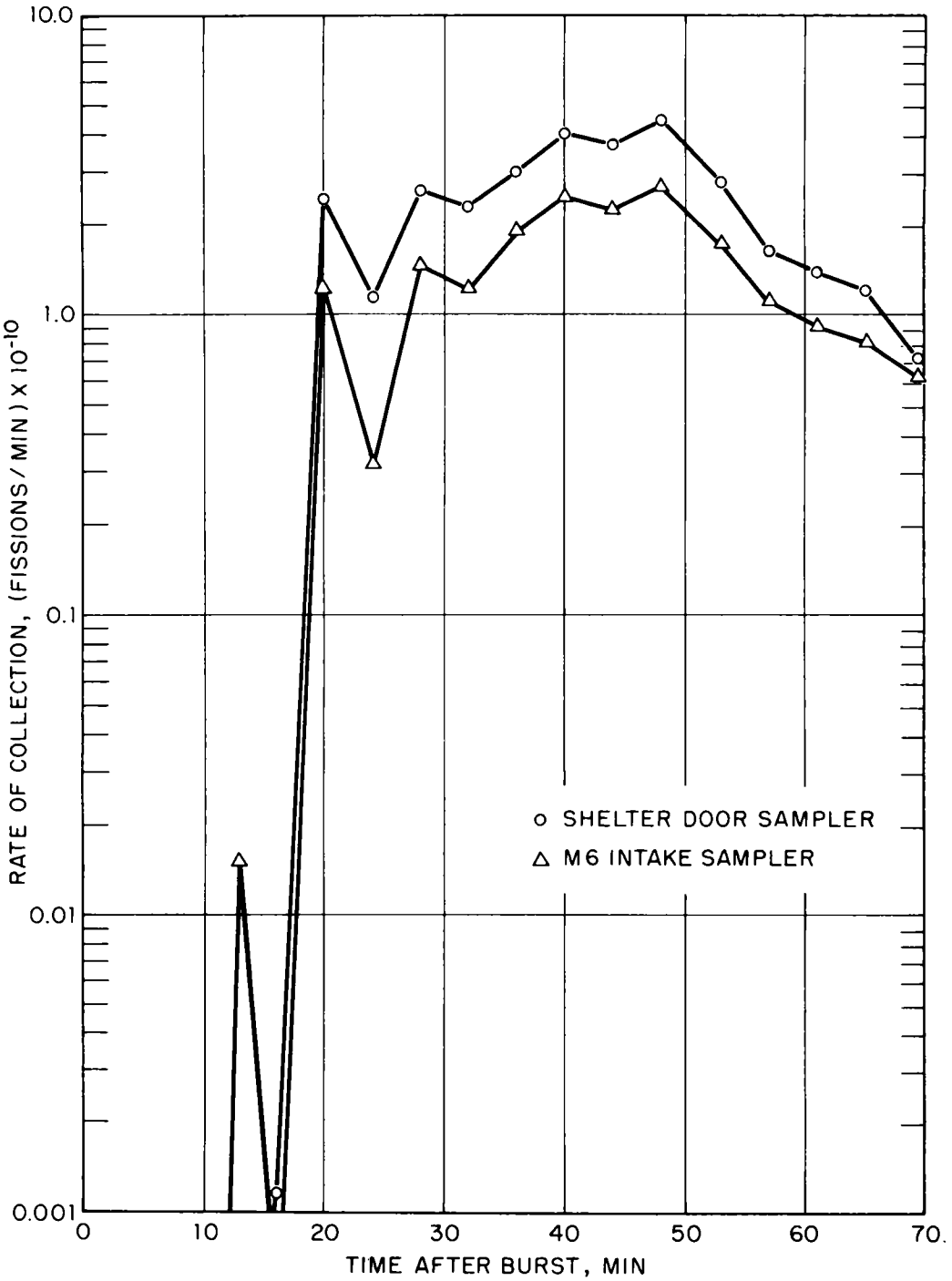

Fig. 3.7—Average (3-min) rate of collection by interior Porta-Vac samplers, shot Shasta.

TABLE 3.10 — MICROSCOPE EXAMINATION OF FILTER SAMPLES, SHOT SHASTA

Sample No.	Observations*
	Cyclic air sampler
1	Most prominent type particles observed were red, yellow, and black grains and some reddish filaments. A 2-in. red circle was visible on filter. Upper limit of grain sizes was about 80 μ; concentration was 10 to 20 per field.
11	Most prominent type particle was black and irregular, less than 15 μ in diameter; concentration was about 1 per field.
20	Most prominent type particle was black and irregular, less than 15 μ in diameter; concentration was less than 1 per field. A few yellow irregular particles up to 50 μ in size were present.
	Shelter-door sampler
3	Most prominent type particle was black and irregular, ranging in size from 5 to 30 μ; concentration was about 20 per field. Occasional black spheres and yellow grains up to a size of 50 μ were present.
8	Most prominent type particle was black and irregular, less than 15 μ in diameter; concentration was 2 to 5 per field.
13	Most prominent type particle was black and irregular, less than 15 μ in diameter; concentration was less than 1 per field.
	M6 intake sampler
3	Description, size, and number of particles for 1 sweep across filter (1.5 × 4.8 min):

Size, μ	No.	Description
7	1	Black sphere
5	2	Yellow-orange flake
15	1	Yellow-orange flake
30	1	Yellow-orange flake
150 × 200	1	Yellow-orange flake
5	1	Black irregular
7	2	Black irregular
10	3	Black irregular
15	3	Black irregular
20	1	Black irregular
30	2	Black irregular
60	2	Black irregular
75	1	Black irregular
135	1	Black irregular
15	1	Gray irregular
35	1	Gray irregular
120	1	Gray irregular
200	1	Gray irregular (black spots)
250	1	Gray irregular
12	1	Gray sphere
60	1	Yellow irregular
75	2	Yellow irregular
90	1	Yellow irregular
300	1	Orange irregular (dark gray scale)
75 × 225	1	Orange needle
120 × 750	1	Orange needle (glossy highlights)
150 × 400	1	Orange needle (glossy highlights)

TABLE 3.10 (Continued)

	Size, μ	No.	Description
	30 × 300	1	Metallic needle
	200	1	Sand particle with black and gray spheres attached
	Total	38	
	The most prominent type particle was black and irregular (16). The total of 38 is about 10 per field.		
8	Most prominent types of particles present were black: irregular in size range from 15 to 30 μ; concentration was less than 1 per field.		
13	Most prominent type particle present was black and irregular, mostly in size range from 15 to 45 μ; concentration was about 1 per field.		

*Standard binocular microscope with field diameter of 1.5 mm.

which decreased very rapidly; the integration of the low sampling rates added only negligible amounts to the total. Hence, the result of operating the M6 collective protector for the longer periods should result in only a small overestimate of the air concentrations at the early times. In reducing the data for shot Shasta, similarity between the two events will be used to estimate the amounts of activity after 71 min; again, the amounts cannot be large since the outside cyclic air sampler showed a large drop in air concentration at that time.

The integrated activity for the interior air samplers are plotted in Figs. 3.8 and 3.9 for shot Diablo and shot Shasta, respectively. The data are summarized in Table 3.11 along with other related data. The total fallout at the shelter on shot Shasta was 1.8 ($^{25}/_{14}$) times that for shot Diablo; however, the total collected by the M6 collective protector on shot Shasta was 4.4 times larger than on shot Diablo. On shot Diablo the integrated activity (to 47 min) for the shelter-door sampler was 1.9 times that collected by the outside Porta-Vac; whereas, that for the M6 intake collector was 0.49 of that collected outside. On shot Shasta the integrated activity (to 71 min) for the shelter-door sampler was 0.73 times that collected by the outside Porto-Vac; whereas, that for the M6 intake collector was 0.43 of that collected outside.

After fallout cessation for shot Diablo (29 min), the collecting rate (except for the period when the helicopter was present) of the interior samplers decreased approximately logarithmically with time. Since the air flow rate through the samplers for each sampling period was approximately constant (9 cfm), the collecting rate is proportional to the air concentration, or

$$C(\text{fissions/cu ft}) = \frac{\text{collecting rate, f(fissions/min)}}{\text{air intake flow rate, v(cu ft/min)}} \tag{3.1}$$

Thus, if

$$f = f_0 e^{-kt} \tag{3.2}$$

where f_0 is the collecting rate at about 29 min, then

$$C = (f_0/v)e^{-kt} \tag{3.3}$$

If C is assumed to be proportional to the number of particles per cubic centimeter (uniform specific activity), then for Stoke's law of fall for small spheres in air

$$k = 3.0 \times 10^5 (\rho/h)d^2 \tag{3.4}$$

where ρ = particle density
h = height for the concentration
C = sampling height
d = median weight diameter of the particles

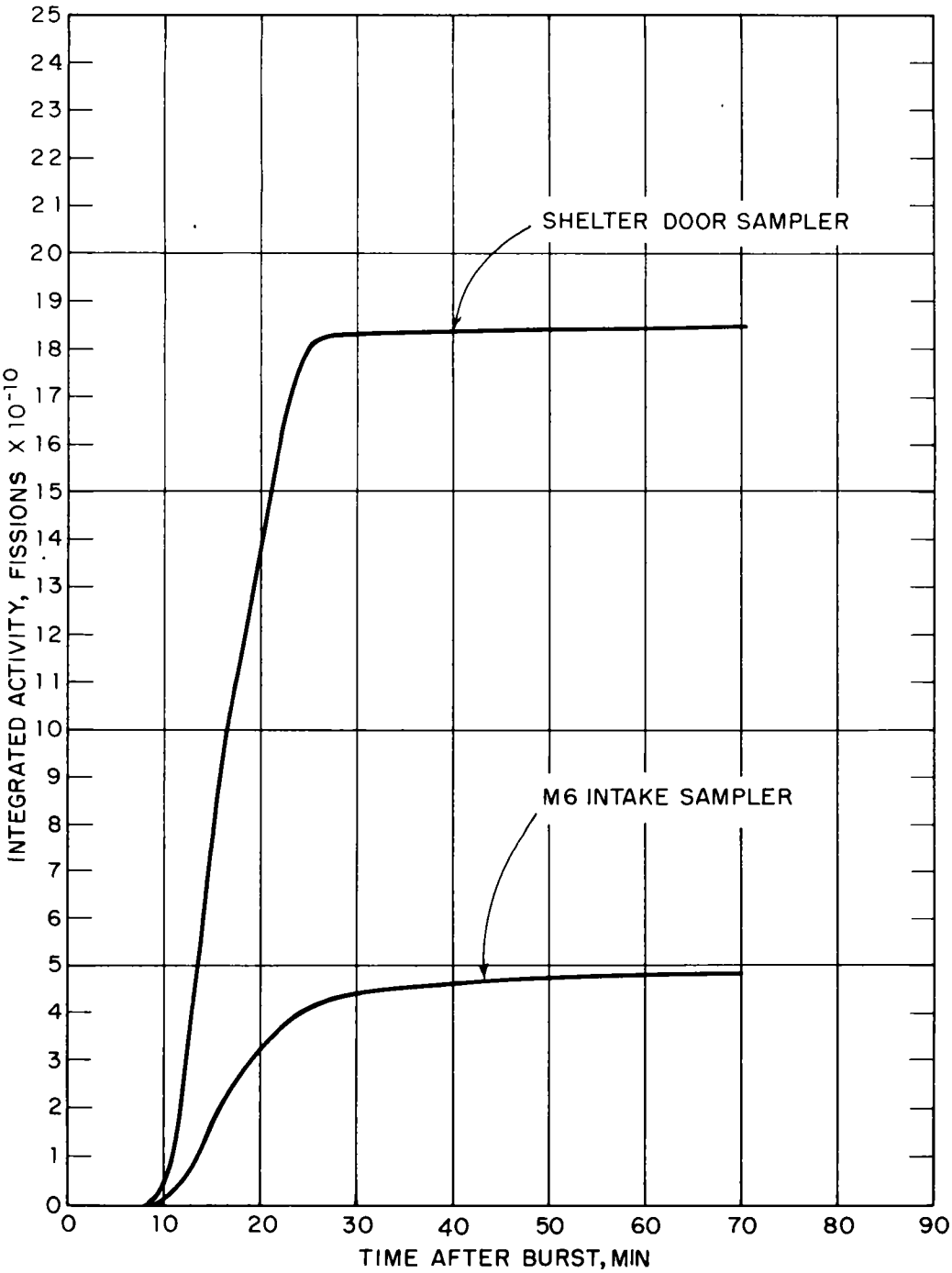

Fig. 3.8—Integrated activity for interior air samplers, shot Diablo.

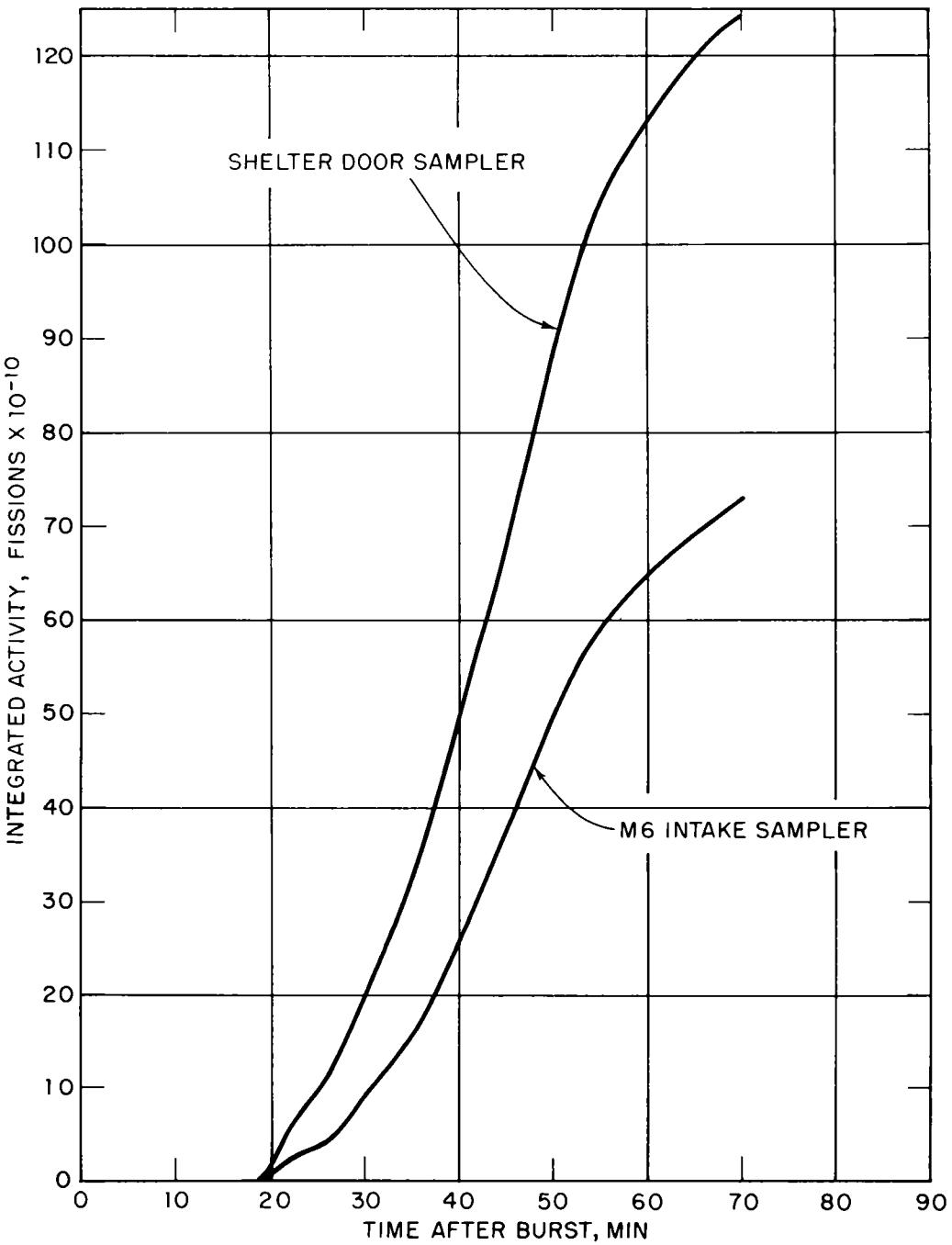

Fig. 3.9—Integrated activity for interior air samplers, shot Shasta.

TABLE 3.11—SUMMARY OF DATA RELATIVE TO AIR SAMPLING AT SHELTER FOR SHOTS DIABLO AND SHASTA

	Shot Diablo	Shot Shasta
Standard intensity*	19 r/hr	36 r/hr
Peak intensity	55 r/hr (GITR)	120 r/hr (GITR)
Outside Porta-Vac sampler (total)	9.57×10^{10} fissions†	1.71×10^{12} fissions‡
Cyclic air-sampler (total)	8.86×10^{10} fissions†	9.39×10^{11} fissions‡
Shelter-door sampler (total)	1.84×10^{11} fissions†,§ 1.85×10^{11} fissions‡,§	1.25×10^{12} fissions‡
M6 intake sampler (total)	4.65×10^{10} fissions†,§ 4.76×10^{10} fissions‡,§	7.35×10^{11} fissions‡
M6 collective protector	8.57×10^{12} fissions	3.76×10^{13} fissions

* Equivalent to AN/PDR-39(T1B) reading at 3 ft.

† To 47 min.

‡ To 71 min.

§ Neglects rise due to helicopter at 41 to 47 min. Sums including helicopter are: shelter-door sampler, 1.86×10^{11} (47 min) and 1.87×10^{11} (71 min); M6 intake sampler, 4.73×10^{10} (47 min) and 4.84×10^{10} (71 min).

TABLE 3.12—COMPUTED CONCENTRATION OF ACTIVITY IN AIR ENTERING SHELTER, SHOT DIABLO

Time after burst, min	Activity calculated for 10^4 fissions,* dis/sec	Adjusted activity, μc/fission	Activity in entering air, fissions/cu ft	Activity in entering air, μc/cu ft
8	8.1	1.1×10^{-8}	7.6×10^{7}	0.85
11	6.1	8.2×10^{-9}	1.6×10^{9}	14
14	5.0	6.5×10^{-9}	3.2×10^{9}	21
17	4.3	5.4×10^{-9}	1.7×10^{9}	9.4
20	3.8	4.7×10^{-9}	1.4×10^{9}	6.6
23	3.4	4.1×10^{-9}	1.1×10^{9}	4.6
26	3.0	3.6×10^{-9}	3.2×10^{8}	1.1
29	2.7	3.2×10^{-9}	1.7×10^{8}	0.53
32	2.5	2.8×10^{-9}	4.7×10^{8}	1.3
35	2.3	2.5×10^{-9}	4.8×10^{7}	0.12
38	2.1	2.3×10^{-9}	7.2×10^{7}	0.16
41	1.9	2.0×10^{-9}	3.9×10^{7}	0.081
44	1.8	1.9×10^{-9}	4.8×10^{7}	0.088
47	1.7	1.7×10^{-9}	5.6×10^{7}	0.095
50	1.6	1.6×10^{-9}	4.2×10^{7}	0.064
53	1.5	1.4×10^{-9}	3.6×10^{7}	0.051
56	1.4	1.3×10^{-9}	2.5×10^{7}	0.033
59	1.3	1.2×10^{-9}	1.5×10^{7}	0.018
62	1.3	1.1×10^{-9}	2.1×10^{7}	0.023
65	1.2	1.0×10^{-9}	2.3×10^{7}	0.025
69.5	1.1	9.4×10^{-10}	1.5×10^{7}	0.014

* Unfractionated radioactive nuclides.

The average sampling rate after fallout cessation (neglecting rise due to helicopter) is given in Fig. 3.10. The slope, 0.043 min^{-1} or 7.2×10^{-4} sec^{-1}; density 2.5 gm/cm^3; and sampling height, 5.5 ft (170 cm), give a median weight diameter, d, of 4 μ. This is in reasonable agreement with the microscope observations. The total collection for this kind of settling of the aerosol for a long time would be f_0/k, in which f_0 is the rate at time of cessation (t = 0 in Eq. 3.4). Using 3 μ (from 0.75×4 based on a size ratio of 15:20 from microscope data) as the median weight diameter for the Shasta particles at time of cessation, the value of k is 0.024 min^{-1}. The value of f_0 and the time of cessation were determined as follows.

Similarity in the plots given in Figs. 3.5 and 3.7 for the collecting rates suggest coordinate transformations in the sampling rate such as

$$f' = af \tag{3.5}$$

in which f is the sampling rate for shot Diablo and f′ for shot Shasta at times corresponding to

$$t' - t'_a = b(t - t_a) \tag{3.6}$$

in which t_a is 6.0 min (for shot Diablo) and t'_a is 16.5 min (for shot Shasta). If F′ and F are the integrated values of f′ and f, respectively, then

$$F' = abF \tag{3.7}$$

It may be noted in Figs. 3.5 and 3.7 that the shelter-door and M6 intake sampling rates are approaching each other at 26 and 69.5 min, respectively. Using each of these times as a first estimate of the same fraction of the fallout period for the two events, b in Eq. 3.6 is 2.65; and, using the average values of the collection rates, 0.105×10^{10} fissions/min for shot Diablo and 0.68×10^{10} fissions/min for Shasta, a is 6.5. The product ab is 17. At 26 min, the integrated activity, F, for shot Diablo is 4.18×10^{10} fissions; at 69.5 min, the integrated activity, F′, for shot Shasta is 72.6×10^{10} fissions. The ratio F′/F = ab is 17; thus the first estimates of a and b are satisfactory for estimating the remainder of the collection rate curve of the M6 intake sampler for shot Shasta from the Diablo data. The time of cessation for shot Shasta, from Eq. 3.6 is 77.5 min. Back extrapolating the M6 intake collector data in Fig. 3.5 according to Eq. 3.2 gives an f_0 value of 0.015×10^{10} fissions/min at 29 min; the corresponding value of f'_0 for shot Shasta is then 0.098×10^{10} fissions/min at 77.5 min.

The integrated activity to infinity for shot Diablo (equivalent to several hours sampling time) was estimated by adding the value of f_0/k to the integrated activity collected up to 29 min. The totals, omitting the amount due to the helicopter, are 18.68×10^{10} fissions for the shelter-door sampler and 4.75×10^{10} fissions for the M6 intake sampler. The totals, including the amount due to the helicopter, are 18.77×10^{10} fissions and 4.84×10^{10} fissions for the respective samplers; the latter values are the ones to be compared with the M6 protective collector filter. The factor for adjusting the sampling rate of the M6 intake sampler to that for the M6 collective protector as representative of the activity that would be entering the shelter if the filter had not been used is given by the ratio of the sum of the activity actually collected on the M6 collective protector filter and M6 intake sampler to 4.84×10^{10} fissions. The factor is $(8.57 + 0.04) \times 10^{12}/4.84 \times 10^{10}$, or 178.

For shot Shasta, the integrated activity up to 78 min for the shelter door sampler is 126×10^{10} fissions, and for the M6 intake sampler it is 75.0×10^{10} fissions. The value of f'_0/k' is 4.08×10^{10} fissions; hence the integrated activities to infinity are 130×10^{10} fissions and 79.1×10^{10} fissions for the respective samplers. The factor for adjusting the sampling rate of the M6 intake sampler to that for the M6 collective protector is $(3.76 + 0.06) \times 10^{13}/7.91 \times 10^{10}$, or 48.3.

If the Porta-Vac samplers collected with an efficiency of 100 per cent at their rated capacity of 9 cfm, the air concentration given by Eq. 3.1 would be

$$C = 0.111f \tag{3.8}$$

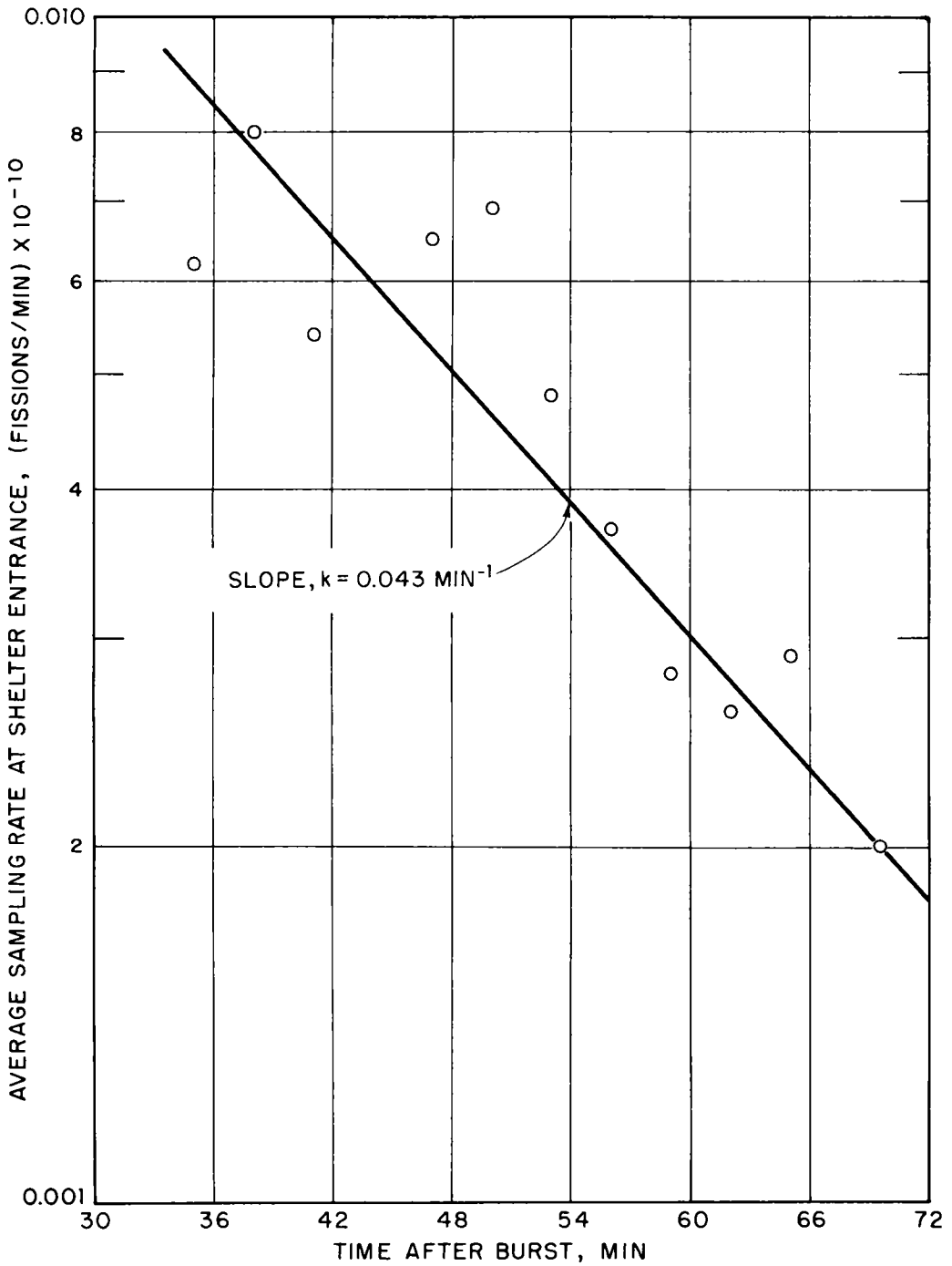

Fig. 3.10—Average sampling rate after fallout cessation, shot Diablo.

Using the multipliers given above and the rated capacity of 300 cfm for the M6 protective collector, the entering air concentration from the M6 intake sampler data is given by

$$C = 0.593f \tag{3.9}$$

for shot Diablo, and

$$C = 0.161f \tag{3.10}$$

for shot Shasta. Thus, in comparison with the M6 collective protector, the Porta-Vac sampler either was not sampling as efficiently or was not pulling in air at its rated capacity (or both). For the shelter-door sampler the f multipliers are 0.154 for shot Diablo and 0.0980 for shot Shasta; these latter values are reasonably near the expected values. For sampling in the range from 8 to 10 cfm, the variation in the multiplier would be from 0.125 to 0.100. The observed values depend on the actual sampling velocities (which, in turn, depend on back pressure, filter loading, and line voltage) and the distribution of activity on the particle sizes. If each particle contained the same amount of activity, then the number of fissions collected per unit time would be proportional to the number of particles per unit volume of air passing the filter. If the activity on the particles was proportional to the square or cube of the particle diameter (surface area or uniform specific activity), then the smaller particles would contain less activity per particle than the larger ones, and the samplers, collecting small particles more efficiently than large ones, would give low estimates of the number of particles per unit volume of air from data based on the activity collected. The large value of the multiplier for shot Diablo (0.593) in Eq. 3.9 suggests the presence of a larger range of particle sizes and also larger particles than for shot Shasta, which the Porta-Vac at 9 cfm could not remove from the intake tube going into the M6 protective collector at a rate of 300 cfm. Although the ratio of the cross-sectional area of the two intake tubes was about 3 to 1 (M6 Porta-Vac), the relative air intake velocity was still almost 4 to 1 in favor of the M6 collective protector.

In order to convert the activity concentrations from fissions to disintegrations per second or curies ($1C = 3.7 \times 10^{10}$ dis/sec), an estimate of the number of disintegrations per second per fission was made from the calculations of Bolles and Ballou[1] and the decay data given in Sec. 3.5. The comparison of the observed decay data with the calculated decay for the USNRDL 4π ionization chamber showed that the fission-product elements in the fallout were severely fractionated (Sec. 3.5). The ratio of the observed ionization rates on the 4π ion chamber to that calculated for unfractionated fission products is plotted in Fig. 3.11. The curve was extrapolated linearly to zero time. Since the observed ionization rate is lower than calculated, the actual disintegration rate must also be lower than calculated. The photon-to-disintegration ratio and the mean photon energy at early times cannot be changing very rapidly (owing to the large mixture of half lives, photon energies, and photon abundances present). Hence, the ratios given by the curve in Fig. 3.11 were used in adjusting downward the disintegrations per second values for the calculated decay of the fallout for both shot Diablo and shot Shasta. The calculations are given in the first two columns of Tables 3.12 and 3.13. The use of the curve in Fig. 3.11 in making the calculations further assumes that the fractionation in the small particles collected was the same as for the gross activity outside. The filter material and the small amounts collected made it impossible to make both radiochemical and decay measurements on the filter samples.

The activity in the entering air in fissions per cubic foot given in Tables 3.12 and 3.13 were obtained by application of Eqs. 3.9 and 3.10 to the data in Figs. 3.5 and 3.7, respectively. The values in microcuries per cubic foot were obtained by multiplying by the corresponding values of the adjusted activity values in microcuries per fission. In terms of the amount of fallout (fissions) entering, the peak air concentration for shot Diablo occurs at about 14 min; the activity in microcuries per cubic foot is also highest at this time. For shot Shasta the peak air concentration in amount of fallout entering occurs at about 48 min; whereas the highest amount of activity in microcuries per cubic foot occurs at 20 min. Although the fallout concentrations entering the shelter on shot Shasta were highest, the "radioactive" peak concentration was about the same as for shot Diablo. In estimating the con-

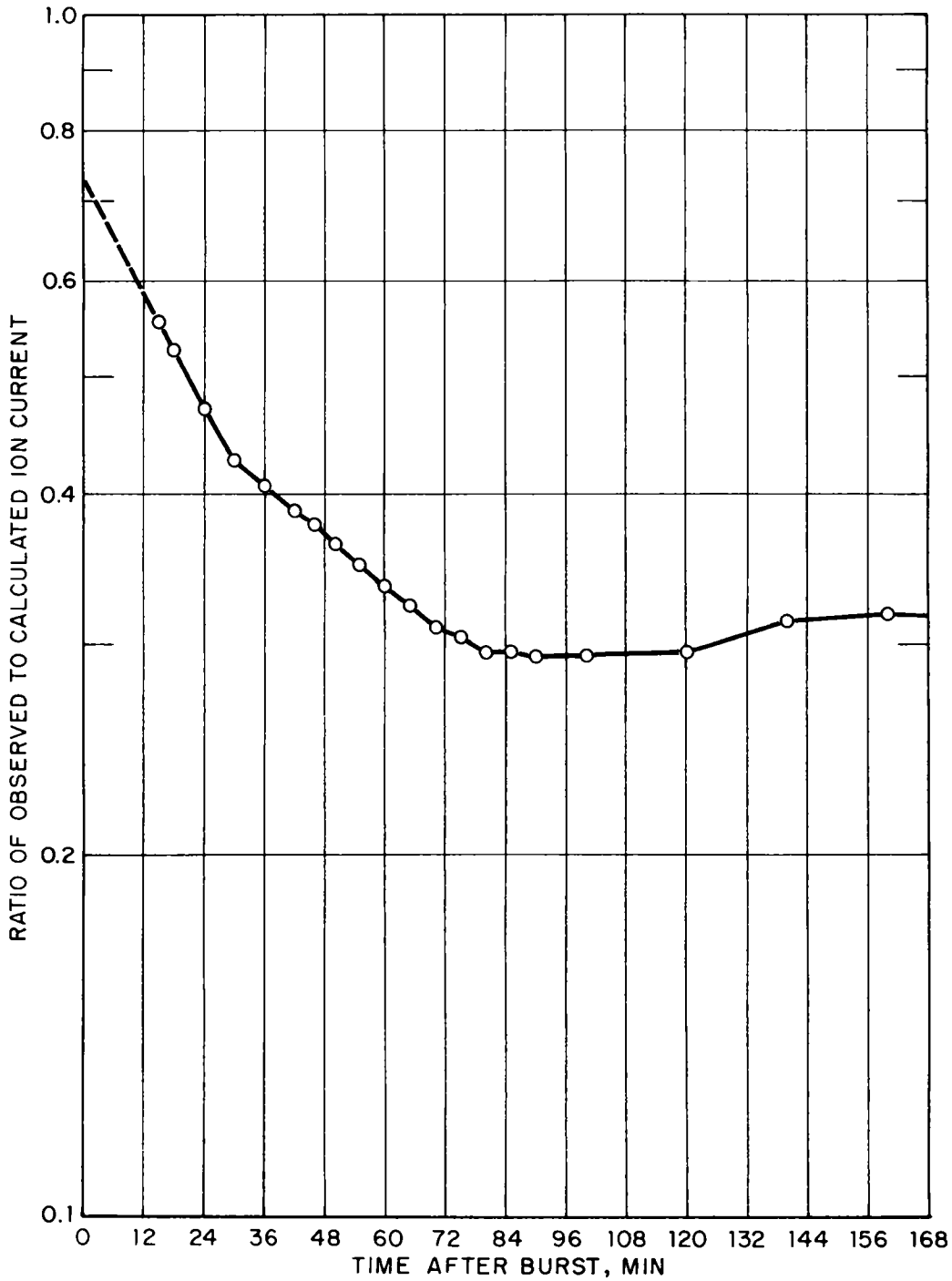

Fig. 3.11—Ratio of observed to computed ionization rate for USNRDL 4π ionization chamber, shot Shasta.

centration of activity in the shelter, it will be assumed that complete mixing of the incoming air (and aerosol) with the shelter air occurs in 1 min. Thus for the first minute of fallout 300 cu ft of contaminated air will enter and mix with the shelter air; also, 300 cu ft of clean air will leave the shelter. For the second minute, 300 cu ft more of contaminated air will enter and 300 cu ft of shelter air contaminated during the first minute will leave. For this method of computation the number of fissions remaining in the shelter volume at the end of the *nth* minute after the first minute of collection is given by

$$F_n = \Delta t K \sum_{i=1}^{i=n} f_i (1-a)^{n-i} \tag{3.11}$$

where i = the running index
f_i = the collecting rates for the M6 intake sampler as given in Figs. 3.5 and 3.7
a = a constant representing the dilution factor for the intake of 300 cu ft/min
Δt = 1 min
K = 178 for shot Diablo and 48.3 for shot Shasta

The shelter volume was 1.18×10^4 cu ft ($\frac{1}{2}\pi \times 12.5^2 \times 48$); thus a is 0.0254. The concentration, in fissions per cubic centimeter, at the end of the *nth* minute is given by

$$C_n = 2.99 \times 10^{-9} F_n \tag{3.12}$$

where 2.99×10^{-9} is the inverse of the shelter volume in cubic centimeters. The activity concentrations in fissions per cubic centimeter of air in the shelter, as obtained by use of Eqs. 3.11 and 3.12, are given in Fig. 3.12. For shot Diablo the peak aerosol concentration

TABLE 3.13—COMPUTED CONCENTRATION OF ACTIVITY IN AIR ENTERING SHELTER, SHOT SHASTA

Time after burst, min	Activity calculated for 10^4 fissions,* dis/sec	Adjusted activity, μc/fission	Activity in entering air, fissions/cu ft	Activity in entering air, μc/cu ft
12.8	5.4	7.0×10^{-9}	2.4×10^7	0.17
16	4.5	5.8×10^{-9}	8.0×10^5	0.0046
20	3.8	4.7×10^{-9}	2.0×10^9	9.4
24	3.2	3.9×10^{-9}	5.1×10^8	2.0
28	2.8	3.3×10^{-9}	2.3×10^9	7.7
32	2.5	2.8×10^{-9}	2.0×10^9	5.5
36	2.2	2.4×10^{-9}	3.1×10^9	7.6
40	2.0	2.1×10^{-9}	4.0×10^9	8.6
44	1.8	1.9×10^{-9}	3.6×10^9	6.8
48	1.7	1.7×10^{-9}	4.4×10^9	7.2
53	1.5	1.4×10^{-9}	2.8×10^9	4.0
57	1.4	1.3×10^{-9}	1.8×10^9	2.3
61	1.3	1.2×10^{-9}	1.5×10^9	1.7
65	1.2	1.0×10^{-9}	1.3×10^9	1.4
69.5	1.1	9.4×10^{-10}	1.0×10^9	0.94
75	1.0	8.2×10^{-10}	2.8×10^8	0.23
80	0.93	7.4×10^{-10}	1.5×10^8	0.11
90	0.80	6.3×10^{-10}	1.2×10^8	0.074
100	0.71	5.6×10^{-10}	9.2×10^7	0.052
120	0.56	4.5×10^{-10}	5.7×10^7	0.025
140	0.47	4.0×10^{-10}	3.5×10^7	0.014
160	0.40	3.5×10^{-10}	2.2×10^7	0.0076
180	0.35	3.0×10^{-10}	1.4×10^7	0.0040

*Unfractionated radioactive nuclides.

occurred at 25 min, when the concentration was 1.9×10^4 fissions/cm^3 (5.3×10^8 fissions/cu ft); the incoming air concentration was highest at 14 min, when the concentration was 3.2×10^9 fissions/cu ft (11 min delay time). For shot Shasta the peak occurred at 57 min, when the concentration was 6.3×10^4 fissions/cm^3 (1.8×10^9 fissions/cu ft), or about three times greater than for shot Diablo. The incoming air concentration was highest at 48 min, when the concentration was 4.4×10^9 fissions/cu ft (9 min delay time).

The activity concentrations in microcuries per cubic centimeter of air in the shelter are given in Fig. 3.13; they were obtained by multiplying the values in Fig. 3.12 by the adjusted decay-curve values in microcuries per fission as was done for the computations for the incoming air concentrations. Owing to decay, the peak concentrations in microcuries per cubic centimeter occur earlier than those in fissions per cubic centimeter. For shot Diablo the peak at 21 min is 7.5×10^{-5} μc/cm^3 (2.1 μc/cu ft); the incoming air concentration peak was 21 μc/cu ft at 14 min (7 min delay time). For shot Shasta the peak at 51 min is 8.9×10^{-5} μc/cm^3 (2.5 μc/cu ft); the incoming air concentration peak was 9.4 μc/cu ft at 20 min (31 min delay time). The peak concentrations in microcuries per cubic centimeter for the two shots are nearly equal. The computed dilution of the activity with relatively clean outside air after the fallout cessation indicates that it is a relatively slow process at 300 cu ft/min. At comparable times after burst the concentrations in the shelter after shot Shasta would have been about eight times higher than for shot Diablo. The computational method, which implied the assumption that only mixing with the shelter air occurs, undoubtedly gives higher concentration values. Many of the particles larger than a few microns would settle out, and smaller ones would adhere to the shelter walls and roof. However, no guide is available for estimating how much such occurrences would decrease the computed air concentrations.

The average air concentration in the shelter for the first 2 hr after fallout arrival (for drawing in 300 cu ft/min of air without filters) would have been about 1.8×10^{-5} μc/cm^3 (10 to 130 min) for shot Diablo and 3.6×10^{-5} μc/cm^3 (20 to 140 min) for shot Shasta. These values were obtained by integrating the curves in Fig. 3.13 and dividing by 120. If the integration were carried further, the averages would be decreased.

No estimates of the inhalation hazard associated with the estimated air concentrations in the shelter were made since no precise data on the size distributions, solubility, and radioactive composition were obtained for the material on the M6 protective collector material. Teresi and Newcombe[2] have estimated the maximum permissible concentrations (MPC) in water and air for small soluble particles (1 to 5 μ) containing mixed fission products (presumably in soluble form) for exposure periods starting as early as 3.5 hr after fission and for exposure periods as short as one day. The computations are based on a continuous exposure to the same aerosol concentration over the exposure period, taking into account radioactive decay. Actually, the cited calculations would be more applicable to fallout from a deep sea-water detonation than to fallout from a land burst.

For MPC calculations based on the concentration of certain fission products in critical organs for fallout from land bursts which is only very slightly soluble, information on the solubility of each fission product as a function of time is required. Thus the use of the calculations of Teresi and Newcombe to assess the degree of inhalation hazard that could have existed in the shelter will result in a high estimate of the hazard. However, in order to make the estimate of the MPC at exposures starting as early as 10 and 20 min after burst and for a 2-hr exposure, the data of Teresi were cross plotted and extrapolated as shown in Figs. 3.14 and 3.15. The curves show that for a given dose the air or water concentrations increase as the start of the exposure decreases and as the period of exposure decreases. Relative to the one-day exposure starting at 3.5 hr giving 150 rem in 30 days, starting the one-day exposure at 10 min would increase the MPC from 4.1×10^{-3} to about 7.5×10^{-2} μc/cm^3, which is a factor of 18. Similarly, decreasing the exposure period from one day to 2 hr (0.0833 day), would increase the MPC by a factor of 49 (0.2 μc/cm^3 divided by 4.1×10^{-3} μc/cm^3). The correction factors and estimated MPC's are summarized in Table 3.14. For shot Diablo the estimated shelter concentration was 7.8×10^{-5} of the estimated MPC for 15 rem in 90 days; for shot Shasta, the estimated shelter concentration was 3.0×10^{-4} of the estimated MPC for 15 rem in 90 days. Thus no inhalation hazard could have existed in the shelter for either shot for the conditions cited.

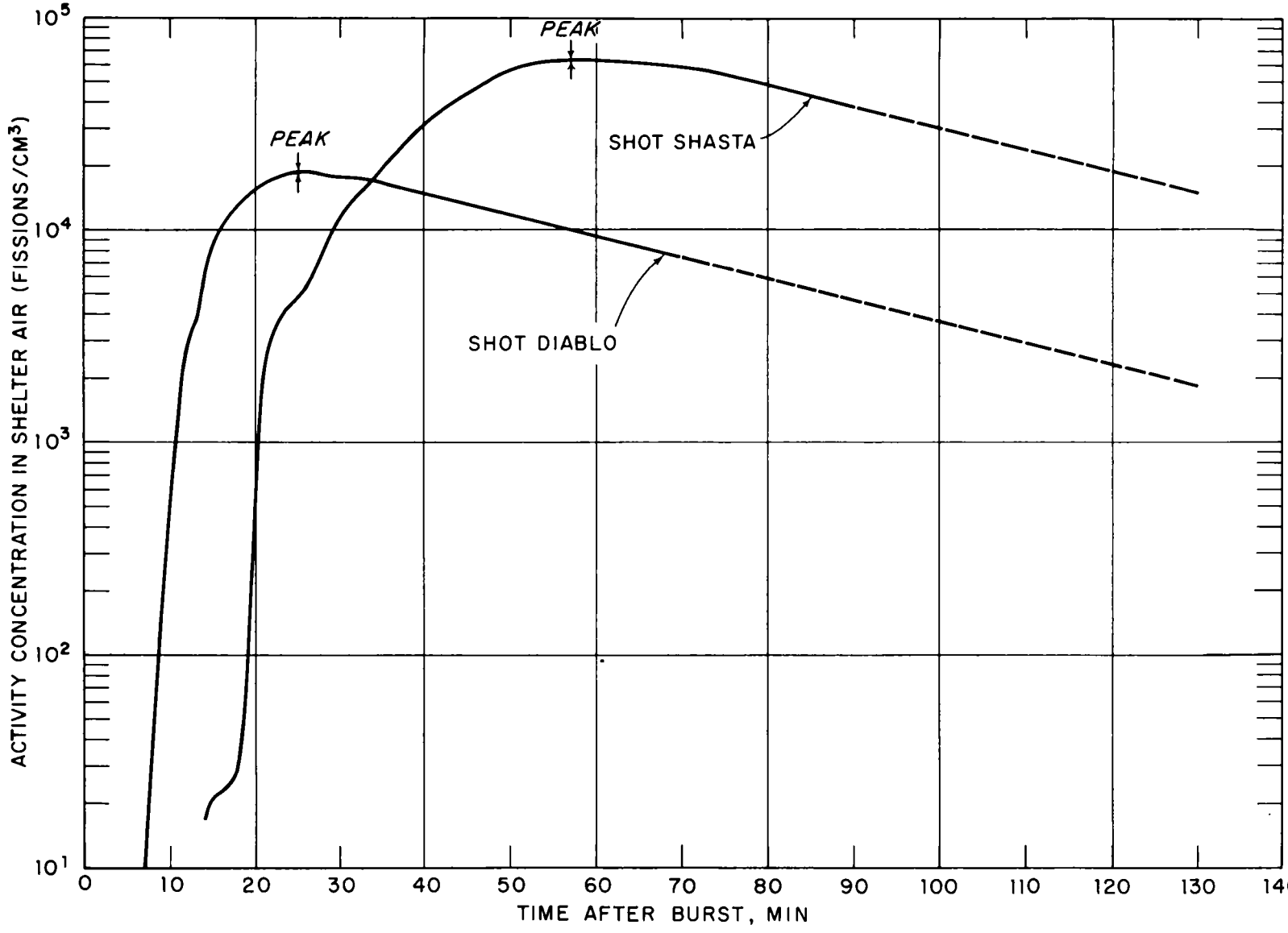

Fig. 3.12—Activity concentration (fissions/cm^3) in shelter air for intake rate of 300 cfm and no filter.

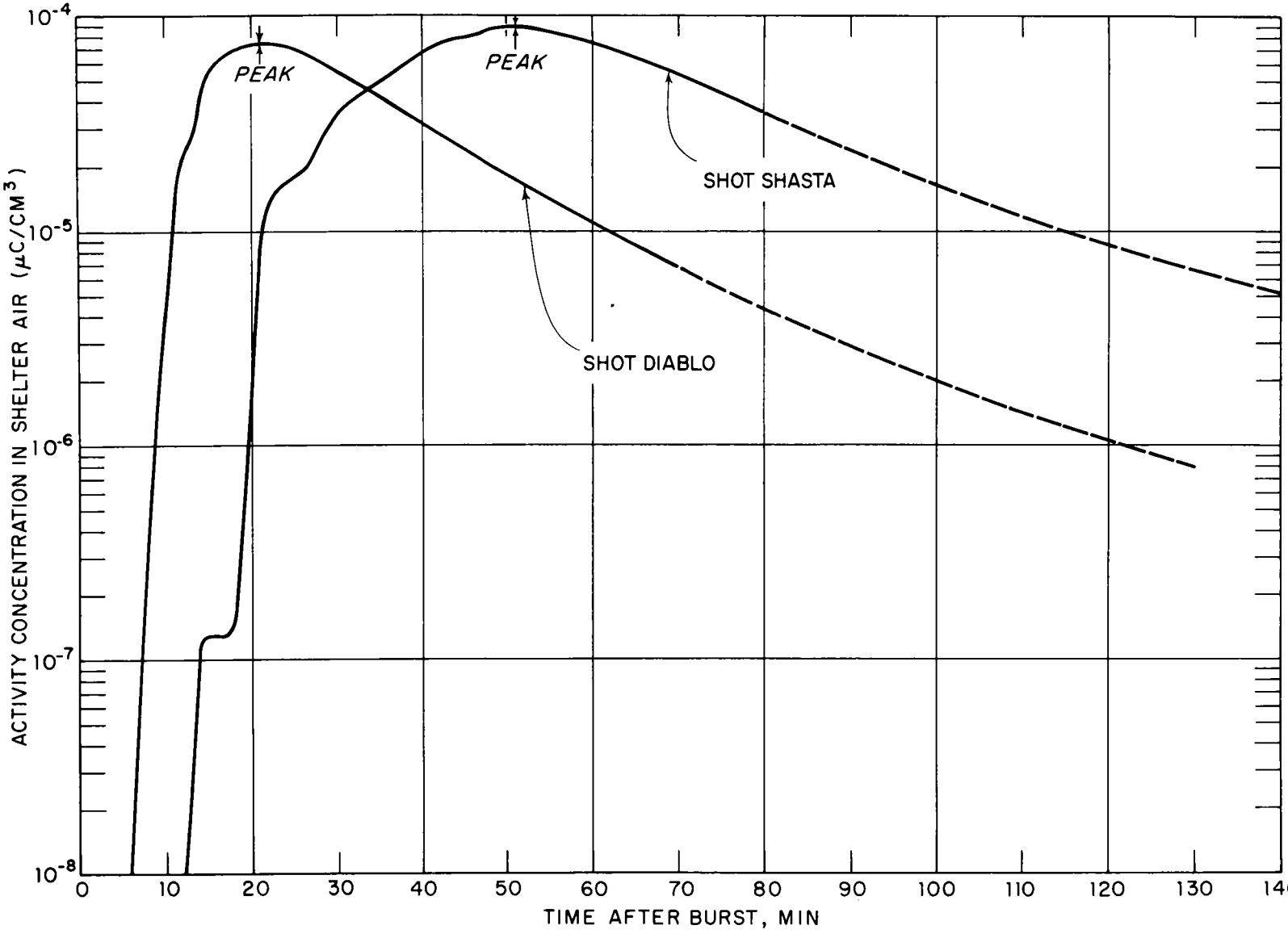

Fig. 3.13—Activity concentration (μc/cm³) in shelter air for intake rate of 300 cfm and no filter.

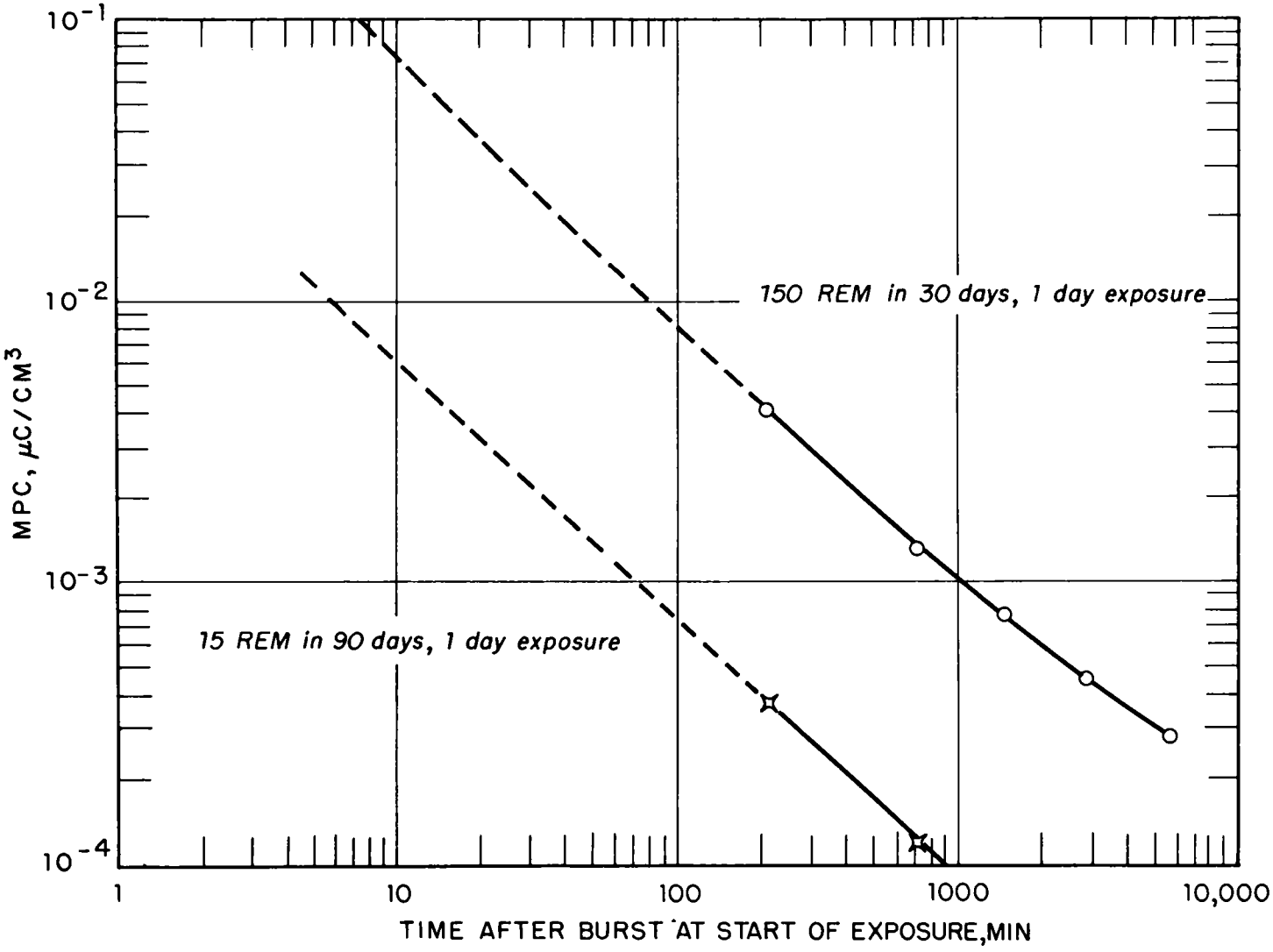

Fig. 3.14—Maximum permissible concentration in water and air for inhalation of small soluble particles of radioactive fallout (unfractionated).

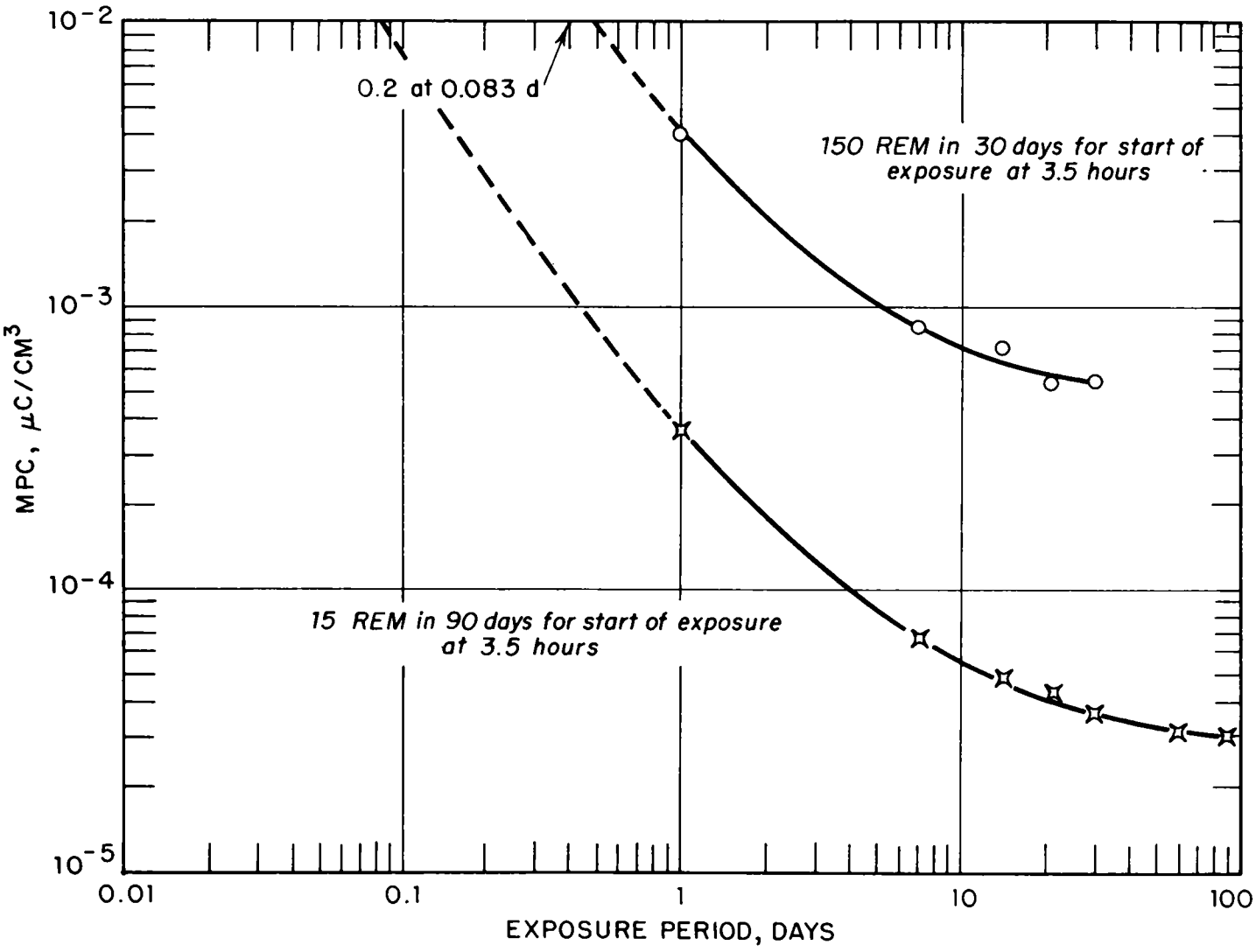

Fig. 3.15—Maximum permissible concentration in water and air for inhalation of small soluble particles of radioactive fallout (unfractionated).

If all conditions surrounding the two events were held constant (air intake flow rate, air intake configurations, particle sizes, etc.) except the amount of fallout that arrived, the estimated MPC for 15 rem in 90 days would have been experienced if the standard intensity increased to $19/7.8 \times 10^{-5}$, or 240,000 r/hr, at 1 hr for shot Diablo and $36/3.0 \times 10^{-4}$, or 120,000 r/hr, at 1 hr for shot Shasta. For reasons previously given, the calculated MPC's are overestimates of the inhalation hazard; therefore the estimates of the upper permissible limits of the standard intensities would be low. On the other hand, only a small fraction of the activity (less than 1 per cent) was carried by particles smaller than 50 to 100 μ at the shelter. For underground and surface detonations, more activity may be carried by the smaller particles, depending on the type of soil at the point of detonation and the down-wind distance from the shot point. Thus the simple estimates could be in considerable error for detonation conditions and ventilation configurations that differ greatly from those described in this report. A few of the important parameters that can influence the air concentrations in shelters are mentioned in Chap. 4.

TABLE 3.14—ESTIMATE OF MPC IN AIR FOR SMALL SOLUBLE PARTICLES OF RADIOACTIVE FALLOUT FOR EXPOSURE TIMES AT SHELTER FOR SHOTS DIABLO AND SHASTA

Item	Dose: 150 rem in 30 days	Dose: 15 rem in 90 days
Diablo		
MPC for 1-day exposure starting at 3.5 hr, $\mu c/cm^3$	4.1×10^{-3}	3.7×10^{-4}
Factor for exposure starting at 10 min	18	17
Factor for exposure period of 2 hr	49	37
MPC for 2-hr exposure starting at 10 min, $\mu c/cm^3$	3.6	0.23
MPC for 1 rem in stated time, $\mu c/cm^3$	2.4×10^{-2}	1.5×10^{-2}
Concentration in shelter (2-hr average), $\mu c/cm^3$	1.8×10^{-5}	1.8×10^{-5}
Fraction of estimated MPC	5.0×10^{-6}	7.8×10^{-5}
Shasta		
MPC for 1-day exposure starting at 3.5 hr, $\mu c/cm^3$	4.1×10^{-3}	3.7×10^{-4}
Factor for exposure starting at 20 min	9.1	8.8
Factor for exposure period of 2 hr	49	37
MPC for 2-hr exposure starting at 20 min, $\mu c/cm^3$	1.8	0.12
MPC for 1 rem in stated time, $\mu c/cm^3$	1.2×10^{-2}	8.0×10^{-3}
Concentration in shelter (2-hr average), $\mu c/cm^3$	3.6×10^{-5}	3.6×10^{-5}
Fraction of estimated MPC	2.0×10^{-5}	3.0×10^{-4}

In addition to the possibility of an inhalation hazard in the shelter, the possibility of dose due to gamma radiation from the aerosol in the air or on shelter surfaces exists. The more simple calculation is that for the dose rate at 3 ft above the surface of the shelter; the results should be within a factor of 2 of that for the activity uniformly mixed in the air. Hence for this calculation it is assumed that all the entering activity is deposited uniformly over the shelter floor. The floor area was 1200 sq ft (25 by 48 ft). For shot Diablo the described dispersion of the aerosol after fallout cessation would have given a surface contamination of $8.6 \times 10^{12}/1.2 \times 10^3$, or 7.2×10^9, fissions/sq ft. For shot Shasta the surface contamination would have been $3.8 \times 10^{13}/1.2 \times 10^3$, or 3.2×10^{10}, fissions/sq ft. For unfractionated activities from the shots, the ionization rate at 3 ft above an infinite smooth plane at 1 hr after burst[3] would be about 7.3×10^{-13} (r/hr)/(fission/sq ft). Multiplying this

value by 0.335, as taken from Fig. 3.11, gives 2.5×10^{-13} (r/hr at 1 hr)/(fission/sq ft). Thus for shot Diablo the equivalent 3-ft radiation rate for an infinite smooth plane would be 1.8×10^{-3} r/hr at 1 hr (1.8 mr/hr); for shot Shasta it would be 8.0×10^{-3} r/hr at 1 hr (8.0 mr/hr). For the 25- by 48-ft slab and for a mean photon energy of about 0.85 Mev, the ratio of the ionization rate at 3 ft above the center of the slab to that for the infinite plane[4] is about 0.5. Thus the two 1-hr ionization rates from the above given amounts of contamination on the shelter floor would be about 1 and 4 mr/hr at 1 hr, 3 ft above the center of the slab, for shot Diablo and shot Shasta, respectively. The ratios of these radiation rates to the standard intensities outside for the two shots are 0.000053 and 0.00011, respectively. The values of these ratios are about the same as those obtained for the shielding residual numbers for the shelter. Thus, if aerosol were increased by a factor of 2 (increasing unfiltered air intake rate from 300 to 600 cu ft/min) and the above assumptions held, the aerosol intake for shot Shasta conditions would have contributed more to the dose in the shelter than the radiation from the outside fallout.

If the activity were actually diluted and mixed with the shelter air without settling, as was assumed for the calculations plotted in Figs. 3.12 and 3.13, the dose rate near the center of a shelter floor can be estimated from

$$I = (1/2)\ 5.22 \times 10^{-2}\ \mu_A \bar{E}_d \times 3.7 \times 10^4 C \int_0^{l_0} e^{-\mu l}\, dl \qquad (3.13)$$

where μ_A = the Klein-Nishina absorption coefficient for air
$\bar{E}_d$ = average photon energy in Mev/disintegration
C = the air concentration in $\mu c/cm^3$
l_0 = the equivalent spherical radius for the shelter volume
I = dose rate in r/hr

Equation 3.13 neglects scattering since the build-up factor has been set equal to 1; this should result in less than a 50 per cent error in the computation. At the times of consideration, $\bar{E}_d$ is about 1.1 Mev/dis, and the average photon energy is about 1.0 Mev. Thus the value of μ_A is 3.6×10^{-5} cm^{-1}, and the value of μ is 0.81×10^{-4} cm^{-1}. Substituting these values and integrating, Eq. 3.13 gives

$$I = 470C\ (1 - e^{-0.8 \times 10^{-4} l_0}) \qquad (3.14)$$

For the hemisphere out to the shelter side walls (l_0 = 12.5 ft or 380 cm), the exponential term is 0.97; for a hemisphere out to the shelter end walls (l_0 = 24 ft or 730 cm), the exponential term would be 0.94. The equivalent spherical radius should give a value between 0.94 and 0.97 for the exponential term; the mid-value was used in the estimates given here. Equation 3.14 then is

$$I = 21C \qquad (3.15)$$

The peak dose rate for nonsettling of the aerosol for shot Diablo would have been about 1.6 mr/hr at H+21 min, and, for shot Shasta at H+51 min, the peak dose rate from the aerosol would have been about 1.9 mr/hr. The dose over the 2-hr exposure period from the aerosol would have been about 0.8 mr for shot Diablo and 1.5 mr for shot Shasta. At H+1 hr, the dose rate for shot Diablo due to the aerosol would have dropped to 0.2 mr/hr, and that for shot Shasta would have only decreased to 1.6 mr/hr. At this time, for shot Shasta, the radiation from the aerosol would have been about one-half the radiation in the shelter from outside fallout.

3.4 EFFECTS OF OPENINGS ON SHIELDING

3.4.1 Dose Measurements, Shot Diablo

Film-badge data from the outside station are given in Tables 3.15 to 3.17. The film badges on the stake stations (see Fig. 2.13) were placed at 1½ to 2½ ft above the ground.

TABLE 3.15—EXTERIOR DOSE DATA FROM FILM BADGES ON STAKE STATIONS, SHOT DIABLO*

Station No.†	Dose, r
1	129
2	151
3	163
4	162
5	161
6	146
7	151
8	145
9	89
10	162
11	164
12	173
13	161
14	161
15	151
16	162
17	164
18	164

*Duration of exposure: H-hour to H+28 hr; height of film badges: 1½ to 2½ ft.
† Refer to Fig. 2.13.

TABLE 3.16—EXTERIOR DOSE DATA FROM FILM BADGES IN DOSIMETER-TUBE CUPS, SHOT DIABLO*

	Dose, r	
Badge No.	510 film	606 film
1	68	70
2	78	86
3	165	170
4	68	78

*Duration of exposure: H+3 min to H+5½ hr.

TABLE 3.17—DOSE DATA FOR OTHER STATIONS, SHOT DIABLO*

Location	Dose, r
Shelter ramp (outside)	78,77
Shelter ramp (12 ft from door)	1.9
Shelter ramp (3 ft from door)	0.41

*Duration of exposure: H to H+28 hr.

These badges were exposed prior to shot time until 28 hr after burst. The film badges in the dosimeter tubes were ejected from inside the shelter through the dosimeter tube at 3 min after burst and were recovered at $5\frac{1}{2}$ hr after burst.

According to the stake-station data, the average value of the dose received outside the shelter in the first 28 hr was 160 r. The large deviation shown for station 9 was due to shielding by the steel ventilator to which the badge was attached. The average value of the dose indicated for the period H+3 min to H+$5\frac{1}{2}$ hr from the badges ejected into the dosimeter-tube cups was about 75 r. The large deviation of badge No. 3 may have resulted from the badge's falling onto the ground when it was ejected from the dosimeter tube.

Two methods were used to estimate the initial dose outside the shelter: (1) dose-distance extrapolation and (2) exposure-period adjustment. The extrapolation using dose (r) and distance (D) was based on dose data from badges close to the burst (1800 to 3000 ft). Extrapolation to 5300 ft was accomplished by using the established procedure of plotting log rD^2 vs. r. The initial dose by this procedure was estimated to be 48 r.

The method of exposure period was based on the film-badge data given in Tables 3.15 and 3.16 and the observed GITR data given in Fig. 3.16. The observed GITR curves were integrated first from 3 min to $5\frac{1}{2}$ hr and the integrated dose was compared to the film-badge data in Table 3.16; the latter were found to be larger by a factor of 1.66. This factor was used to adjust the dose from the observed GITR data as integrated from 1 min to 28 hr, and the adjusted integrated dose was subtracted from the average dose in Table 3.15 to give the second estimate of initial dose at the shelter. Results from the two methods are summarized in Table 3.18. Thus up to 28 hr after shot about 36 per cent of the outside dose was from initial dose delivered within the first minute after burst.

The average value of the dose from fallout, 103 r, was used to determine the correction factor for the observed GITR data, 1.82. When this is applied to the observed data, the peak radiation rate increases from 55 to 100 r/hr and the one-hour rate increases from 14 to 25.5 r/hr. Comparison of the adjusted GITR and some AN/PDR-39(T1B) readings are given in Table 3.19. The calculated response of the AN/PDR-39(T1B) to an extended source of fission products varies between 0.73 and 0.78; thus the adjustment of the GITR data from the film-badge data is in agreement with the AN/PDR-39(T1B) data.

The dose data for interior stations for various exposure periods are given in Table 3.20. Three 200-mr electroscope dosimeters were grouped at each height under the ventilators. The other stations had one 200-mr dosimeter and one 1-mr dosimeter. The residual numbers (RN) for initial radiation were calculated by using the average outside initial dose of 57 r as given in Table 3.18 and the average of the three interior dose measurements at each location; the results are given in Table 3.21. The shielding residual numbers for fallout radiation given in Table 3.22 were calculated from the interior dose data and estimates of the dose from fallout radiation obtained by integrating the adjusted GITR curve (Fig. 3.16).

Except for the 3-ft measurements, the residual numbers for the initial radiation under the center ventilator are about two times those for fallout radiation. At the rear ventilator the values are only slightly higher (about 40 per cent on the average). In general, for initial radiation, at heights less than 9 ft the residual numbers were less than 0.001.

For fallout radiation the shielding residual numbers based on dose indicate that residual numbers better than 0.001 can be expected under the ventilator openings. The one exception occurs at the 12-ft station under the center ventilator. For stations under ventilators the residual numbers based on dose agree within a factor of 2 with residual numbers based on dose rate. The residual numbers for other stations show large discrepancies, probably owing to the small doses recorded.

Attenuation of radiation below the exhaust ventilators is indicated by the dose measurements. A comparison of doses at various distances below the vent to the dose at the vent is given in Fig. 3.17. The data show that radiation has been reduced at the 3-ft level to 10 to 20 per cent of that at the 12-ft level.

3.4.2 Intensity Measurements, Shot Diablo

Measurements of gamma intensity were made on top of the shelter at H+$5\frac{1}{2}$ hr with AN/PDR-39(T1B) survey instruments. Results are shown in Table 3.23.

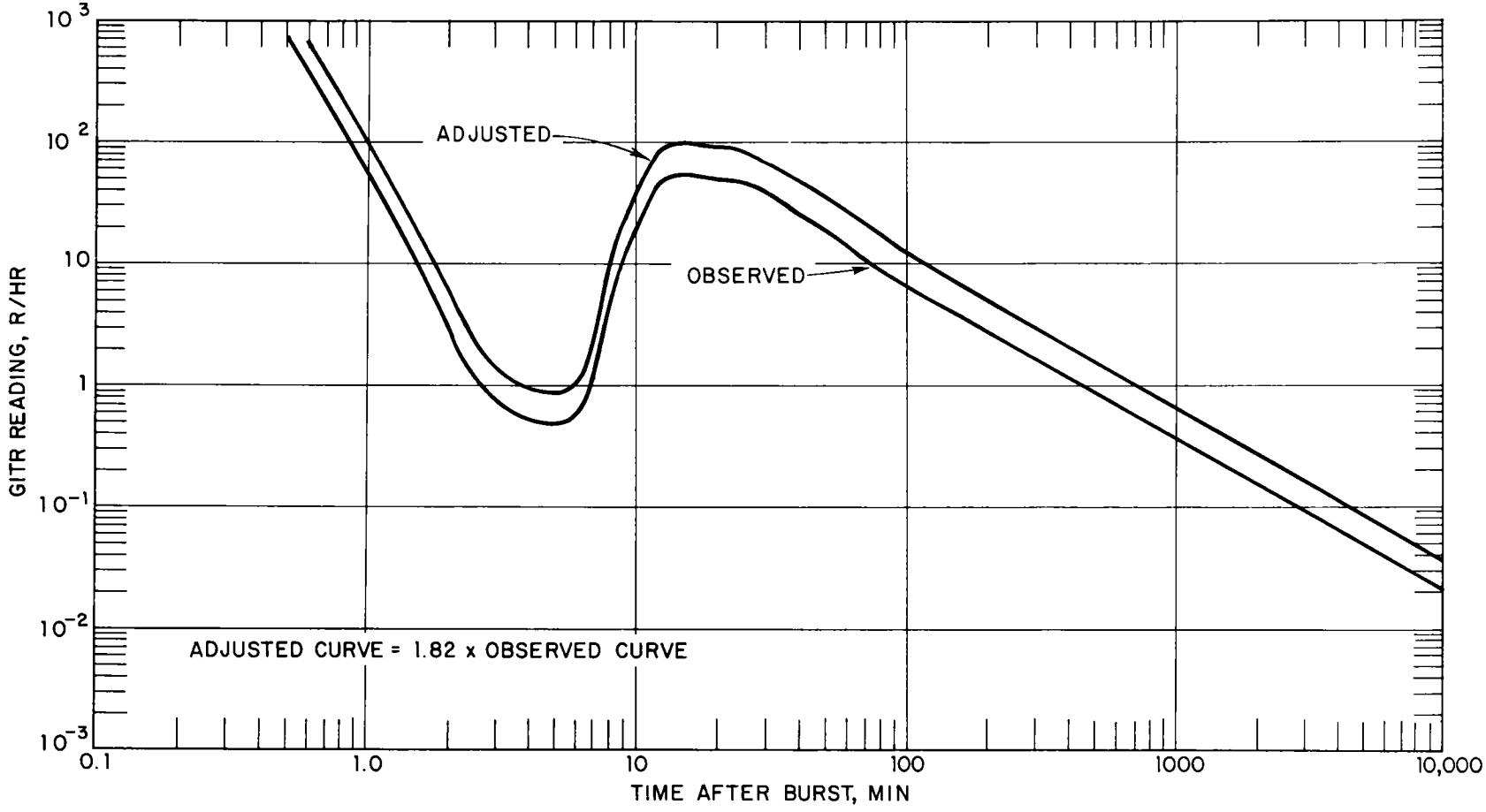

Fig. 3.16—GITR data, shot Diablo.

TABLE 3.18—ESTIMATES OF INITIAL DOSE AND DOSE FROM FALLOUT

Dose fraction	Dose, r		
	Method 1	Method 2	Average
Initial, 0 to 1 min	48	66	57
Fallout (transit and deposit), 1 min to 28 hr	112	94	103
Total, 0 to 28 hr	160	160	160

TABLE 3.19—COMPARISON OF ADJUSTED GITR AND AN/PDR-39(T1B) READINGS

Time after burst, hr	Adjusted GITR reading, mr/hr	AN/PDR-39(T1B) reading, mr/hr	Ratio, (T1B/GITR)
5.5	2700	2200	0.81
27.5	370	260	0.70
30.0	320	250	0.78
		Av.	0.76

TABLE 3.20—INTERIOR DOSE DATA, SHOT DIABLO

Location*	Height, ft	Initial gamma dose, mr			Fallout gamma dose, mr		
		1	2	3	1	2	3
		Center Ventilator†					
C4	12	200+	190	180	110	110	95
C4	9	70	60	70	25	35	30
C4	6	30	30	20	12	10	10
C4	3	10	20	20	10	17	22
		Rear Ventilator‡					
C7	12	30	30	20	20	20	23
C7	9	10	10	10	8	20	11
C7	6	0	10	10	8	6	5
C7	3	3	7	4	0	5	5

Other Stations (3-ft Height)§

Location*	Initial gamma dose, 200-mr dosimeter, mr	Fallout gamma dose, mr	
		200-mr dosimeter	Background dosimeter
A1	4	30	10+
A4	4.5	3	4.5
A7	4	5	10+
E1	0.5	18	10+
E4	2	10	10+
E6	3.5	1	0.5

* Locations are shown in Fig. 2.11.

† Initial exposure was from H-hour to H+5 min; fallout exposure was from H+5 min to H+76 min.

‡ Initial exposure was from H-hour to H+4½ min; fallout exposure was from H+6 min to H+77 min.

§ Initial exposure was from H-hour to H+3 min; fallout exposure was from H+8 min to H+76 min.

TABLE 3.21—SHIELDING RESIDUAL NUMBERS FOR INITIAL RADIATION

Station No.	Height, ft	Interior average dose, r	Residual No.*
	Center Ventilator		
C4	12	0.190	0.0033
C4	9	0.067	0.0012
C4	6	0.027	0.0005
C4	3	0.017	0.0003
	Rear Ventilator		
C7	12	0.027	0.0005
C7	9	0.010	0.0002
C7	6	0.010	0.0002
C7	3	0.005	0.0001

*Exterior dose taken as 57 r (Table 3.18).

TABLE 3.22—SHIELDING RESIDUAL NUMBERS FOR FALLOUT RADIATION

Station No.	Height, ft	Interior average dose,* r	Exterior average dose,* r	Residual No.
	Center Ventilator			
C4	12	0.105	55.5	0.0019
C4	9	0.030	55.5	0.00054
C4	6	0.011	55.5	0.00020
C4	3	0.016	55.5	0.00029
	Rear Ventilator			
C7	12	0.021	55.5	0.00038
C7	9	0.013	55.5	0.00024
C7	6	0.006	55.5	0.00011
C7	3	0.005	55.5	0.00009
	Other Stations			
A1	3	0.030†	55.2	> 0.00055
A4	3	0.0045	55.2	0.00008
A7	3	0.010	55.2	0.00018
E1	3	0.018	55.2	0.00033
E4	3	0.010	55.2	0.00018
E7	3	0.0005	55.2	0.00001

*See Table 3.20 for time periods used.
†In shielded location, unrepresentative of radiation through the door.

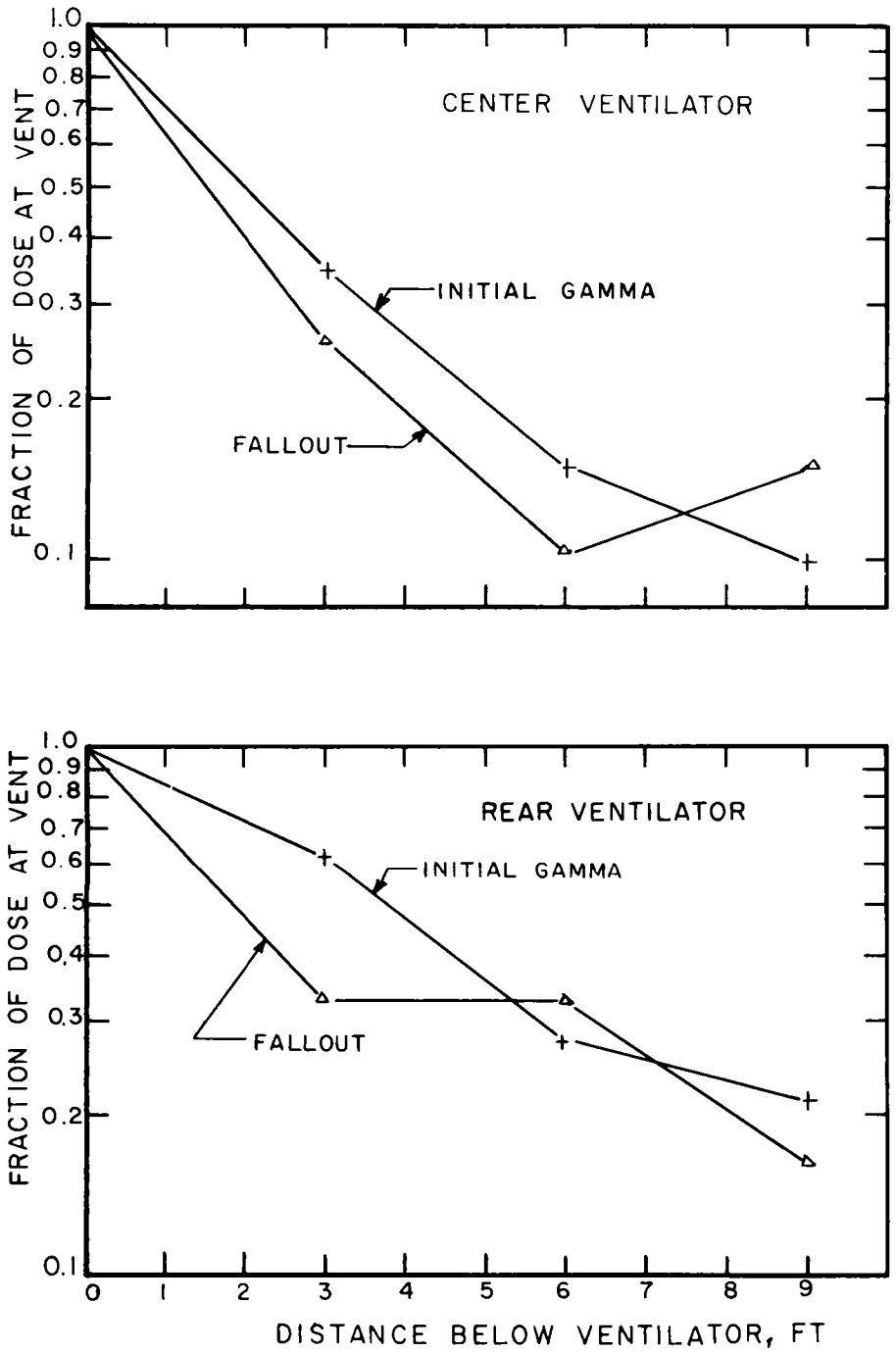

Fig. 3.17—Reduction of intensity below ventilators, expressed as fraction of intensity at vent opening, shot Diablo.

The first survey of the interior of the shelter was made after cessation of fallout during the period H+94 to H+108 min. Measurements made with AN/PDR-27C radiacs at the various stations shown in Fig. 2.11 are given in Table 3.24. Residual numbers for each station were obtained by correcting the average of the exterior AN/PDR-39(T1B) measurements to H+100 using the observed GITR data (Fig. 3.16) for determining the decay correction factor. The response of the AN/PDR-27C to the photon spectrum inside the shelter was the same as that of the AN/PDR-39(T1B) to the photon spectrum outside the shelter; hence the two sets of measurements require no additional correction in computing the residual numbers. The response of the AN/PDR-27C to the photon spectrum inside the shelter is discussed in Appendix D.

Residual-number contours were developed from the data in Table 3.24. Figure 3.18 shows contours on horizontal-plane sections at 3, 6, and 9 ft above the shelter floor, on a vertical section through the center line of the shelter, and on a vertical section through grid column 4.

Residual numbers given in Table 3.24 and contours in Fig. 3.18 show that almost all the shelter gave residual numbers better than 0.001; most of the shelter gave residual numbers approaching 0.00001. Restricted areas near the entrance and within about 1 ft of the center vent gave residual numbers poorer than 0.001.

Attenuation of radiation below the vents was determined from the data in Table 3.24; results are plotted in Fig. 3.19. Attenuation is essentially proportional to the distance from the vent down to 6 ft from the floor. This rate is substantially greater than the attenuation based on dose measurements (Fig. 3.17).

A second interior survey, made after sandbagging the center vent, gave the results shown in Table 3.24. Shielding the vent did not result in appreciable improvement of residual numbers in most parts of the shelter. However, a threefold reduction was noted directly below the vent. Observable reductions also were noted at stations C3, C4, and C5. Residual numbers given in Table 3.24 for the second survey were obtained by correcting the interior readings to H+100 min using the observed GITR data and then comparing the interior readings to the exterior readings corrected to the same time.

Additional intensity measurements were taken in the shelter by five AN/PDR-27C low-range radiacs whose signals were recorded on Brown recorders. The traces of these instruments for the first 2 hr are shown in Fig. 3.20, together with the interior survey measurements made at the same locations. The data are in fair agreement, the interior survey measurements tending to be somewhat higher than the recorded data.

3.4.3 Intensity Measurements, Shot Shasta

The observed GITR data for the GITR location on top of the shelter are given in Fig. 3.21. Data from the Geiger-tube rate meter underneath the center ventilator are given in Fig. 3.22; the rate-meter readings were converted to AN/PDR-39(T1B) ionization rates by taking several readings on the latter instrument at the Geiger-tube location. The Geiger-tube position was protected on the sides by lead bricks; the opening pointed upward. Hence the readings (and residual numbers) for the rate meter were somewhat lower than those under the ventilator for an unshielded reading.

Exterior rate measurements taken with the AN/PDR-39(T1B) and their correlation with the GITR measurements are given in Table 3.25. The ratios of the corrected AN/PDR-39 (T1B) readings to the GITR readings are in agreement with the value, 1.8, found on shot Diablo. The difference in the ratio between the two early measurements and the later one is probably due more to the calibration of the AN/PDR-39(T1B) instruments (first two were on instruments checked out from Rad-Safe) than to relative change in the response of the two instruments with photon energy. For the computation of residual numbers, the observed GITR data were corrected to observed AN/PDR-39(T1B) by multiplying them by 1.62. This value of the ratio is an average for the first two measurements; it was used since all the interior measurements were taken on, or converted to equivalent readings on, the Rad-Safe calibrated AN/PDR-39(T1B) instruments. This treatment assumes the same over-all response of the AN/PDR-39(T1B) to the radiation inside and outside the shelter (the energy and geometries of the radiation were different).

(Text continues on page 84.)

TABLE 3.23—EXTERIOR SURVEY DATA, SHOT DIABLO*

Station No.†	Intensity, r/hr	Station No.†	Intensity, r/hr	Station No.†	Intensity, r/hr
1	2.0	7	2.2	13	2.2
2	2.2	8	2.2	14	2.2
3	2.3	9	2.0	15	2.2
4	2.2	10	2.1	16	2.2
5	2.3	11	2.4	17	2.2
6	2.2	12	2.2	18	2.2

*Time of survey, H + 5½ hr; instrument, AN/PDR-39(T1B).
†Refer to Fig. 2.13.

TABLE 3.24—INTERIOR SURVEY DATA, SHOT DIABLO

		First survey (H + 100 min)		Second survey (H + 5½ hr)	
Location*	Height, ft	Reading, mr/hr	Residual No.	Reading, mr/hr	Residual No.
A1	3	50	0.0050	3.5	0.0018
B1	3	10	0.0010	5.0	0.0026
C1	3	14	0.0014	2.3	0.0012
D1	3	10	0.0010	2.4	0.0013
E1	3	5	0.0005 0.0003†	1.5	0.00078
E1	6	11	0.0011	1.5	0.00078
D1	3	9	0.0009	2.5	0.0013
D1	6	21	0.0021	2.2	0.0011
D1	9	11	0.0011	1.4	0.00073
C1	3	13	0.0013	2.8	0.0015
C1	6	15	0.0015	4.0	0.0021
C1	9	8	0.0008	1.8	0.00094
C1	12	2	0.0002	0.7	0.00036
B1	3	11	0.0011	3.5	0.0018
B1	6	13	0.0013	3.0	0.0016
B1	9	5	0.0005	0.9	0.00047
A1	3	32	0.0032	5.0	0.0026
A1	6	36	0.0036	4.7	0.0024
A2	3	6	0.0006	1.5	0.00078
B2	3	5	0.0005	0.9	0.00047
C2	3	3.5	0.00035	1.0	0.00052
D2	3	3	0.00030	1.0	0.00052
E2	3	3.5	0.00035	0.7	0.00036
E2	6			0.4	0.00021
D2	3	4.3	0.00043	0.8	0.00042
D2	6	3.2	0.00032	0.8	0.00042
D2	9	2.6	0.00026	0.6	0.00031
C2	3	3.4	0.00034	0.9	0.00047
C2	6	3.3	0.00033	0.8	0.00042
C2	9	2.1	0.00021	0.4	0.00021
C2	12	1.1	0.00011	0.3	0.00016
B2	3	4.3	0.00043	0.7	0.00037
B2	6	3.4	0.00034	0.4	0.00021
B2	9	1.3	0.00013	0.4	0.00021
A2	3	13	0.0013	1.7	0.00088
A2	6	4	0.00040	1.4	0.00073
A3	3	1.5	0.00015	0.30	0.00016

TABLE 3.24 (Continued)

Location*	Height, ft	First survey (H + 100 min) Reading, mr/hr	First survey (H + 100 min) Residual No.	Second survey (H + 5½ hr) Reading, mr/hr	Second survey (H + 5½ hr) Residual No.
B3	3	1.3	0.00013	0.25	0.00013
C3	3	1.1	0.00011	0.17	0.000089
D3	3	0.7	0.00007	0.10	0.000052
E3	3	0.4	0.00004	0.07	0.000036
E3	6	0.5	0.00005	0.10	0.000052
D3	3	0.7	0.00007	0.12	0.000062
D3	6	0.6	0.00006	0.09	0.000047
D3	9	0.3	0.00003	0.11	0.000057
C3	3	1.2	0.00012	0.15	0.000078
C3	6	1.2	0.00012	0.16	0.000083
C3	9	1.1	0.00011	0.14	0.000073
C3	12	1.1	0.00011	0.20	0.00010
B3	3	1.4	0.00014	0.25	0.00013
B3	6	1.1	0.00011	0.22	0.00011
B3	9	0.8	0.00008	0.19	0.000078
A3	3	1.3	0.00013	0.27	0.00014
A3	6	0.8	0.00008	0.25	0.00013
A4	3	0.2	0.00002	0.09	0.000047
B4	3	0.4	0.00004	0.15	0.000078
C4	3	1.6	0.00016 0.00029†	0.17	0.000088
D4	3	0.8	0.00008	0.17	0.000088
E4	3	0.4	0.00004 0.00018†	0.10	0.000052
E4	6	0.4	0.00004	0.09	0.000047
D4	3	0.7	0.00007	0.13	0.000068
D4	6	0.8	0.00008	0.13	0.000068
D4	9	0.6	0.00006	0.11	0.000057
C4	3	1.4	0.00014	0.18	0.000094
C4	6	1.4	0.00014 0.00020†	0.20	0.00010
C4	9	4.1	0.00041 0.00054†	0.21	0.00011
C4	12	30	0.0030 0.0019*	2.0	0.0010
B4	3	0.3	0.00004	0.14	0.000073
B4	6	0.4	0.00004	0.16	0.000083
B4	9	0.4	0.00004	0.14	0.000073
A4	3	0.2	0.00002 0.00008†	0.09	0.000047
A4	6	0.2	0.00002	0.11	0.000057
A5	3	0.2	0.00002	0.15	0.000078
B5	3	0.5	0.00005	0.18	0.000094
C5	3	1.0	0.00010	0.25	0.00013
D5	3	0.5	0.00005	0.17	0.000088
E5	3	0.5	0.00005	0.13	0.000068
E5	6	0.2	0.00002	0.09	0.000047
D5	3	0.5	0.00005	0.15	0.000078
D5	6	0.5	0.00005	0.12	0.000062
D5	9	0.5	0.00005	0.13	0.000068
C5	3	1.0	0.00010	0.18	0.000094
C5	6	1.3	0.00013	0.20	0.00010
C5	9	1.4	0.00014	0.23	0.00012

TABLE 3.24 (Continued)

Location*	Height, ft	First survey (H + 100 min) Reading, mr/hr	First survey (H + 100 min) Residual No.	Second survey (H + 5½ hr) Reading, mr/hr	Second survey (H + 5½ hr) Residual No.
C5	12	1.5	0.00015	0.21	0.00011
B5	3	0.6	0.00006	0.17	0.000088
B5	6	0.5	0.00005	0.12	0.000062
B5	9	0.4	0.00004	0.10	0.000052
A5	3	0.2	0.00002	0.12	0.000062
A5	6	0.2	0.00002	0.10	0.000052
A6	3	0.2	0.00002		
B6	3	0.3	0.00003		
C6	3	1.5	0.00015		
D6	3	0.5	0.00005		
E6	3	0.3	0.00003		
E6	6	0.5	0.00005	0.15	0.000078
D6	3	0.5	0.00005	0.15	0.000078
D6	6	0.4	0.00004	0.17	0.000088
D6	9	0.4	0.00004	0.15	0.000078
C6	3	0.7	0.00007	0.20	0.00010
C6	6	1.0	0.00010	0.25	0.00013
C6	9	1.6	0.00016	0.27	0.00015
C6	12	2.7	0.00027	0.30	0.00016
B6	3	0.4	0.00004	0.15	0.000078
B6	6	0.5	0.00005	0.10	0.000052
B6	9	0.4	0.00004	0.10	0.000052
A6	3	0.3	0.00003	0.09	0.000047
A6	6	0.3	0.00003	0.11	0.000057
A7	3	0.1	0.00001 0.00018†	0.05	0.000026
B7	3	0.3	0.00003	0.08	0.000042
C7	3	1.0	0.00010 0.00009†	0.13	0.000068
D7	3	0.5	0.00005	0.08	0.000042
E7	3	0.2	0.00002 0.00001†	0.04	0.000021
E7	6	0.2	0.00002	0.05	0.000026
D7	3	0.4	0.00004	0.10	0.000052
D7	6	0.5	0.00005	0.09	0.000047
D7	9	0.5	0.00005	0.07	0.00036
C7	3	0.6	0.00006	0.11	0.000057
C7	6	0.7	0.00007 0.00011†	0.14	0.000074
C7	9	1.1	0.00011 0.00024†	0.17	0.000088
C7	12	2.0	0.00020 0.00038†	0.20	0.00010
B7	3	0.4	0.00004	0.07	0.000036
B7	6	0.6	0.00006	0.05	0.000026
B7	9	0.3	0.00003	0.07	0.000036
A7	3	0.1	0.00001	0.06	0.000031
A7	6	0.4	0.00004	0.07	0.000036

* Locations are shown in Fig. 2.11.

† Residual numbers from dose measurements (Table 3.22) given for comparison.

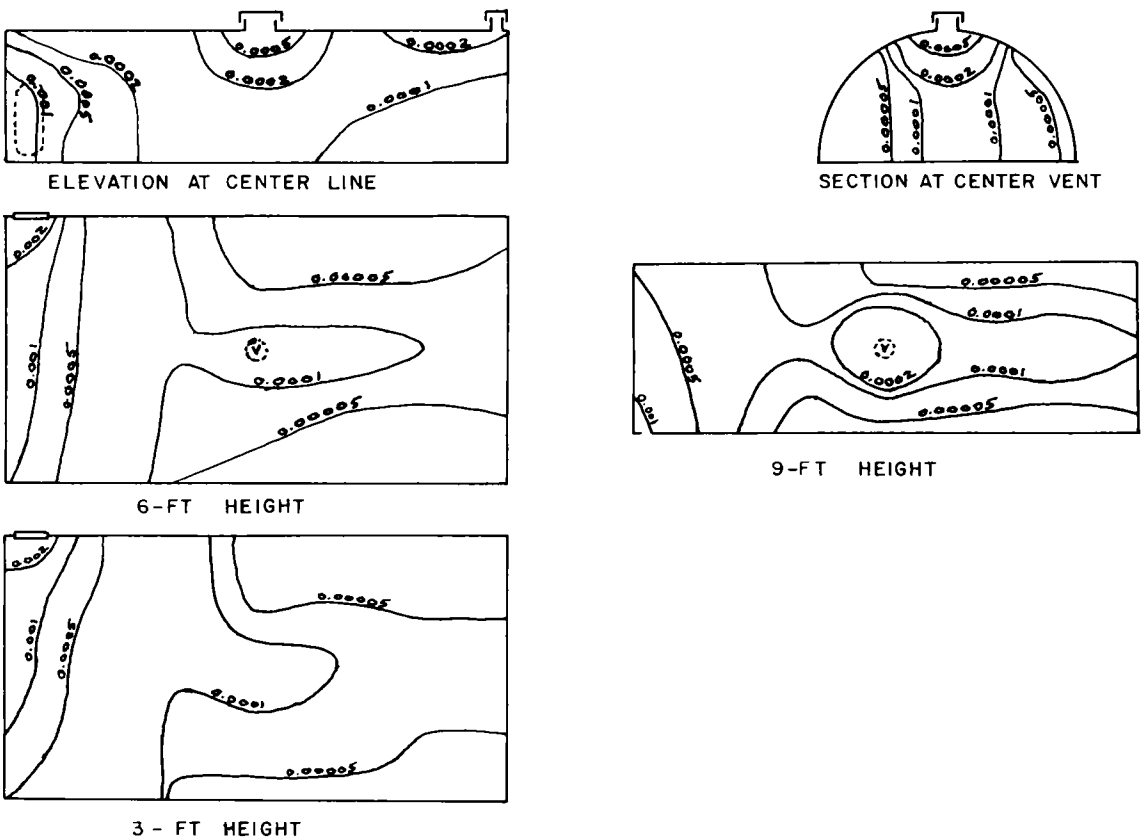

Fig. 3.18—Residual-number contours for first interior survey, shot Diablo.

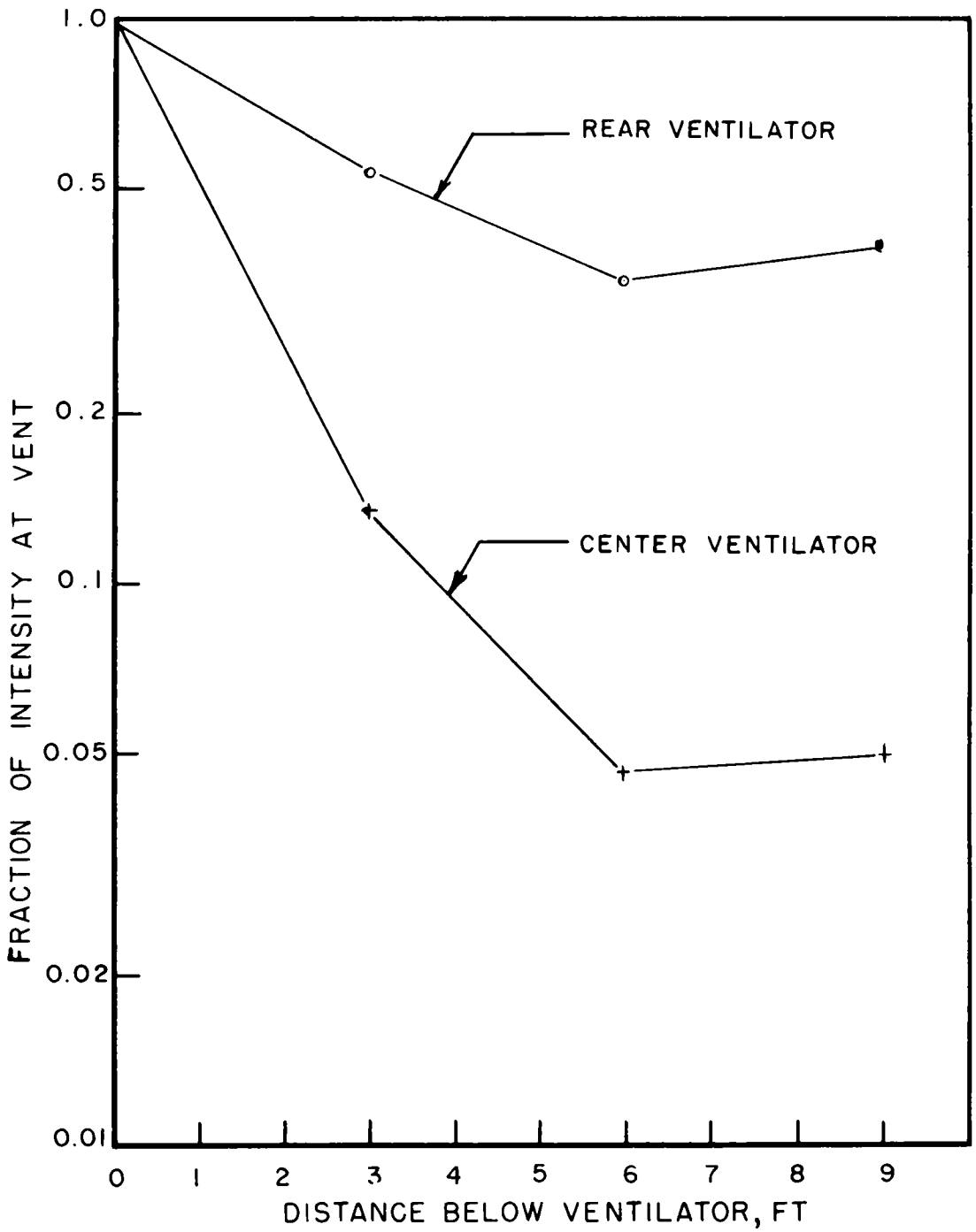

Fig. 3.19—Reduction of intensity below ventilators, expressed as fraction of intensity at vent opening, shot Diablo.

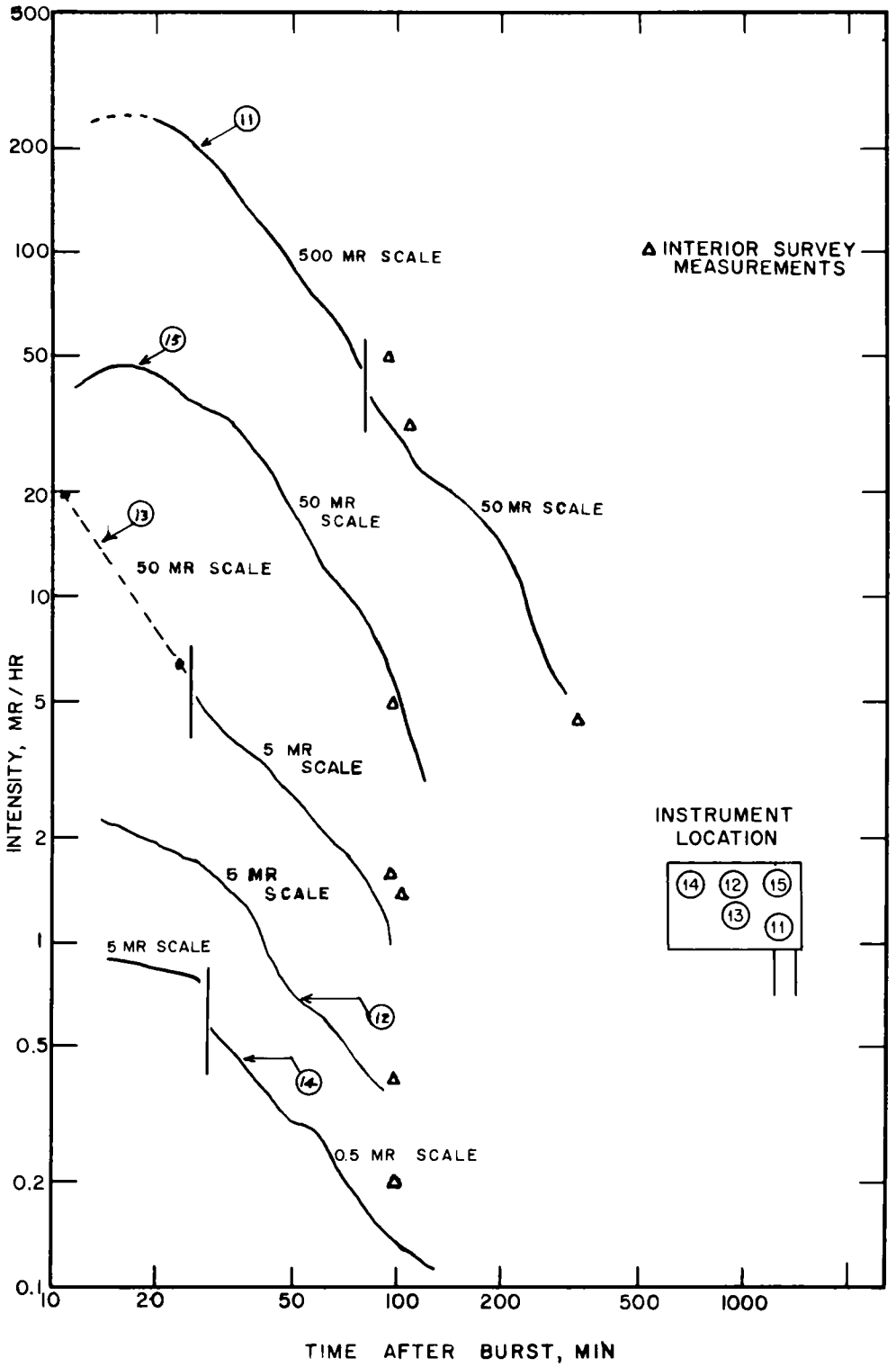

Fig. 3.20—Results from fixed AN/PDR-27C instruments in shelter, shot Diablo.

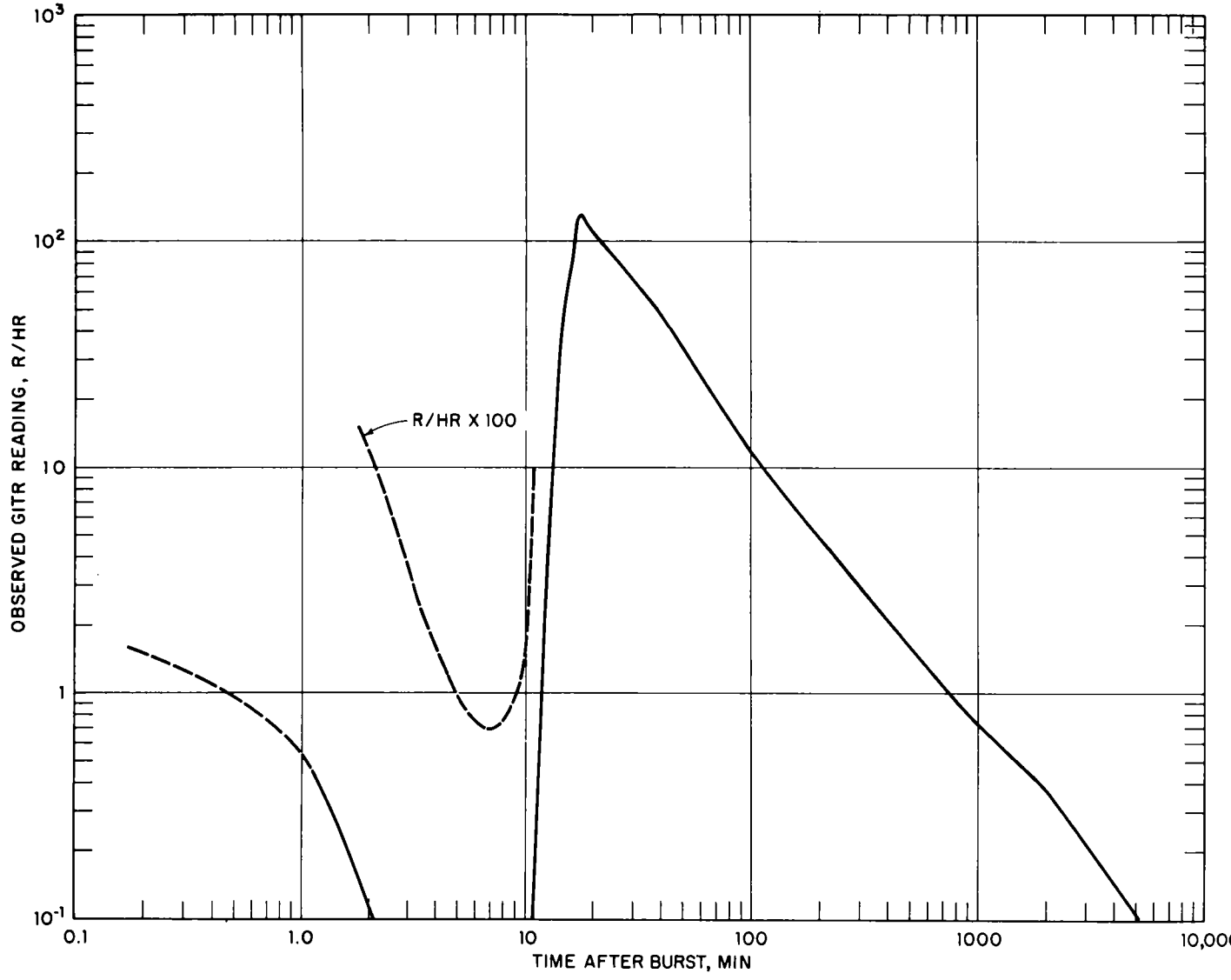

Fig. 3.21—GITR data, shot Shasta.

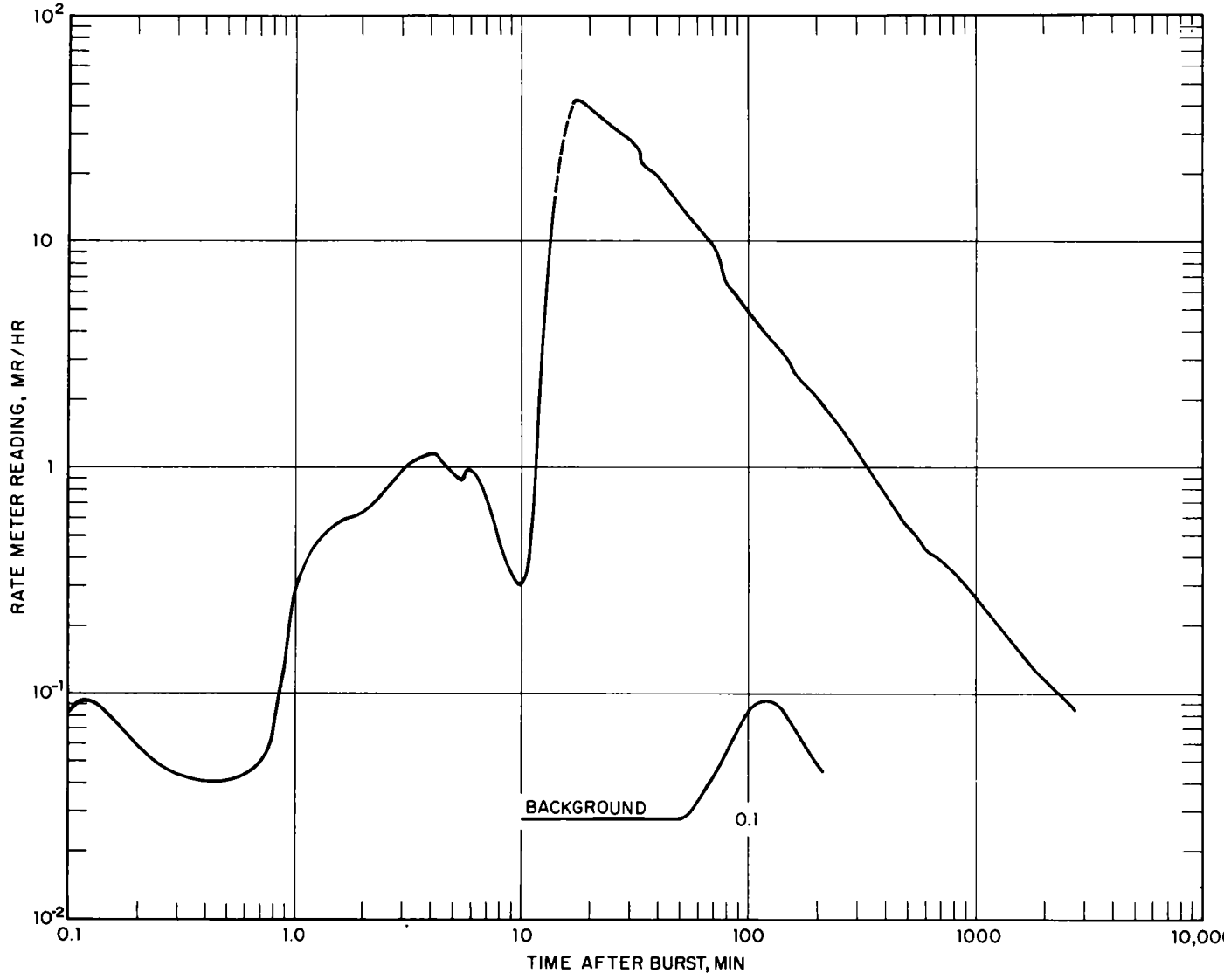

Fig. 3.22—Rate-meter data, converted to milliroentgens per hour from correlation data with the AN/PDR-39(T1B), shot Shasta.

The residual number at the Geiger-tube rate-meter location under the center ventilator is plotted as a function of time in Fig. 3.23. Since the geometry for the rate meter pointed upward, the contribution of the radiation down the vent to the observed count-rate on this instrument was large. The data show a peak in the residual number at 6 to 7 min due to radioactive sources directly over the ventilator. This time was just prior to fallout arrival; therefore it must have been due to radiation from the cloud overhead. After most of the fallout had arrived, the residual number remained almost constant up to about 250 min (4 hr); the decrease after 250 min was probably due to a general decrease in the energy of the photons.

A single shelter survey was made at H+2½ hr using the AN/PDR-39(T1B) instruments; the data and residual numbers are given in Table 3.26. The AN/PDR-39(T1B) equivalent reading from the GITR data at that time was 11.3 r/hr; this value was used in computing the residual numbers. Except for the residual numbers for positions under the center vent and open periscope (C_3, C_4, C_5, and C_6) and near the M6 collective protector (A_3), the residual numbers on the average are a little less than two times those given in Table 3.24 for shot Diablo. Under the openings the residual numbers are between 0.0007 and 0.0008; hence the requirement for a residual number of 0.001 was met. The higher numbers could, in part, be due to a higher relative response of the AN/PDR-39(T1B) to the radiations inside the shelter.

3.4.4 Directional Gamma Measurements, Shot Diablo

Data obtained by the directional gamma instrument are plotted in Figs. 3.24 through 3.27. The instrument records have been corrected to 1 hr after burst. The unit of measurement is milliroentgens per hour per 10 degrees of solid angle. When properly summed over 4π, the result of the directional survey should equal the measured intensity at the point of interest. Figure 3.24 shows the result of a transverse rotation of the instrument in a plane including the shelter door. Figure 3.25 gives the results of a transverse rotation midway between the door and the center ventilator, showing the greatly reduced contribution from the door. Figure 3.26 is a longitudinal rotation approximately under the center ventilator, and Fig. 3.27 shows two longitudinal rotations, one under the rear ventilator and one midway between the door and center ventilator.

3.4.5 Energy-spectrum Measurements, Shot Diablo

Data on the gamma spectrum inside the shelter are given in Appendix D along with the computations on the response of the AN/PDR-27C to the radiations in the shelter.

3.5 SUPPORTING TECHNICAL STUDIES

3.5.1 Shot Diablo

The technical supporting studies on shot Diablo consisted in (1) the intensity-time record from the GITR on the shelter roof, (2) the decay of fallout samples measured in the 4π ionization chamber, (3) the rate and accumulation of fallout at the shelter as collected by the incremental fallout collector, (4) intensity-time records on an AN/PDR-27C instrument inside the shelter, and (5) directional gamma measurements on top of the shelter.

The GITR data for shot Diablo are given in Fig. 3.16. Figure 3.28 gives a comparison of the planning decay curve, the intensity-time record from the GITR, and the average decay of fallout samples measured in the 4π ionization chamber. The measurements of the incremental fallout collector trays are given in Table 3.27. The early intensity-time data from an AN/PDR-27C instrument attached to a Brown recorder are shown in Fig. 3.29. Directional measurements of the radiation field on top of the shelter are shown in Fig. 3.30.

The GITR data indicate fallout arrival at about H+6 min and peak intensity at H+15 min. The incremental-collector data show a slight increase from background between H+5½ min and H+6½ min; in the following minute a single large particle counting about a million counts per minute at H+31½ hr was collected. The variability in the data between successive trays is a statistical one owing to small tray size. The bulk of the activity collected

(Text continues on page 94.)

TABLE 3.25—COMPARISON OF AN/PDR-39(T1B) AND OBSERVED GITR MEASUREMENTS, SHOT SHASTA

Time after burst, hr	AN/PDR-39(T1B) reading, r/hr	Corrected AN/PDR-39(T1B) reading,* r/hr	Observed GITR reading, r/hr	Ratio, corrected T1B/GITR
10.0	2.2	2.9	1.3	2.2
13.5	1.4	1.9	0.91	2.1
53.8	0.20†	0.27	0.19	1.4

* Relative response of 0.75 used to correct readings.
† AN/PDR-146(T1B) calibrated and used by Project 32.4 personnel.

TABLE 3.26—INTERIOR AN/PDR-39(T1B) MEASUREMENTS, SHOT SHASTA

Location*	Reading, mr/hr	Residual No.	Location*	Reading, mr/hr	Residual No.
A1	6.0	0.00053	A5	0.5	0.00004
B1	10	0.00088	B5	1.0	0.00009
C1	12	0.0011	C5	8.0	0.00071
D1	14	0.0012	D5	1.1	0.00010
E1	6.0	0.00053	E5	1.0	0.00009
A2	10	0.00088	A6	0.7	0.00006
B2	10	0.00088	B6	1.4	0.00012
C2	12	0.0011	C6†	9.0	0.00080
D2	8.0	0.00071	D6	1.3	0.00012
E2	6.0	0.00053	E6	0.4	0.00004
A3	1.4	0.0012	A7	0.6	0.00005
B3	3.0	0.00027	B7	1.0	0.00009
C3	8.0	0.00071	C7	3.0	0.00027
D3	2.4	0.00021	D7	1.0	0.00009
E3	1.5	0.00013	E7	0.3	0.00003
A4	0.7	0.00006	At door	80	0.0071
B4	1.3	0.00012	6 ft from door	49	0.0043
C4	8.0	0.00071	Outside door‡	17	0.0077
D4	2.1	0.00019	Chamber entrance‡	1400	0.64
E4	1.2	0.00011			

* Locations are shown in Fig. 2.11.
† Periscope lid off, periscope in up position; time of survey, H + 2.5 hr.
‡ Taken at H + 10 hr; outside reading, 2.2 r/hr.

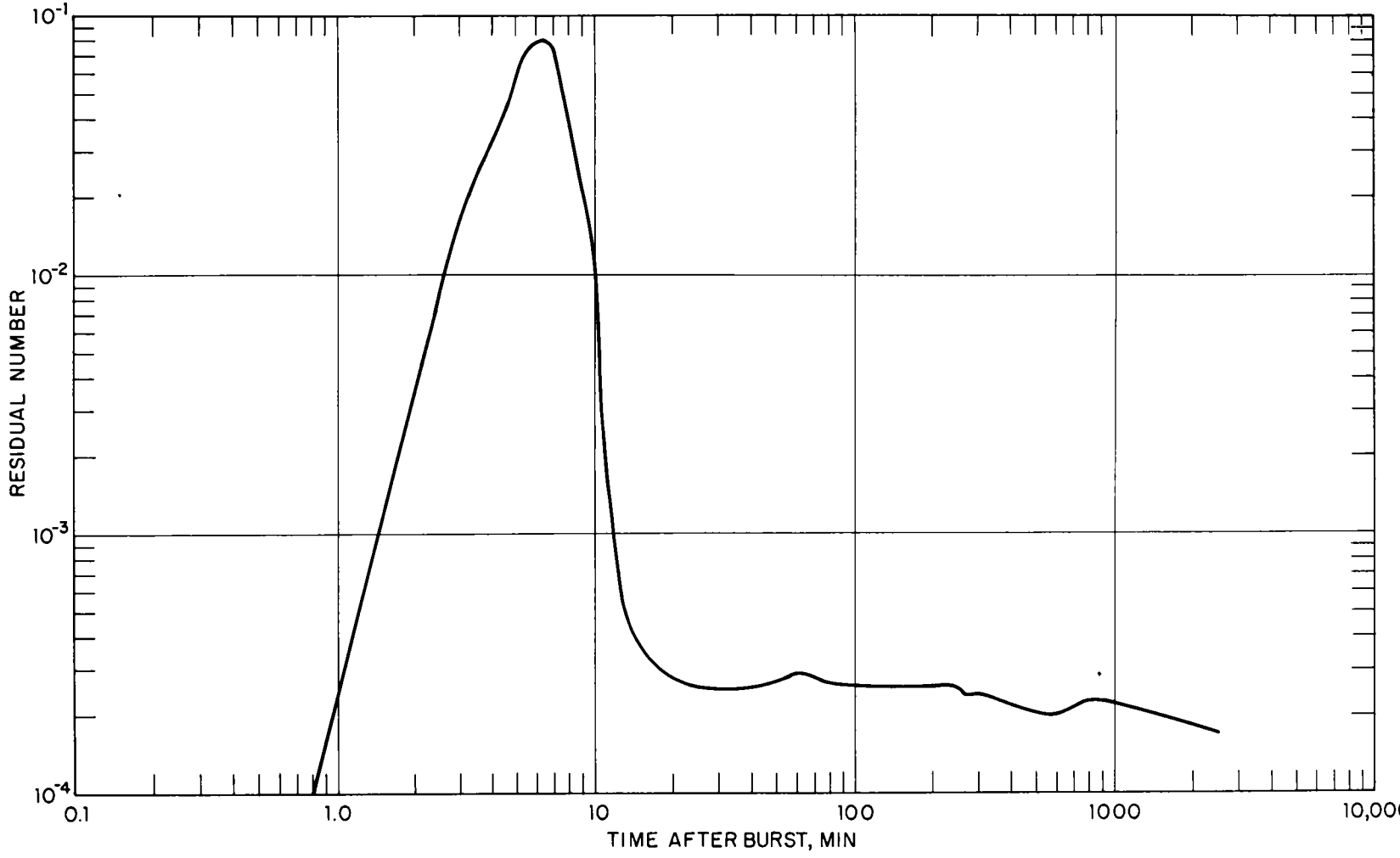

Fig. 3.23—Residual number at rate-meter location under center ventilator, shot Shasta.

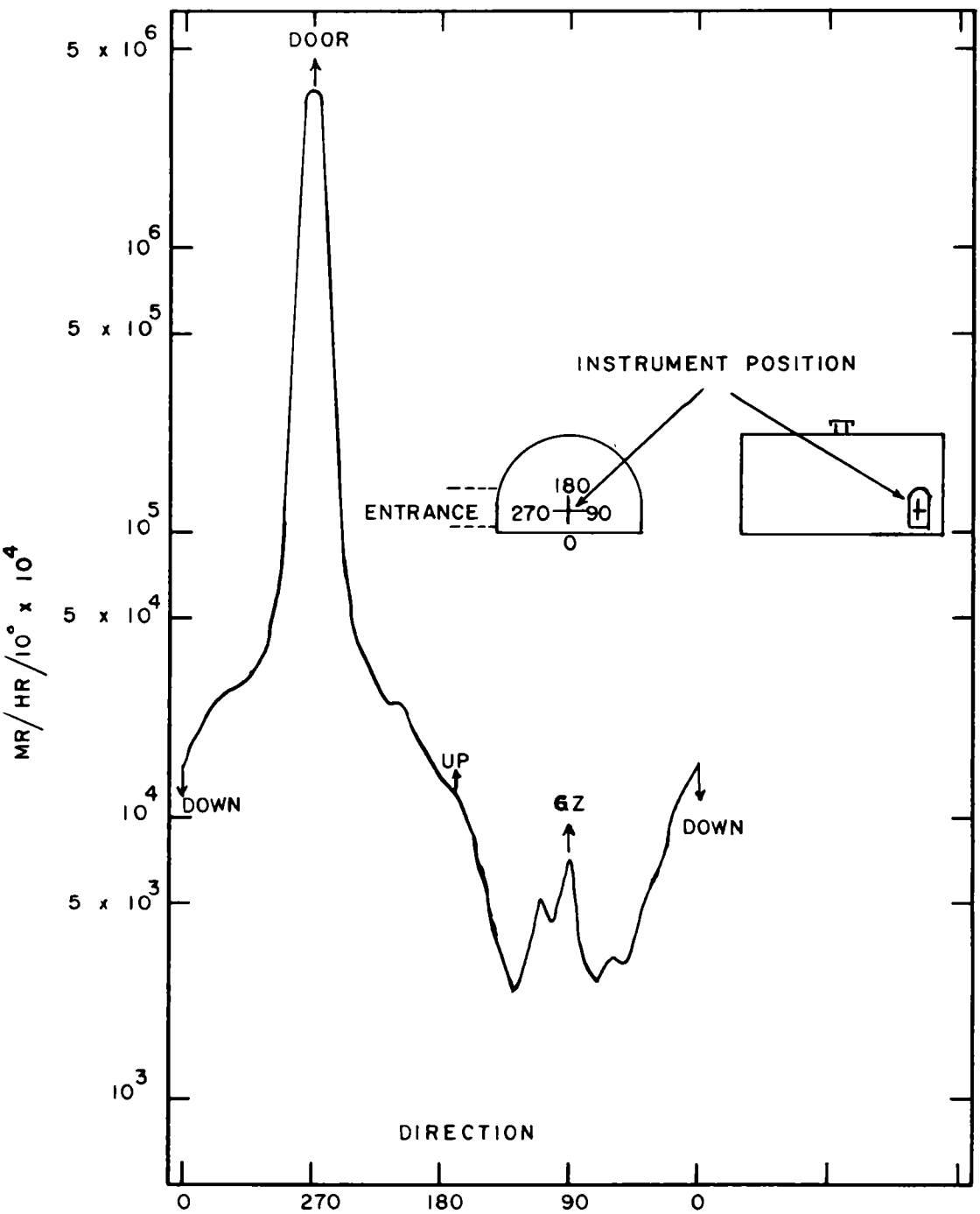

Fig. 3.24—Directional characteristics of gamma-radiation flux on center line of shelter opposite door, shot Diablo.

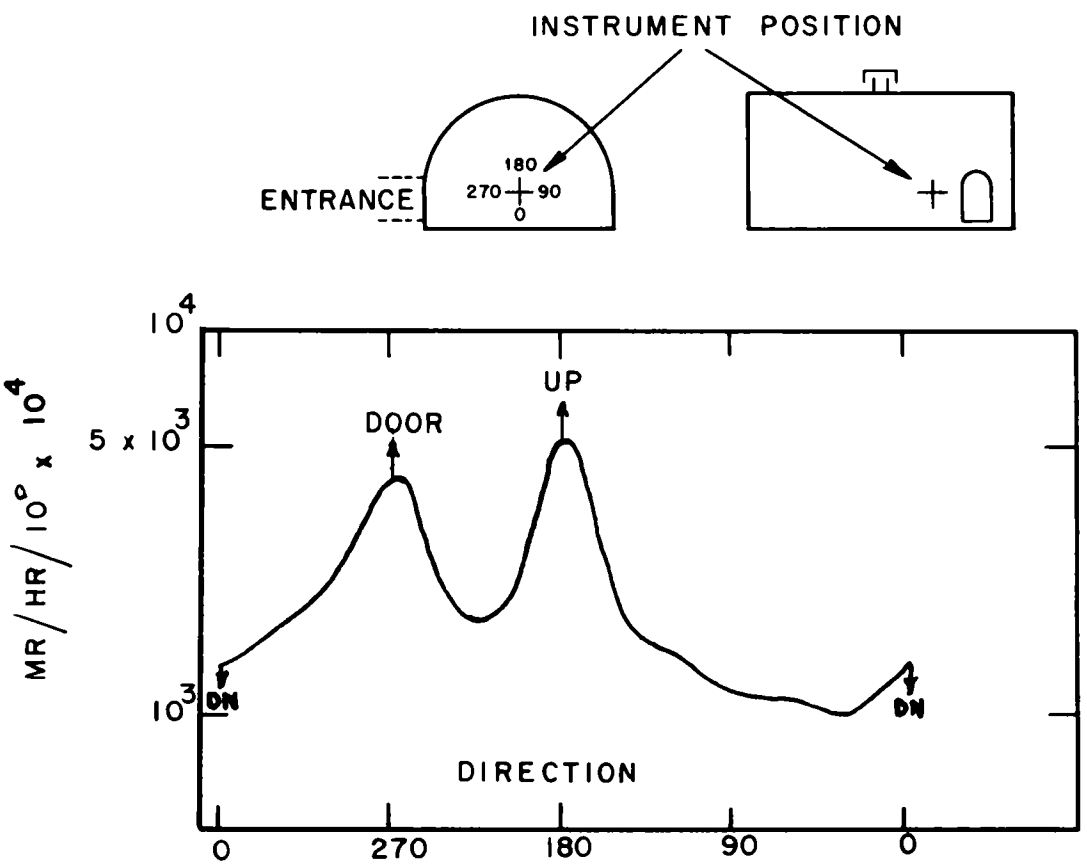

Fig. 3.25—Directional characteristics of gamma-radiation flux on transverse plane midway between door and center ventilator, shot Diablo.

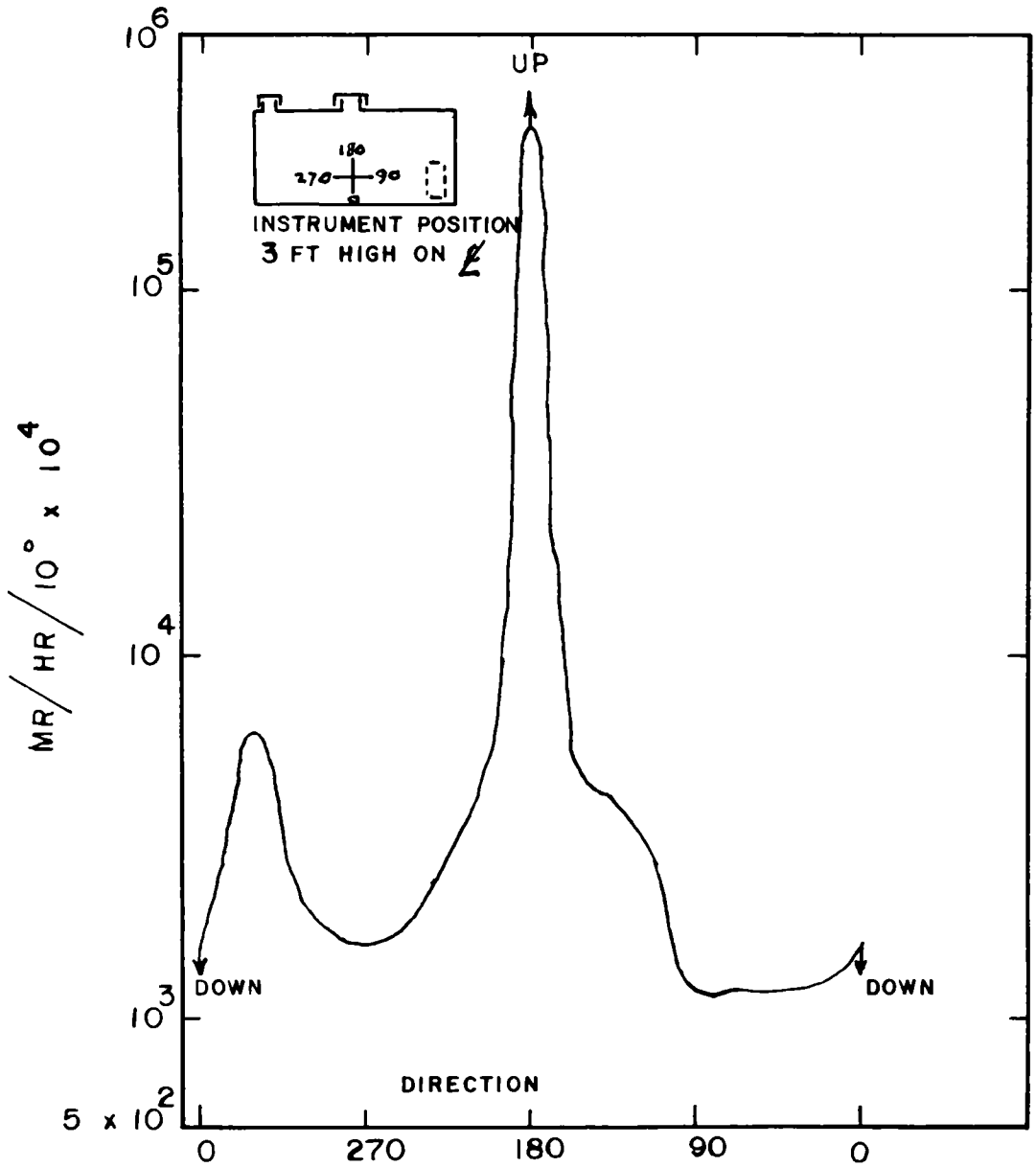

Fig. 3.26—Directional characteristics of gamma-radiation flux along shelter axis under center ventilator, shot Diablo.

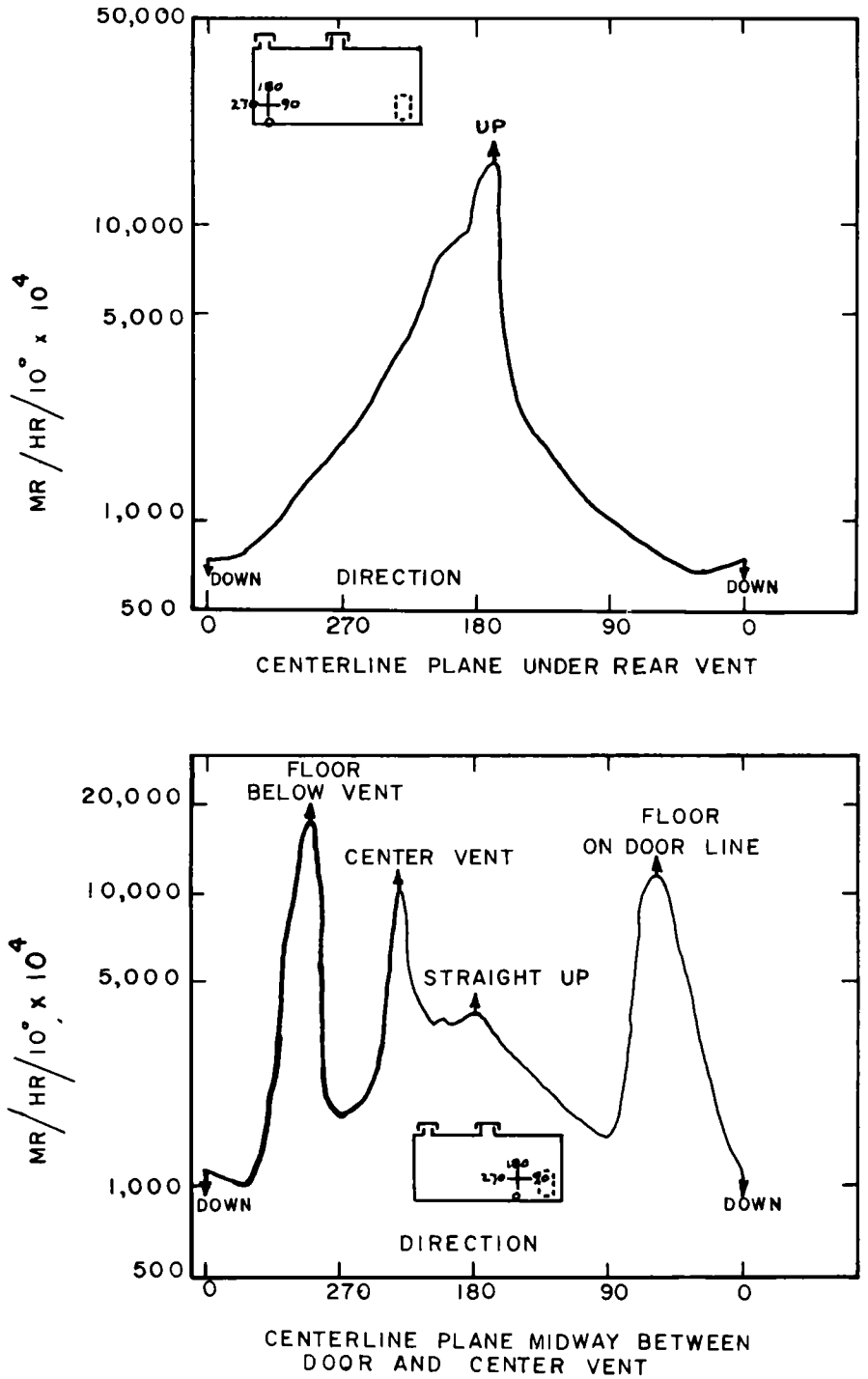

Fig. 3.27—Directional characteristics of gamma-radiation flux along shelter axis at two points of measurement, shot Diablo.

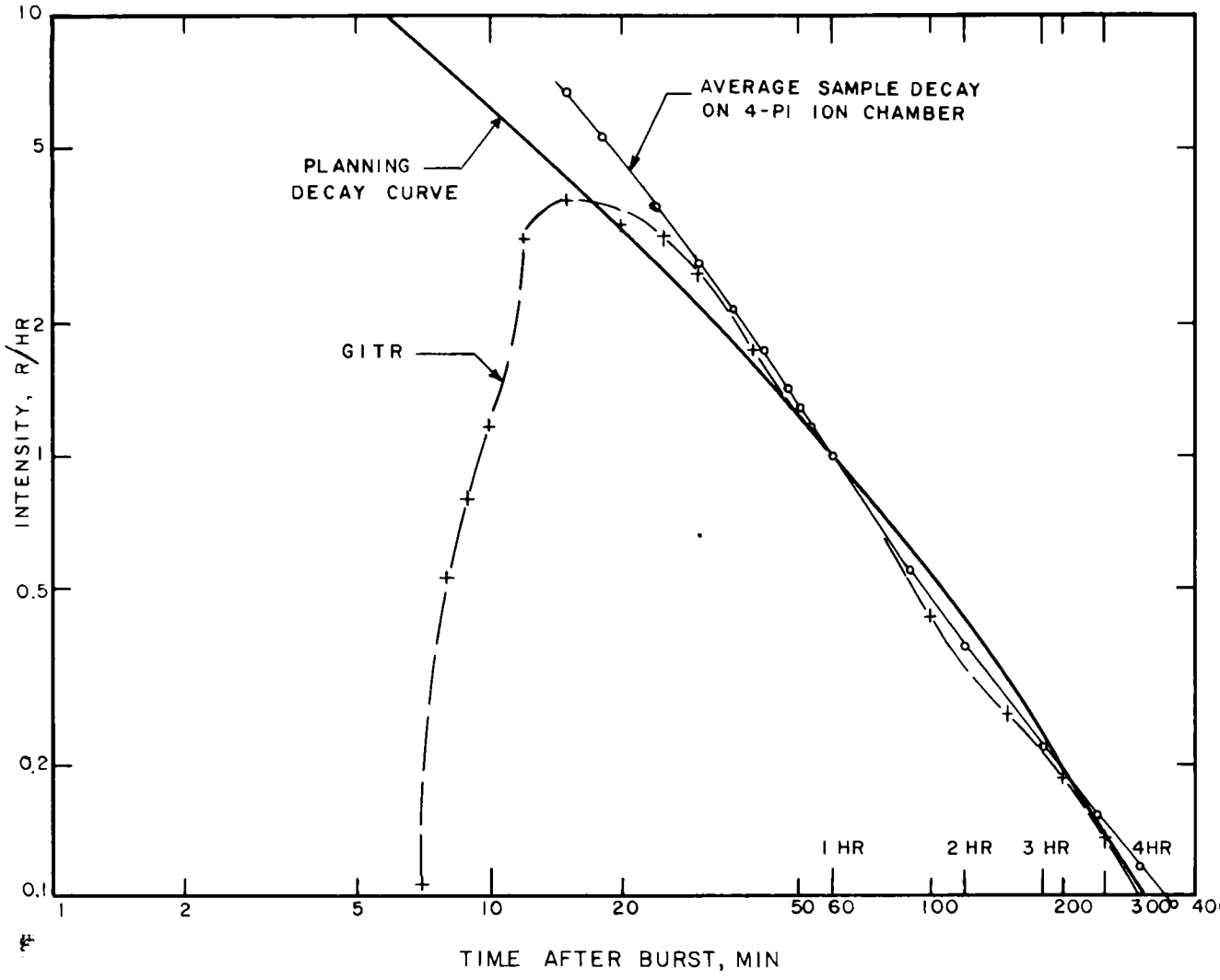

Fig. 3.28—Early decay measurements on shot Diablo, normalized to unit standard intensity.

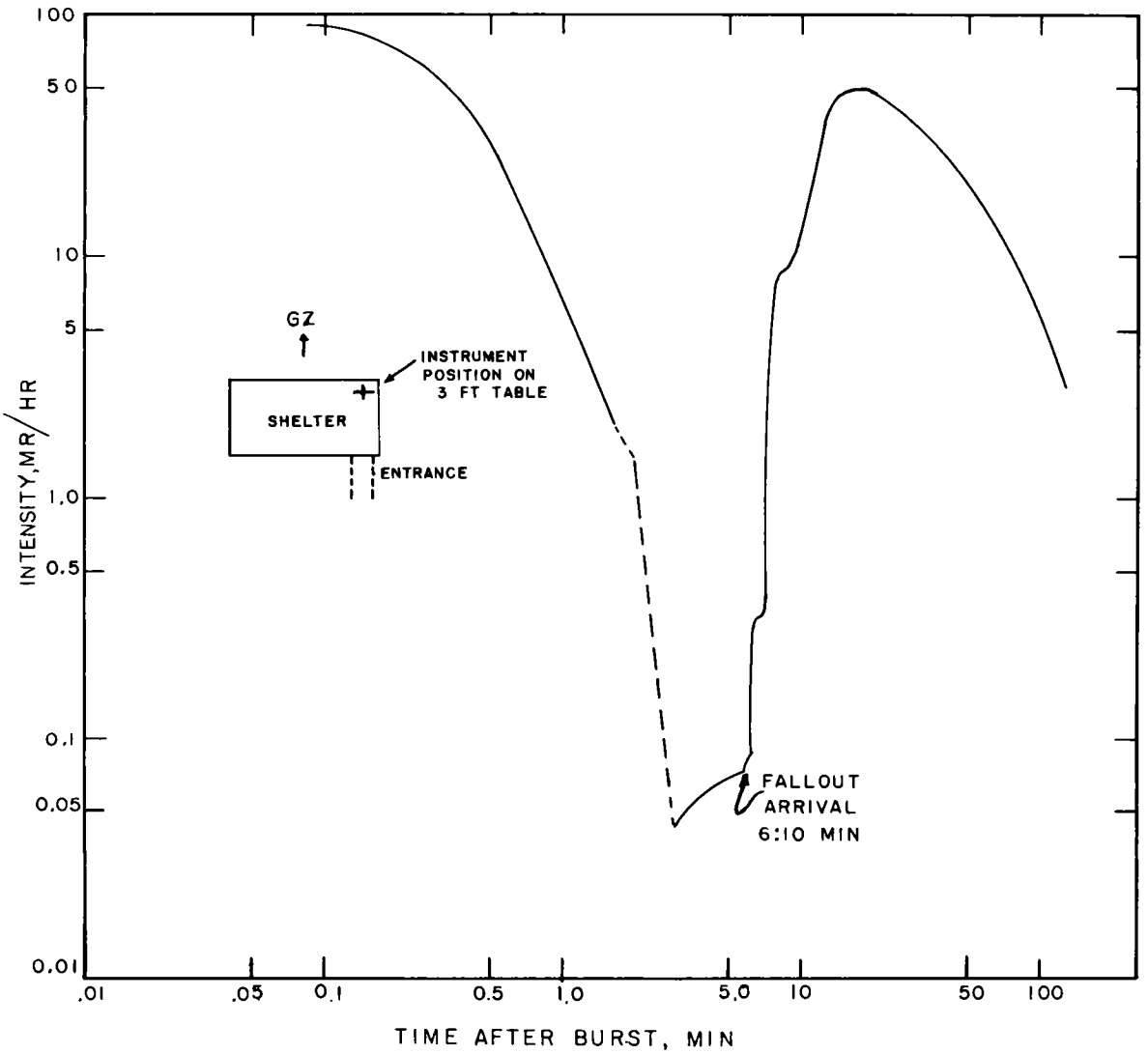

Fig. 3.29—Early intensity-time record on fixed AN/PDR-27C, shot Diablo.

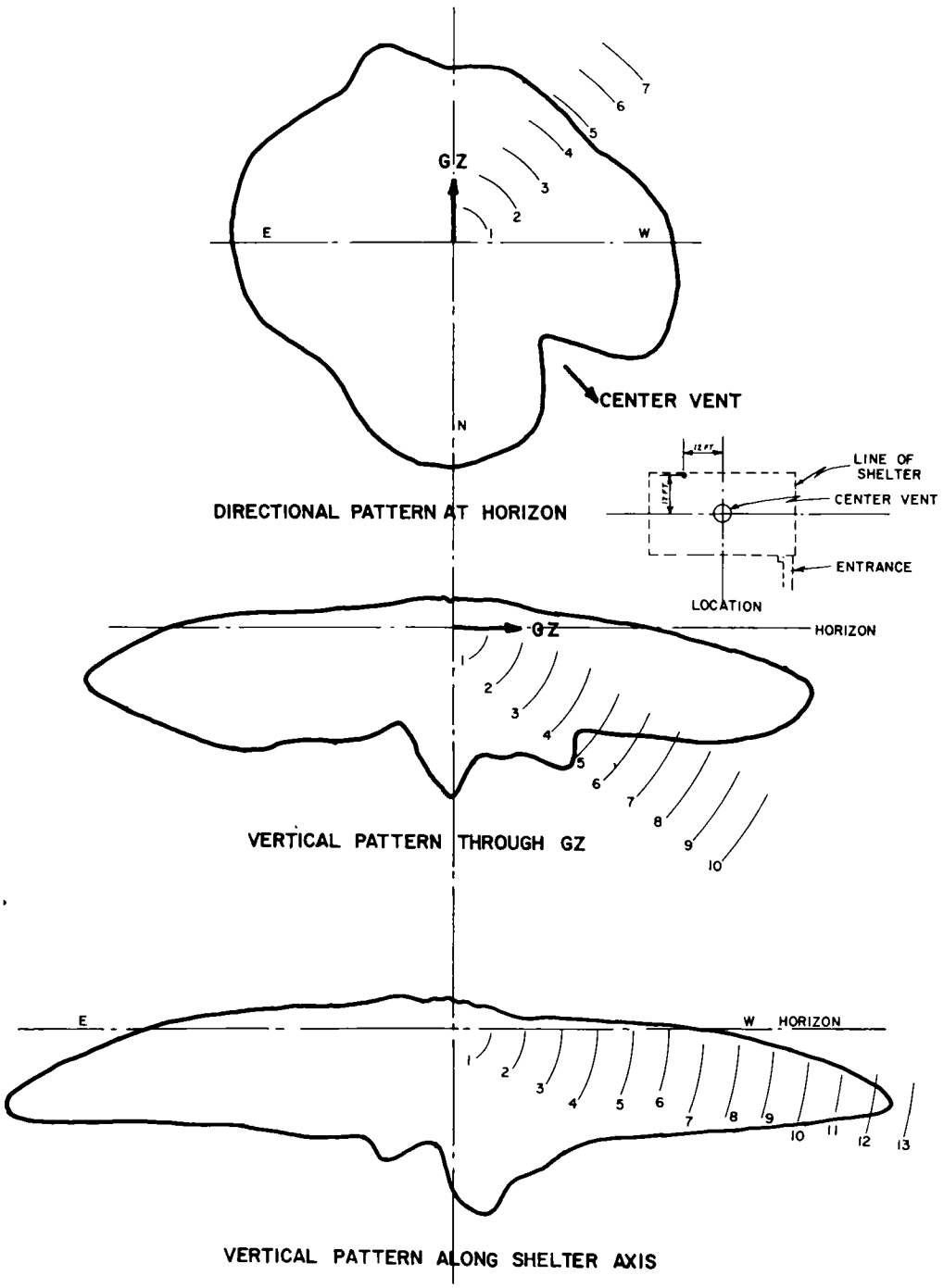

Fig. 3.30—Directional characteristics of radiation field on top of shelter, shot Diablo.

was contained in rather large spherical glassy fallout particles. The hottest tray (single particle) was collected between H+10½ and H+11½ min. The increase in collection due to the dust raised by the helicopter noted for the air samples is also shown in the incremental collector data between H+40 and H+46 min. The time of fallout arrival from the AN/PDR-27C inside the shelter indicated arrival of the first particle(s) on the shelter ramp at 6.17 min; it may be noted, from Fig. 3.29, that the instrument was in a particularly good position to observe the radiation beam through the entrance tunnel. The peak in the record of 50 mr/hr occurred at about H+17 min. Data from the directional gamma instrument, which was pointed directly upward at shot time, are shown in Fig. 3.31; the curve indicates fallout arrival between H+5 and H+6 min. The AN/PDR-27C was probably the most sensitive indicator of fallout arrival; the best value of fallout arrival for shot Diablo was therefore 6.2 min.

TABLE 3.27—INCREMENTAL-COLLECTOR DATA, SHOT DIABLO

Time interval, min	Activity,* counts/min	Cumulative activity, counts/min	Time interval, min	Activity,* counts/min	Cumulative activity, counts/min
0–1.25	0		30.2–31.2	10	10,493,000
1.25–2.25	13		31.2–32.2	17	10,493,000
2.25–3.25	17		32.2–33.2	0	10,493,000
3.25–4.25	14		33.2–34.2	0	10,493,000
4.25–5.25	0		34.2–35.2	0	10,493,000
5.25–6.25	97	97	35.2–36.2	0	10,493,000
6.25–7.25	1,026,000	1,026,000	36.2–37.2	20	10,493,000
7.25–8.25	47	1,026,000	37.2–38.2	0	10,493,000
8.25–9.25	1,671,000	2,697,000	38.2–39.2	0	10,493,000
9.25–10.2	1,117,000	3,814,000	39.2–40.2	17	10,493,000
10.2–11.2	1,688,000	5,502,000	40.2–41.2	20	10,493,000
11.2–12.2	488,900	5,991,000	41.2–42.2	34	10,493,000
12.2–13.2	163	5,991,000	42.2–43.2	167	10,493,000
13.2–14.2	1,208,000	7,199,000	43.2–44.2	467	10,494,000
14.2–15.2	117	7,199,000	44.2–45.2	0	10,494,000
15.2–16.2	938,800	8,138,000	45.2–46.2	22,460	10,516,000
16.2–17.2	541,000	8,679,000	46.2–47.2	0	10,516,000
17.2–18.2	97	8,679,000	47.2–48.2	0	10;516,000
18.2–19.2	434,600	9,114,000	48.2–49.2	0	10,516,000
19.2–20.2	60	9,114,000	49.2–50.2	0	10,516,000
20.2–21.2	70	9,114,000	50.2–51.2	0	10,516,000
21.2–22.2	33	9,114,000	51.2–52.2	47	10,516,000
22.2–23.2	168,000	9,282,000	52.2–53.2	34	10,516,000
23.2–24.2	308,900	9,591,000	53.2–54.2	281	10,517,000
24.2–25.2	393	9,591,000			
25.2–26.2	383,400	9,975,000			
26.2–27.2	518,300	10,493,000			
27.2–28.2	27	10,493,000			
28.2–29.2	0	10,493,000			
29.2–30.2	6	10,493,000			

*Counts per minute on an end-window gamma scintillation counter at H+31.5 hr.

The normalized and average decay curve from the 4π ion chamber data observed at the shelter was obtained from seven samples consisting of single particles (at early times) and groups of particles. The shapes of the decay curves from the different samples were the same within a few per cent (measurement error); the curves were therefore normalized at one time and averaged. The decay of particles later collected at station T2C (about 5 miles downwind) was the same as those collected at the shelter. The radioactive composition of

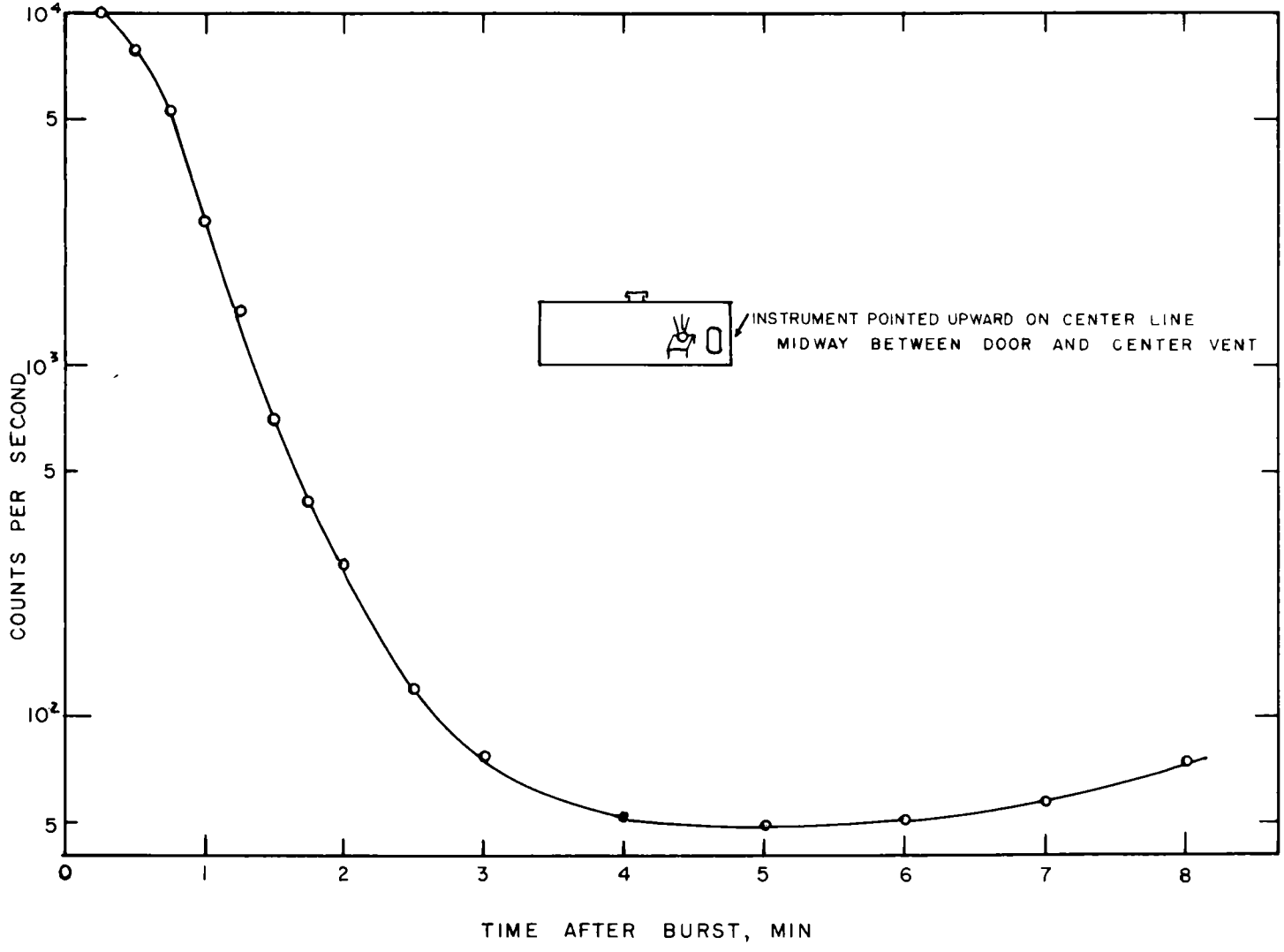

Fig. 3.31—Early intensity-time record on directional gamma instrument, shot Diablo.

all the large fallout particles must therefore have been about the same. Decay data from Project 32.4 fallout collectors and one cloud sample were obtained at USNRDL. The combined data, together with a curve calculated for unfractionated fission products,[3] are plotted in Fig. 3.32. It may be noted that the calculated curve and the curve from the cloud sample data are the same and that the data for the fallout particles and samples fall below the calculated curve by as much as a factor of 3. However, at later times the curves are tending to approach each other. Thus the fallout samples must have been depleted in many of the shorter lived fission products in order to exhibit the observed decay behavior.

The radiation field, as measured at about 3 ft above the top of the shelter (Fig. 3.30), was very flat or uniform in the horizontal plane. The direction of the maximum observed gamma count rate on the vertical pattern was 9°30′ below the horizon for both directions. Except for the larger readings at 90° from the horizontal, the bumps in the curves occur at angles corresponding to a line of sight through the cone of the detector to the edge of the dirt fill over the shelter. In these directions the detector "sees" more radioactive sources per unit of horizontal area.

The data in Fig. B.4 (Appendix B), when integrated in 4π for a thin spherical source about the detector, show that greater than 99 per cent of the count rate comes from the surface area of the source intercepted by a cone of 15° solid angle at the detector; this solid angle was used to estimate the fraction of the gamma radiation on top of the shelter which was emitted from sources various distances away.

If θ_0 is the angle down from the horizon for the center line of the 15° cone, h is the height of the instrument above the surface, and r is the distance from the observation point to the intersection of the center line of the cone with ground, then

$$r = h \cot \theta_0 \tag{3.16}$$

The distance, d, from the detector to the intersection is

$$d = \frac{r}{\cos} \theta_0 \tag{3.17}$$

The lateral distance, r^1, from the intersection of the center line of the cone (distance, d) is given by

$$r^1 = d \tan \phi \tag{3.18}$$

in which ϕ is the angle at the detector between the vertical plane through the center of the cone and the line along the edge of the cone that connects the end of r^1 to the point of the cone at the detector. Therefore ϕ can have values between 0° and 7°30′. Substituting for d in Eq. 3.18 gives

$$r^1 = \frac{h \tan \phi}{\sin \theta_0} \tag{3.19}$$

The total area seen by the detector is that bounded by the angle limits, $\theta_0 \pm 7°30'$ and $\phi = 0 \pm 7°30'$. Since the cone angle is fixed, the corresponding values θ and θ_0 and ϕ can be obtained from

$$x^2 + y^2 = 1 \tag{3.20}$$

and

$$\tan \theta = 0.1316y \tag{3.21}$$

and

$$\tan \phi = 0.1316x \tag{3.22}$$

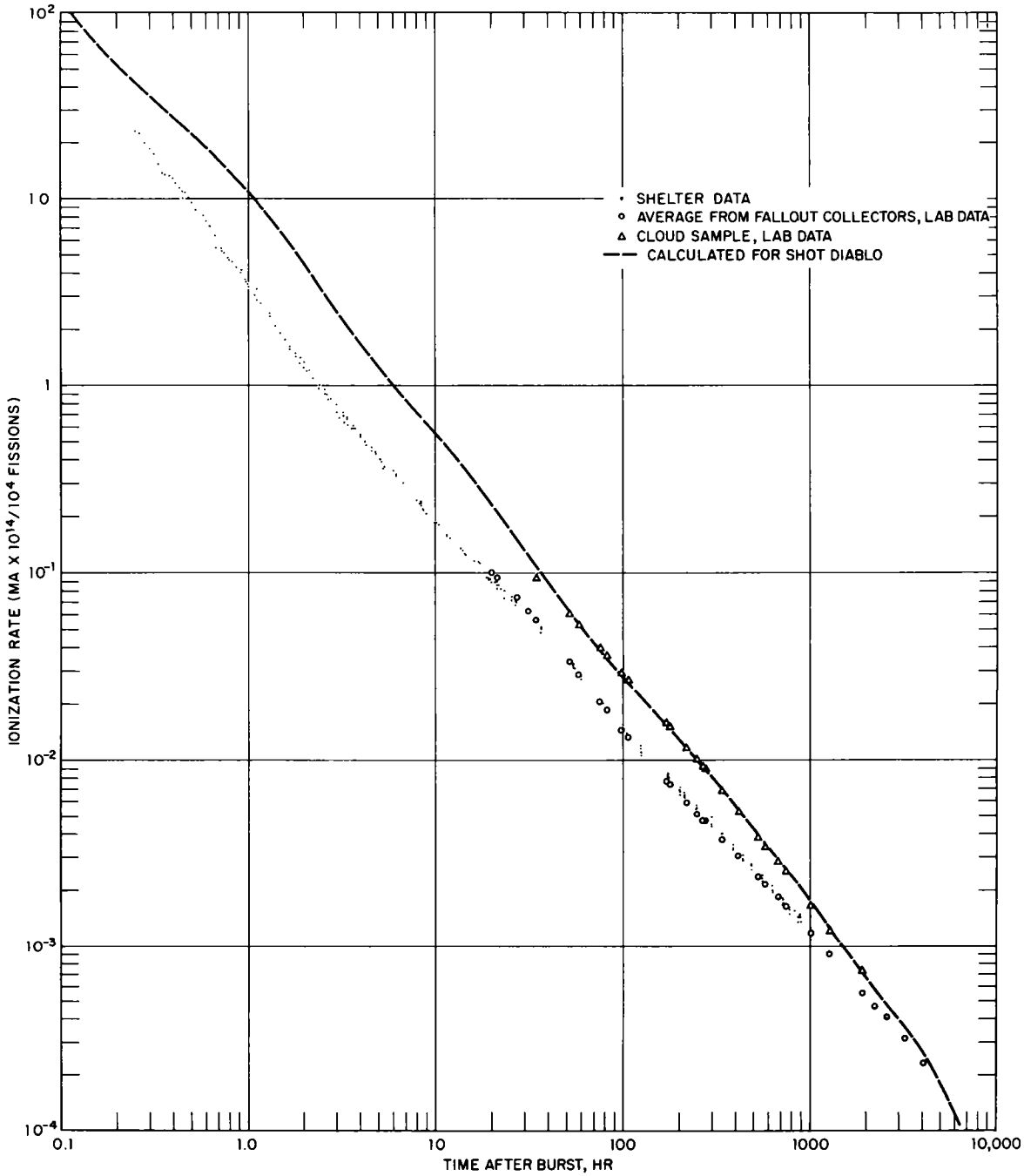

Fig. 3.32—USNRDL 4π ionization chamber data, shot Diablo.

where tan 7°30′ = 0.1316. The values of the equation constants are equivalent to a cone radius of 1 in. and a height of 7.6 in., where x and y are the coordinates of the base of the cone (zero at the center). A few paired values of θ, ϕ, r/h, and r^1/h for $\theta_0 = 15°$ are given in Table 3.28; the surface area seen by the detector for the 15° setting is shown in Fig. 3.33. The area within the elliptical figure is given by

$$A = \pi h^2(\Delta/2) \cot \theta \tan \bar{\phi}/\sin \bar{\theta} \tag{3.23}$$

in which $(\Delta/2) \cot \theta$ is half the difference between the values of cot $(\theta_0 - 7°30')$ and cot $(\theta_0 + 7°30')$, $\bar{\theta}$ is defined by

$$\cot \bar{\theta} = \tfrac{1}{2} [\cot (\theta_0 - 7°30') + \cot (\theta_0 + 7°30')] \tag{3.24}$$

and $\bar{\phi}$ is the angle corresponding to $\bar{\theta}$ via Eqs. 3.20, 3.21, and 3.22. The angle $\bar{\theta}$ is the angle to the center of gravity of the ellipse, and the distance from the detector defined by $\bar{\theta}$ was used as the distance of the equivalent point source from the detector. Using Eq. 3.23, the areas seen by the detector, given as $A/(\pi h^2)$, are computed in Table 3.29. The lowest angle used was 8°; at 7°30′ the maximum value of cot θ and $A/\pi h^2$ would be infinity. At 7°30′ above the horizon the detector observes only scattered radiation (assuming the radiations all arise from a plane source).

It will be assumed that the sources are uniformly distributed in estimating the contribution of the radiation from various distances to that measured by the detector. A more refined calculation could be made by using fallout pattern data in which the source strength from a given area would be weighted according to its pattern values. The observed count rates (values are proportional to those given in Fig. 3.30) and average count rate per unit area are given in Table 3.30. All the count-rate values, of course, contain contributions from radiations scattered into the cone from sources outside the surface area seen by the detector. The relative contribution of the sources per unit area is relatively small from the areas farthest away. Since the detector was 3 ft above the ground, the center of gravity for the 8° angle is 177 ft away, the distance to the farthest source in the area would be 344 ft, and the distance to the near source would be about 11 ft. The values of the relative count rate per unit area are plotted against distance to the center of gravity for the area in Fig. 3.34.

If the distance from the detector to the center of gravity of the area seen by the detector is defined as $\bar{r}$, then the total radiation that would be received by an unshielded detector would be $2\pi\bar{r}$ times that coming from the center of gravity (i.e., as a point source) to the shielded detector. Since $\bar{r}$ is the same as h cot $\bar{\theta}$, new relative count-rate units will be obtained if the values in Table 3.30 are simply multiplied by cot $\bar{\theta}$. If a calibrated detector were used, then the total radiation received from the distance $\bar{r}$ away would be given by

$$I(\bar{r}) = \frac{4 I_A \cos \bar{\theta}}{h(\Delta \cot \theta) \tan \bar{\phi}} \tag{3.25}$$

in which $I(\bar{r})$ is the intensity at the unshielded detector from the distance $\bar{r}$, and I_A is the intensity at the collimated detector from the area A (averaged for an equivalent point source at the distance $\bar{r}$). The values of $I(\bar{r})$, in relative units, are plotted in Fig. 3.35 against cot $\bar{\theta}$. The peak contribution comes from a distance of cot $\bar{\theta}$ equal to about 0.92, or about $2\frac{3}{4}$ ft from the detector rather than from an angle of about 10° (17 ft) shown in Fig. 3.30 for the observed data.

Integrating the curve in Fig. 3.35 out to $I(\bar{r}) = 0$ and normalizing the relative values to the total should give the per cent contribution to the count rate up to a given distance from an unshielded detector. The results are given in Table 3.31 and are plotted in Fig. 3.36. The unshielded detector must have the same response to the radiations as the shielded detector that was used to take the measurements. For these calculations from the data, 50 per cent of the total comes from distances up to cot $\bar{\theta} = 12$ (36 ft), 99 per cent comes from distances up to cot $\bar{\theta} = 83$ (249 ft), and essentially 100 per cent comes from within a 300-ft circle.

TABLE 3.28—COMPUTATION OF CONE-EDGE INTERCEPT WITH THE SURFACE FOR $\theta_0 = 15°$*

θ^1	θ	r/h = cot θ	ϕ	tan ϕ	sin θ	$r^1h = \frac{\tan \phi}{\sin \theta}$
0	15°	3.73	7°30′	0.1316	0.259	0.508
0	15°	3.73	7°30′	0.1316	0.259	0.508
+3°46′	18°46′	2.94	6°33′	0.1140	0.322	0.354
−3°46′	11°14′	5.04	6°33′	0.1140	0.195	0.584
+5°19′	20°19′	2.70	5°19′	0.0930	0.347	0.268
−5°19′	9°41′	5.86	5°19′	0.0930	0.168	0.554
+6°33′	21°33′	2.53	3°46′	0.0658	0.367	0.179
−6°33′	8°27′	6.73	3°46′	0.0658	0.147	0.448
+7°30′	22°30′	2.41	0	0	0.383	0
+7°30′	7°30′	7.60	0	0	0.131	0
+7°16′	22°16′	2.44	1°53′	0.0329	0.379	0.0868
−7°16′	7°44′	7.36	1°53′	0.0329	0.135	0.244
−3°42′	11°18′	5.00	6°32′	0.1145	0.196	0.584

* $\theta = \theta_0 \pm \theta^1$.

TABLE 3.29—COMPUTATION OF THE AREAS SEEN BY THE DETECTOR AT SEVERAL VALUES OF θ_0

θ_0	Cot θ_0	(Δ/2) cot θ	Cot $\bar{\theta}$	tan $\bar{\phi}$	sin $\bar{\theta}$	$A/\pi h^2$
8°	7.12	55.49	59.10	0.0456	0.0169	150
10°	5.67	9.86	13.04	0.0874	0.0764	11.3
15°	3.73	2.60	5.00	0.1145	0.196	1.52
22°30′	2.41	1.00	2.73	0.1248	0.344	0.363
30°	1.73	0.555	1.86	0.1280	0.474	0.150
37°30′	1.303	0.365	1.36	0.1300	0.592	0.0801
45°	1.00	0.268	1.04	0.1304	0.695	0.0503
52°30′	0.767	0.212	0.788	0.1309	0.785	0.0353
60°	0.577	0.176	0.590	0.1311	0.861	0.0268
67°30′	0.414	0.154	0.422	0.1313	0.921	0.0220
75°	0.268	0.141	0.273	0.1315	0.965	0.0192
82°30′	0.132	0.134	0.134	0.1316	0.991	0.0178
90°	0.000	0.1316	0.000	0.1316	1.000	0.0173

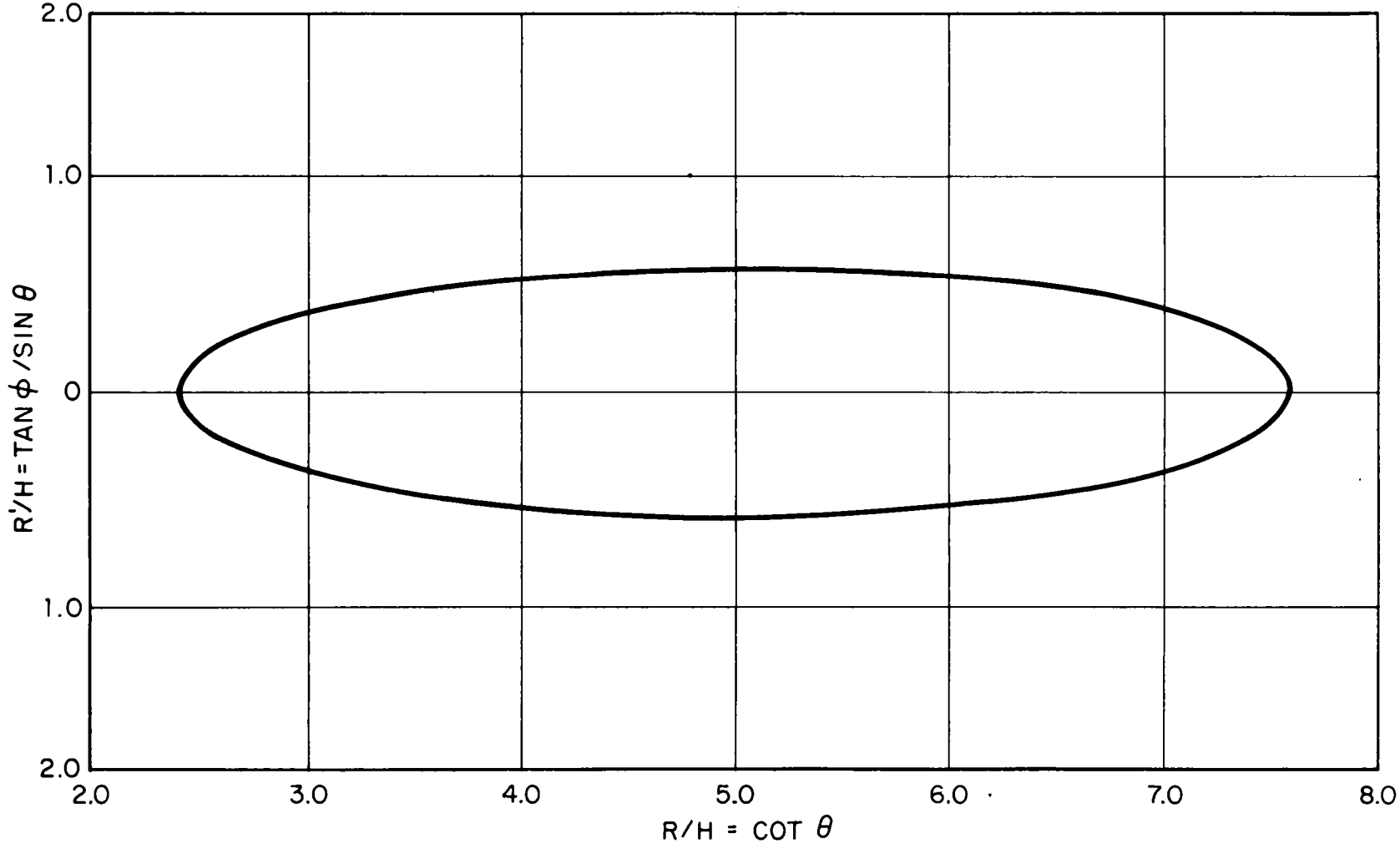

Fig. 3.33—Surface area seen by detector for $\theta_0 = 15°$, detector at r/h = 0.

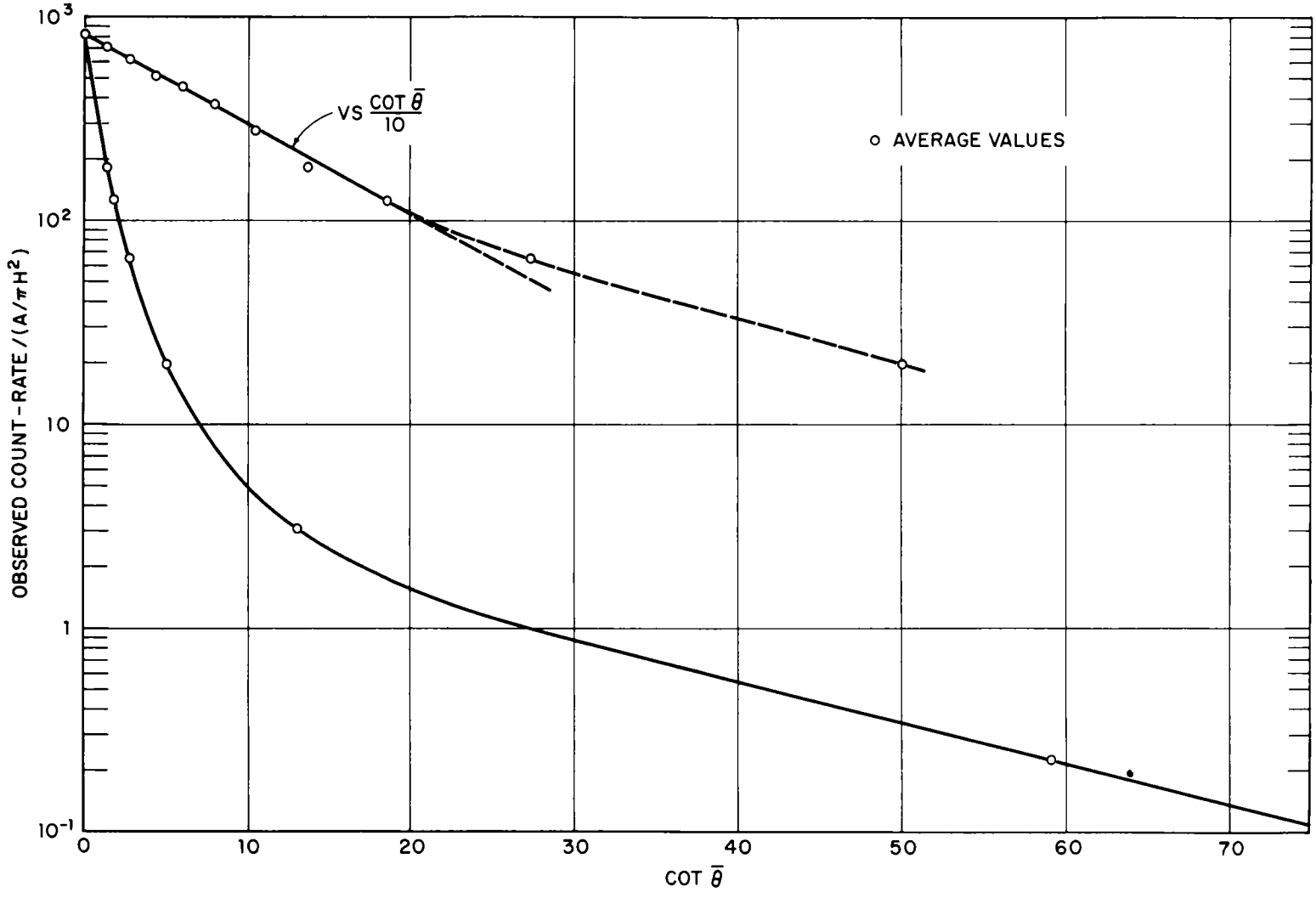

Fig. 3.34—Variation of count rate per unit area with distance of center of gravity of area seen by the detector.

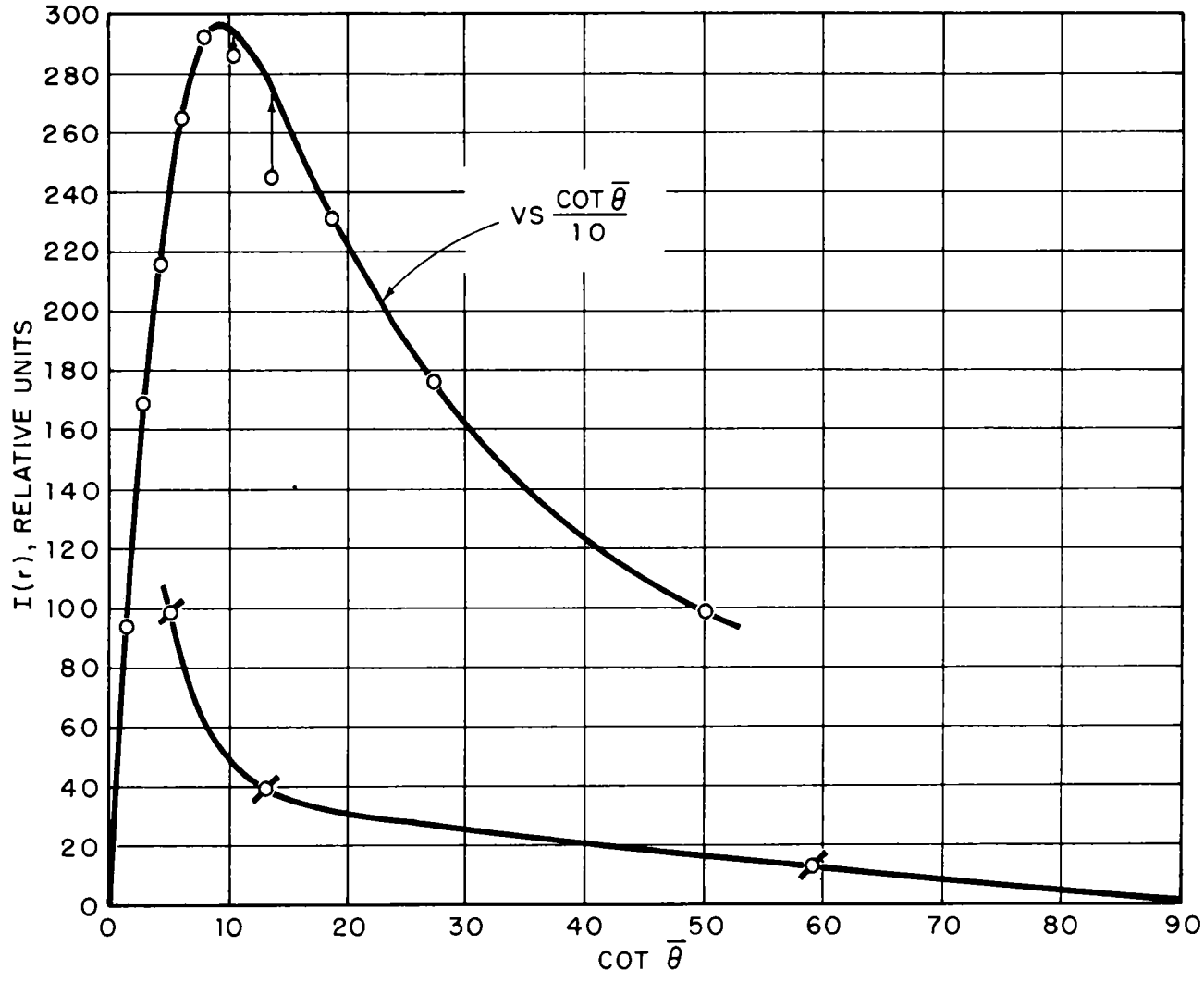

Fig. 3.35—Variation of relative contribution of sources for uniform contamination about the shelter with distance from an unshielded detector.

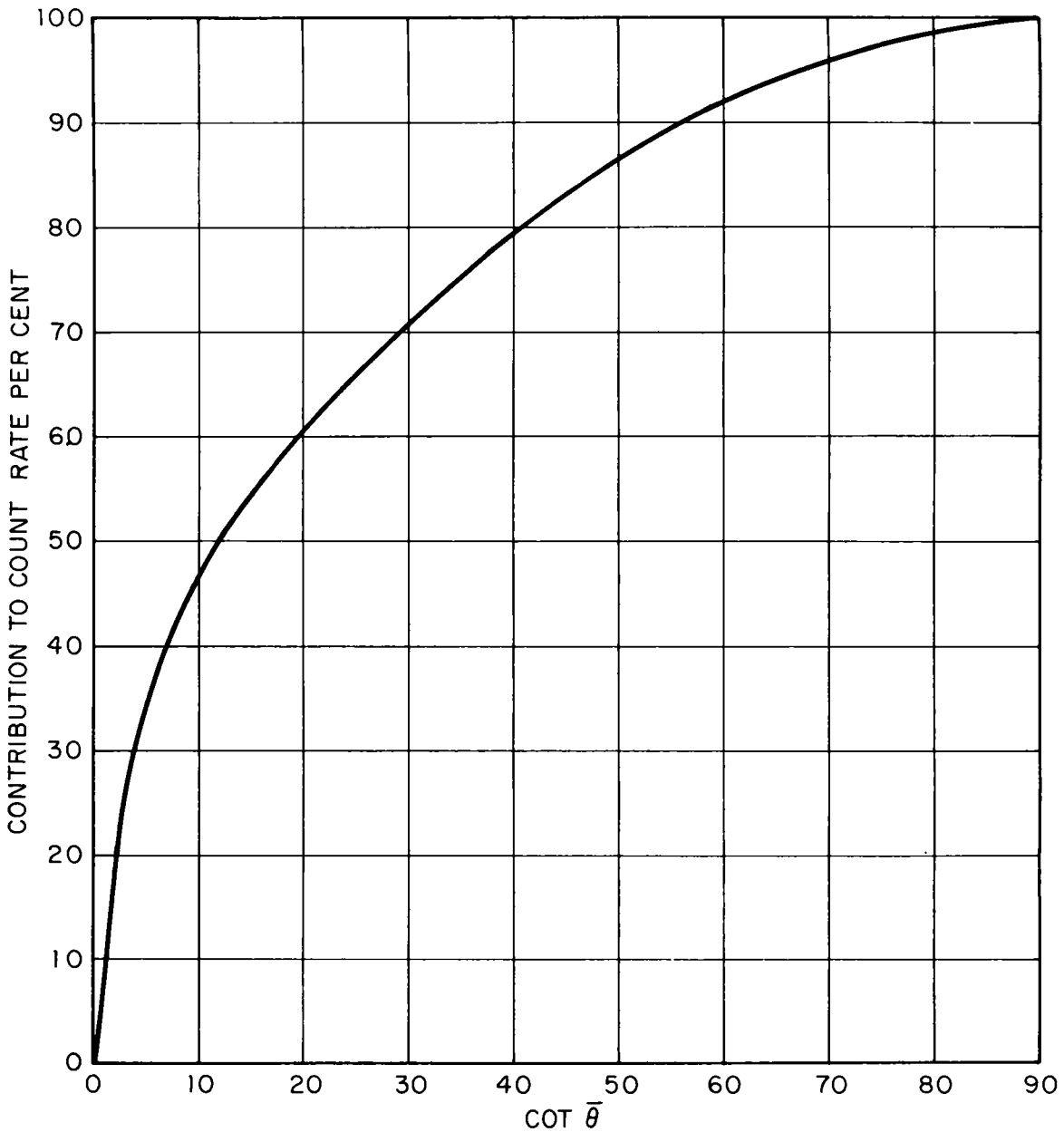

Fig. 3.36—Contribution to radiation seen by an unshielded detector up to a given distance from the shelter, shot Diablo.

The calculations given are actually only first approximations of the contributions from the various areas seen by the detector; these calculations and the actual fallout contour values could be used to redetermine a more accurate relative count-rate value and location of the center of gravity for each area seen by the detector.

3.5.2 Shot Shasta

The technical supporting studies on shot Shasta consisted in (1) the GITR data, (2) the incremental fallout collector data, and (3) the decay of fallout samples as measured in the 4π ion chamber.

TABLE 3.30—OBSERVED COUNT RATES AND COUNT RATES AT THE DETECTOR PER UNIT AREA OF SURFACE

	Observed count rate, relative units				Average observed count rate/$(A/\pi h^2)$, relative units				
θ_0	North	East	South	West	North	East	South	West	Average
8°	31.3	37.1	29.3	36.3	0.209	0.247	0.195	0.242	0.223
10°	30.9	38.3	30.7	37.4	2.74	3.39	2.72	3.31	3.04
15°	27.9	31.1	29.8	31.0	18.4	20.4	19.6	20.4	19.7
22°30′	24.0	21.4	25.0	23.0	66.1	59.0	68.8	63.4	64.3
30°	20.7	17.6	18.2	18.3	138	117	121	122	124
37°30′	14.6	13.3	14.3	15.6	182	166	178	195	180
45°	13.6	13.2	14.4	14.3	270	262	286	284	275
52°30′	11.7	11.9	14.8	14.0	331	337	419	397	371
60°	9.3	12.4	12.4	14.0	347	463	463	522	449
67°30′	9.7	11.8	11.8	11.8	441	536	536	536	512
75°	11.2	10.2	11.0	15.3	583	531	573	797	620
82°30′	12.7	10.1	11.7	15.6	713	567	657	876	703
90°	14.2	13.8	14.2	13.8	821	798	821	798	810

TABLE 3.31—SUMMARY OF ACCUMULATIVE RELATIVE CONTRIBUTION TO RADIATION AT AN UNSHIELDED DETECTOR AT THE SHELTER FOR UNIFORM CONTAMINATION ABOUT THE SHELTER

Cot $\bar{\theta}$	Contribution to count rate, %	Cot $\bar{\theta}$	Contribution to count rate, %
0	0	20	60.2
1	7.92	30	70.6
2	17.6	40	79.4
3	24.7	50	86.5
4	30.0	60	91.8
5	34.0	70	95.8
6	37.4	80	98.5
8	42.6	90	99.8
10	46.6	100	100
15	54.2		

The GITR data are given in Fig. 3.21; the data indicate fallout arrival at H+8 min and a peak at H+18 min. The rate-meter data in Fig. 3.22 indicate a time of arrival of H+9.7 min. The incremental-collector data are given in Table 3.32; these data show a time of arrival between H+9 and H+10 min. The peak rate of collection occurred between H+12 and H+13 min. After H+17 min only two fairly large particles were collected, one between H+19 and H+20 min and the other between H+24 and H+25 min. Small amounts of activity were collected after H+25 min, but, so far as the cumulative sum is concerned, the amounts were negligible.

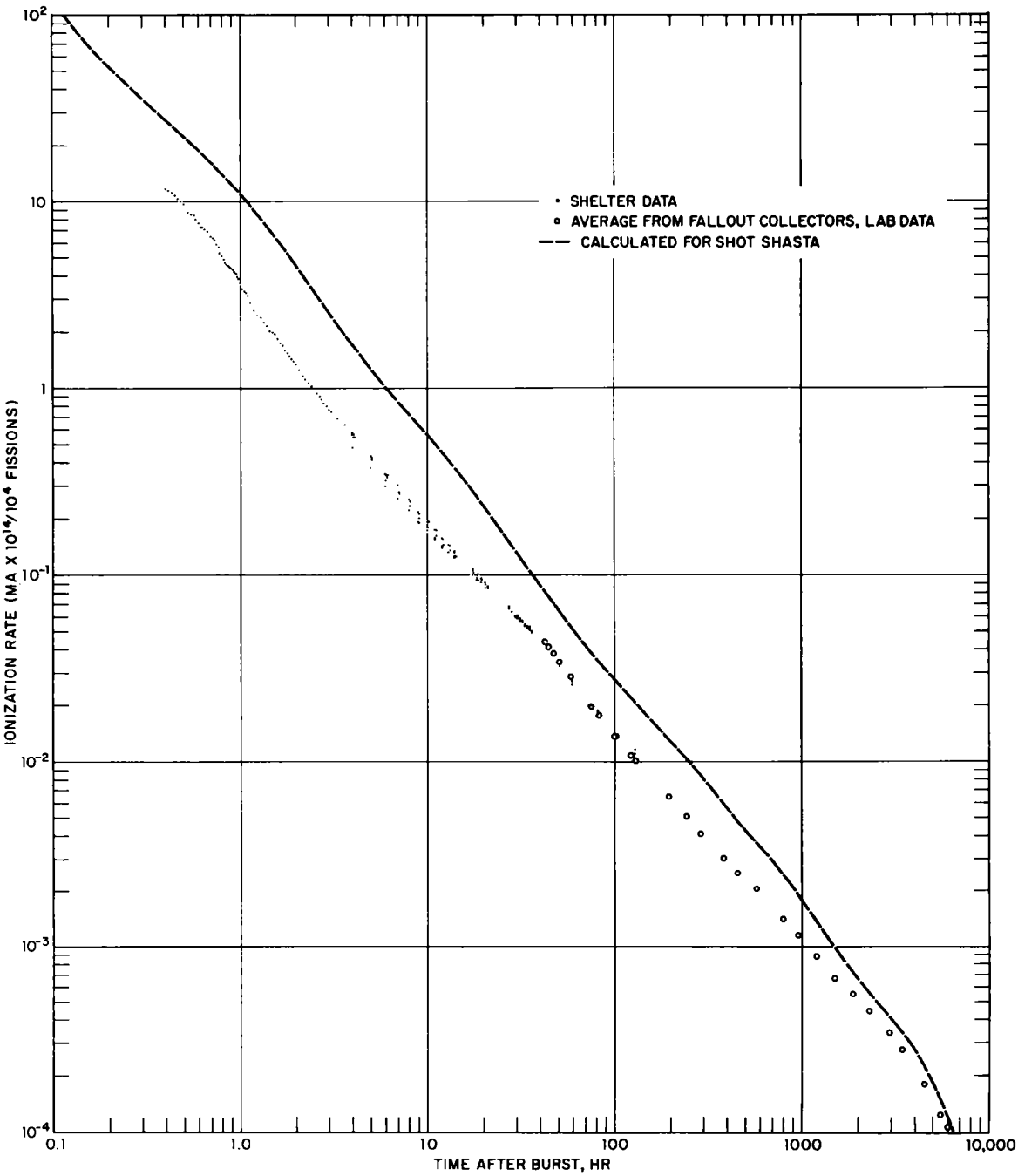

Fig. 3.37—USNRDL 4π ionization chamber data, shot Shasta.

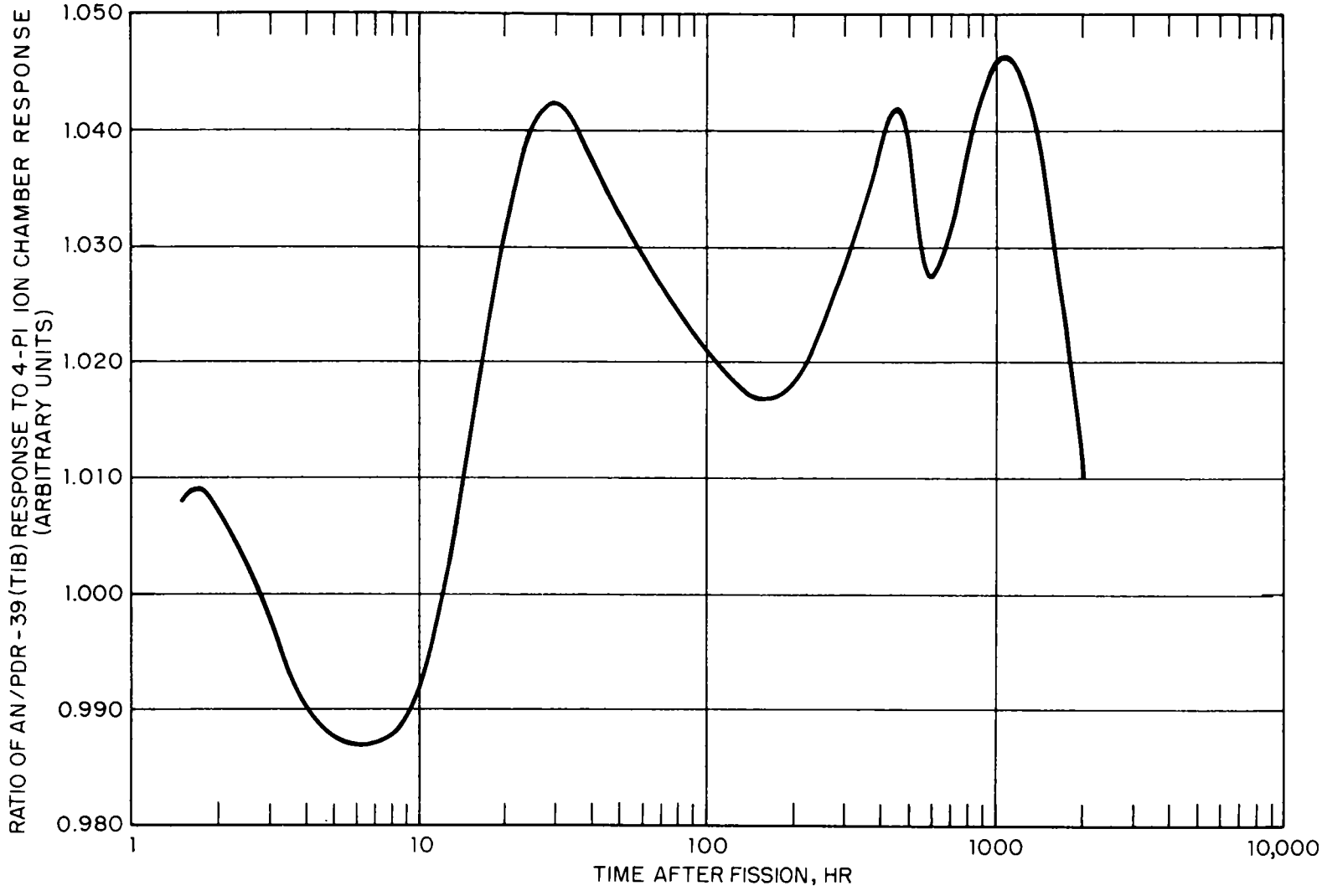

Fig. 3.38—Ratio of AN/PDR-39(T1B) response to a distributed fission-product source to the 4π ion chamber response to small samples of fission products.

The decay of five fallout particles and three groups of particles was taken at the shelter starting at H+24 min. Decay of five fallout samples collected by Project 32.4 was taken at USNRDL. The data are plotted in Fig. 3.37. The averaged decay data are identical to those observed for shot Diablo. From about H+½ to H+2½ hr, the logarithmic slope is −1.46; a single line from H+4 to H+1000 hr gives a slope of −1.14. The difference between the observed decay data of samples for the 4π ion chamber and those for a radiac instrument used to measure an extended source of fission products is shown in Fig. 3.38, where the ratio of the AN/PDR-39(T1B) response to that of the 4π ion chamber for fission products is plotted as a function of time after fission. The ratio was arbitrarily adjusted to 1.000 at H+1 hr;

TABLE 3.32—INCREMENTAL-COLLECTOR DATA, SHOT SHASTA

Time interval, min	Activity,* counts/min	Cumulative activity, counts/min	Time interval, min	Activity,* counts/min	Cumulative activity, counts/min
0 −5.25	429		34.2−35.2	280	12,210,000
5.25−6.25	159		35.2−36.2	355	12,210,000
6.25−7.25	3		36.2−37.2	220	12,210,000
7.25−8.25	23		37.2−38.2	180	12,210,000
8.25−9.25	87	87	38.2−39.2	175	12,210,000
9.25−10.2	970,000	970,100	39.2−40.2	125	12,210,000
10.2 −11.2	2,390,000	3,360,000	40.2−41.2	180	12,210,000
11.2 −12.2	2,160,000	5,520,000	41.2−42.2	165	12,210,000
12.2 −13.2	4,300,000	9,820,000	42.2−43.2	175	12,210,000
13.2 −14.2	830,000	10,650,000	43.2−44.2	135	12,210,000
14.2 −15.2	420,000	11,070,000	44.2−45.2	225	12,210,000
15.2 −16.2	176,000	11,250,000	45.2−46.2	210	12,210,000
16.2 −17.2	630,000	11,880,200	46.2−47.2	195	12,210,000
17.2 −18.2	135	11,880,000	47.2−48.2	160	12,210,000
18.2 −19.2	1,210	11,880,000	48.2−49.2	195	12,210,000
19.2 −20.2	126,850	12,010,000	49.2−50.2	180	12,210,000
20.2 −21.2	75	12,010,000	50.2−51.2	135	12,210,000
21.2 −22.2	40	12,010,000	51.2−52.2	185	12,210,000
22.2 −23.2	5	12,010,000	52.2−53.2	80	12,210,000
23.2 −24.2	110	12,010,000	53.2−54.2	85	12,210,000
24.2 −25.2	202,000	12,210,000	54.2−55.2	145	12,210,000
25.2 −26.2	135	12,210,000	55.2−56.2	50	12,210,000
26.2 −27.2	95	12,210,000	56.2−57.2	65	12,210,000
27.2 −28.2	115	12,210,000			
28.2 −29.2	125	12,210,000			
29.2 −30.2	115	12,210,000			
30.2 −31.2	165	12,210,000			
31.2 −32.2	120	12,210,000			
32.2 −33.2	200	12,210,000			
33.2 −34.2	215	12,210,000			

*Counts per minute on an end-window gamma scintillation counter at H+77 hr.

the maximum difference in the ratio up to H+2000 hr (83 days) is about 6 per cent. Hence the shape of the ion-chamber decay curve would be almost identical to the shape of the roentgens per hour decay curve.

If calculated and observed decay curves become coincident at a later date, it may be possible to determine, by subtraction and curve resolution, some of the important radionuclides that are missing in the fallout samples at earlier times.

3.5.3 Comparison of GITR and Incremental-collector Data for Shots Diablo and Shasta

Decay-correcting the GITR data to a given time after detonation should result in a curve with time after burst similar in shape to that for the accumulated activity from the incremental collector (1) if the GITR readings are due mainly to radiations from fallout deposited on the ground and (2) if the incremental collections are a reasonably reliable representation of the accumulation of fallout at the shelter during the fallout period. If, at any time, the contribution of airborne (falling) particles to the radiation intensity as measured by the GITR is an appreciable fraction of the total, then the decay-corrected GITR data should lie above the accumulated activity data for the incremental collector when the two are normalized to the same value at the cessation of fallout.

The decay-corrected GITR data and incremental-collector data for shot Diablo adjusted to 14.0 r/hr at 1 hr are shown in Fig. 3.39. The rise of I(1), roentgens per hour at 1 hr, for the GITR between 3 and 6 min after burst is due to transit radiation from the approaching particle cloud. The single particle collected some time between 6.25 and 7.25 min contributed about 10 per cent to the total activity in all the increments collected. The incremental-collector data show that only about a dozen large particles were collected over the whole fallout period; thus the small collectors (3 in. diameter) did not give a quantitative measure of the rate of fallout arrival.

If the time of fallout cessation is defined as the time when 99 per cent had been deposited, the GITR data give a cessation time of 26.3 min, and the incremental-collector data give 26.5 min. The same treatment of the data from the outside cyclic air-sampler data gives a cessation time for 99 per cent collection of 27.9 min. This result is reasonable since the cyclic air sampler collected none of the large particles that contained most of the activity and since the small particles, which did not contribute significantly to the GITR readings or to the total count rate for the collector, continued to arrive at later times than the large particles.

If fallout arrival is defined as the time when 0.1 per cent of the fallout had arrived (i.e., a measurable amount), the arrival time from the incremental-collector data was 6.4 min. The GITR data cannot be used to determine an arrival time by this definition since the transit radiation gave I(1) values that were greater than 0.1 per cent at the minimum. If arrival time of 6.1 min is associated with the GITR data, then the defined fallout period was 20.2 min for that data and 20.4 min from the incremental-collector data.

The decay-corrected GITR data and the incremental-collector data for shot Shasta, adjusted to 24.6 r/hr at 1 hr, are given in Fig. 3.40. In this case a single particle that contributed about 10 per cent of the total activity collected arrived between 9.25 and 10.25 min after burst, and, since additional large particles were collected in all intervals up to 16.25 min, all the early incremental-collector I(1) values are further above the GITR I(1) values than they were for shot Diablo. The time of cessation values, however, again are in good agreement; the time for 99 per cent deposited is 23.8 min from the GITR data and 24.3 min from the incremental-collector data. The depression in the difference curve between H+16 and H+20 min for the GITR I(1) values is an indication of the presence of more radiation contributing to the GITR reading than can be attributed to that from the deposited material alone. Thus, at this time, a measurable amount of transit radiation was evidenced. The fallout cessation time for the outside cyclic air sampler was about 69 min. The large difference in the cessation time between that for the "fallout" data and the "aerosol" data indicates the presence of many more small particles arriving for shot Shasta (2 miles from GZ) than for shot Diablo (1 mile from GZ). The continuing arrival of small amounts of activity is also shown by the incremental-collector data for shot Shasta (Table 3.32), but the amounts are not large enough to make significant contributions to the cumulative sum. Actually, fallout never ceases in an absolute sense; extremely small particles from the shots will be falling over the world (including the shelter location) for many years to come. The above definitions of arrival and cessation time were made to bound the amount of fallout to within 1.2 per cent of that which is readily measured.

The time of arrival for 0.1 per cent on shot Shasta from the GITR data is 11.2 min, which gives a defined fallout interval of 12.6 min. The arrival time from the incremental-collector data is 9.9 min, giving a defined fallout interval of 14.4 min. The minimum in the

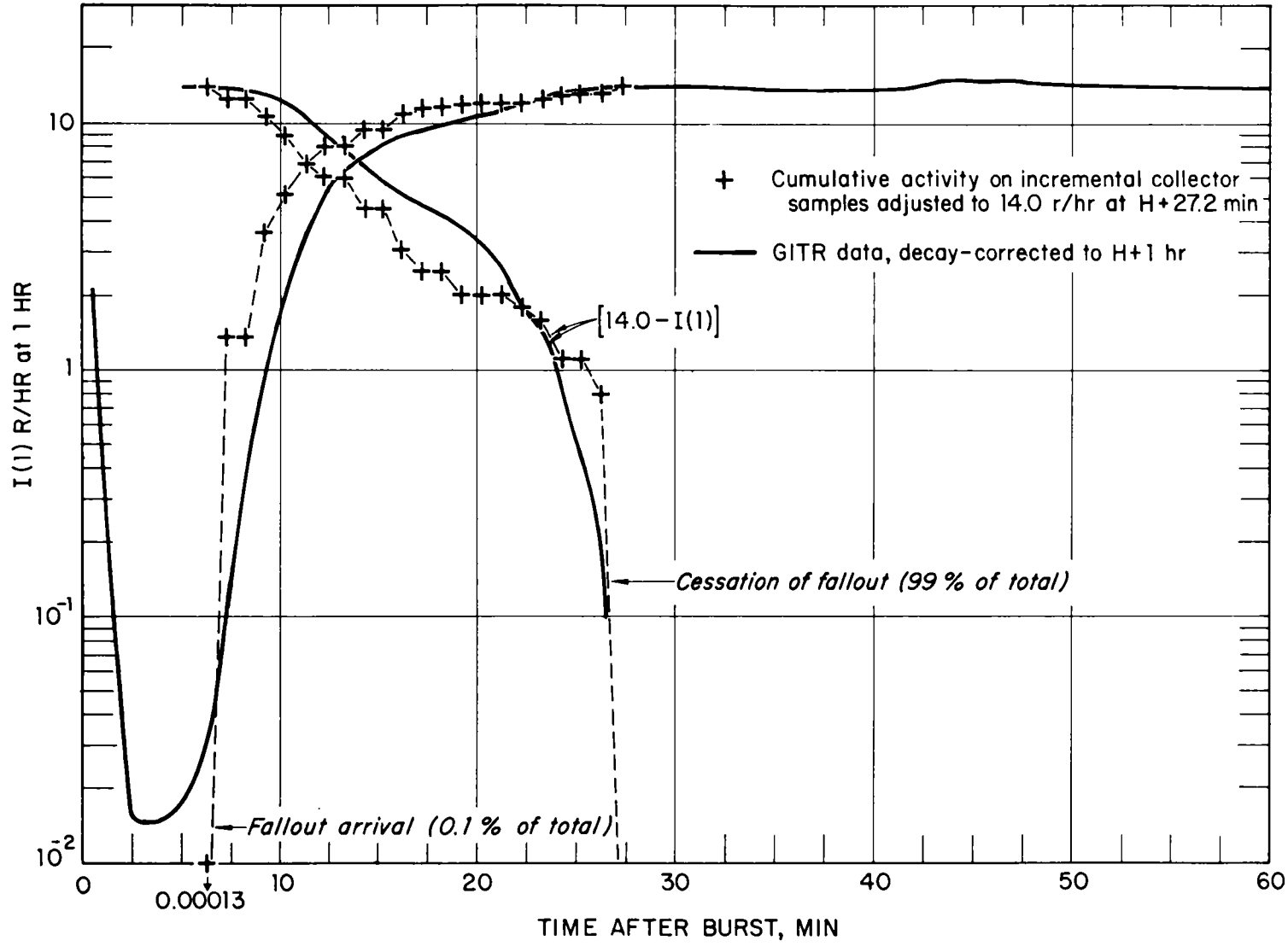

Fig. 3.39—Decay-corrected GITR data and incremental-collector data, shot Diablo.

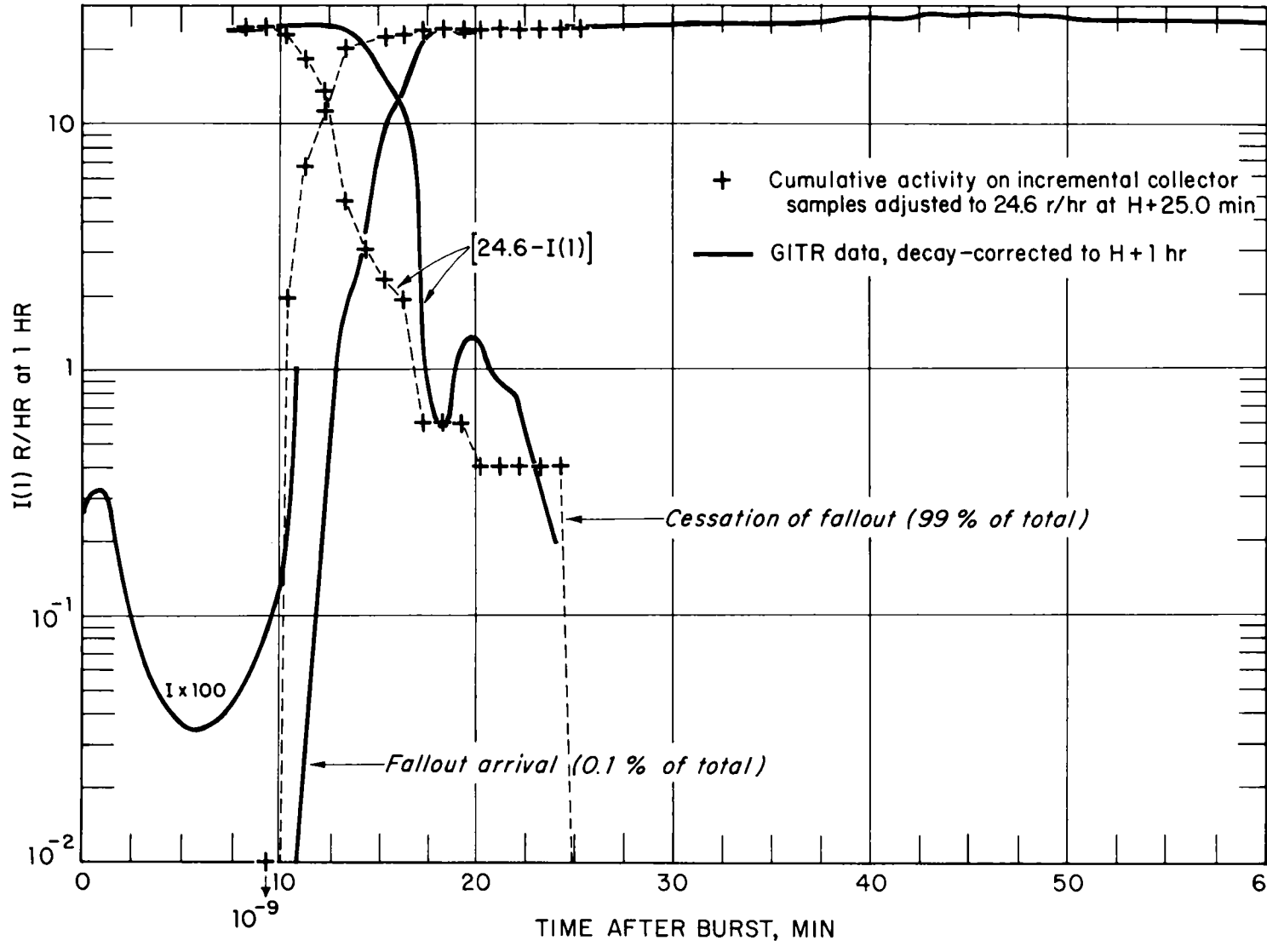

Fig. 3.40—Decay-corrected GITR data and incremental-collector data, shot Shasta.

GITR data occurred at about 6 min with an I(1) value of 0.00034 r/hr at 1 hr; this is much less than 0.1 per cent of the total at fallout cessation, and hence it was possible to obtain an arrival time from the GITR data.

The relative amount of fallout collected up to a given fraction of the fallout interval is given in Fig. 3.41. Although the sampling was undoubtedly statistically poor, the curves show, qualitatively, that, up to 0.3 or 0.4 of the fallout interval, the fallout arrived at a more rapid rate than it did toward the end of the period. On shot Shasta the shelter was nearer the center, or hot line, of the fallout area than for shot Diablo. This may account for the more rapid accumulation for shot Shasta during the first half of the fallout interval.

The relative decay-corrected GITR readings at fractions of the fallout interval are given in Fig. 3.42. If the GITR readings included no contribution from transit radiation and if the incremental-collector data accurately represented the accumulation of fallout at the shelter, the curves in the two figures should be identical for the respective shots. Except for the bump in the curve for the GITR data from shot Shasta, the respective curves are qualitatively similar. This similarity was used to trace in the line on the curve for estimating the contribution from the deposited fallout for shot Shasta. The difference curve (transit contribution) shows that the peak contribution from transit radiation between 0.5 and 0.6 of the fallout interval for shot Shasta was about 10 per cent. On shot Diablo there was little or no contribution from transit radiation after about 0.3 of the fallout interval. On both shots the curved portion of the plots from 0.0 to 0.2 of the fallout interval indicates the detection of some transit radiation owing to the approach of the falling particles. The incremental-collector data do not show any such curvature at the beginning of fallout. The discrepancy between the two sets of curves (decay-corrected GITR vs. incremental collector) at the times when the curves are the steepest is equivalent to about 0.14 to 0.18 of the fallout interval. This would be about a 3-min error for a 20-min fallout interval and larger than a 2-min error for a 13-min fallout interval. But, since the arrival and cessation times for the two sets of data differed only by 0.3 and 0.2 min, respectively, for shot Diablo and 1.3 and 0.5 min, respectively, for shot Shasta, most of the error must have been due to the poor sampling statistics of the incremental collector.

Smoothed values of the rate of fallout arrival (GITR data) as a function of the fraction of the fallout interval are plotted in Fig. 3.43. The rate curves show that the peak in the rate of fallout occurred between 0.2 and 0.3 of the fallout interval for shot Diablo; in real time this would be between H+10.2 and H+12.2 min. For shot Shasta the peak rate occurred between 0.35 and 0.45 of the fallout interval; in real time this would be between H+15.7 and H+16.9 min. Since the yields and heights of detonation of the two shots were essentially equal, the difference in the two rate-of-fallout curves must be due mainly to the difference in the distance of the shelter from shot point and in the relative location of the shelter in the fallout area. For shot Diablo (shelter at 1 mile from GZ and on the edge of the fallout area), the rate curve is unsymmetrical, and the peak rate occurred early in the fallout interval. For shot Shasta (shelter at 2 miles from GZ and on the hot line of the fallout area), the rate curve is nearly symmetrical, and the peak rate occurred nearer 0.5 of the fallout interval than for shot Diablo. The height of the peak is probably associated with the lateral distance of the location relative to the hot line (center of path of fallout) through the fallout area. The shape of the rate-of-arrival curve and relative position of the peak rate are probably associated with the distance of the location from GZ. If the trends shown by the two curves are general, then it might be expected that the peak in the rate of arrival would shift toward 0.5 of the interval at the distance corresponding to the area of maximum amount of fallout [i.e., location at which highest value of I(1) occurs], which is always located some distance from GZ, and for greater distances the peak would remain at 0.5 of the interval. Also, the shape of the rate curve would become symmetrical about the peak rate (approximately normally distributed about 0.5) at this distance. It is also likely that the peak rate itself would be a maximum at the location of the maximum value of I(1) and would decrease with distance beyond this location. The data presented here, of course, are insufficient to verify these interpretations of the trends suggested by the two rate-of-fallout curves.

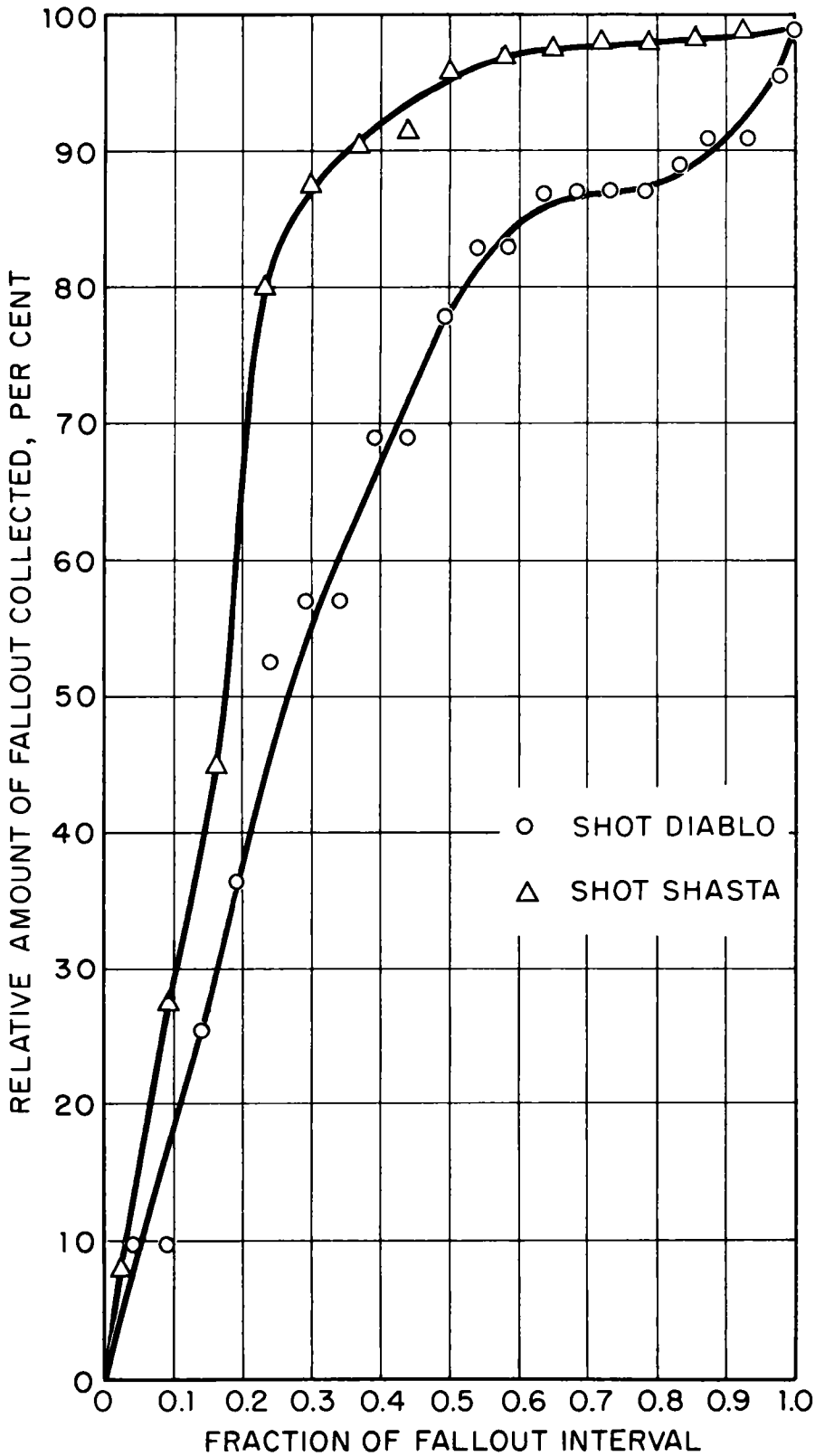

Fig. 3.41—Relative amount of fallout collected by the incremental collector up to a given fraction of the fallout interval.

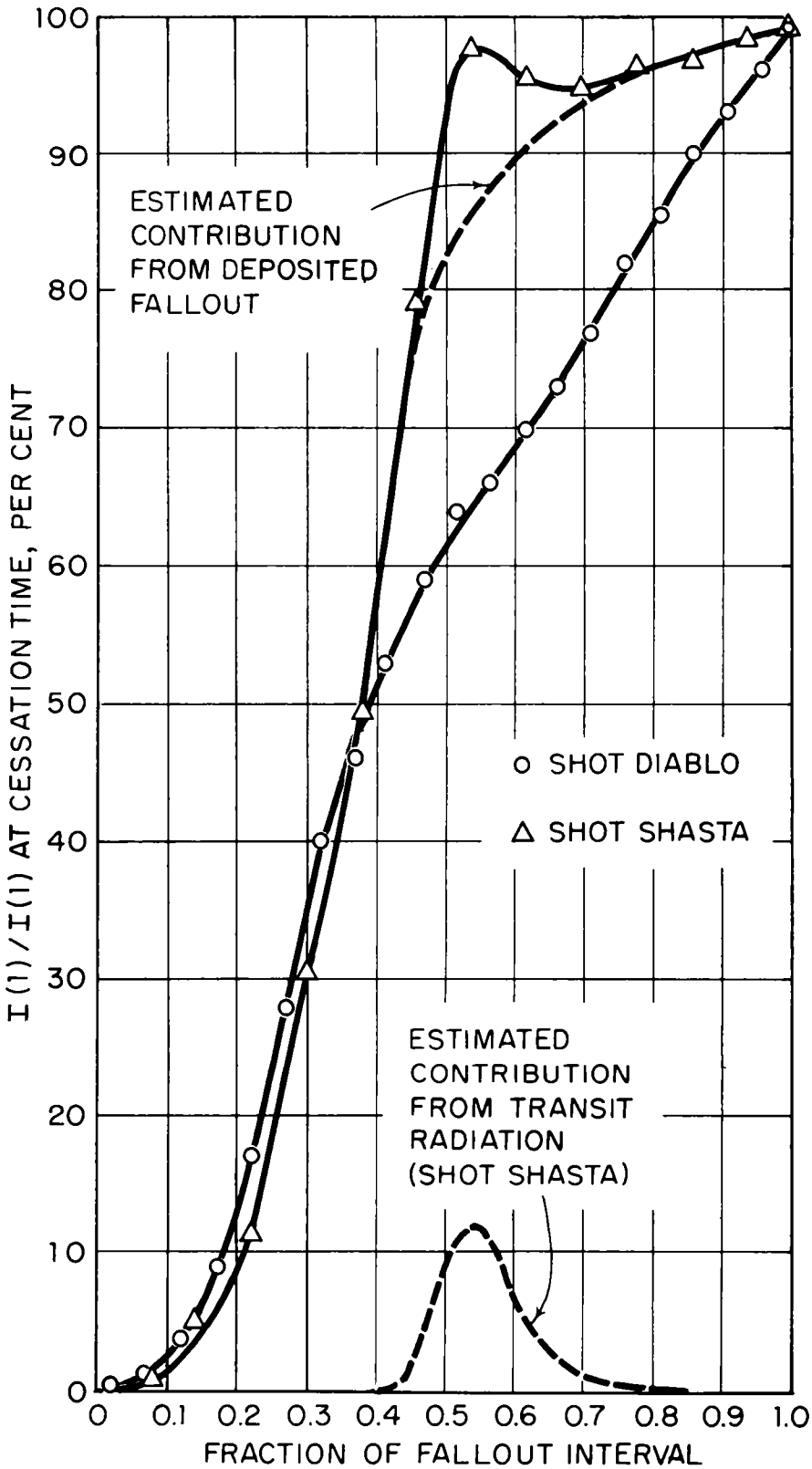

Fig. 3.42—Relative decay-corrected GITR data at a given fraction of the fallout interval.

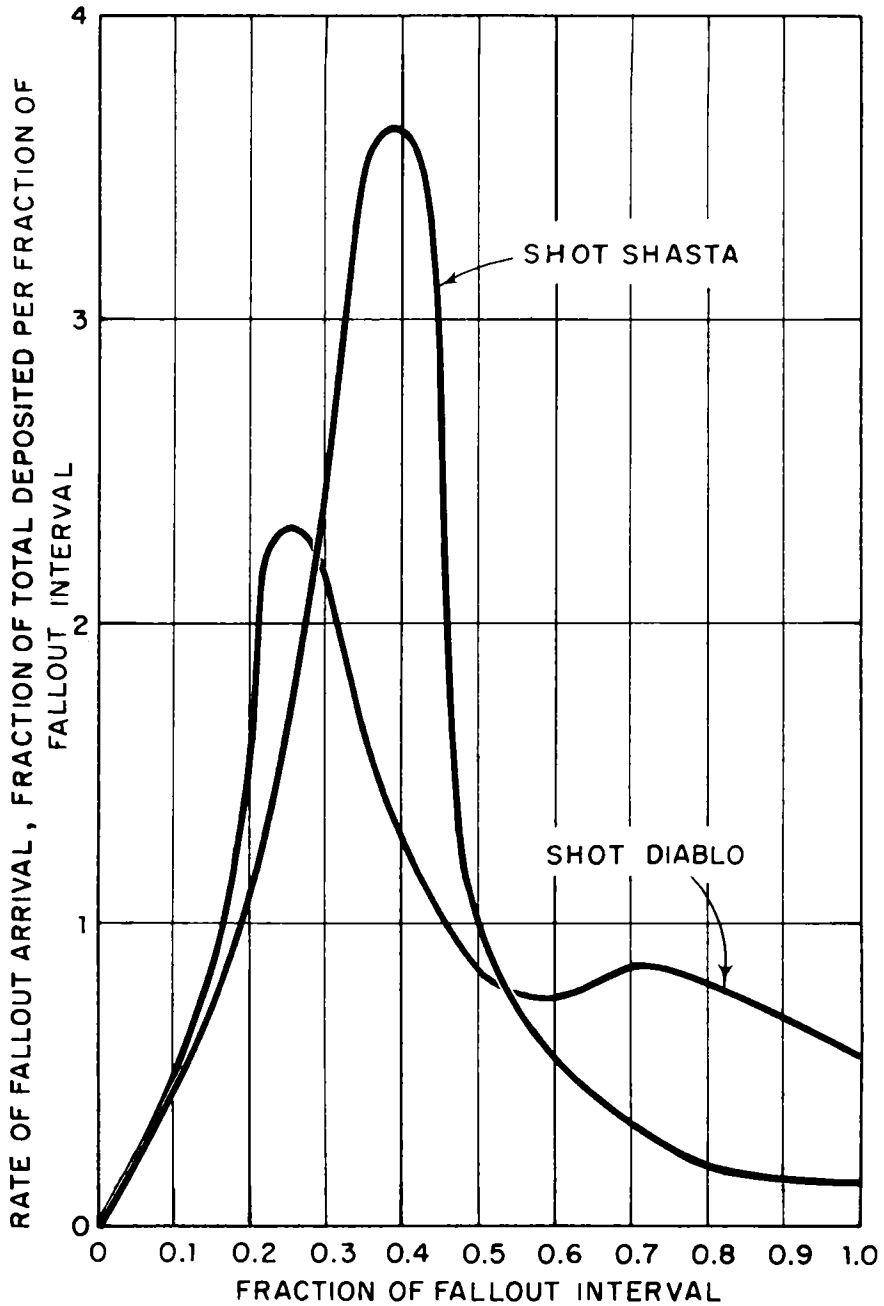

Fig. 3.43—Smoothed rate of fallout arrival as a function of fraction of fallout interval.

3.6 INITIAL MONITORING FROM SHELTER, SHOT DIABLO

Because of the high intensities resulting from shot Diablo, initial monitoring from the shelter was delayed until 7 hr after burst. Measurements were made at Areas 1 and 3 (Fig. 2.1); telemeter data showed that the reading on Area 3 was 6 r/hr. The gradient was very flat, the lowest reading being 5 r/hr and the highest reading 7 r/hr. The single-point reading was sufficient for decision purposes at the shelter. The single-point reading in Area 1 at H+7 hr was 3 r/hr. The gradient was also flat; the single-point reading was a sufficient measure of the situation.

TABLE 3.33—DATA TAKEN FOR PROOF OF TEST METHODS*

Height of reading, ft	Center, mr/hr				Two paces, mr/hr			
	North	East	South	West	North	East	South	West
				Uncleared Area				
3	280	270	290	290	280	280	290	290
2	280	290	310	310	290	300	310	310
1	300	300	310	310	290	300	320	320
				After Clearing 40- by 40-ft Area				
3	100	90	100	100	110	120	100	130
2	80	80	90	90	100	100	90	120
1	70	70	80	80	80	80	70	110
				After Clearing 60- by 60-ft Area				
3	80	80	80	80	90	100	100	80
2	70	70	70	70	80	90	80	70
1	60	60	60	60	70	70	70	50
				After Clearing 100- by 100-ft Area				
3	60	60	60	70	70	80	70	60
2	60	60	60	60	60	70	60	50
1	60	50	50	50	60	60	60	50

*Data taken on D+2 day.

3.7 STAGING-AREA RECLAMATION AND TEST METHODS, SHOT DIABLO

The center area, Area 1, was selected for phase II operations. Because of the high intensity resulting from shot Diablo, these operations were conducted on D+2 day, when the intensity in the area was about 300 mr/hr. The residual number in the center of the area after one complete pass of the equipment was about 0.16. A second pass over the central 100- by 100-ft area reduced the residual number to 0.11. Working conditions for the second pass were very poor; large numbers of rocks were turned up by the grader. Further attempts to lower the residual number by locating spills with AN/PDR-27C instruments and by removing the spills with a front-end loader and dump truck were unsuccessful.

Results of the proof test of the reclamation test methods are given in Tables 3.33 and 3.34. Table 3.33 gives the actual readings made near the center of the area during the process of successive enlargement of the square. Table 3.34 gives the resulting ratios obtained from these readings. These data are plotted in Fig. 3.44 according to the vertical method of predicting residual number. The measured value for the 500- by 500-ft area has been introduced as the criterion of successful prediction.* Figure 3.45 gives the result of

*It was estimated in Sec. 3.5.1 that about 99 per cent of the initial reading was contributed by sources within 250 ft of the detector.

applying the horizontal method of prediction. The measured value for the 500- by 500-ft area has been introduced as a criterion of successful prediction.

Data were obtained on the doses received by the grader and scraper operators following the operation. The dose measured on self-reading dosimeters over an operating period of approximately 3 hr was 175 mr. The equivalent free-field dose during this period was 820 mr. Therefore the residual number for this operation (because of equipment shielding and the effect of the reclaimed part of the area) was 0.21.

3.8 ALTERNATE BUFFER-ZONE TECHNIQUE, SHOT DIABLO

The test of a barrier as a substitute for a buffer zone was first accomplished in Area 3 on D+4 day. A barrier having an average height of 3 ft was constructed around a 100- by 100-ft cleared area. Results are given in Table 3.35. The residual number achieved by a

TABLE 3.34—RATIOS FOR PROOF OF TEST METHODS*

Height of reading, ft	Center average	Two paces				Grand average
		North	East	South	West	
		40-ft Clearing				
3	0.345	0.393	0.429	0.448	0.345	0.392
	(0.655)	(0.607)	(0.571)	(0.552)	(0.655)	(0.608)
2	0.286	0.345	0.333	0.387	0.240	0.329
	(0.714)	(0.655)	(0.667)	(0.613)	(0.710)	(0.671)
1	0.246	0.276	0.267	0.344	0.219	0.270
	(0.754)	(0.724)	(0.733)	(0.656)	(0.781)	(0.730)
		60-ft Clearing				
3	0.283	0.322	0.357	0.345	0.276	0.316
	(0.717)	(0.678)	(0.643)	(0.655)	(0.724)	(0.684)
2	0.235	0.276	0.300	0.258	0.226	0.259
	(0.765)	(0.724)	(0.700)	(0.742)	(0.774)	(0.741)
1	0.197	0.242	0.234	0.218	0.156	0.208
	(0.803)	(0.758)	(0.766)	(0.782)	(0.844)	(0.792)
		100-ft Clearing				
3	0.221	0.250	0.286	0.241	0.207	0.242
	(0.779)	(0.750)	(0.714)	(0.759)	(0.793)	(0.758)
2	0.202	0.207	0.234	0.194	0.162	0.200
	(0.798)	(0.793)	(0.766)	(0.806)	(0.838)	(0.800)
1	0.172	0.207	0.200	0.188	0.156	0.184
	(0.828)	(0.793)	(0.800)	(0.812)	(0.844)	(0.816)
		Final 500-ft Clearing (3-ft Reading)				
Actual reading, mr	44	50	35	60	40	45.2
Ratio, RN	0.156	0.176	0.123	0.210	0.140	0.159

* Values in parentheses are $1 - (R_2/R_1)$.

500- by 500-ft cleared area (from Table 3.34) is also given. The results indicate that the 3-ft barrier is as effective as a 200-ft-wide buffer zone. The barrier required 1.3 hr of work by a D-8 bulldozer; therefore the rate of operation was approximately 300 linear feet of barrier per equipment-hour.

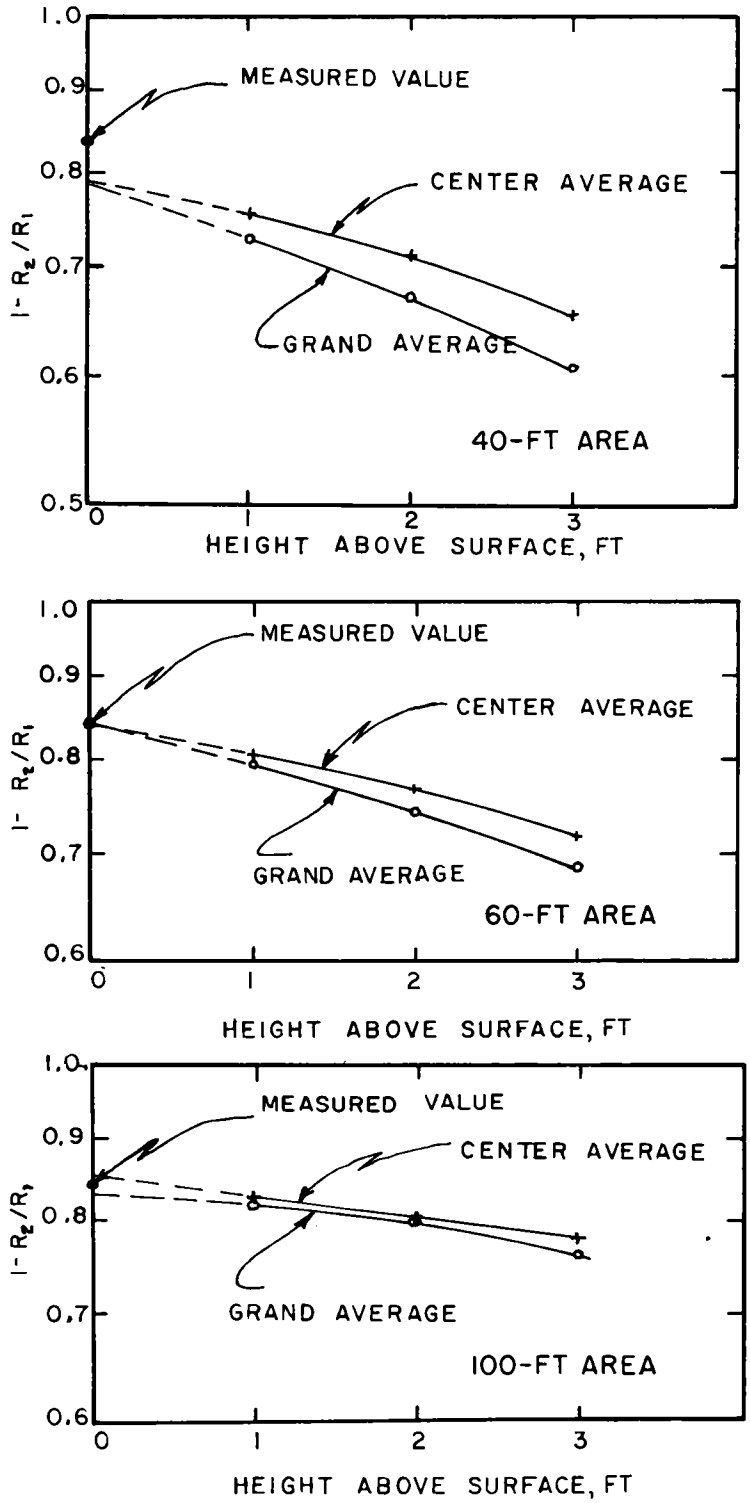

Fig. 3.44—Results of vertical method of predicting reclamation effectiveness, shot Diablo.

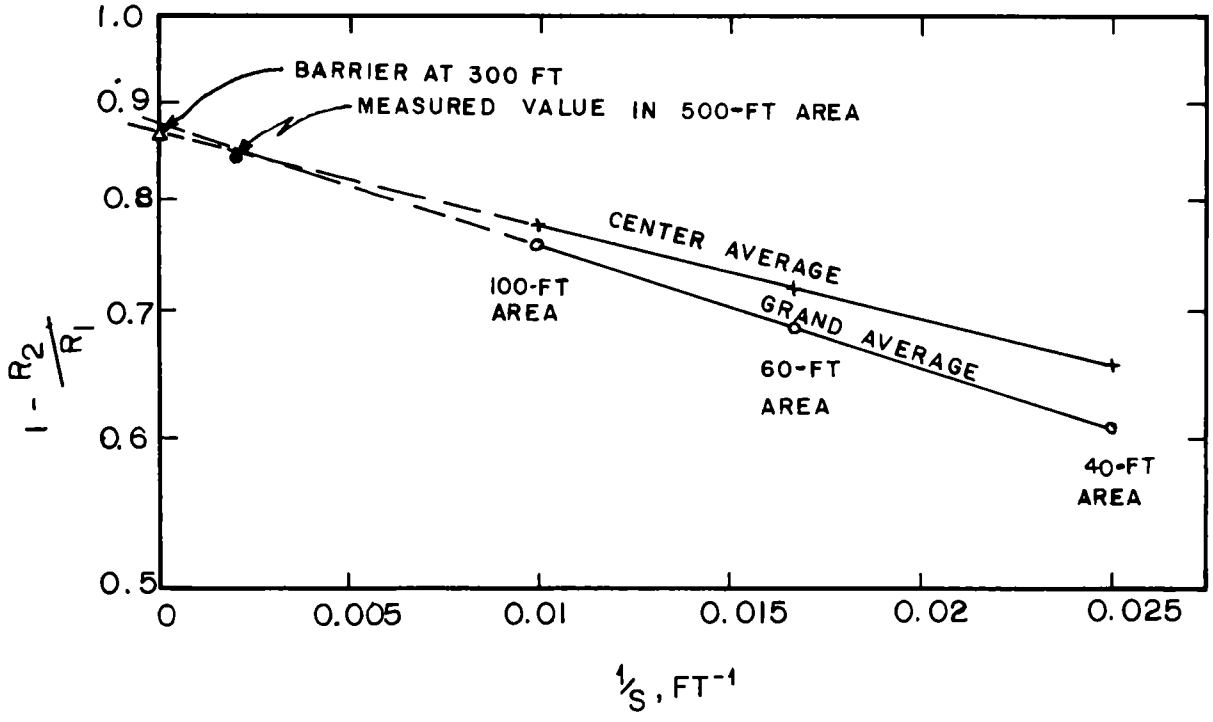

Fig. 3.45—Results of horizontal method of predicting reclamation effectiveness, shot Diablo.

TABLE 3.35—BARRIER TEST DATA, SHOT DIABLO*

	Center					Two paces				
	North	East	South	West	Av.	North	East	South	West	Av.
Uncleared area	230	240	240	240	237.5	230	230	240	250	237.5
100-ft area	50	50	60	60	55	60	50	60	60	57.5
After barrier	44	45	32	32	38	44	40	30	38	38
Residual number without barrier	0.22	0.21	0.25	0.25	0.23	0.26	0.22	0.25	0.24	0.24
Residual number with barrier	0.19	0.19	0.13	0.13	0.16	0.19	0.17	0.12	0.15	0.16
Residual number in 500-ft area (see Table 3.34)					0.156					0.162

*Readings were taken at a height of 3 ft.

On D+7 a barrier approximately 4 ft high was constructed around a square 300 ft on a side in the center of the 500- by 500-ft cleared area in Area 1. The residual number achieved by this effort has been introduced into Fig. 3.44. The effectiveness of the barrier appeared to be equivalent to a cleared area of infinite extent.

REFERENCES

1. R. C. Bolles and N. E. Ballou, Calculated Activities and Abundances of U^{235} Fission Products, Report USNRDL-456, August 1956.
2. J. D. Teresi and C. L. Newcombe, A Study of Maximum Permissible Concentrations of Radioactive Fallout in Water and Air Based Upon Military Exposure Criteria, Report USNRDL-TR-182, August 1957.
3. C. F. Miller and Peter Loeb, Ionization Rate and Photon-Pulse-Decay of Fission Products from the Slow-neutron Fission of U^{235}, Report USNRDL-TR-247, July 27, 1958.
4. C. F. Ksanda et al., Gamma Radiations from Contaminated Planes and Slabs, Report USNRDL-TM-27, 1955.

Chapter 4

DISCUSSION

The complete experimental plan for the project was carried out on shot Diablo. Measurements covering all project objectives were made, and all project objectives were met, except two: (1) the aerosol sampling data, together with the fallout conditions from the two shots, were not sufficient to allow a generalized conclusion to be derived about air filtration requirements in shelters and (2) the requirement for a staging-area residual number of 0.01 was not fulfilled by the reclamation procedure on Nevada Test Site soil. These exceptions are further noted in the following sections. Owing to the lengthy delay in detonating shot Shasta, only partial participation by the project was possible; on this shot some of the operational measurements and most of the technical measurements were made. The results obtained were in good agreement with the measurements taken on shot Diablo. The results from the data are discussed in the following sections.

4.1 OPERATIONAL MONITOR SYSTEM

The dosimeter-tube procedure was effective in providing information on the course of the radiological event outside the shelter, despite the exaggerated readings introduced by the film-badge cup at the top of the tube (Sec. 3.2). There are some anomalies in the data for the forward tube on shot Diablo; a constant intensity was measured for nearly 15 min at the peak, and there was wild oscillation in the measurements at about 45 min after burst. Even these data would have provided necessary radiological information. Data for the after tube were much more stable and closely approximate the GITR information, except for absolute level for both shots.

Several additional pieces of operational data were obtained from the dosimeter tubes. No significant problem was encountered concerning the contamination of the dosimeter; industrial wiping tissue was used to clean the dosimeter before reading. The 200-mr dosimeters were quickly overtaxed as the intensity increased, forcing a shift to the 5-r dosimeter. Experience proved that an operational dosimeter tube would require a number of dosimeters covering the possible range of intensities to be encountered.

Converting the measured intensity to standard intensities by means of an assumed decay curve proved to be an effective way of determining fallout cessation. The fact that the actual decay was somewhat faster than the assumed decay during the first hour (Fig. 3.28) caused a peak in the standard intensity plot at fallout cessation (Fig. 3.3).

4.2 INGRESS OF CONTAMINATED AIR

If one assumes that the M6 collective protective filter is an absolute filter, then no significant hazard due to inhalation or to gamma radiation would have resulted in the shelter on either shot Diablo or shot Shasta with an intake ventilation flow rate of 300 or 600 cu ft/min. On shot Diablo, where there was a blow-in of the wall separating the generator room from the

plenum chamber, the Porta-Vac sampler at the shelter door, with a flow rate of 600 cu ft/min, collected about twice as much activity as the outside Porta-Vac sampler. This could have been caused by the large air flow rate down the chamber, which would have accelerated particles toward the shelter door from greater distances away than the sampling velocity of the Porta-Vac alone would have. Many of the smaller particles, of course, were lost from the plenum chamber into the generator exhaust stack since they would make the turn into the generator room more easily than the larger particles. On shot Shasta the shelter-door sampler, with a flow rate of 300 cu ft/min, collected about 0.7 of the activity of the outside Porta-Vac sampler. The two ratios show qualitatively the effect of flow rate on the fraction of aerosol that would be available at the shelter door. Here, of course, the particle sizes that are included in the term "aerosol" are defined as those collected by the Porta-Vac sampler.

The relative fraction of the total activity in the aerosol for the two shots can be estimated from the totals collected outside the shelter and the standard intensities. On shot Diablo, where the shelter was 1 mile from GZ, the total aerosol collected was 5.1×10^9 fissions/(r/hr) at 1 hr. On shot Shasta, where the shelter was 2 miles from GZ, the total aerosol collected was 4.8×10^{10} fissions/(r/hr) at 1 hr. Thus, for shot Shasta, the collectable aerosol was 10 times the fraction on shot Diablo. The two ratios show the effect of distance from GZ on the fraction of available aerosols (or fraction of activity arriving in small particles). If 0.1 per cent of the total activity were carried by the small particles at 1 mile from GZ, then 1.0 per cent of the total would be carried by the same sizes at 2 miles. For surface and underground detonations of the same yield, the fraction of the total in the small particles would be higher at both locations, probably more like 1.0 per cent at 1 mile and 10 per cent at 2 miles.

The maximum size of fallout particles that passed the ventilation system intake (plenum chamber plus hooded vent) was about 120 μ in diameter on shot Diablo and about 80 μ in diameter on shot Shasta. The maximum size, as well as the total number of particles collected, is thus affected by the intake flow rate. At 300 cu ft/min the intake flow rate in the chamber was 15 ft/min in the entrance tunnel. Since the tunnel was 30 ft long and 8 ft high, all particles falling faster than 4 ft/min (about 25 μ) should have settled out in the tunnel if gravity fall only occurred. Since the maximum size particles were larger for shot Shasta, there must have been considerable turbulence in the entrance tunnel, perhaps due, in large part, to the exposed 12- by 2-in. studs along the tunnel walls and ceiling. Howevèr, the fact that the shelter-door sampler collected 0.7 of the amount collected by the outside sampler shows that the concentration of the larger particles was reduced in the air passing through the entrance tunnel. The effect of the hooded vent on discriminating against the larger particles in the aerosol cannot be clearly shown because the M6 intake sampler was pulling air against the M6 collective protector.

The important factors in determining the amount of contaminated air are the design of the air entrance path, the flow rate of the air, the particle-size distribution of the fallout (and activity distribution among the particles), the outside air concentration, and the time after detonation when fallout occurs. At a given distance downwind from GZ, the mean particle size should increase with yield and wind speed; for a given yield and wind speed, the mean particle size should decrease with distance from GZ. The outside air concentration should increase with the standard intensity but should decrease with the duration of the fallout period (i.e., with decreasing wind speed and increasing yield). The activity in the aerosol, of course, decreases rapidly at early times after detonation; thus the radiation dose decreases with distance from GZ and with a decreasing wind speed. The interaction of all these parameters are too complicated or too little known to be given simple treatment for making estimates of the ingress into structures in a variety of contaminating situations. It may be noted that some of the parameters have opposite effects on different important factors. This should tend to limit the range of possible aerosol hazards; therefore the results of the data reported in Chap. 3 may have more general application than presently considered.

4.3 EFFECTS OF OPENINGS ON SHIELDING

Both the dose and dose-rate data on shot Diablo gave residual numbers for the shelter of less than the required value[1] of 0.001. Dose-rate data on shot Shasta also gave residual numbers less than 0.001. In many locations in the shelter, residual numbers less than 0.0001 were

observed. The center ventilator, which was a mock-up of a combination exhaust ventilator and escape hatch, was satisfactory from a radiological point of view. The periscope opening also was satisfactory. The major source of radiation in the shelter was shine from the outside ramp down the entrance tunnel. One 90° bend in the tunnel would reduce this contribution to an acceptable level.

4.4 SUPPORTING TECHNICAL STUDIES

The technical data, including film-badge measurements, GITR measurements, 4π ionization chamber decay measurements, spectral measurements, and others, were introduced in the report as they were used to interpret and evaluate the operational data. The several methods used to determine the time of fallout arrival agreed well on both shots. The GITR data generally gave low values of the ionization rate by almost a factor of 2; this was probably due to the shielding of one detector by others, to excessive shielding around the detectors, and to calibration methods. The two 4π ion chamber decay curves were started earlier than any reported in the literature to date. The data showed that the radioactive composition of the fallout from shots Diablo and Shasta was the same. Since the 4π ionization chamber decay curve has, to within 6 per cent, the same shape as that for the AN/PDR-39(T1B) for extended radiation-field measurements, the decay data on the samples will be continued beyond this reporting to determine whether the observed and calculated decay curves join at some later time.

4.5 INITIAL MONITORING FROM SHELTER

The fallout radiation field resulting from shot Diablo was very uniform. Consequently, the single-point measurements in the center of the areas were adequate indicators of the radiological situation in the general region. No significant additional information was provided by either the corner measurements or the detailed survey. Since the fallout field was similar to that expected in most of the region contaminated by large-yield nuclear weapons, it would appear that single-point measurements obtained from within shelters or by early monitoring missions provide an adequate basis for decisions with respect to operational recovery.

4.6 STAGING-AREA RECLAMATION

The attempt to achieve a residual number of 0.01 in a cleared area was unsuccessful. However, the soil conditions in the test area were extremely unfavorable. A 3-in. layer of clean fill had to be introduced to establish the conditions for a single pass of the scraping equipment. Since the desired residual number was known to require multiple passes of the equipment, serious difficulties were anticipated for this objective when the areas were initially laid out. This experiment must be rescheduled under other soil and terrain conditions before the range of feasibility can be evaluated.

The operational-dose data gave a residual number of approximately 0.2 for the equipment operators. This is considerably better than the value of 0.5 currently used in planning for operational recovery.[2] There appeared to be little variation in protection afforded by the various types of land reclamation equipment.

4.7 RECLAMATION TEST METHODS

Both methods of predicting the effectiveness of reclamation methods on the basis of use in a small test area performed well in this test. The vertical method gave a good prediction in the 60- by 60-ft and 100- by 100-ft areas. The overestimate of residual number for the 40- by 40-ft area was largely due to spills at the edge of the area where the graders lifted blades. The pass that increased the cleared area to 60 by 60 ft removed this source of radiation. Although both methods gave good estimates, the vertical method appears preferable since less reclamation effort is required to get a result. The over-all test requires less time and therefore exposes the test crew to a smaller dose than the horizontal method.

The results indicate that, for both methods, an accurate prediction can be obtained only if the ratios are based on the average of many readings around the center of the test area. Plots of ratios based on individual readings are relatively unreliable.

4.8 ALTERNATE BUFFER-ZONE TECHNIQUE

Two tests were made of the barrier technique. Both indicated that a barrier 3 to 4 ft high would effectively reduce the contribution of radiation from outside a reclaimed area to a negligible amount. A rate of about 300 linear feet per equipment-hour was observed. The same length of buffer zone 200 ft wide would require approximately 2 equipment-hours of plowing. Scraping is even slower. Thus the barrier appears to be about twice as fast as the fastest buffer-zone technique. It would be desirable to determine the effect of barriers of other heights than those tested as well as more detailed measurements of the radiation field over the cleared area inside a barrier in order to develop an optimum procedure. For example, barriers along access routes may need to be quite high to shield vehicle occupants properly.

REFERENCES

1. W. E. Strope, Performance Specifications for a Sound National Shelter System, Report USNRDL-TR-132, Feb. 13, 1957.
2. Radiological Recovery of Fixed Military Installations, Report NavDocks TP-PL-13, Apr. 16, 1958.

Chapter 5

CONCLUSIONS

The following conclusions are offered as a result of the analysis of the data obtained from the measurements taken on shots Diablo and Shasta:

1. The standard Navy ammunition storage magazine (Armco Multi-plate structure), buried so as to provide a minimum thickness of 3 ft of earth cover over the crown and provided with all necessary openings for entrances, ventilation, and control purposes, offers a high degree of radiological protection. An average residual number of about 0.0001 was observed.

2. A 2-ft-diameter straight exhaust ventilator that can be designed as an escape hatch is radiologically acceptable.

3. A simple device consisting of a 1-in. pipe projecting through the shelter roof and fitted with a rod carrying a self-reading dosimeter will provide the shelter commander with all necessary radiological information for decision purposes within the shelter.

4. On shots Diablo and Shasta there was no need for filtration of the shelter air supply. However, the data were not sufficient to establish a generalized conclusion with respect to this requirement.

5. Both the vertical and horizontal methods of predicting reclamation effectiveness give satisfactory predictions in small test areas (less than 100 by 100 ft) under field conditions using land reclamation equipment.

6. An earth barrier 3 to 4 ft high is a satisfactory substitute for a buffer zone and can be created with half the effort required for the fastest buffer-zone method.

7. Single-point monitoring gives adequate radiological information in radiation fields that are relatively uniform for making general decisions regarding shelter stay-time, suitable staging areas, and selection of plans for reclaiming vital facilities.

8. The feasibility of obtaining a residual number of 0.01 in a cleared area by means of multiple passes with land reclamation equipment has not been established.

Appendix A

DESIGN DETAILS OF RADIOLOGICAL SHELTER AND ASSOCIATED EXPERIMENTAL EQUIPMENT

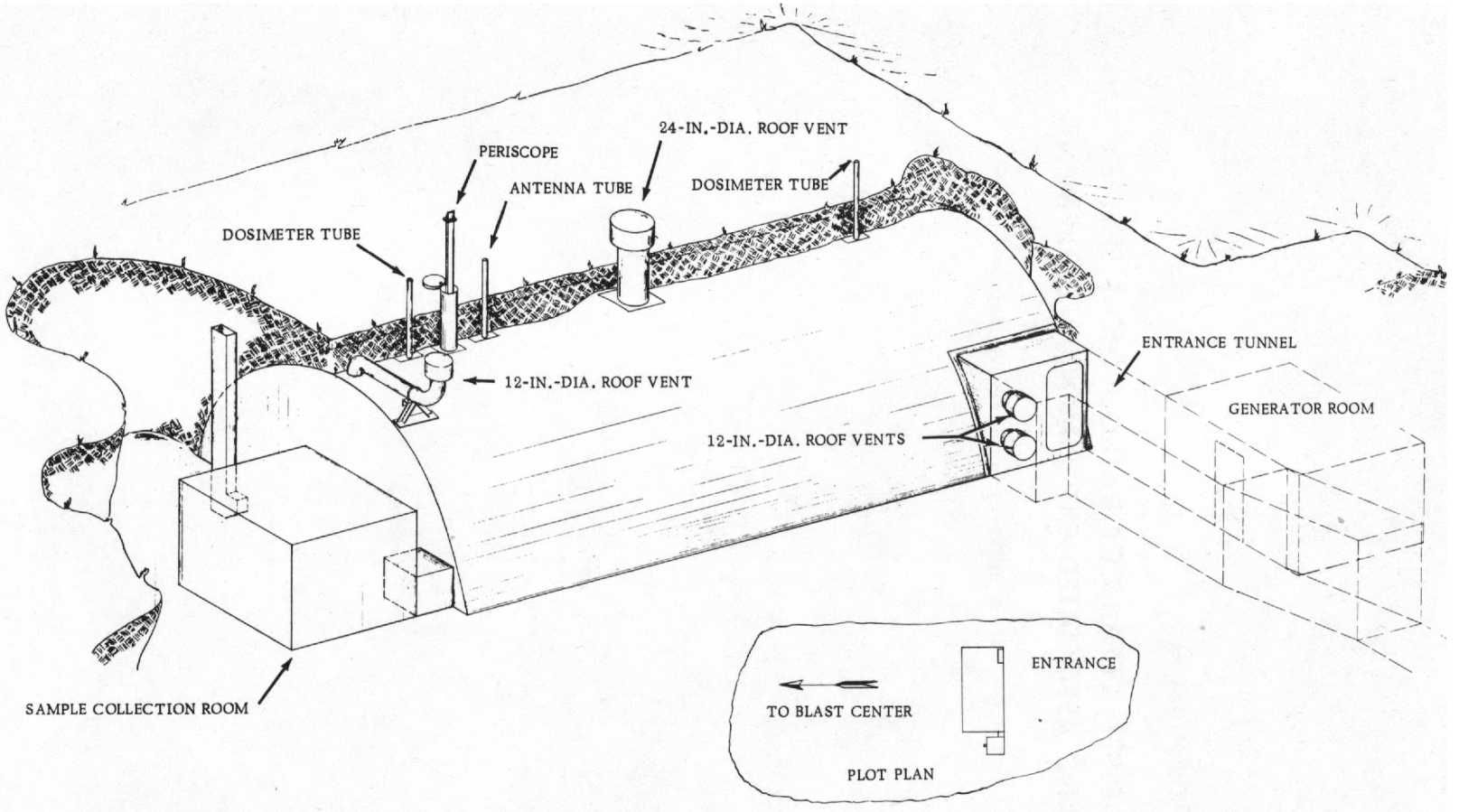

Fig. A.1—Underground personnel shelter for Project 32.3.

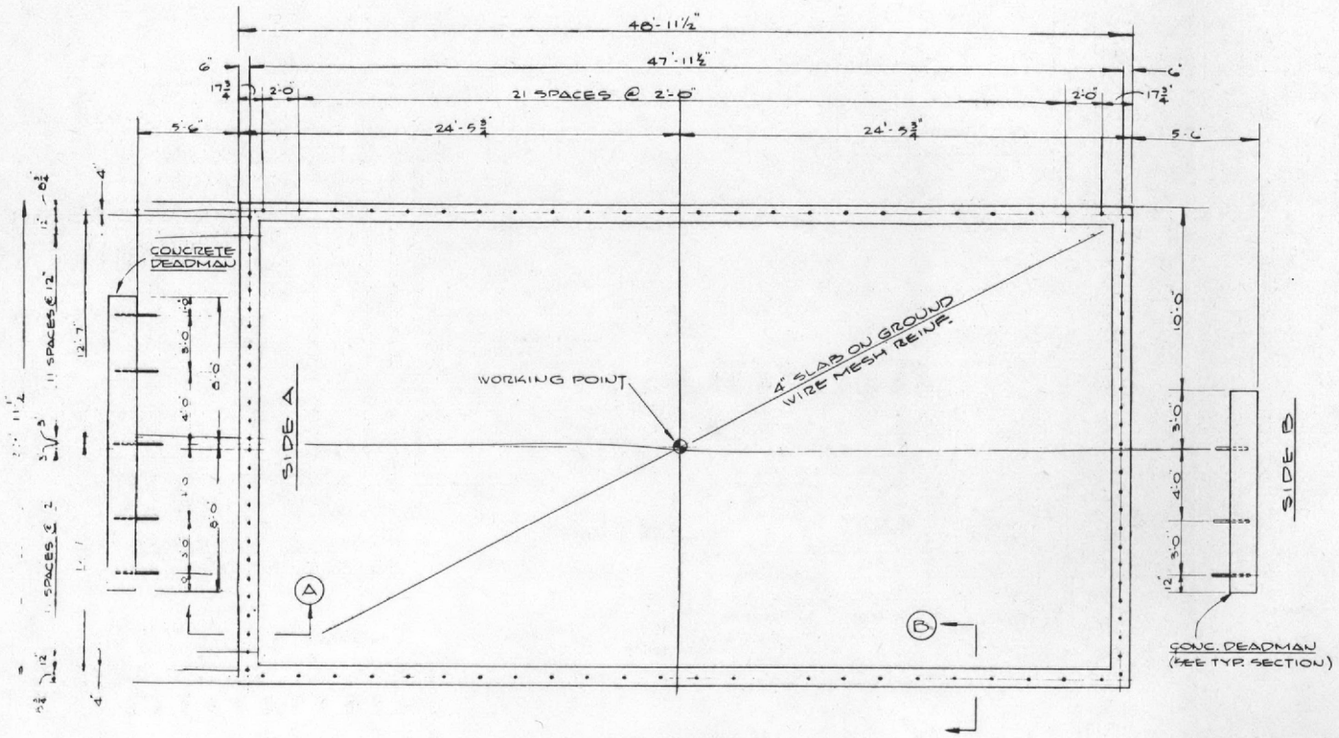

FOUNDATION & ANCHOR BOLT PLAN

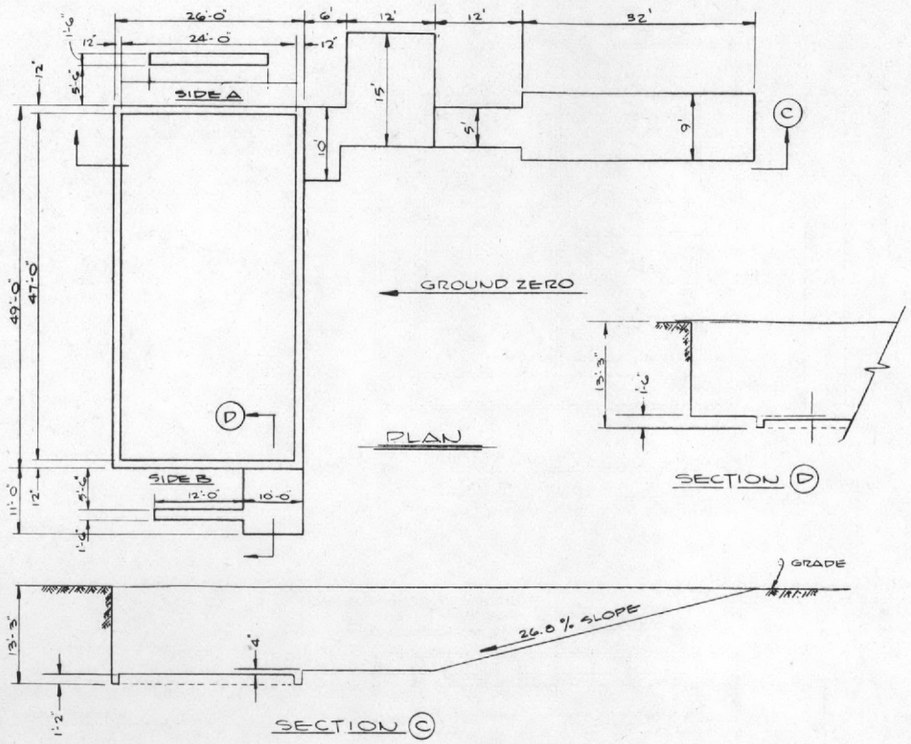

NET EXCAVATION f/ RADIOLOGICAL SHELTER & TUNNEL

(CONTRACTOR MAY INCREASE AS NEEDED for CONSTRUCTION PURPOSES)

GENERAL NOTES

1. REINFORCED CONCRETE SHALL CONFORM TO LATEST A.C.I. CODE
2. CONCRETE SHALL HAVE A MINIMUM ULTIMATE COMPRESSIVE STRENGTH of 3000 PSI AT 28 DAYS.
3. REINFORCING STEEL SHALL CONFORM TO A.S.T.M. SPEC. A15-54T
4. LAP BAR SPLICES 30 DIA. UNLESS OTHERWISE SHOWN.

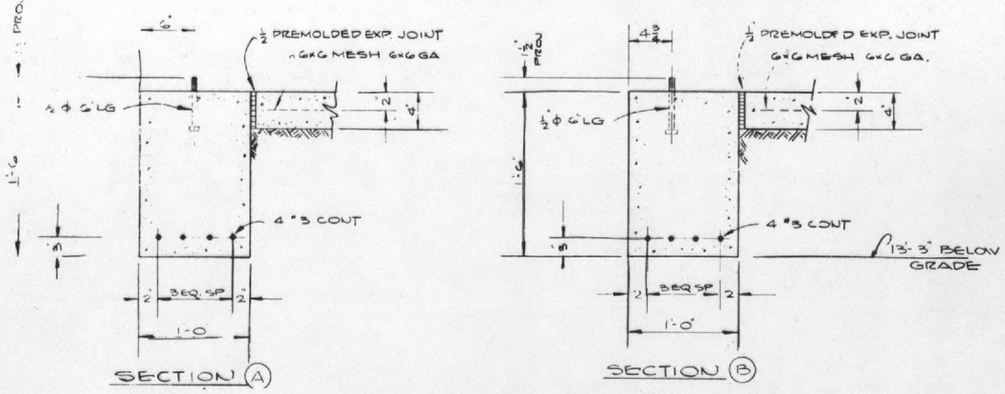

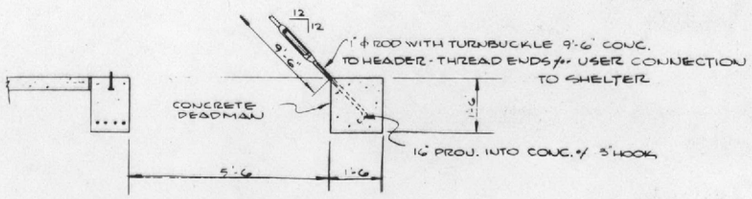

TYPICAL SECTION SHOWING DEADMAN

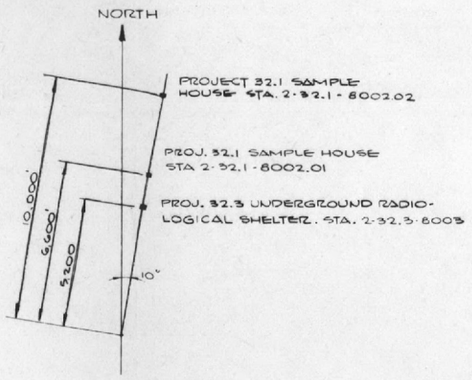

Fig. A.2—Foundation and floor slab.

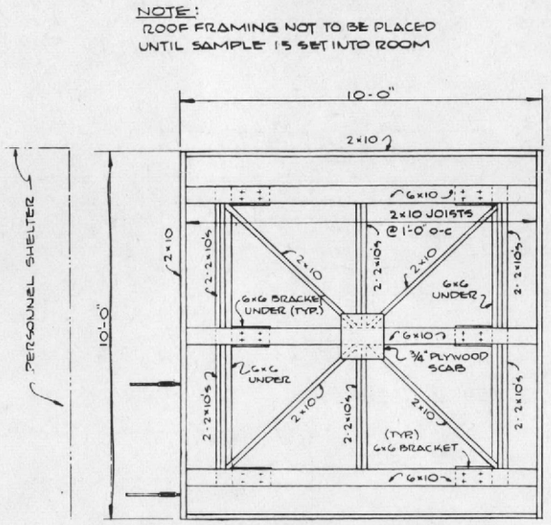

SAMPLE COLLECTION ROOM
ROOF FRAMING PLAN
(JOIST & ROOF DECKING NOT SHOWN)

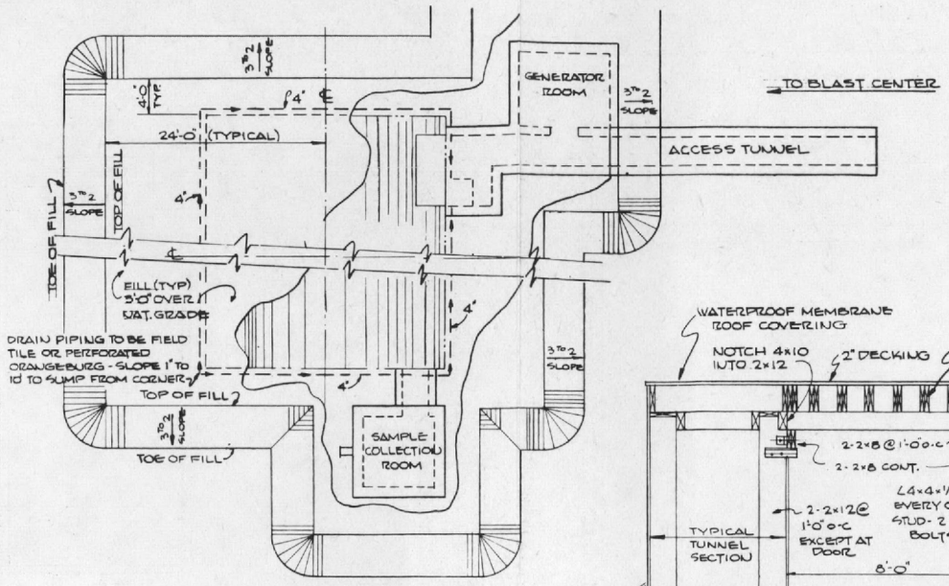

PLOT PLAN

NOTE: BACKFILL TO NATURAL GRADE - TO BE COMPACTED TO 80%

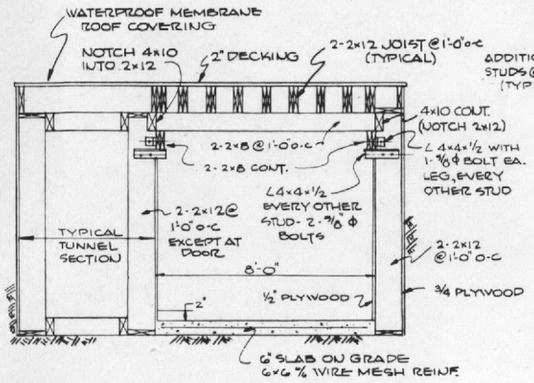

SECTION (F)

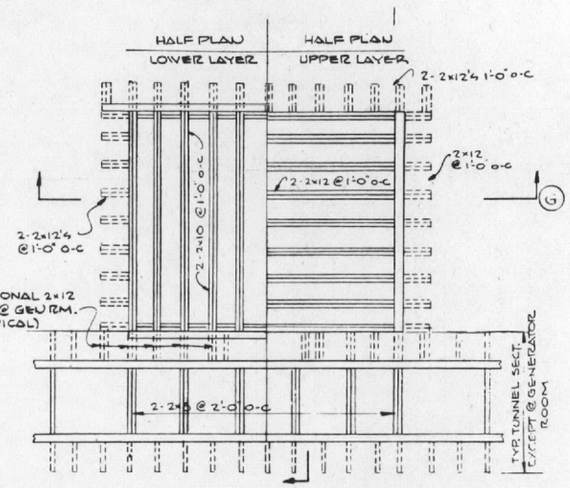

GENERATOR ROOM
ROOF FRAMING PLAN

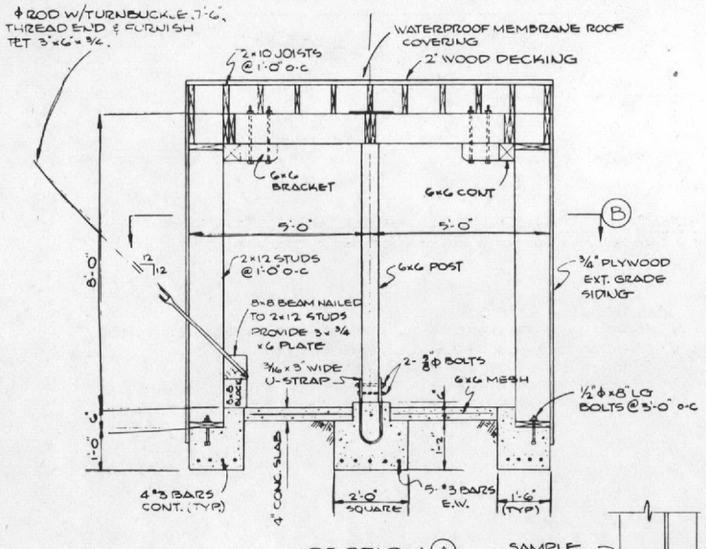

SECTION (A)

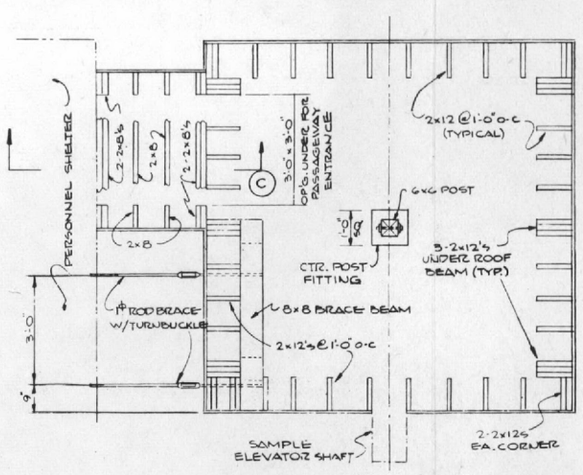

SECTION (B)

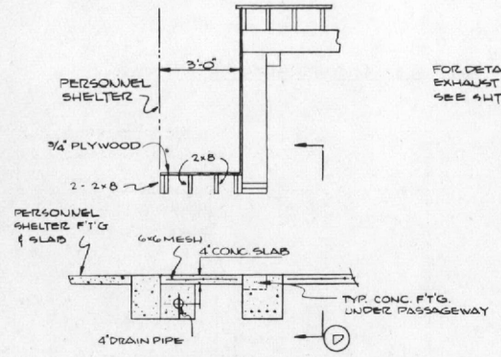

SECTION (C)

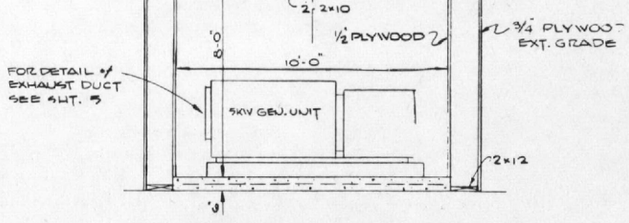

SECTION (G)

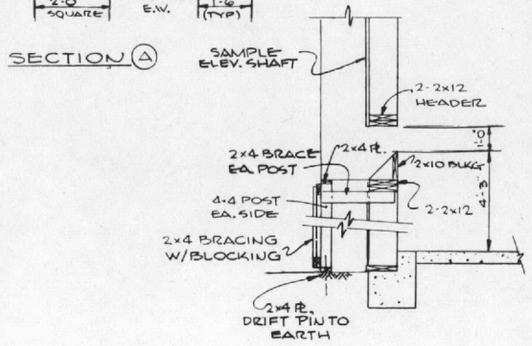

SECTION (E)

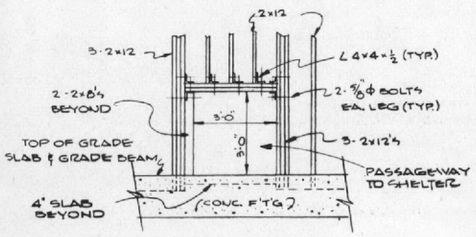

SECTION (D)

Fig. A.3—Plans, sections, and details.

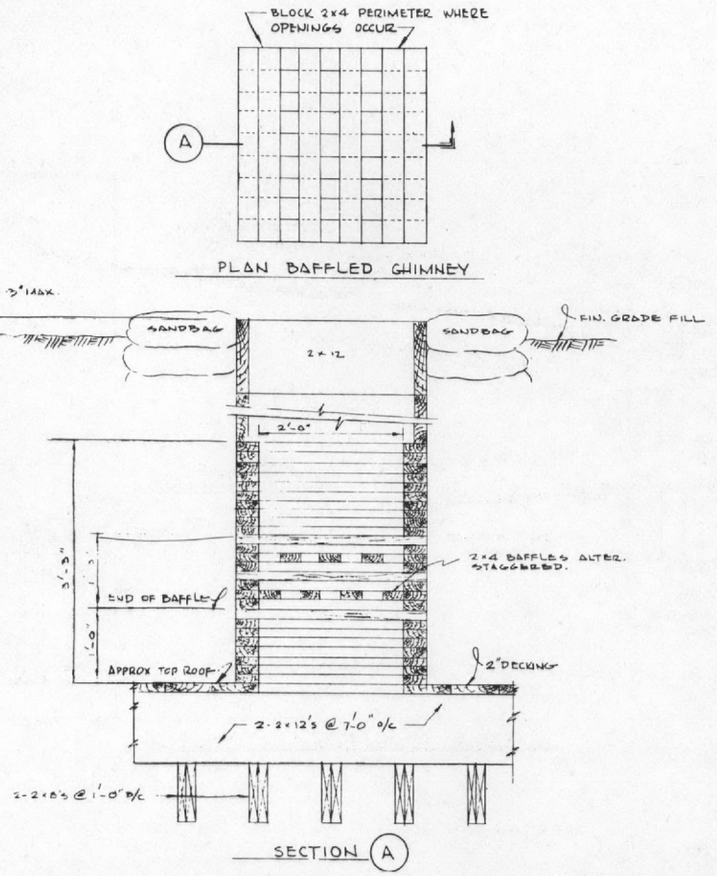

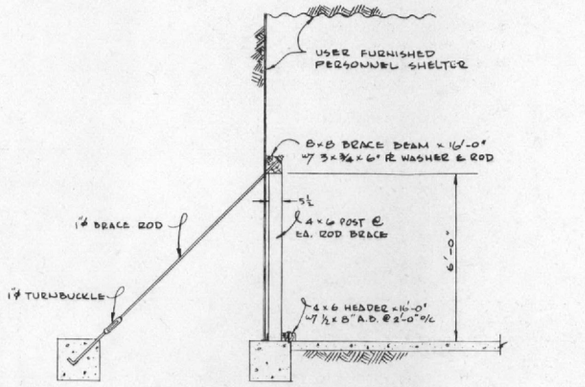

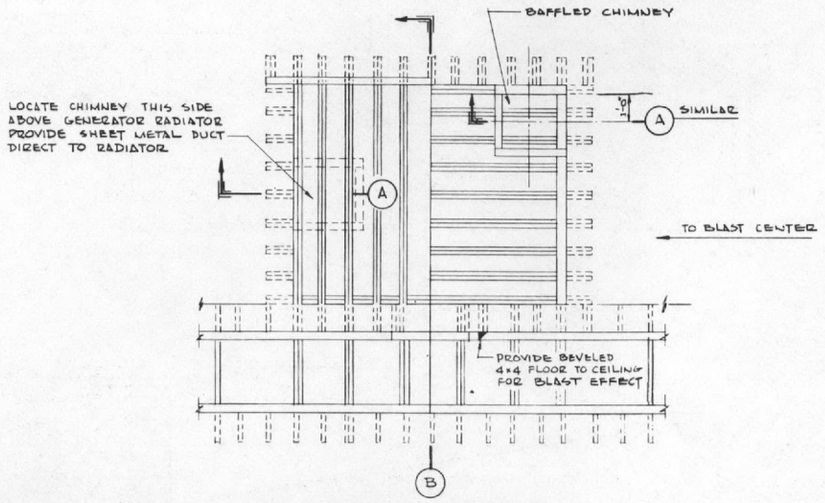

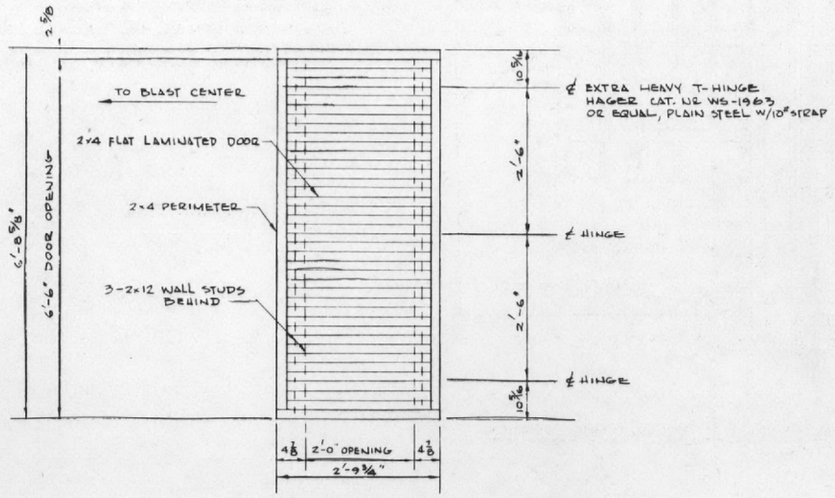

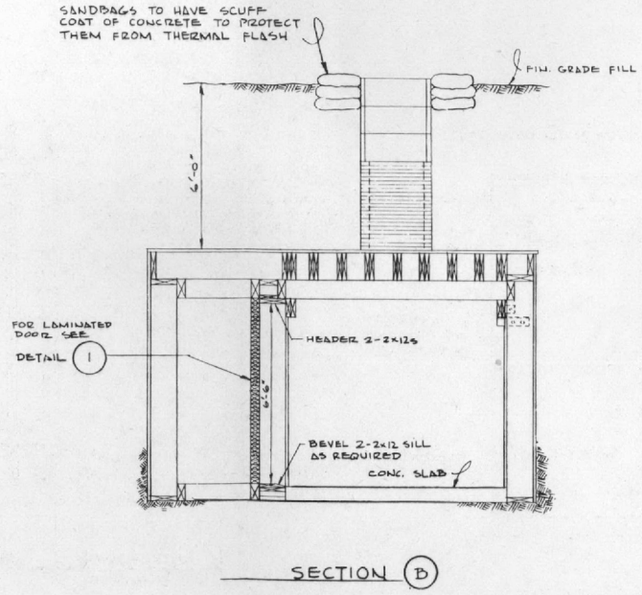

Fig. A.4—Door and chimney plan, section and details.

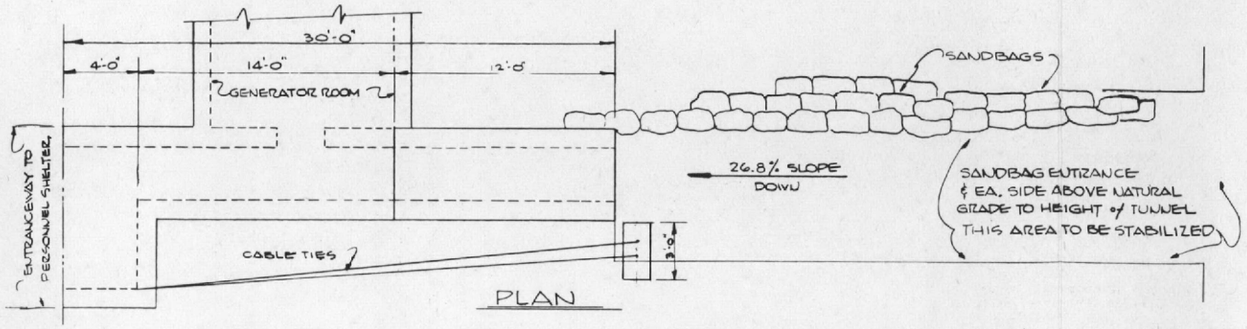

PLAN

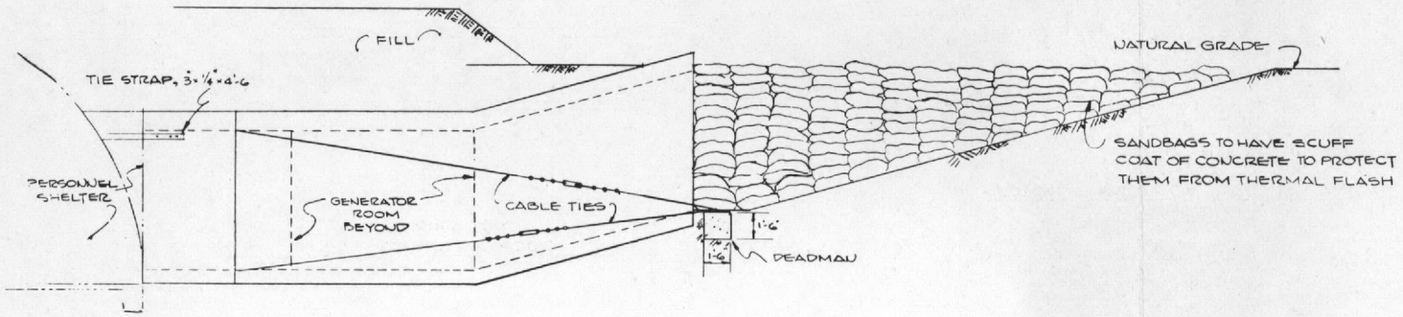

ELEVATION

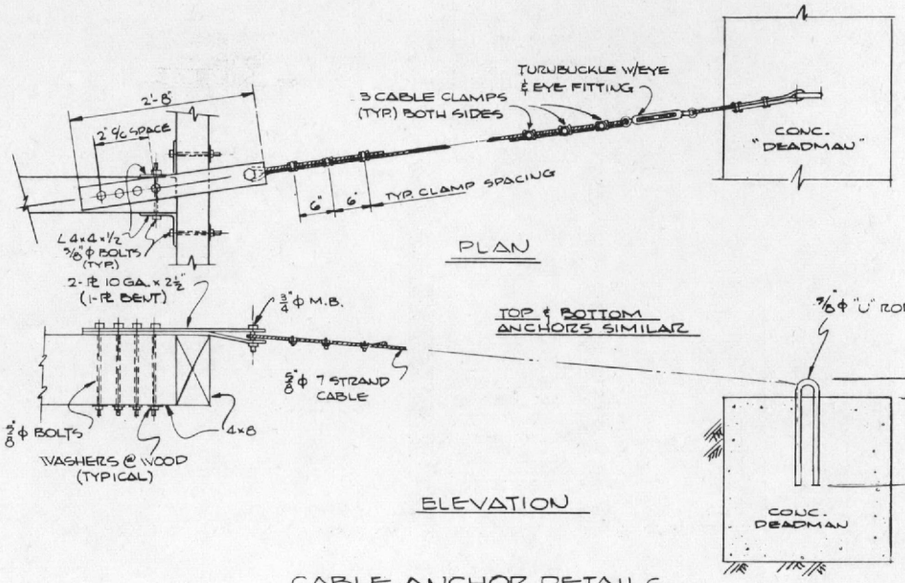

PLAN

ELEVATION

CABLE ANCHOR DETAILS

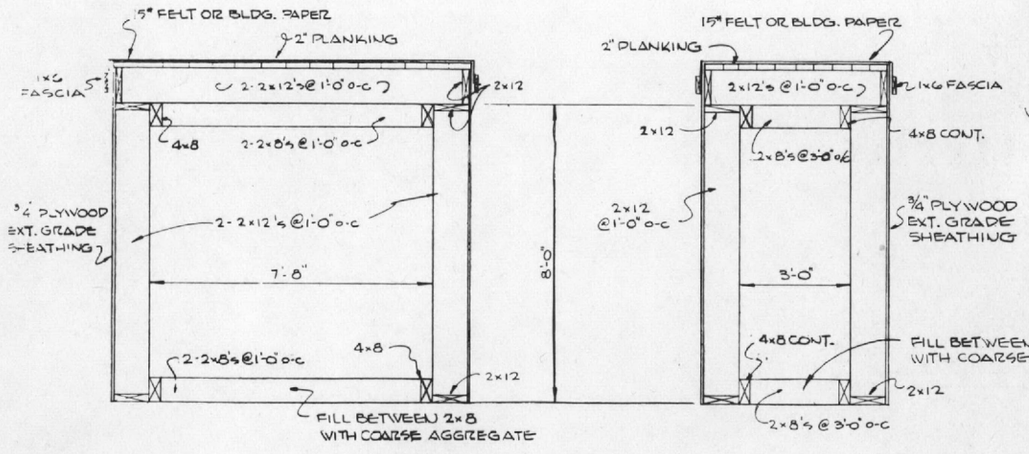

SECTION THRU TUNNEL AT SHELTER ENTRANCE

TYPICAL TUNNEL SECTION

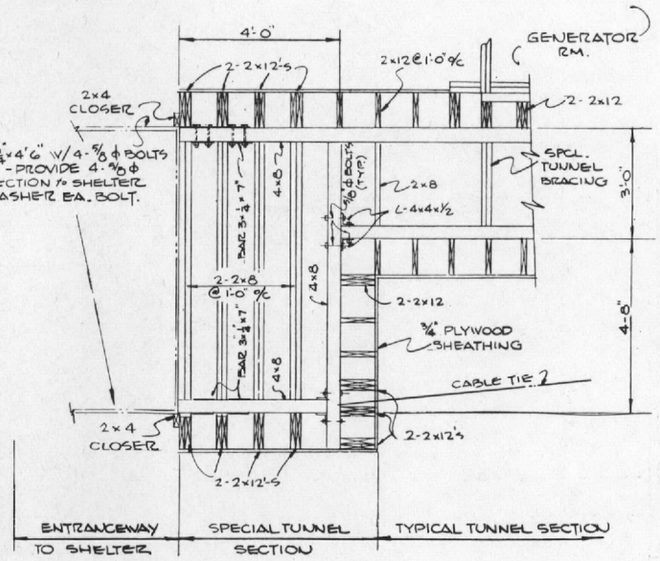

PART FRAMING PLAN - TUNNEL ROOF

FRAMING @ FLR SIMILAR

(JOISTS NOT SHOWN)

GENERAL NOTES

1. ALL WOOD SHALL BE #1 GRADE DOUGLAS FIR.
2. CONCRETE SHALL HAVE ULTIMATE COMPRESSIVE STRENGTH of 3,000 PSI @ 28 DAYS.

Fig. A.5—Entrance tunnel details.

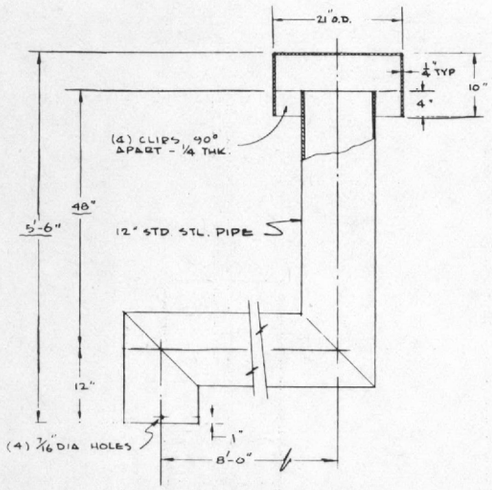

12" DIA. ROOF VENT

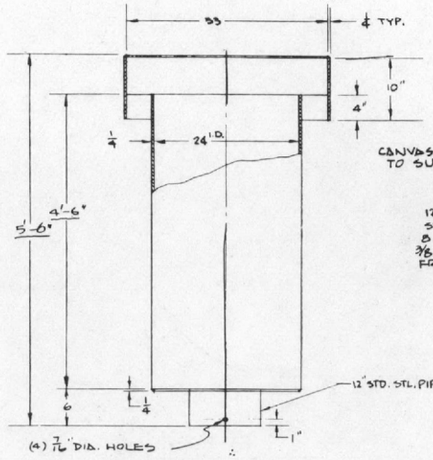

24" DIA. ROOF VENT

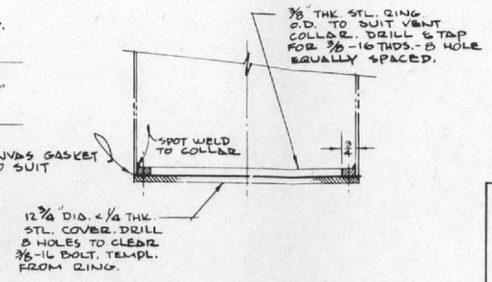

BLAST SHIELD
FOR ROOF VENTS
(2 REQ'D.)

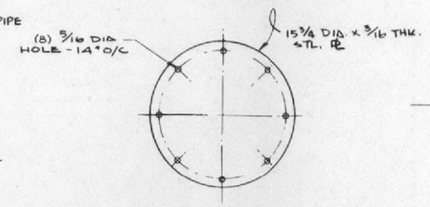

BLAST SHIELD
FOR SIDE VENTS
(2 REQ'D.)

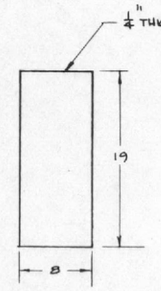

DETAIL "C"
(4 REQ'D.)

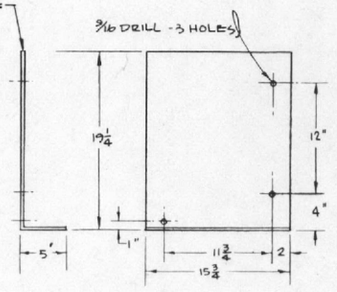

DETAIL "B"
(1 REQ'D.)

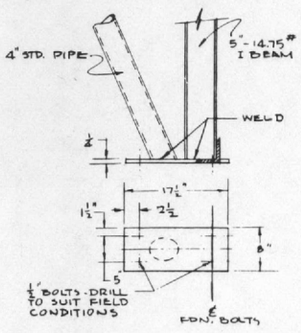

DETAIL "A"
(1 REQ'D.)

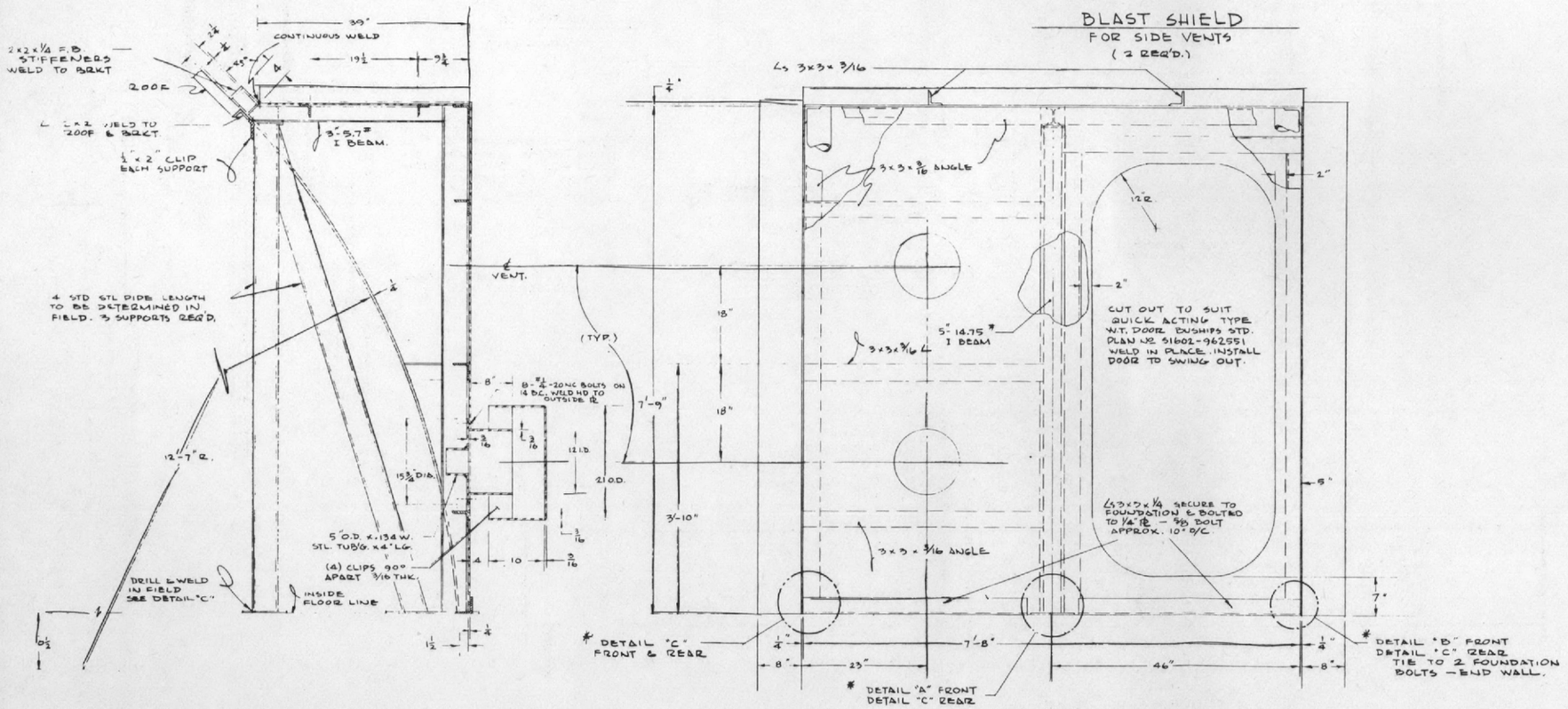

FRONT VIEW

* PLATES SHOULD BE IN PLACE PRIOR TO LOCATING ENTRANCE WAY.

NOTES

ALL ITEMS SHOWN IN THIS DRAWING ARE TO BE FABRICATED FROM MILD STEEL

Fig. A.6—Entrance and vent details.

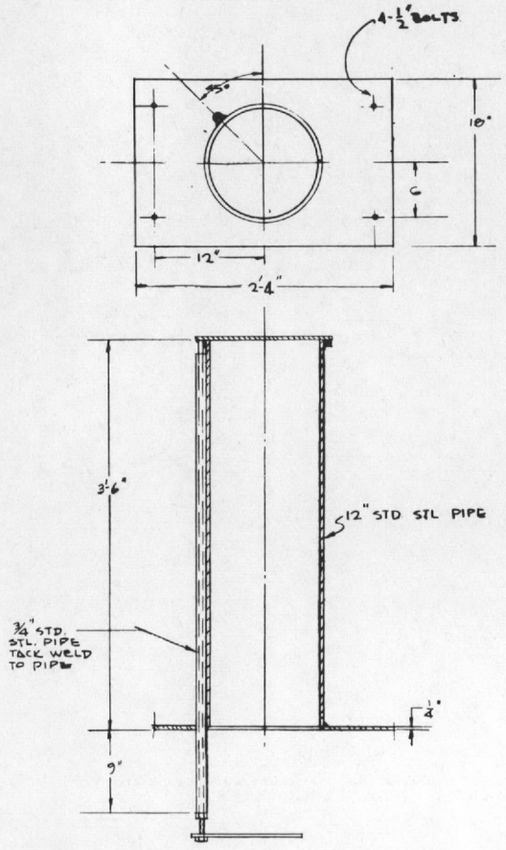

GUIDE TUBE ASSEMBLY

(SECURED POSITION)

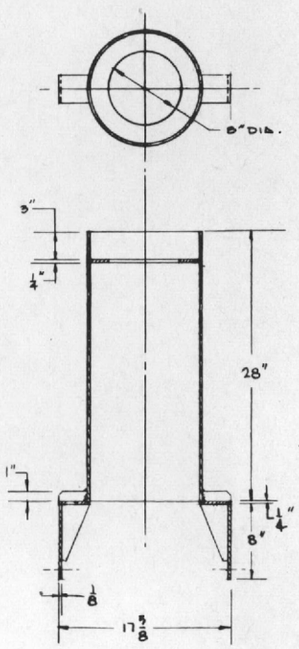

ELEVATING TUBE

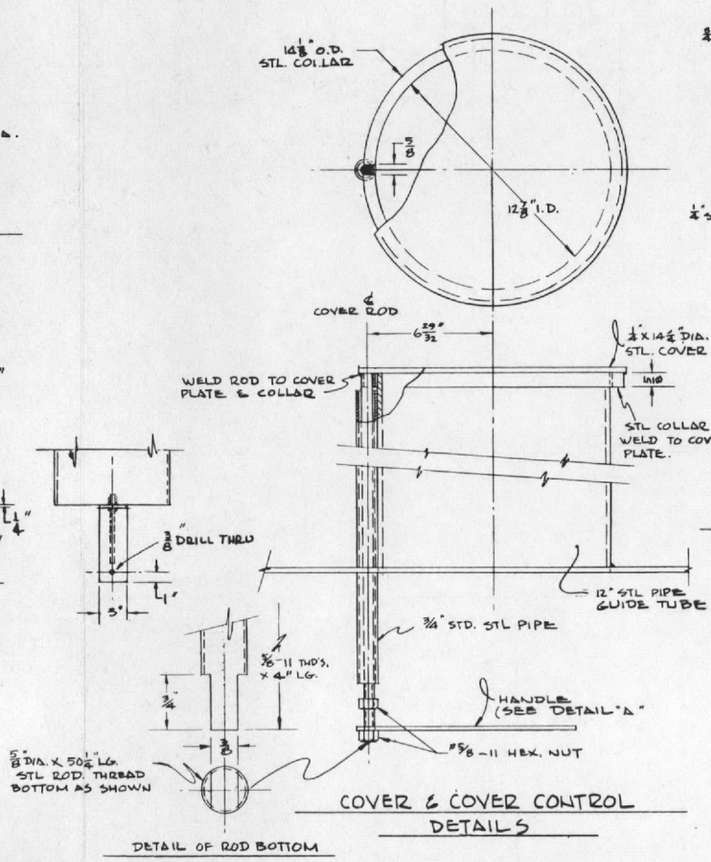

DETAIL OF ROD BOTTOM

COVER & COVER CONTROL DETAILS

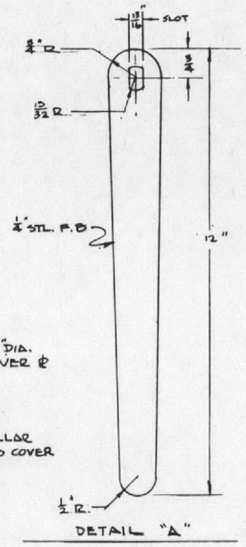

DETAIL "A"

(HANDLE)

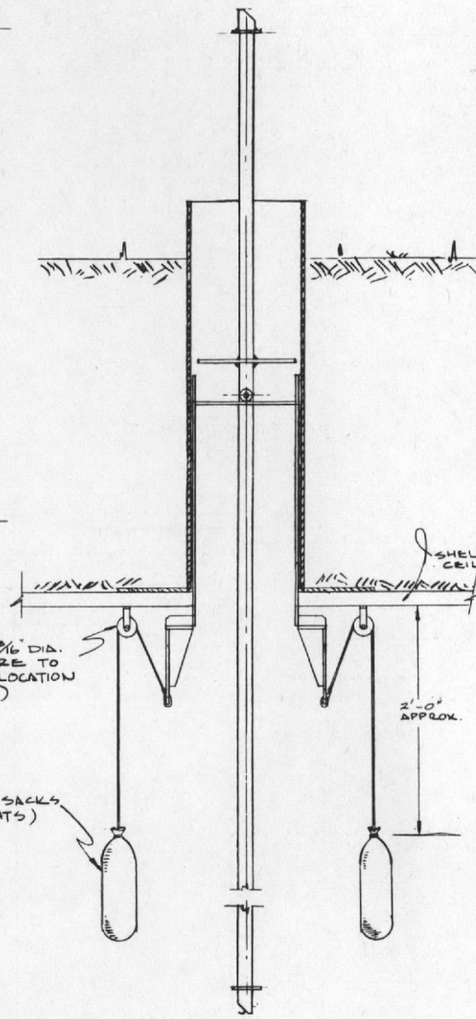

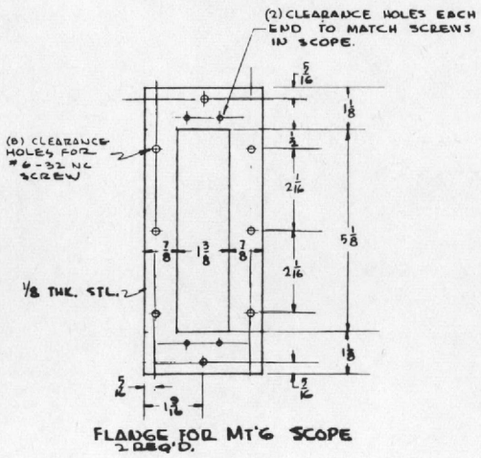

FLANGE FOR MT'G SCOPE

2 REQ'D.

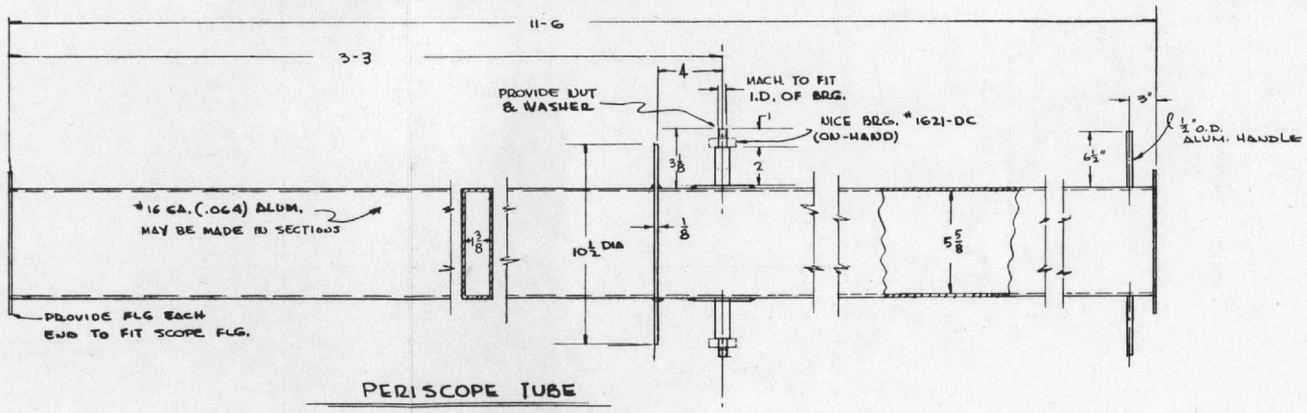

PERISCOPE TUBE

NOTE: PAINT INSIDE OF TUBE BLACK

Fig. A.7—Periscope mounting details.

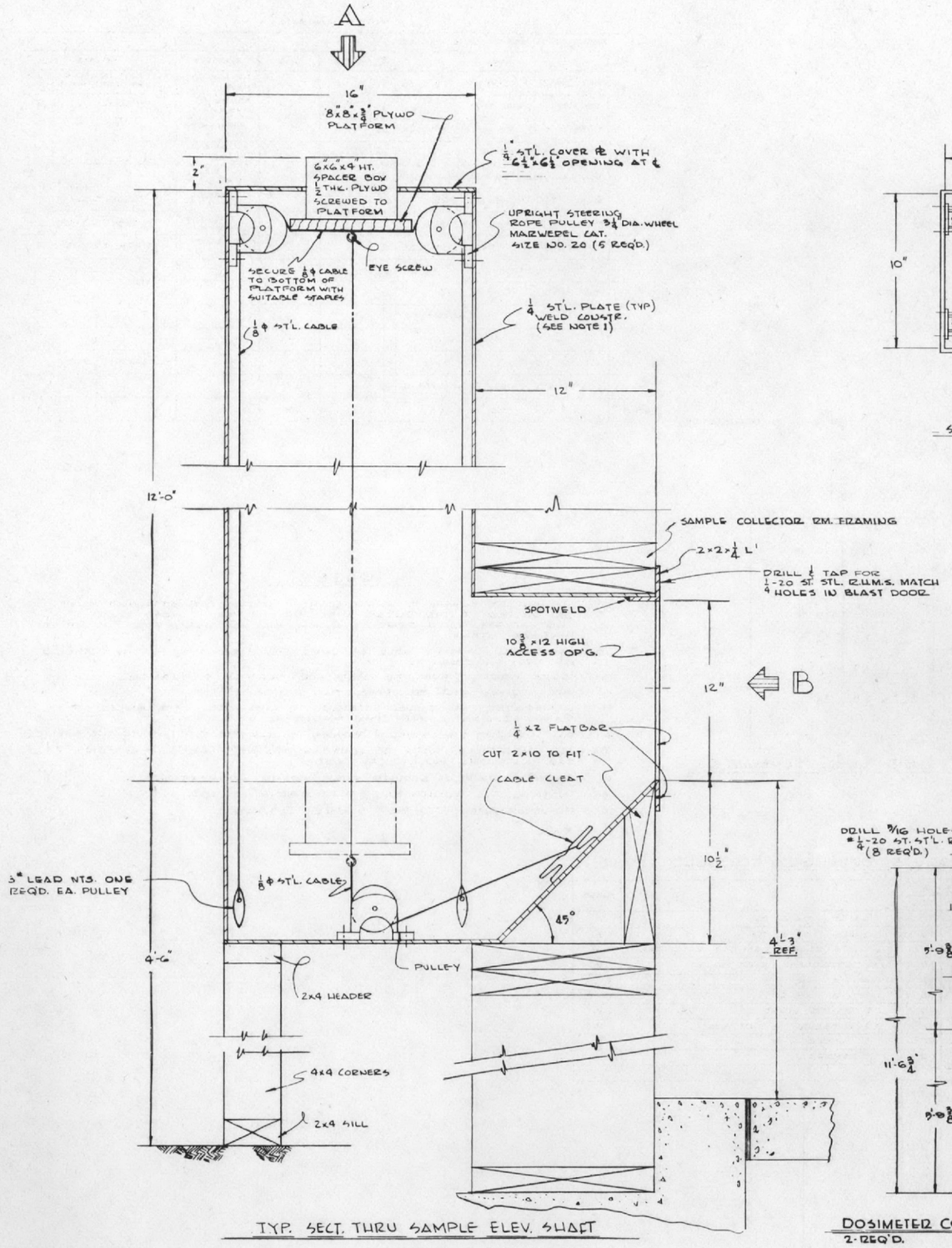

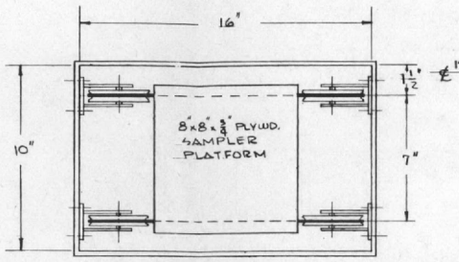

VIEW A

SHOWN WITH COVER PL REMOVED

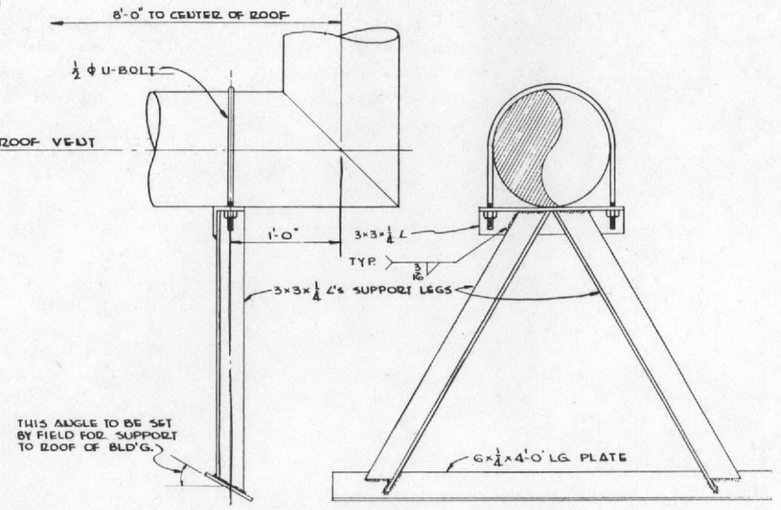

SUPPORT FOR 12" DIA. ROOF VENT

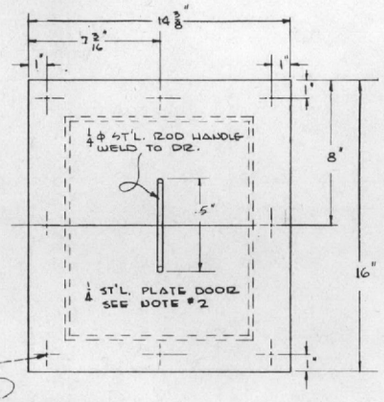

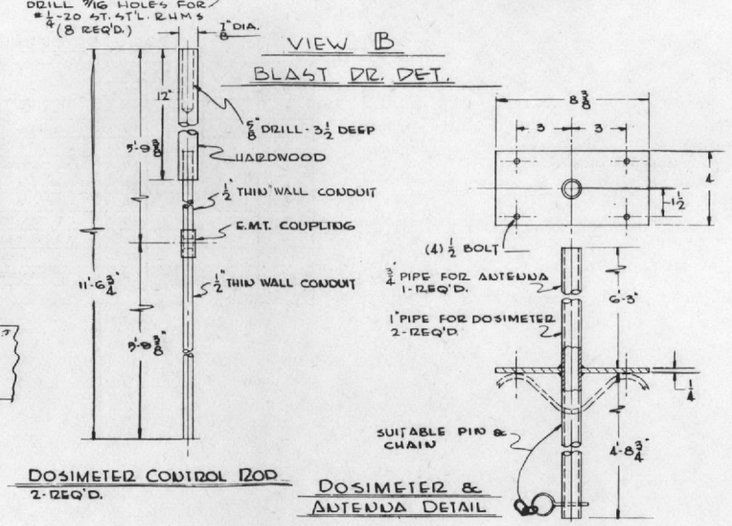

VIEW B

BLAST DR. DET.

DOSIMETER CONTROL ROD

2-REQ'D.

DOSIMETER & ANTENNA DETAIL

NOTES

1. STRUCTURAL WELDS TO BE 1/4" BEAD WELDS, 3" LG ON 6" CENTERS. TYPICAL FOR ALL WELDS.
2. INSTALL 1/4" THK. SPONGE RUBBER GASKET BETWEEN BLAST DOOR & FRAME.
3. THE BOTTOM END OF DOSIMETER CONDUIT IS TO BE PROVIDED WITH A STD. 3/4" PIPE CAP
4. THE ANTENNA TUBE IS TO BE PROVIDED WITH A STD. STUFFING TUBE. SIZE TO SUIT
5. ALL ITEMS SHOWN ON THIS DRAWING ARE TO BE FABRICATED FROM MILD STEEL.

Fig. A.8—Sample elevator shaft and shelter details.

LEGEND

EF○	ENTRANCE FITTING	PP	POWER PANEL
○	RLM FIXTURE 50W	TS	SERVICE SWITCH
◯	RLM FIXTURE 100W	○	OUTLET BOX
⋔	RECEPTACLE	SS	SAFETY SWITCH
S	SP SWITCH	—#—	2-#10-¾" CONDUIT
		—###	3-#3-1½" RIGID CONDUIT

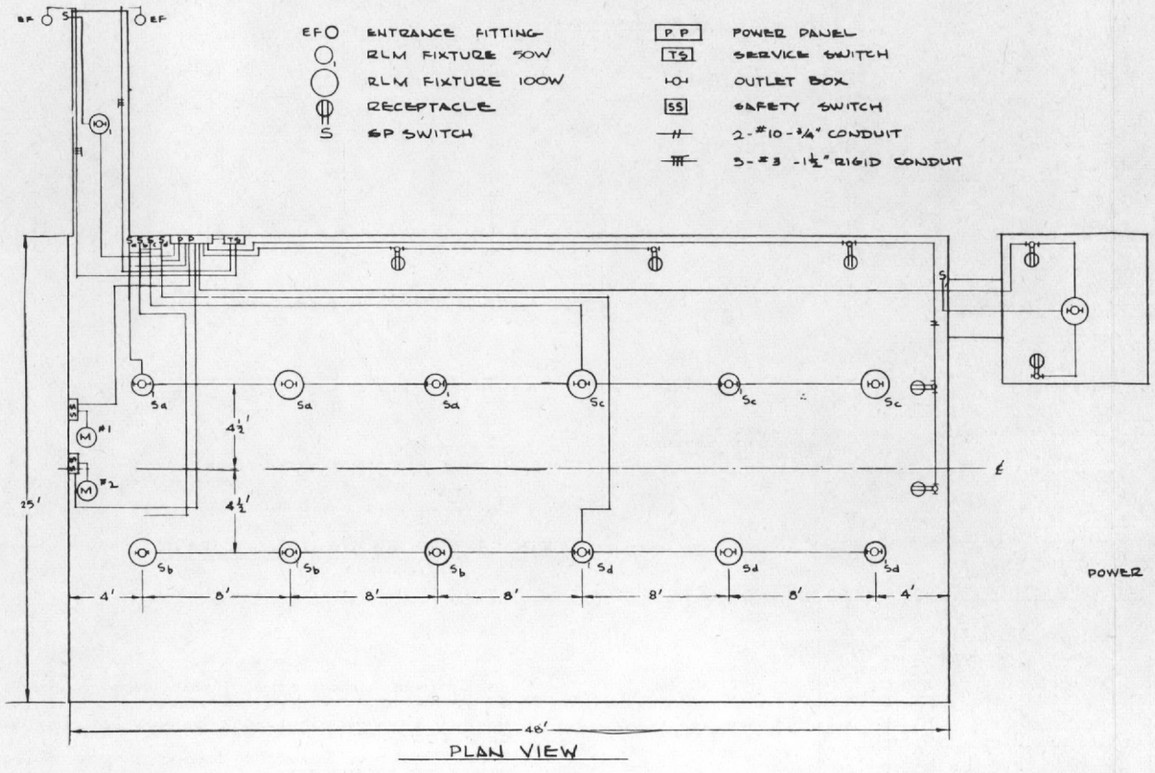

PLAN VIEW

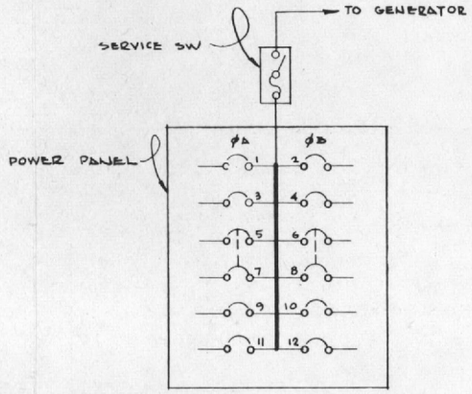

POWER PANEL SCHEMATIC

LIST OF MATERIAL

QUANTITIES SHOWN ARE FOR ONE SHELTER

PC. NO.	NAME	NO. REQ.	MATL.	MATL SPACE	STOCK SIZE	REMARKS
	CIR. BRKR. PWR. PANEL 125/250V.	1			SQUARE D #NBGR 12-32	3W, 12CKT, 100A MAINS, 5-30A, 7-20A BREAKERS, BOX MH20
	TRANSFER SW, 3PDT 100A FUSIBLE	1			SQUARE D # B2353F	SHEET METAL ENCLOSURE
	SAFETY SW, 2P-30A-250V, FUSIBLE	2			BULLDOG # SN-321	
	TOGGLE SW, SP-15A-120V	6			HUBBELL #1201	
	DUPLEX RECEPTACLES, 15A-120V	7			HUBBELL #5252	
	RLM STD. DOME FIXTURE	7			WHEELER # HRS-100	100W LAMP
	RLM STD. DOME FIXTURE	7			WHEELER # HS-100	90W LAMP
	ENTRANCE FITTING, 1½"-3 HOLES	2			APPLETON #EF-F-150	TYPE FEBS
	OUTLET BOX	AS REQ.				
	TW WIRE #3 AWG					
	#12 AWG					
	#10 AWG					
	RIGID CONDUIT, 1½"					WITH FITTINGS
	CONDUIT, ½" THIN WALL					
	¾"					

NOTES

1. ALL OUTLET BOXES TO WHICH LIGHT FIXTURES ARE ATTACHED MUST BE BOLTED TO THE OUTER SHELL OF SHELTER. THESE BOXES MUST ACCEPT RIGID CONDUIT WHICH WILL BE USED FOR THE LIGHT FIXTURE STEM.
2. THIN WALL CONDUIT WILL BE USED FOR RACEWAYS IN THE INTERIOR OF THE SHELTER.
3. RIGID CONDUIT WILL BE USED FOR SERVICE ENTRANCE.
4. ALL WIRING WILL BE TYPE TW.
5. GENERATOR MUST BE LOCATED TO MINIMIZE ENTRANCE OF EXHAUST GASES INTO THE SHELTER.
6. ALL CONDUIT & SWITCH BOXES SHALL BE BOLTED TO THE SHELTER.
7. ALL ELECTRICAL WORK TO CONFORM TO APPLICABLE SECTIONS OF THE NATIONAL ELECTRICAL CODE.
8. PROVIDE DRIVEN GROUND FOR GROUND CONNECTIONS.
9. INSTALL ALL EQUIPMENT 5 FT. ABOVE FLOOR.
10. POWER SUPPLY TO BE 3 WIRE 120/208 V.

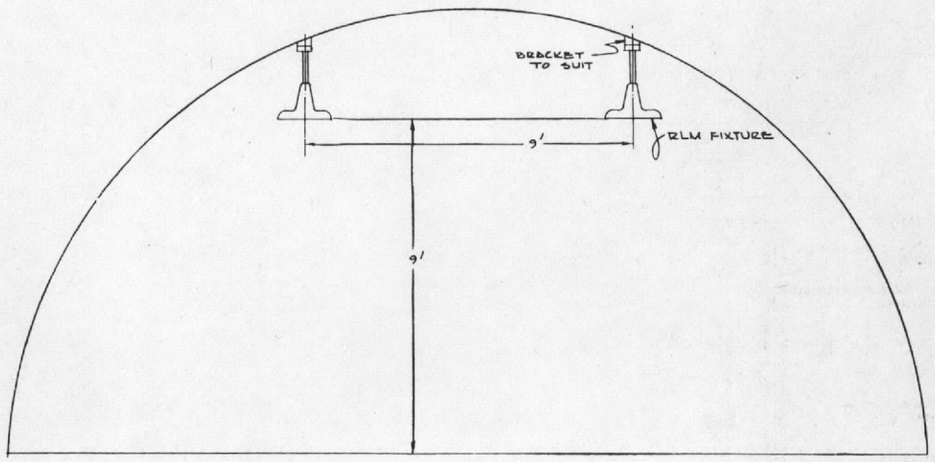

ELEVATION

CIRCUIT BREAKER SCHEDULE

BREAKER NO.	NO. OF POLES	RATING FRAME	RATING TRIP		PHASE
1	1	30 A	20 A	LIGHTS Sa & Sc	A
2	1		20 A	LIGHTS Sb & Sd	B
3	1		20 A	LIGHTS RECEPT. SAMPLE COLL. RM.	A
4	1		30 A	RECEPTACLES - END WALL	B
5 & 7	2		30 A	MOTOR NO 1	A-B
6 & 8	2		30 A	MOTOR NO 2	B-A
9	1		20 A	ENTRANCE LIGHT	A
10	1		20 A	RECEPTACLES - SIDE WALL	B
11	1		20 A	SPARE	A
12	1		20 A	SPARE	B

Fig. A.9—Electrical installation.

Appendix B

INSTRUMENTATION

B.1 INTERIOR SURVEY EQUIPMENT

Gamma-radiation surveys were carried out inside the shelter using seven AN/PDR-27C low-range survey instruments. Since it was possible that the interior intensities might be too low to provide reasonable rate-meter indication, the output of these instruments was connected to a Heiland oscillographic recorder. Each G-M tube pulse appears on the recorder trace. Very low radiation levels can be accurately resolved by a pulse-counting technique. In addition, the recorder traces provide a check on the accuracy with which the instruments were read by the operators. Details of the system are given in Fig. B.1.

B.2 FIXED SURVEY-INSTRUMENT SYSTEM

Five low-range survey instruments (AN/PDR-27C) were placed in the shelter at the locations shown in Fig. B.2. The indication on each instrument was recorded, providing a continuous measure of the radiation intensity throughout the shelter. Only one of the five instruments was continuously connected to a Brown recorder. The other four were intermittently connected to a second Brown recorder by a manually operated selector switch. An operator was required to switch the output of the instruments, in sequence, to the second recorder and to periodically adjust the range switches of all instruments. System details are shown in Fig. B.2.

B.3 DIRECTIONAL GAMMA APPARATUS

Instrumentation used to determine directional properties of gamma-radiation fluxes inside and outside consisted of a 1- by 1-in. cylindrical sodium iodide crystal enclosed with an associated photomultiplier tube in an elliptical lead collimator. This assembly was mounted on a rubber-tired metal dolly at a height of 1 meter above the surface. The apparatus was constructed so that the lead collimator could be rotated through a complete circle.

The output of the crystal–photomultiplier combination, in the form of electrical pulses, was used to drive both rate-meter and pulse-counting circuits, as shown in Fig. B.3. The output of the logarithmic rate-meter circuit was recorded on an Esterline-Angus chart during the first 10 min after burst. At later times, when directional measurements were being made, counts were accumulated during 10-sec runs by a Berkeley Digital Scanner, which made a permanent record on printed tape.

The angular resolution of the system, as determined with a radium source, is shown in Fig. B.4.

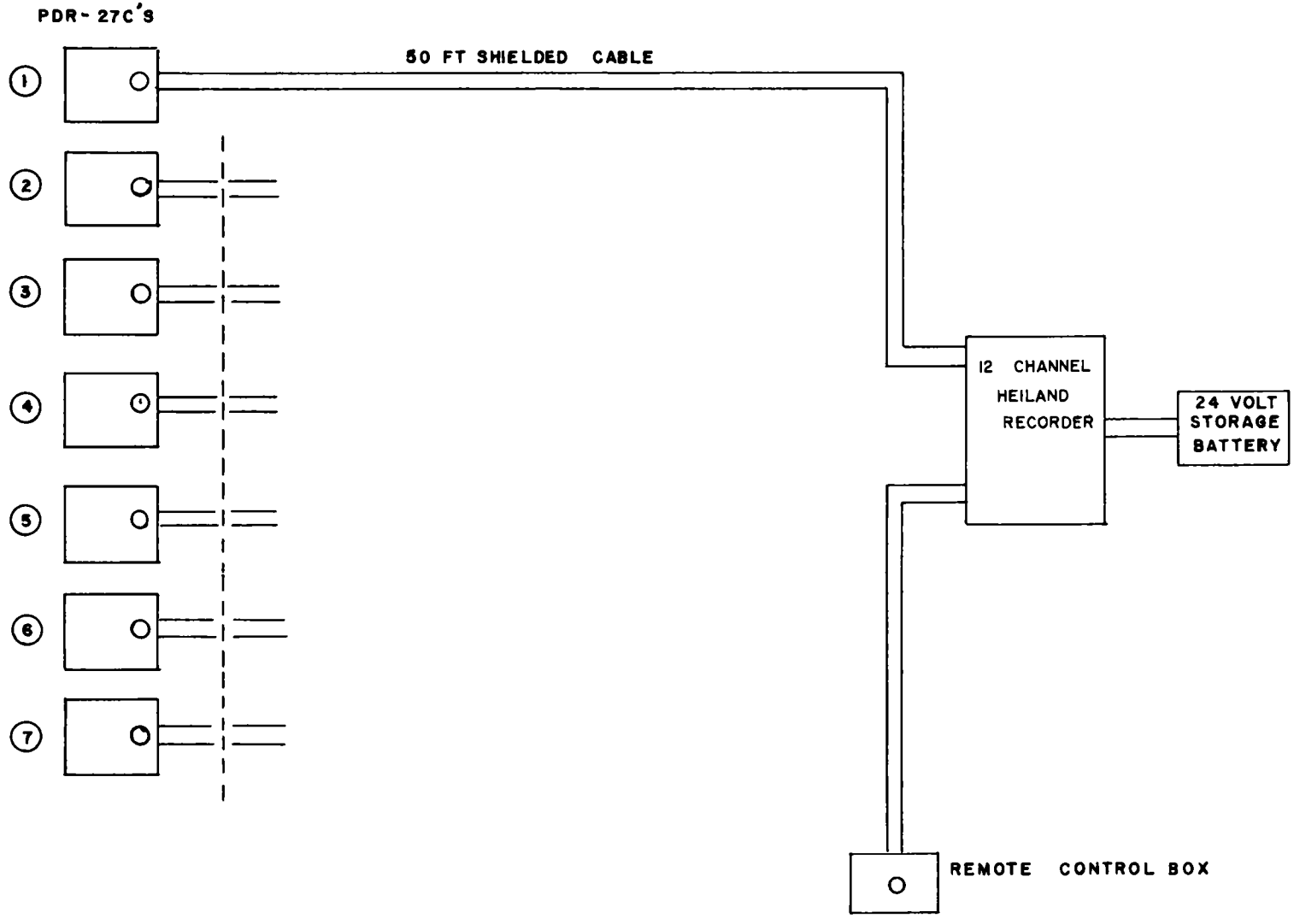

Fig. B.1—Block diagram of recording system for interior survey measurements.

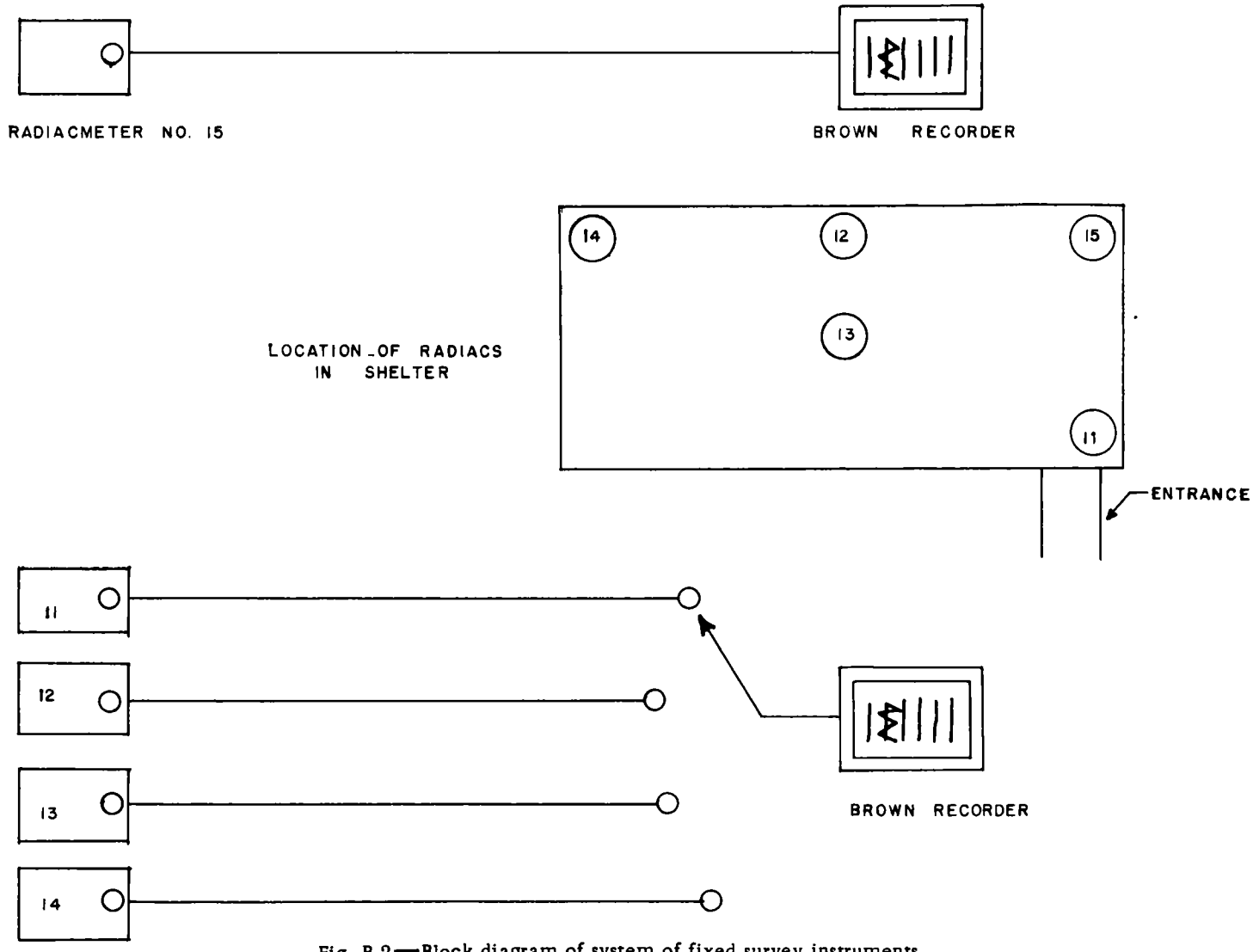

Fig. B.2—Block diagram of system of fixed survey instruments.

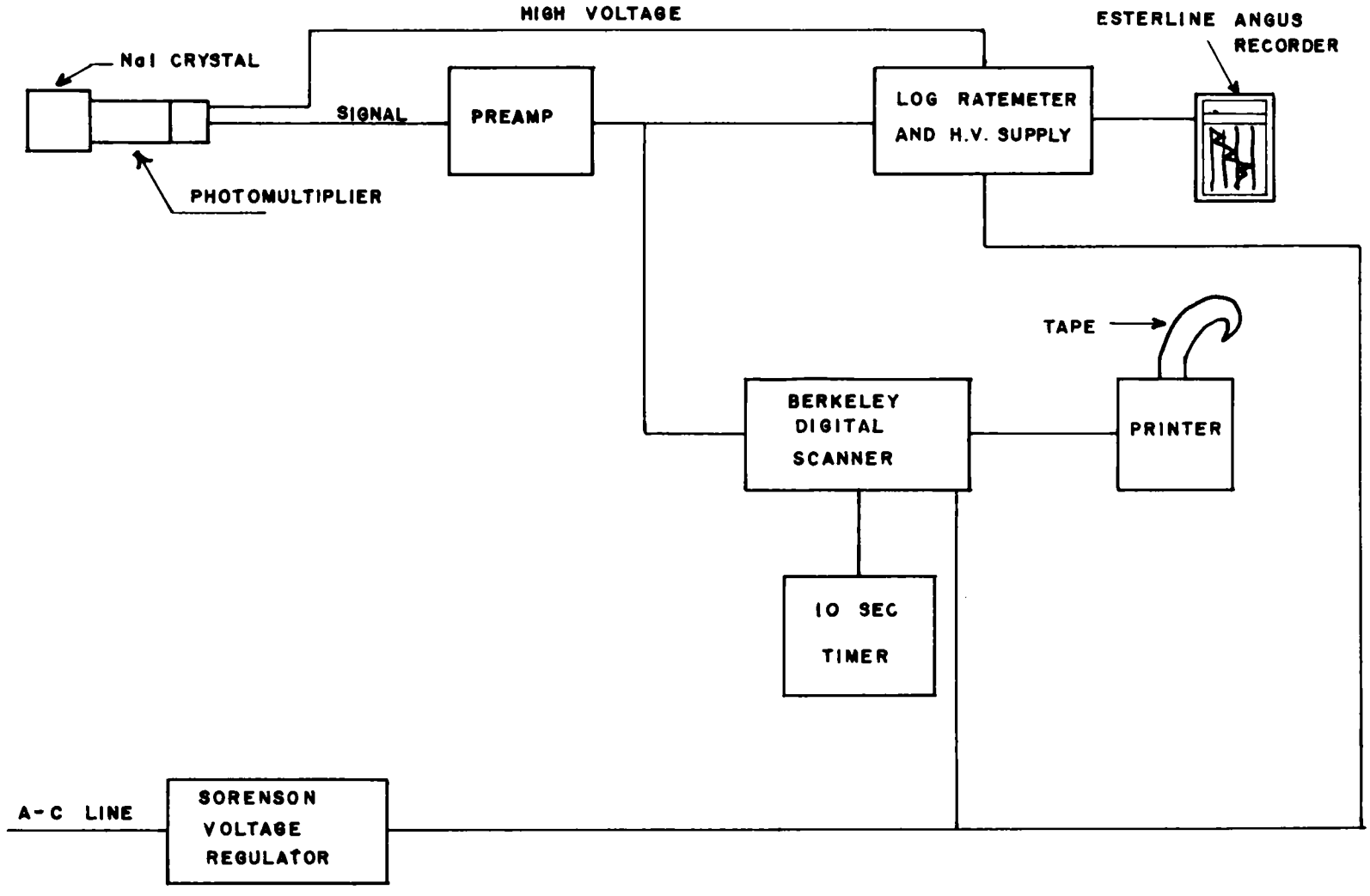

Fig. B.3—Block diagram of directional gamma apparatus.

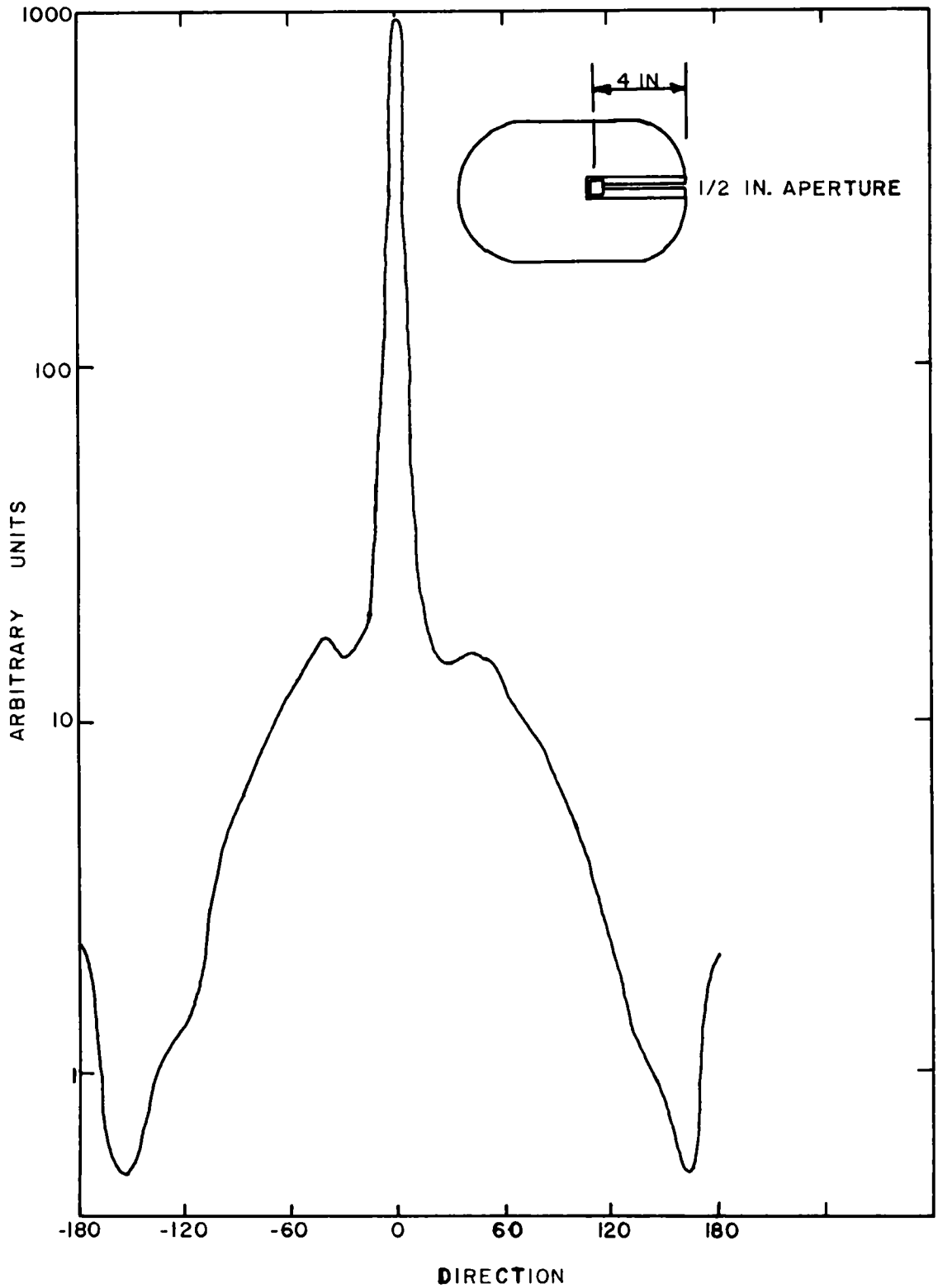

Fig. B.4—Angular resolution of a point source by the directional gamma apparatus.

B.4 SINGLE-CHANNEL PULSE-HEIGHT ANALYZER

Gamma spectra of fallout samples were obtained with an automatic step-scanning single-channel analyzer. Samples were prepared as point sources and placed in a 4-in. lead collimator with a $\frac{1}{2}$-in. hole. The distance from sample to the detector was maintained at 49 cm. The detector assembly consisted of a 3-in.-diameter cylinder of NaI(TI) and photomultiplier (Dumont 6363). This was shielded by an iron-brick cave. The single-channel analyzer was a USNRDL model 1, operated with a 5-volt window through a span of 100 volts. Data were recorded with a Berkeley Digital Scanner and were printed on tape. The equipment is shown in Fig. B.5.

B.5 USNRDL 4π ION CHAMBER

The USNRDL 4π ionization chamber is a high-pressure argon-gas chamber operated at 600 psig. The ion current is collected on a screen inside the chamber and is measured by use of an electronic electrometer. The current is read on a sensitive ammeter and is recorded through an amplifier by an Esterline-Angus recorder. Fallout particles, which were received in the sample-room collector, were transferred to $1\frac{1}{4}$-in.-diameter Lusteroid test tubes; the ionization current was measured by inserting the test tube into a cylindrical well extending into the chamber from the top. The sample, when placed at the bottom of the well, is located at the center of the chamber. Decay data can be obtained either by taking measurements from time to time or by leaving the sample in place and recording the ion current on the recorder. The equipment is shown in Fig. B.6.

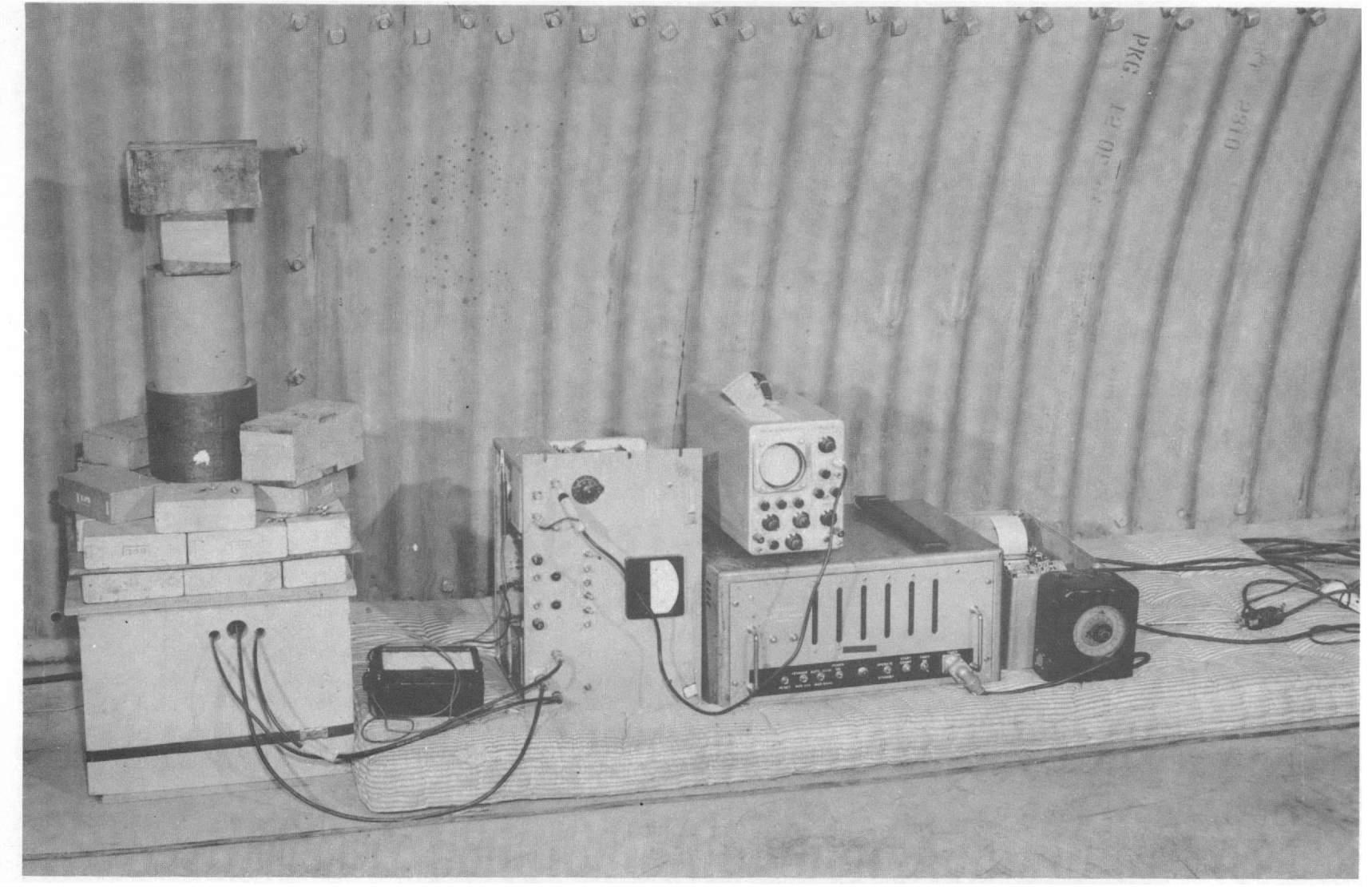

Fig. B.5—View of single-channel pulse-height analyzer.

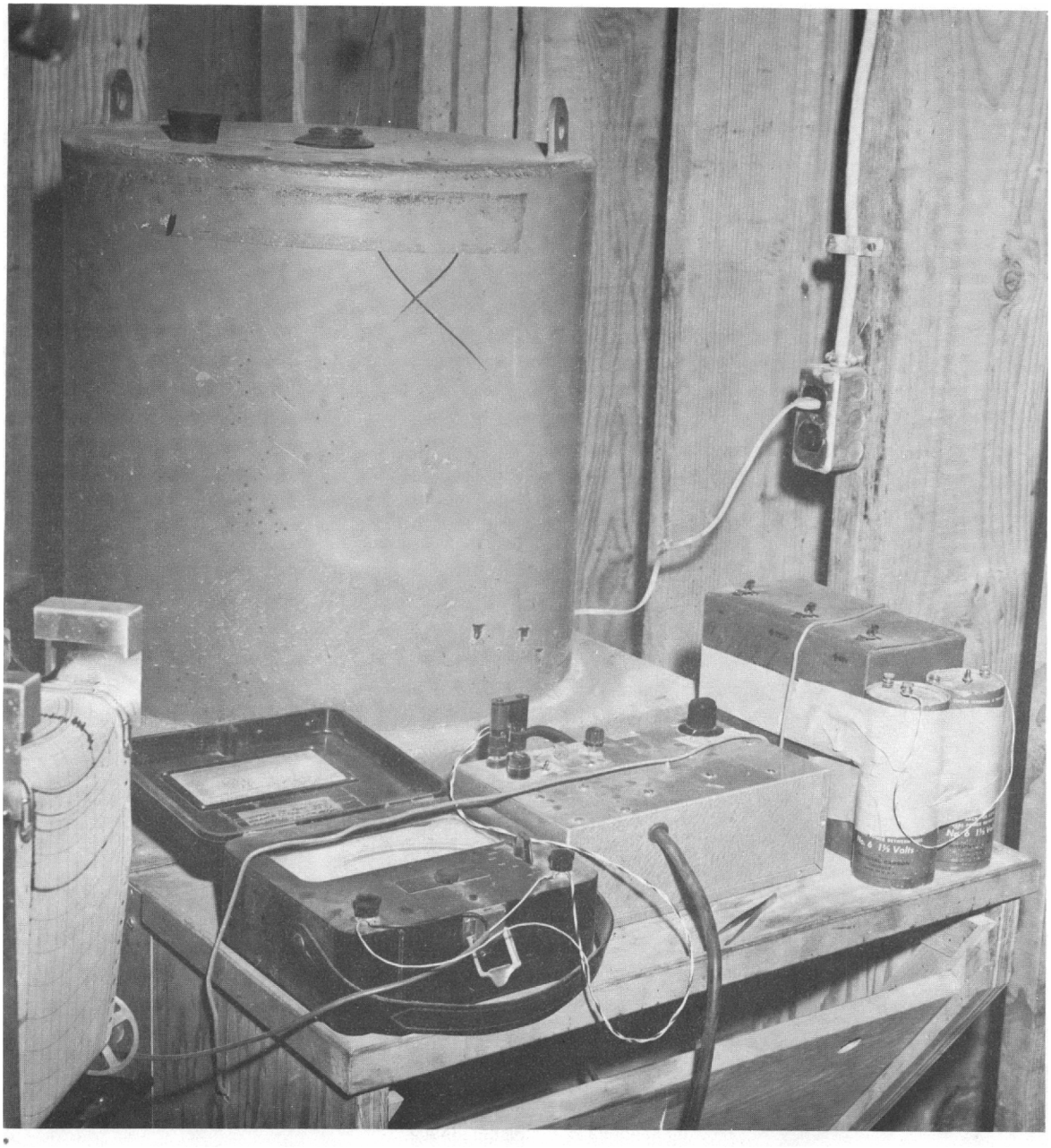

Fig. B.6 — View of 4π ion chamber in sample-collecting room.

Appendix C

EVENT SCHEDULES

TABLE C.1 — SHOT DIABLO, PROJECT 32.3 EVENT SCHEDULE

Time relative to shot time	Time relative to fallout event	Action	Personnel
D−1 day		Gas jeeps and deliver to CP	Unruh, Jamison, Thrall, Trolenberg, Phillips
		Refuel shelter generator	Nuckolls
H−8 hr		Leave Mercury for CP in carryall and sedan	All personnel
H−7 hr		Arrive CP area; dress out at Rad-Safe.	All personnel
H−6½ hr		Man jeeps; clear check station for station 2-32.3-8003	All personnel
H−6 hr		Arrive at station 2-32.3-8003	All personnel
		Start generator	Nuckolls
		Report station manned to CP	Strope
		Communication check: check radio link to CP. Monitors move by jeep to reclamation areas 2 and 3: check portable radio net	Sword, Unruh, Phillips, Lee, Jamison
		Check all instrumentation and shelter equipment	Miller, Work, Nuckolls, Brown, Laurino, Giboney
		Place jeeps in revetment, cover and tie down	Unruh, Phillips, Jamison, Lee
		Report completion of check to CP	Strope
H−2 hr		Button up entrance; no personnel to leave shelter until called for in event schedule after H-hour	Laurino
		Report status to CP	Strope
		Start GITR	Miller
H−30 min		Stop ventilation, close intake vents	Brown, Giboney
		Close exhaust vents	(a) Center vent: Laurino, Phillips (b) Rear vent: Thrall, Trolenberg
		House periscope; check dosimeter rods	Strope
		Charge dosimeters	Jamison, Lee
		Dress out	Unruh, Phillips, Jamison, Lee, Laurino, Brown, Giboney, Work
H−25 min		Report completion of shelter closure to CP; request fallout prediction	Strope

TABLE C.1 — (Continued)

Time relative to shot time	Time relative to fallout event	Action	Personnel
H − 5 min		All personnel assume shot-time position: sitting position on center line at rear of shelter; observe audible count-down	All personnel
H hour		Observe survey meters for initial gamma pulse	All personnel
		Start timing watches	Strope, Sword
		Start count-up	Strope
H + 15 sec		Check condition of shelter and personnel	Strope, Miller
		Raise ladder, open periscope, then open rear vent	Trolenberg, LaSpada
		Open vent intakes, start one M6	Brown, Giboney
		Run up periscope, check condition of superstructure and vehicles	Strope
		Switch count-down	Sword
		Man sample room	Nuckolls
H + 1 min		Report shelter condition to CP	Strope
H + 1½ min		Open up center exhaust vent	Laurino, Phillips
		Man Brown recorders	LaSpada
H + 2 min		Run film badges up dosimeter tubes	Thrall, Trolenberg
		Run film badges up center vent	Laurino, Phillips
		Read all self-reading dosimeters; charge background dosimeters and place in measurement locations	Lee, Unruh
H + 3 min		Begin I(a) routine on forward dosimeter tube, using 6-min cycle	Thrall
H + 4 min		Replace dosimeters	Lee, Unruh
H + 5 min		Start second M6	Giboney
H + 6 min		Start I(a) routine on after dosimeter tube, using 6-min cycle	Trolenberg
H + 6 min (est.)	Approach of fallout	Start aerosol sampling	Brown, Giboney
		Open fallout collectors; start incremental samplers	Miller, Laurino
		Begin directional gamma	Work, Jamison
		Begin absorption measurements	Unruh, Phillips
H + 6 to H + 10 min (est.)	Fallout arrival	Report fallout arrival to CP	Strope
H + 15 min		Equipment operators, with Rad-Safe monitor, leave CP for equipment location	Covey
H + 20 min (est.)	Peak intensity	Report peak intensity to CP	Strope
H + 20 min		Helicopter makes sample pickup and returns to CP	
H + 25 min		Prepare for I(c) survey	Unruh, Phillips, Jamison, Lee, Laurino, Work
		Terminate directional work	Work, Jamison
		Terminate absorption measurements	Unruh, Phillips
H + 30 min (est.)	Fallout cessation	Terminate aerosol sampling	Brown, Giboney
		Shut off exterior aerosol samplers	Miller
		Commence I(c) survey routine	Laurino, Unruh, Phillips, Jamison, Lee, Brown, Work, Giboney
		Report fallout cessation time and estimate of standard intensity to CP	Strope

TABLE C.1 — (Continued)

Time relative to shot time	Time relative to fallout event	Action	Personnel
H + 30 min		Equipment operators arrive at equipment; start engines	
H + 35 min		Make initial Phase II decision based on standard intensity at shelter; request available fallout information from CP if shelter situation is unsatisfactory	Strope, Miller, Sword
H + 40 min (est.)	Intensity less than 1 r/hr	Advise CP of Phase II situation; request permission to execute	Strope
H + 45 min (est.)		Terminate shelter survey	
		Two 2-man monitor teams man jeeps and execute survey of reclamation areas 2 and 3	Unruh, Phillips, Jamison, Lee
		Start exterior measurements	Laurino, Brown, Giboney, Work
		Retrieve exterior air samples	Brown, Giboney
H + 50 min		Receive first key-point measurements from monitors; select area most suitable or cancel Phase II; advise equipment crew and CP	Strope, Miller, Sword
H + 55 min (est.)		Receive second key-point measurements from monitors; make final decision on Phase II; advise equipment crew and CP	Strope, Miller, Sword
		Phase II monitors move to selected area	Unruh, Phillips, Thrall, Lee, Trolenberg, Giboney
H + 1 hr (est.)		Begin Phase II operations; monitor area and record data	See second entry in preceding item (plus equipment operators)
		Close fallout trays; terminate incremental samplers	Miller
		Set up Rad-Safe and dosimeter charge point at shelter entrance	Brown
		Read all dosimeters	Work, Jamison, Laurino
H + 1 hr 10 min		Grade and scrape 40- by 40-ft area; move spoil 500 ft from area	
H + 1 hr 25 min		Monitor 40- by 40-ft area	
H + 1 hr 35 min		Grade and scrape 60- by 60-ft area	
H + 1 hr 55 min		Monitor 60- by 60-ft area	
H + 2 hr 5 min		Grade and scrape 100- by 100-ft area	
H + 2 hr 35 min		Monitor 100- by 100-ft area	
H + 2 hr 45 min		Plow around 100- by 100-ft area to 500-ft perimeter	
H + 4 hr 45 min		Monitor 500- by 500-ft area	
H + 4 hr 45 min		Grade and scrape 100- by 100-ft area second time	
H + 5 hr 25 min		Monitor 100- by 100-ft area	
H + 5 hr 30 min		Further clearing of 100- by 100-ft area by front-end loader and dump truck	
H + 4 hr 45 min		Final monitoring of area	
H + 5 hr 55 min		Test completed	
H + 6 hr (est.)		Close down shelter; man jeeps; return to CP Rad-Safe area; process through change station; return to Mercury in carryall and sedan	All personnel

TABLE C.2—SHOT KEPLER, PROJECT 32.3 EVENT SCHEDULE

Time relative to shot time	Time relative to fallout event	Action	Personnel
D-1 day		Refuel shelter generator	Nuckolls
H-6½ hr		Leave Mercury for CP in carryall and sedan	All personnel
H-6 hr		Arrive CP area; dress out at Rad-Safe	All personnel
H-5½ hr		Man jeeps; clear check station for station 2-32.3-8003	All personnel
H-5 hr		Arrive at station 2-32.3-8003	All personnel
		Start generator	Nuckolls
		Report station manned to CP	Strope
		Communication check: check radio link to CP	Sword, Unruh
		Check all instrumentation and shelter equipment	Miller, Work, Nuckolls, Brown, Laurino, Harris
		Place jeeps in revetment; cover and tie down.	Unruh, Jamison, Lee, Osborne
		Report completion of check to CP	Strope
H-2 hr		Button up entrance; no personnel to leave shelter until called for in event schedule after H hour	Laurino
		Report status to CP	Strope
		Start GITR	Miller
H-30 min		Stop ventilation, close intake vents	Brown, Harris
		Close exhaust vents	(a) Center vent: Laurino, Osborne; (b) Rear vent: Thrall, Home
		House periscope; check dosimeter rods	Strope
		Charge dosimeters	Jamison, Lee
H-25 min		Report completion of shelter closure to CP; request fallout prediction	Strope
H-5 min		All personnel assume shot-time position: sitting position on center line at rear of shelter; observe audible count-down	All personnel
H hour		Observe survey meters for initial gamma pulse	All personnel
		Start timing watches	Strope, Sword
		Start count-up	Strope
H+15 sec		Check condition of shelter and personnel	Strope, Miller
		Raise ladder, open periscope, then rear vent	Home, Covey
		Open vent intakes, start one M6	Brown, Harris
		Run up periscope; check condition of superstructure and vehicles	Strope
		Switch count-down	Sword
		Man sample room	Nuckolls, MacDonald
H+1 min		Report shelter condition to CP	Strope
H+1½ min		Open center exhaust vent	Laurino, Osborne
H+2 min		Run film badges up center vent	Laurino, Osborne
		Read all self-reading dosimeters Charge background dosimeters and place in measurement locations	Lee, Unruh, Schuert, Anderson
		Man Brown recorder	Covey
H+3 min		Begin I(a) routine on forward dosimeter tube, using 6-min cycle	Thrall

TABLE C.2 — (Continued)

Time relative to shot time	Time relative to fallout event	Action	Personnel
H + 4 min		Replace dosimeters	Lee, Unruh, Schuert, Anderson
H + 6 min		Start I(a) routine on after dosimeter tube, using 6-min cycle	Home
H + 8 min (est.)	Approach of fallout	Start aerosol sampling	Brown, Harris
		Open fallout collectors; start incremental samplers	Laurino, Miller
		Begin absorption measurments	Unruh, Osborne
H + 8 to H + 10 min (est.)	Fallout arrival	Report fallout arrival to CP	Strope
H + 20 min (est.)	Peak intensity	Report peak intensity to CP	Strope
H + 25 min		Prepare for I(c) survey	Unruh, Osborne, Jamison, Lee, Laurino, Work
		Terminate absorption measurements	Unruh, Osborne
H + 30 min (est.)	Fallout cessation	Terminate aerosol sampling	Brown, Harris
		Shut off exterior aerosol samplers	Miller
		Commence I(c) survey routine	Laurino, Unruh, Osborne, Jamison, Lee, Brown, Work, Harris
		Report fallout cessation time and estimate of standard intensity to CP	Strope
H + 45 min (est.)		Terminate shelter survey	
		Start exterior measurements	Laurino, Brown, Work, Harris
		Retrieve exterior air samples	Brown, Harris
H + 1 hr (est.)		Start directional gamma measurements on shelter roof	Work, Jamison
		Close fallout trays; terminate incremental sampling	Miller
		Set up Rad-Safe and dosimeter charge point at shelter entrance	Brown
		Read all dosimeters	Work, Jamison, Laurino

TABLE C.3—SHOT SHASTA, PROJECT 32.3 EVENT SCHEDULE

Time relative to shot time	Time relative to fallout event	Action	Personnel
D−1 day		Refuel generator	Nuckolls
H−2 hr		Leave Mercury for station 2-32.3-8003 in two jeeps	All personnel
H−1½ hr		Arrive at station 2-32.3-8003	All personnel
		Start generator	Nuckolls
		Report station manned to CP	Miller
		Check all instrumentation	Miller, Covey, Nuckolls, Sively, Johnson
		Secure jeeps in revetment	Covey, Sively
H−1 hr		Close entrance	Miller
		Report status to CP	Miller
H−30 min		Stop ventilation, close intake and exhaust vents	All personnel
H−5 min		Assume shot-time position in rear of shelter	All personnel
H hour		Observe survey meters for initial gamma pulse	All personnel
H+30 sec		Check condition of shelter	Miller, Covey
		Open exhaust vents	Covey, Sively
		Open vent intake and start M6	Johnson
		Man sample room	Nuckolls
H+1 min		Report shelter condition to CP	Miller
H+5 min		Open sample collectors	Miller
H+6 min		Start incremental collectors	Miller
H+8 min		Start aerosol sampling	Covey, Sively
H+10 to H+15 min (est.)	Fallout arrival	Report fallout arrival to CP	Miller
H+15 to H+20 min (est.)	Peak intensity	Report peak intensity to CP	Miller
H+45 to H+60 min (est.)	Fallout cessation	Report fallout cessation to CP	Miller
		Terminate aerosol sampling	Covey, Sively, Johnson
		Close fallout collectors	Miller
H+2 hr		Make shelter survey	All personnel
H+6 hr		Recover fallout samples	Sively, Johnson
		Recover outside aerosol samples	Covey

Appendix D

CONVERSION OF R/HR AS OBSERVED ON THE AN/PDR-27C TO TRUE R/HR

D.1 SOURCE OF DATA AND INSTRUMENTATION

The photon distributions in the shelter on shot Diablo used in the following calculations were obtained by removing the lead collimator shield from the single-channel pulse-height analyzer described in Appendix B. The counts observed for a given time interval and channel number are presented in the columns of Table D.1. The number at the top of the various columns represents the time at which the measurements for that column were commenced.

D.2 TREATMENT OF DATA

The spectral data taken at H−105 min were used as the shelter background; the background counts were subtracted from the corresponding counts in the columns to the right. The energies corresponding to the various channel numbers were obtained from observed spectral data on standard samples of radionuclides with well-known decay schemes. The energy calibration curve for the analyzer settings used in taking the data is shown in Fig. D.1. From this figure and the net counts per time interval, plots of the number of counts in a given energy interval were made. It may be noted from Fig. D.1 that the pulse-height analyzer was not adjusted to zero energy and did not record photon energies below about 0.15 Mev. Since complete spectral coverage to zero energy was required for the analysis, it was necessary to extrapolate the observed data to zero energy. Extrapolations from both linear and logarithmic activity vs. channel curves were considered. When both of these methods were applied to the H+11 min measurements, the values obtained from the semilog plot were about 10 per cent higher than those obtained from linear plot. Since this difference is negligible when considered in terms of the over-all distribution and the attendant approximations in the calculations and since the use of the linear plot was more convenient, linear extrapolation was employed.

With the aid of the extrapolation it became possible to estimate the relative number of counts contained in selected energy intervals as shown in Table D.2. From these estimates the relative number of counts in each interval was determined. The data taken at H-hour were not included because at that time the radiation levels from the initial gamma were changing much more rapidly than the rate at which the data were being taken. The data taken at H+140 min were considered to duplicate those taken at H+118 min and H+129 min; therefore they were not included in the analysis. Finally, because many of the data taken at H+790 min were near the background level, many of the resultant net counts are subject to large uncertainties, and consequently the H+790 min data were not reduced. The relative distribution for the remainder of the data is given in Table D.2.

To convert from relative number of counts in a given energy interval to the relative number of incident photons in that interval, one must first divide the former quantity by the de-

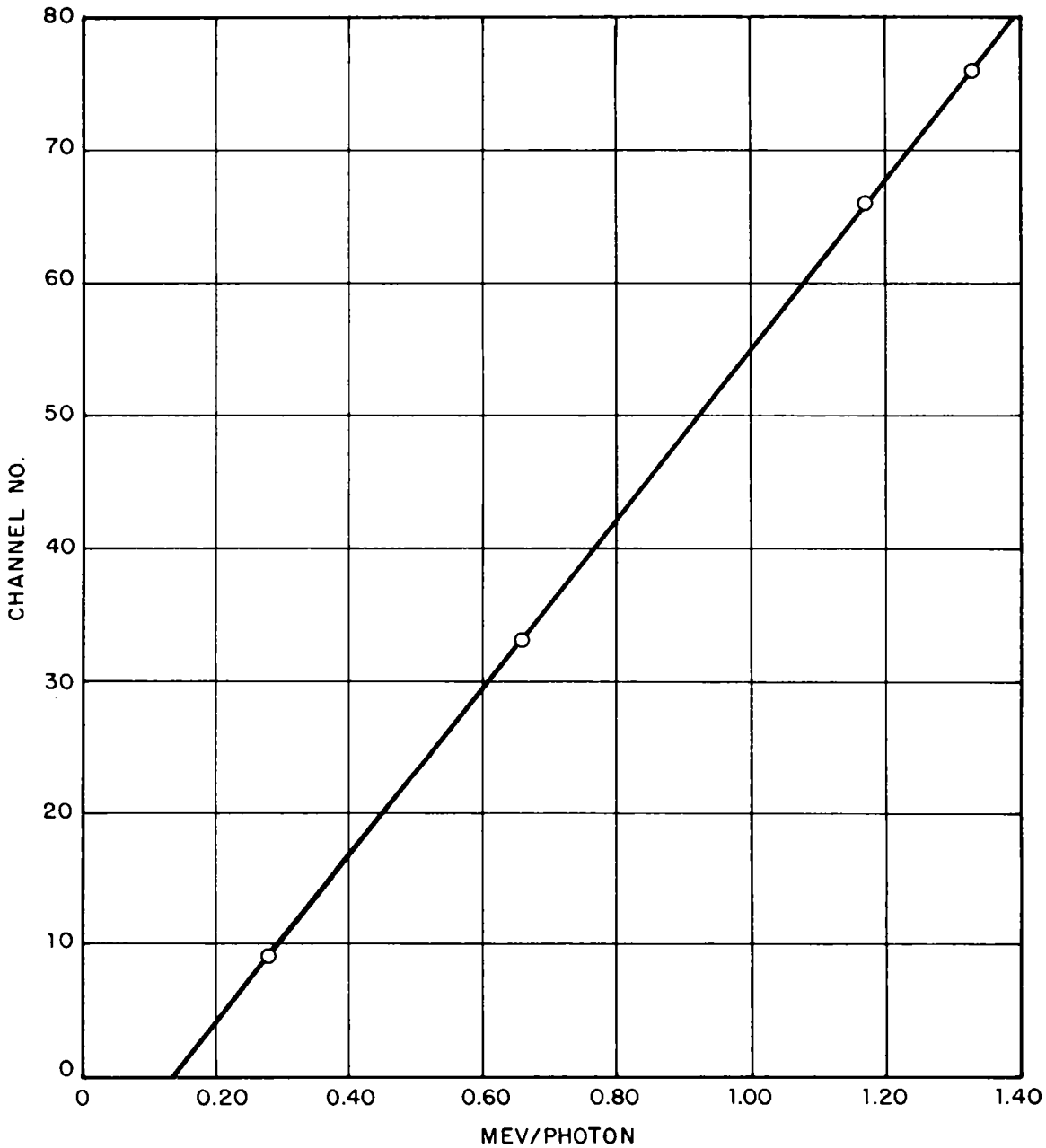

Fig. D.1—Pulse-height analyzer energy calibration curve.

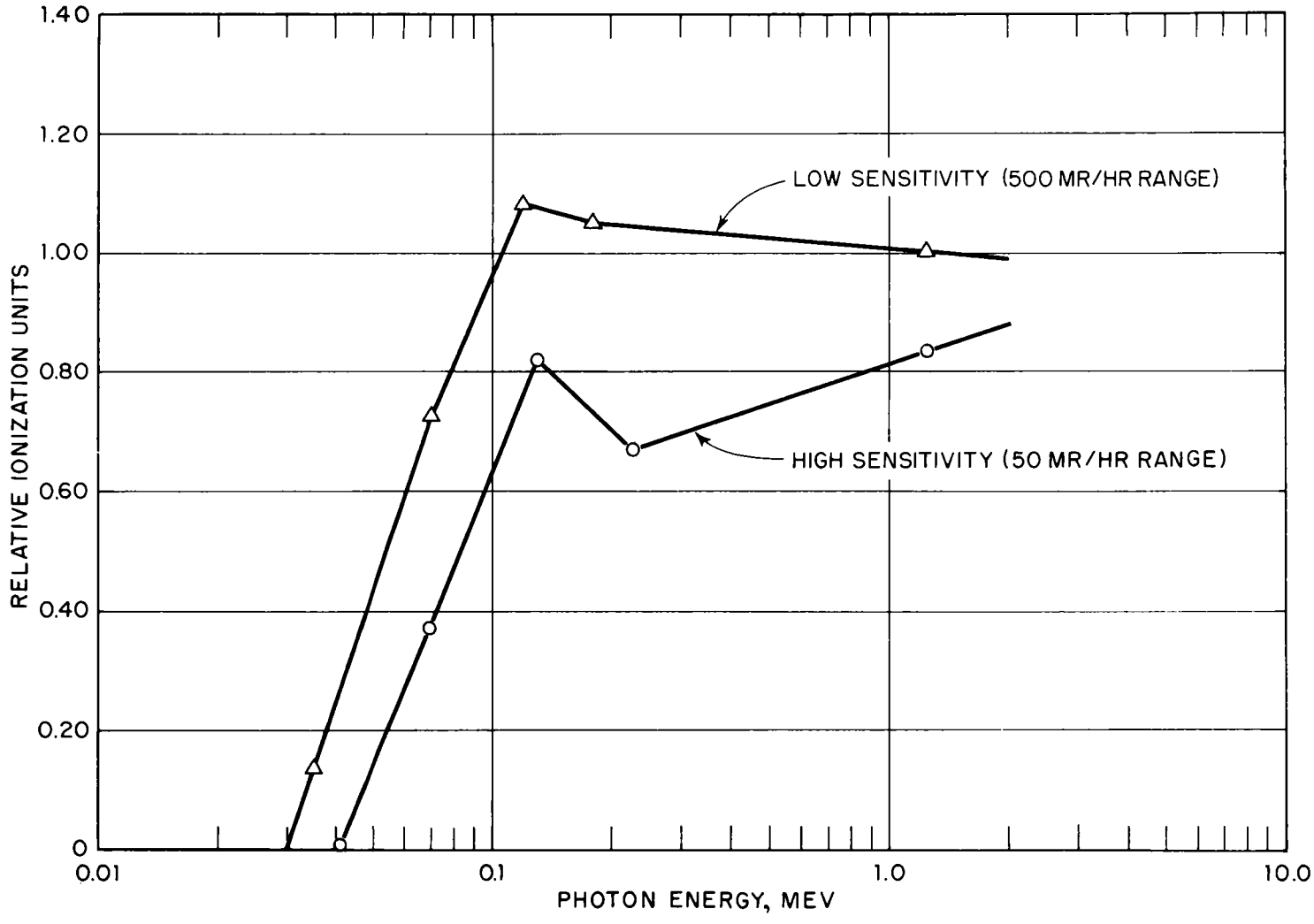

Fig. D.2—Response of AN/PDR-27C relative to Co^{60} for a source geometry that is symmetrical about a vertical plane through the long axis of the instrument (integrated response with phantom).

tector efficiency. The detector efficiency is dependent upon the median energy for the interval, the size of the detecting crystal, and the geometrical arrangement of the source material with respect to the detecting element. The latter quantity for the shelter is not known in any detail, and, even if it were, it is unlikely that the corresponding detector efficiencies would be known. However, reference 1 gives the efficiencies for a crystal like that used in the pulse-height analyzer (Appendix B) for a point source located at various distances up to a maximum of 20 cm from the crystal. Inspection of the data in reference 1 shows that, although the efficiencies corresponding to the 20-cm distance are different in absolute magnitude from the efficiencies at, say, contact distance, the relative efficiencies, i.e., ratio of efficiency at one energy to that at another, are about the same. Because a better choice was not possible, it was assumed that this observation would also apply between the relative efficiencies corresponding to the 20-cm distance and the actual source geometry. The relative efficiencies for the 20-cm distance are reproduced in Table D.3; these were applied to the numbers in Table D.2 to estimate the energy distribution of photons in the shelter. The results are given in Table D.4.

To convert the spectra to the relative contribution to the ionization rate of a given energy interval, one must multiply the relative number of photons in each energy interval by the product of median energy for that interval and the Klein-Nishina absorption coefficient for air corresponding to the median energy.[2] Values for the latter quantity were obtained from reference 2 and are listed in column 3 of Table D.3. The product is given in column 4. The instrument (AN/PDR-27C) ratios are given in the last two columns of Table D.3. The percentage of the ionization rate contributed from a given energy interval is listed in Table D.5.

Conversion of the air ionization rate, Table D.5, to the gross response in roentgens per hour as observed on the AN/PDR-27C requires that the ratio of the two quantities be known for each energy interval. Data on the response of the AN/PDR-27C to various source geometries as a function of source energy were furnished by G. A. Work.[3] The geometry most appropriate to the present calculation is the one designated as the vertical plane in which the source consists, in essence, of a uniformly active ring centered about the detector, located in a vertical plane through the long axis of the instrument. The response of the AN/PDR-27C for this geometry and for both ranges of detection on the instrument are presented in Fig. D.2. With the aid of this figure it was possible to obtain the relative response for each energy interval given in the last two columns of Table D.3. The latter values were used to compute, in relative terms, the contribution of the photons in each energy interval to the over-all response of the AN/PDR-27C from the values given in Table D.5. The results are given in Table D.6; the sum is included for appropriate columns. This sum, when divided into 100 yields the conversion ratio for the AN/PDR-27C, i.e., the factor that converts observed reading in roentgens per hour into the estimated value of the true ionization rate. The latter set of values are summarized in Table D.7.

D.3 DISCUSSION OF RESULTS

It will be recalled that it was necessary to extrapolate the number of counts in the channels for photons from 0 to 0.15 Mev. Inspection of Tables D.2 and D.4 makes it evident that a considerable fraction of these photon-energy distributions is contained in the extrapolated region. However, if reference is now made to Tables D.5 and D.6, it will be seen that the corresponding relative contribution of the photons up to 0.15 Mev in energy is considerably smaller. Thus at H+118 min some 60 per cent of the photons in the shelter are contained in the region of extrapolation, but only 17 per cent of the true air ionization and 13 per cent of the AN/PDR-27C (low-range) response are contributed by these photons. Therefore it is apparent that errors in the extrapolation would not contribute corresponding errors in the values of Table D.7. Inspection of Table D.3 shows that the biggest change in the relative distribution is brought about by use of the product of the Klein-Nishina factor and the median energy. This is probably the most accurate set of conversion numbers used. Although much larger uncertainties are associated with the other conversion factors, the smaller variation from interval to interval does not make the final result equally sensitive to such uncertainties.

From Table D.7 it can be seen that there is excellent agreement among the results in each sensitivity range. This is noteworthy because the spectral distributions from which they were computed are quite different, and the good agreement indicates that the conversion factor is quite insensitive to changes in the photon spectrum. The relative response of the low range (50 mr/hr) of the AN/PDR-27C to the photon-energy distribution in the shelter, 1/1.37(0.735), is very close to that given in the text for the response of the AN/PDR-39(TIB) to the photons from a distributed source of fission products.

REFERENCES

1. E. A. Wolicki, Calculated Efficiencies of NaI Crystals, Report NRL-4833, Oct. 5, 1956.
2. S. L. Glasstone, "The Effects of Atomic Weapons," U. S. Government Printing Office, Washington 25, D. C., September 1950.
3. G. A. Work et al., Directional Response of AN/PDR-27C, private communication, USNRDL.

TABLE D.1 — PULSE-HEIGHT ANALYZER DATA FROM PHOTON SPECTRA INSIDE THE SHELTER, SHOT DIABLO

Channel No.	Time relative to shot times							
	H−105 min, counts/15 sec	H+0 min, counts/15 sec	H+11 min, counts/15 sec	H+118 min, counts/15 sec	H+129 min, counts/15 sec	H+140 min, counts/15 sec	H+315 min, counts/15 sec	H+790 min, counts/30 sec
0	189	8813	3632	3729	3324	2975	1169	843
1	212	800	3680	2984	2728	2481	1129	801
2	199	2501	3551	2485	2284	1921	995	760
3	161	2395	3466	2117	1904	1701	986	731
4	140	9208	3110	1771	1514	1475	907	630
5	174	5387	3092	1566	1378	1317	872	548
6	147	6763	2891	1413	1191	1099	763	540
7	123	704	2709	1220	1095	996	660	503
8	140	7899	2430	1079	1027	930	596	413
9	104	4322	2451	1086	890	855	495	377
10	79	3563	2376	953	831	741	444	318
11	107	702	2217	878	768	659	391	308
12	87	949	2127	760	674	673	398	267
13	76	555	2065	731	603	588	304	235
14	69	4649	1986	663	555	474	343	192
15	55	3173	1930	569	504	453	262	173
16	62	2286	1861	509	455	414	250	154
17	60	1650	1651	475	422	421	208	177
18	40	1166	1677	474	403	357	186	158
19	47	902	1555	425	351	340	201	132
20	28	704	1653	425	374	346	210	141
21	54	511	1601	369	307	315	199	161
22	40	435	1460	330	325	297	195	122
23	41	359	1463	320	296	277	227	141
24	24	315	1371	358	298	250	178	146
25	31	289	1230	322	273	246	170	124
26	39	239	1207	276	264	244	169	103
27	30	200	1193	269	226	216	111	109
28	25	195	1067	245	216	201	143	98
29	34	156	987	229	235	203	107	92

TABLE D.1 — (Continued)

Channel No.	Time relative to shot times							
	H − 105 min, counts/15 sec	H + 0 min, counts/15 sec	H + 11 min, counts/15 sec	H + 118 min, counts/15 sec	H + 129 min, counts/15 sec	H + 140 min, counts/15 sec	H + 135 min, counts/15 sec	H + 790 min, counts/30 sec
30	23	139	926	222	215	199	93	67
31	24	137	897	230	193	162	106	75
32	25	151	883	195	200	166	93	85
33	23	138	853	206	201	150	82	60
34	23	142	795	161	155	143	76	66
35	19	120	754	185	162	133	85	49
36	18	130	698	170	139	179	66	61
37	18	133	700	168	158	125	73	48
38	15	115	682	147	159	128	94	68
39	21	122	620	147	124	125	66	67
40	21	101	606	143	134	101	74	36
41	14	109	626	132	96	115	70	66
42	22	118	592	145	123	125	48	45
43	17	97	555	130	129	99	73	49
44	20	90	556	138	123	125	73	35
45	19	109	509	146	127	128	57	31
46	12	105	488	118	129	88	58	33
47	11	102	502	110	114	97	54	44
48	15	100	514	101	93	99	51	30
49	16	86	496	110	99	70	55	36
50	15	95	464	79	99	82	45	40
51	14	102	442	102	76	85	40	31
52	13	90	419	91	93	71	55	33
53	15	96	417	113	82	69	39	38
54	15	98	376	68	81	58	43	25
55	10	92	349	83	72	54	43	33
56	8	82	351	63	61	71	39	36
57	11	88	347	54	64	72	36	22
58	11	114	341	74	75	50	37	29
59	10	100	322	70	58	63	31	27

TABLE D.1 — (Continued)

Channel No.	Time relative to shot times							
	H−105 min, counts/15 sec	H+0 min, counts/15 sec	H+11 min, counts/15 sec	H+118 min, counts/15 sec	H+129 min, counts/15 sec	H+140 min, counts/15 sec	H+315 min, counts/15 sec	H+790 min, counts/30 sec
60	15	98	344	53	74	54	25	18
61	12	113	337	58	74	43	47	18
62	10	86	331	70	59	32	36	27
63	8	93	312	62	54	45	35	20
64	10	86	331	47	51	51	32	16
65	6	93	294	61	46	45	31	15
66	7	100	276	44	38	50	26	17
67	4	79	279	53	63	33	26	13
68	8	91	277	58	31	47	25	25
69	5	94	282	58	40	27	18	18
70	5	96	289	49	40	27	26	14
71	5	94	253	42	43	38	21	7
72	2	101	236	35	44	34	21	18
73	5	92	227	55	29	45	19	12
74	9	85	212	34	26	39	20	16
75	5	84	215	42	36	36	23	19
76	9	96	215	38	30	34	24	13
77	7	107	186	38	37	32	24	21
78	5	93	200	46	33	25	18	15
79	4	84	200	35	20	37	12	13
80	8	97	189	26	22	27	17	11
81	5	96	200	29	21	20	26	19
82	8	105	209	35	24	33	29	21
83	4	119	175	26	17	34	30	25
84	3	104	215	23	17	31	17	22
85	9	113	187	31	12	28	22	29
86	4	115	163	28	15	23	25	25
87	0	110	177	28	23	29	16	19
88	5	132	164	35	25	22	18	18
89	3	110	171	27	11	27	18	14

TABLE D.1 — (Continued)

Channel No.	Time relative to shot times: H−105 min, counts/15 sec	H+0 min, counts/15 sec	H+11 min, counts/15 sec	H+118 min, counts/15 sec	H+129 min, counts/15 sec	H+140 min, counts/15 sec	H+315 min, counts/15 sec	H+790 min, counts/30 sec
90	2	100	164	22	11	22	15	26
91	3	108	165	20	17	15	20	16
92	5	141	154	32	20	21	12	11
93	3	152	160	30	11	28	9	11
94	4	148	135	23	15		12	8
95	2	119	129	12	17		8	5
96	0	115	156	24	24		14	3
97	3	135	872	13	7		12	7
98	0	128	710	20	9		7	5
99	6	142	139	14	10		11	3

TABLE D.2—RELATIVE DISTRIBUTION OF OBSERVED PHOTON COUNTS FROM THE PULSE-HEIGHT ANALYZER IN SELECTED ENERGY INTERVALS

Energy interval, Mev	Relative distribution (at indicated time after burst), %			
	H + 11 min	H + 118 min	H + 129 min	H + 315 min
0 – 0.06	14.7	32.1	35.2	23.2
0.06 – 0.08	4.2	8.7	8.9	6.5
0.08 – 0.10	4.1	7.8	7.9	6.1
0.10 – 0.15	10.7	17.2	17.0	15.0
0.15 – 0.20	9.5	10.3	9.0	11.9
0.20 – 0.30	15.0	11.1	8.0	16.8
0.30 – 0.40	10.2	3.9	4.4	6.2
0.40 – 0.50	7.4	2.4	2.4	3.7
0.50 – 0.60	6.3	1.8	2.0	3.3
0.60 – 0.80	7.2	2.1	2.2	2.8
0.80 – 1.00	4.7	1.2	1.5	1.9
1.00 – 1.50	6.0	1.4	1.6	2.5
Total	100.0	100.0	100.1	99.9

TABLE D.3—FACTORS USED TO CONVERT SPECTRAL DATA TO GROSS RESPONSE TO THE AN/PDR-27C

Energy interval, Mev	Crystal efficiency, relative units	Klein-Nishina factor, 10^5/cm	Klein-Nishina factor × Median energy, (Mev × 10^{-5})/cm	Low range, instrument ratio relative units	High range, instrument ratio relative units
0 – 0.06	8.8	2.10	0.063	0.05	0.18
0.06 – 0.08	8.8	2.63	0.184	0.38	0.73
0.08 – 0.10	8.7	2.80	0.252	0.56	0.91
0.10 – 0.15	8.5	3.02	0.378	0.72	1.06
0.15 – 0.20	8.2	3.28	0.574	0.74	1.05
0.20 – 0.30	7.6	3.56	0.89	0.69	1.04
0.30 – 0.40	7.1	3.78	1.32	0.71	1.03
0.40 – 0.50	6.7	3.84	1.73	0.73	1.03
0.50 – 0.60	6.4	3.38	2.11	0.75	1.02
0.60 – 0.80	6.0	3.76	2.63	0.78	1.01
0.80 – 1.0	5.6	3.64	3.28	0.80	1.01
1.0 – 1.5	5.0	3.34	4.18	0.83	1.00

TABLE D.4 — ESTIMATED ENERGY DISTRIBUTION OF PHOTONS IN SHELTER, SHOT DIABLO

Energy interval, Mev	Estimated energy distribution (at indicated time after burst), % H+11 min	H+118 min	H+129 min	H+315 min
0 – 0.06	12.2	29.7	32.5	20.7
0.06 – 0.08	3.5	8.1	8.3	5.8
0.08 – 0.10	3.4	7.3	7.4	5.5
0.10 – 0.15	9.1	16.5	16.3	13.8
0.15 – 0.20	8.4	10.2	8.9	11.3
0.20 – 0.30	14.3	11.9	8.5	17.3
0.30 – 0.40	10.4	4.5	5.0	6.9
0.40 – 0.50	8.0	2.9	2.9	4.4
0.50 – 0.60	7.2	2.2	2.6	4.1
0.60 – 0.80	8.7	2.8	3.0	3.7
0.80 – 1.00	6.2	1.8	2.1	2.7
1.00 – 1.50	8.7	2.3	2.6	3.9
Total	100.1	100.2	100.1	99.6

TABLE D.5 — CONTRIBUTION OF EACH ENERGY INTERVAL TO THE IONIZATION RATE IN SHELTER, SHOT DIABLO

Energy interval, Mev	Contribution (at indicated time after burst), % H+11 min	H+118 min	H+129 min	H+315 min
0 – 0.06	0.5	2.8	3.1	1.4
0.06 – 0.08	0.4	2.2	2.3	1.2
0.08 – 0.10	0.6	2.8	2.8	1.5
0.10 – 0.15	2.4	9.4	9.2	5.7
0.15 – 0.20	3.3	8.9	7.6	7.2
0.20 – 0.30	8.7	16.0	11.4	16.9
0.30 – 0.40	9.4	8.9	9.8	9.9
0.40 – 0.50	9.5	7.5	7.5	8.3
0.50 – 0.60	10.4	7.1	8.1	9.5
0.60 – 0.80	15.7	11.2	11.8	10.7
0.80 – 1.00	13.9	8.9	10.4	9.7
1.00 – 1.50	25.0	14.3	16.1	17.8
Total	99.8	100.0	100.1	99.8

TABLE D.6—RELATIVE CONTRIBUTION OF PHOTONS IN SELECTED ENERGY INTERVALS TO TOTAL RESPONSE OF THE AN/PDR-27C INSIDE THE SHELTER, SHOT DIABLO*

Energy interval, Mev	Low range (5 mr/hr)				High range (500 mr/hr)			
	H+11 min	H+118 min	H+129 min	H+315 min	H+11 min	H+118 min	H+129 min	H+315 min
0 –0.06	0.0	0.1	0.1	0.1	0.1	0.5	0.6	0.3
0.06–0.08	0.2	0.9	0.9	0.4	0.3	1.7	1.7	0.9
0.08–0.10	0.3	1.6	1.6	0.9	0.5	2.6	2.6	1.4
0.10–0.15	1.7	6.8	6.6	4.1	2.5	10.4	9.8	6.1
0.15–0.20	2.5	6.6	5.7	5.3	3.5	9.7	8.0	7.5
0.20–0.30	6.0	11.0	7.8	11.0	9.1	17.2	11.8	17.6
0.30–0.40	6.7	6.4	7.0	7.1	9.7	9.6	10.1	10.2
0.40–0.50	7.0	5.5	5.5	6.1	9.8	8.0	7.7	8.6
0.50–0.60	7.8	5.3	6.0	7.1	10.6	7.5	8.2	9.6
0.60–0.60	12.3	8.7	9.2	8.4	15.9	11.8	11.9	10.8
0.80–1.00	11.1	7.1	8.3	7.8	14.0	9.3	10.5	9.8
1.00–1.50	20.8	11.9	13.3	14.8	25.0	11.0	16.1	17.8
Total	76.4	71.9	72.0	73.1	101.0	99.3	99.0	100.6

* Values in percentage contribution of the air ionization rate to the instrument reading.

TABLE D.7—GROSS RESPONSE OF THE AN/PDR-27C TO PHOTON SPECTRUM INSIDE THE SHELTER, SHOT DIABLO*

	Time after burst				
	H+11 min	H+118 min	H+129 min	H+315 min	Average
Low range (5 mr/hr)	1.31	1.39	1.39	1.37	1.36
High range (500 mr/hr)	0.99	1.01	1.01	0.99	1.00

* Conversion ratio: true ionization rate/instrument reading.